To the Graduate Council:

I am submitting herewith a thesis written by Lee Reynolds Allen entitled “Numerical Analysis for Determination of Fiber Orientation in Nonwoven Mats.” I have examined the final electronic copy of this thesis for form and content and recommend that it be accepted in partial fulfillment of the requirements for the degree of Master of Science, with a major in Mechanical Engineering.

_____

Dr. Ahmad Vakili, Major Professor

We have read this thesis
And recommend its acceptance:

_____

Dr. Basil Antar

_____

Dr. Louis Deken

Accepted for the Council:

Carolyn R. Hodges
Vice Provost and Dean of the Graduate School

(Original signatures are on file with official student records.)

Numerical Analysis for Determination of Fiber Orientation in Nonwoven Mats

A Thesis Presented for
the Master of Science
Degree
The University of Tennessee, Knoxville

Lee Reynolds Allen
December 2008

Copyright © 2008 by Lee R. Allen
All rights reserved.

ACKNOWLEDGEMENTS

Thank you:

Dr. Vakili, Dr. Antar & Dr. Deken for your advice and support

My family & Jennifer for your unwavering love and words of encouragement

ABSTRACT

The University of Tennessee Space Institute is interested in pitch-based carbon fibers. A need has arisen for characterizing relative alignment of nonwoven fiber mats, produced by the spinning gathering technology implemented. Knowledge of this alignment is relevant in the validation of production methodology as well as aiding in the analysis of carbon fiber composite materials made with the fiber mats. A digital image processing method was developed presented and evaluated in this thesis consisting of three steps: preprocessing using image smoothing, edge detection based upon local intensity gradients, and line detection via the Hough Transform. A summary of typical results are provided in both Chapter 4; a more extensive examples of analysis as well as Matlab™ codes are provided in the Appendix. This method was applied to digital photographs taken from two sources: a carbon fiber mat produced by the University and a generic anti-static dryer sheet.

Four preprocessing methods are explored: Averaging, Median, Gaussian, and Laplacian of Gaussian smoothing. In each case, a convolution kernel is created based upon specified dimensions and standard deviation σ (for Gaussian and Laplacian of Gaussian). Original images are convolved with each kernel, producing a smoothed image. Noise reduction is quantified by the difference between the original image and the smoothed image; this noise is analyzed in histograms generated from Matlab™. Using parameters such as mean, median, and maximum grayscale value as well as processing time, a 5 x 5 Averaging kernel is identified as the optimum preprocessing method explored.

In this thesis, three edge detection techniques are evaluated: the Roberts Method, the Sobel Method, and the Canny Method. Roberts and Sobel, considered first-order methods, are evaluated solely over a specified range of thresholds. The second-order Canny Method (with standard deviation $\sigma = 2.75$) varied over a range of thresholds of a higher order of magnitude. Histograms generated from binary edge images, as well as processing time and relative error introduced from image orientation are used for evaluation purposes. The Canny Method, using a threshold interval of (0.010, 0.250) is chosen as the most appropriate method for this analysis.

The Hough Transform is used to determine characteristics of the lines found in the edge images. Each line is translated into Hough-space using parametric terms ρ and Θ. Using built-in Matlab™ functions, each edge image is divided into grids ranging from 1 x 1 to 10 x 10. In each grid, the mean angle θ, total length L, and processing time t are determined. Results are returned in an array of the specified dimensions.

TABLE OF CONTENTS

Chapter Page

CHAPTER 1 1
Introduction 1
1.1 UTSI High Performance Carbon Fibers 1
1.2 Manufacturing Process 1
1.3 Need For Alignment Evaluation / Measurement 2
CHAPTER 2 3
Concepts And Literature Review 3
2.1 Mechanical Evaluation 3
2.2 Optical Evaluation 3
2.3 Image Analysis 3
2.3.1 Digital Images 4
2.3.2 Image Smoothing 4
2.3.2.1 Averaging Smoothing 5
2.3.2.2 Median Smoothing 5
2.3.2.3 Gaussian Smoothing 6
2.3.2.4 Laplacian of Gaussian (LoG) Smoothing 6
2.3.3 Edge Detection 7
2.3.3.1 Roberts Operator 7
2.3.3.2 Sobel Operator 7
2.3.3.3 Canny Method 8
2.3.3.4 Demonstration 8
2.3.4 The Hough Transform 10
2.3.5 Benchmark Evaluation 11
CHAPTER 3 13
Methods and Analysis 13
3.1 Preprocessing / Smoothing 13
3.1.1 Average Smoothing 14
3.1.2 Median Smoothing 18
3.1.3 Gaussian Smoothing 18
3.1.4 LoG Smoothing 18
3.1.5 Comparison and Method Selection 20
3.2 Edge Detection 23
3.2.1 Roberts Method 24
3.2.2 Sobel Method 25
3.2.3 Canny Method 26
3.2.4 Comparison and Method Selection 27
Figure 14. Processing Time, Rotational Error Study 29
3.3 Line Detection via the Hough Transform 30
CHAPTER 4 34
Typical Results 34
CHAPTER 5 53

Conclusions and Recommendations 53
5.1 Conclusions 53
5.2 Recommendations 53
LIST OF REFERENCES 55
APPENDIX 57
Appendix A: Analysis of Image 0013-2-2a 58
Appendix B: Analysis of Image fiber02a 158
Appendix C: Matlab™ Codes 258
Vita 281

LIST OF TABLES

Table Page

Table 1. Averaging Smoothing Results 11
Table 2. Averaging Smoothing Results 20
Table 3. Median Smoothing Results 20
Table 4. Gaussian Smoothing Results 22
Table 5. Smoothing Method Evaluation 23
Table 6. Line Detection Results 31
Table 7. Averaging Method Summary 44
Table 8. Averaging Method Time Summary 44
Table 9. Median Method Summary 45
Table 10. Median Method Time Summary 45
Table 11. Gaussian Method Summary 46
Table 12. Gaussian Method Time Summary 47
Table 13. LoG Method Summary 48
Table 14. LoG Method Time Summary 49
Table 15. 0013-2-2a Averaging Smoothing Histogram Data 65
Table 16. 0013-2-2a Median Smoothing Histogram Data 79
Table 17. 0013-2-2a Gaussian Smoothing Histogram Data 93
Table 18. 0013-2-2a LoG Smoothing Histogram Data 106
Table 19. 0013-2-2a Roberts Edge Detection Histogram Data 116
Table 20. 0013-2-2a Sobel Edge Detection Histogram Data 120
Table 21. 0013-2-2a Canny Edge Detection Histogram Data 124
Table 22. 0013-2-2a Line Detection θ_{mean}, Grid = 1 x 1 126
Table 23. 0013-2-2a Line Detection θ_{mean}, Grid = 2 x 2 126
Table 24. 0013-2-2a Line Detection θ_{mean}, Grid = 4 x 4 127
Table 25. 0013-2-2a Line Detection θ_{mean}, Grid = 5 x 5 128
Table 26. 0013-2-2a Line Detection θ_{mean}, Grid = 6 x 6 130
Table 27. 0013-2-2a Line Detection θ_{mean}, Grid = 8 x 8 132
Table 28. 0013-2-2a Line Detection θ_{mean}, Grid = 10 x 10 134
Table 29. 0013-2-2a Line Detection L_{total}, Grid = 1 x 1 137
Table 30. 0013-2-2a Line Detection L_{total}, Grid = 2 x 2 137
Table 31. 0013-2-2a Line Detection L_{total}, Grid = 4 x 4 138
Table 32. 0013-2-2a Line Detection L_{total}, Grid = 5 x 5 139
Table 33. 0013-2-2a Line Detection L_{total}, Grid = 6 x 6 141
Table 34. 0013-2-2a Line Detection L_{total}, Grid = 8 x 8 143
Table 35. 0013-2-2a Line Detection L_{total}, Grid = 10 x 10 145
Table 36. 0013-2-2a Line Detection t_{total}, Grid = 1 x 1 148
Table 37. 0013-2-2a Line Detection t_{total}, Grid = 2 x 2 148
Table 38. 0013-2-2a Line Detection t_{total}, Grid = 4 x 4 149
Table 39. 0013-2-2a Line Detection t_{total}, Grid = 5 x 5 150
Table 40. 0013-2-2a Line Detection t_{total}, Grid = 6 x 6 152

Table 41. 0013-2-2a Line Detection t_{total}, Grid = 8 x 8 154
Table 42. 0013-2-2a Line Detection t_{total}, Grid = 10 x 10 155
Table 43. fiber02a Averaging Smoothing Histogram Data 164
Table 44. fiber02a Median Smoothing Histogram Data 178
Table 45. fiber02a Gaussian Smoothing Histogram Data 192
Table 46. fiber02a LoG Smoothing Histogram Data 205
Table 47. fiber02a Roberts Edge Detection Histogram Data 215
Table 48. fiber02a Sobel Edge Detection Histogram Data 219
Table 49. fiber02a Canny Edge Detection Histogram Data 223
Table 50. fiber02a Line Detection θ_{mean}, Grid = 1 x 1 225
Table 51. fiber02a Line Detection θ_{mean}, Grid = 2 x 2 225
Table 52. fiber02a Line Detection θ_{mean}, Grid = 4 x 4 226
Table 53. fiber02a Line Detection θ_{mean}, Grid = 5 x 5 227
Table 54. fiber02a Line Detection θ_{mean}, Grid = 6 x 6 229
Table 55. fiber02a Line Detection θ_{mean}, Grid = 8 x 8 231
Table 56. fiber02a Line Detection θ_{mean}, Grid = 10 x 10 233
Table 57. fiber02a Line Detection L_{total}, Grid = 1 x 1 236
Table 58. fiber02a Line Detection L_{total}, Grid = 2 x 2 236
Table 59. fiber02a Line Detection L_{total}, Grid = 4 x 4 237
Table 60. fiber02a Line Detection L_{total}, Grid = 5 x 5 238
Table 61. fiber02a Line Detection L_{total}, Grid = 6 x 6 240
Table 62. fiber02a Line Detection L_{total}, Grid = 8 x 8 242
Table 63. fiber02a Line Detection L_{total}, Grid = 10 x 10 244
Table 64. fiber02a Line Detection t_{total}, Grid = 1 x 1 247
Table 65. fiber02a Line Detection t_{total}, Grid = 2 x 2 247
Table 66. fiber02a Line Detection t_{total}, Grid = 4 x 4 248
Table 67. fiber02a Line Detection t_{total}, Grid = 5 x 5 249
Table 68. fiber02a Line Detection t_{total}, Grid = 6 x 6 251
Table 69. fiber02a Line Detection t_{total}, Grid = 8 x 8 253
Table 70. fiber02a Line Detection t_{total}, Grid = 10 x 10 255

LIST OF FIGURES

Figure Page

Figure 1. Fiber Image 0013-2-1a 12
Figure 2. Fiber Image 0013-2-1a 14
Figure 3. Average Smoothing, Image 0013-2-1a, 3 x 3 kernel 15
Figure 4. Noise from Original Image using Averaging Smoothing 16
Figure 5. Averaging Noise Histogram, 3 x 3 kernel 17
Figure 6. Effect of standard deviation on Gaussian Smoothing 19
Figure 7. Noise from 0013-2-1a, LoG Smoothing, $\sigma = 4$ 19
Figure 8. Image 0013-2-1a, Roberts Edge Detection, Threshold = 0.001 24
Figure 9. Image 0013-2-1a, Sobel Edge Detection, Threshold = 0.001 25
Figure 10. Image 0013-2-1a, Canny Edge Detection, Threshold = [0.010 0.025] 26
Figure 11. Composite 90° Rotation Sensitivity, Canny Method 27
Figure 12. Composite Detection Percentages of Roberts, Sobel, and Canny 28
Figure 13. Composite Detection Percentages of Roberts, Sobel, and Canny (Zoom) 28
Figure 14. Processing Time, Rotational Error Study 29
Figure 15. Percentage of Measured / Expected Length 33
Figure 16. Averaging Smoothing, 3 x 3 kernel 34
Figure 17. Averaging Smoothing, 5 x 5 kernel 35
Figure 18. Averaging Smoothing, 7 x 7 kernel 35
Figure 19. Averaging Smoothing, 9 x 9 kernel 36
Figure 20. Averaging Smoothing, 11 x 11 kernel 36
Figure 21. Median Smoothing, 3 x 3 kernel 37
Figure 22. Median Smoothing, 5 x 5 kernel 37
Figure 23. Median Smoothing, 7 x 7 kernel 38
Figure 24. Median Smoothing, 9 x 9 kernel 38
Figure 25. Median Smoothing, 11 x 11 kernel 39
Figure 26. Gaussian Smoothing, $\sigma = 1.00$ 39
Figure 27. Gaussian Smoothing, $\sigma = 2.00$ 40
Figure 28. Gaussian Smoothing, $\sigma = 3.00$ 40
Figure 29. Gaussian Smoothing, $\sigma = 4.00$ 41
Figure 30. Gaussian Smoothing, $\sigma = 5.00$ 41
Figure 31. Gaussian Smoothing, $\sigma = 6.00$ 42
Figure 32. LoG Smoothing, $\sigma = 1.00$ 42
Figure 33. LoG Smoothing, $\sigma = 2.00$ 43
Figure 34. LoG Smoothing, $\sigma = 3.00$ 43
Figure 35. LoG Smoothing, $\sigma = 4.00$ 44
Figure 36. Roberts Histograms 50
Figure 37. Roberts Processing Time 50
Figure 38. Sobel Histograms 51
Figure 39. Sobel Processing Time 51
Figure 40. Canny Histograms 52

Figure 41. Canny Processing Time 52
Figure 42. 0013-2-2a 58
Figure 43. 0013-2-2a Averaging Smoothing, 3 x 3 kernel 59
Figure 44. 0013-2-2a Averaging Smoothing Noise, 3 x 3 kernel 59
Figure 45. 0013-2-2a Averaging Smoothing, 5 x 5 kernel 60
Figure 46. 0013-2-2a Averaging Smoothing Noise, 5 x 5 kernel 60
Figure 47. 0013-2-2a Averaging Smoothing, 5 x 5 kernel 61
Figure 48. 0013-2-2a Averaging Smoothing Noise, 5 x 5 kernel 61
Figure 49. 0013-2-2a Averaging Smoothing, 7 x 7 kernel 62
Figure 50. 0013-2-2a Averaging Smoothing Noise, 7 x 7 kernel 62
Figure 51. 0013-2-2a Averaging Smoothing, 9 x 9 kernel 63
Figure 52. 0013-2-2a Averaging Smoothing Noise, 9 x 9 kernel 63
Figure 53. 0013-2-2a Averaging Smoothing, 11 x 11 kernel 64
Figure 54. 0013-2-2a Averaging Smoothing Noise, 11 x 11 kernel 64
Figure 55. 0013-2-2a Averaging Smoothing Histogram, 3 x 3 kernel 71
Figure 56. 0013-2-2a Averaging Smoothing Histogram, 5 x 5 kernel 71
Figure 57. 0013-2-2a Averaging Smoothing Histogram, 7 x 7 kernel 72
Figure 58. 0013-2-2a Averaging Smoothing Histogram, 9 x 9 kernel 72
Figure 59. 0013-2-2a Averaging Smoothing Histogram, 11 x 11 kernel 73
Figure 60. 0013-2-2a Median Smoothing, 3 x 3 kernel 74
Figure 61. 0013-2-2a Median Smoothing Noise, 3 x 3 kernel 74
Figure 62. 0013-2-2a Median Smoothing, 5 x 5 kernel 75
Figure 63. 0013-2-2a Median Smoothing Noise, 5 x 5 kernel 75
Figure 64. 0013-2-2a Median Smoothing, 7 x 7 kernel 76
Figure 65. 0013-2-2a Median Smoothing Noise, 7 x 7 kernel 76
Figure 66. 0013-2-2a Median Smoothing, 9 x 9 kernel 77
Figure 67. 0013-2-2a Median Smoothing Noise, 9 x 9 kernel 77
Figure 68. 0013-2-2a Median Smoothing, 11 x 11 kernel 78
Figure 69. 0013-2-2a Median Smoothing Noise, 11 x 11 kernel 78
Figure 70. 0013-2-2a Median Smoothing Histogram, 3 x 3 kernel 85
Figure 71. 0013-2-2a Median Smoothing Histogram, 5 x 5 kernel 85
Figure 72. 0013-2-2a Median Smoothing Histogram, 7 x 7 kernel 86
Figure 73. 0013-2-2a Median Smoothing Histogram, 9 x 9 kernel 86
Figure 74. 0013-2-2a Median Smoothing Histogram, 11 x 11 kernel 87
Figure 75. 0013-2-2a Gaussian Smoothing, $\sigma = 1.00$ kernel 88
Figure 76. 0013-2-2a Gaussian Smoothing Noise, $\sigma = 1.00$ kernel 88
Figure 77. 0013-2-2a Gaussian Smoothing, $\sigma = 2.00$ kernel 89
Figure 78. 0013-2-2a Gaussian Smoothing Noise, $\sigma = 2.00$ kernel 89
Figure 79. 0013-2-2a Gaussian Smoothing, $\sigma = 3.00$ kernel 90
Figure 80. 0013-2-2a Gaussian Smoothing Noise, $\sigma = 3.00$ kernel 90
Figure 81. 0013-2-2a Gaussian Smoothing, $\sigma = 4.00$ kernel 91
Figure 82. 0013-2-2a Gaussian Smoothing Noise, $\sigma = 4.00$ kernel 91
Figure 83. 0013-2-2a Gaussian Smoothing, $\sigma = 5.00$ kernel 92
Figure 84. 0013-2-2a Gaussian Smoothing Noise, $\sigma = 5.00$ kernel 92

Figure 85. 0013-2-2a Gaussian Smoothing Histogram, σ = 1.00 kernel 99
Figure 86. 0013-2-2a Gaussian Smoothing Histogram, σ = 2.00 kernel 99
Figure 87. 0013-2-2a Gaussian Smoothing Histogram, σ = 3.00 kernel 100
Figure 88. 0013-2-2a Gaussian Smoothing Histogram, σ = 4.00 kernel 100
Figure 89. 0013-2-2a Gaussian Smoothing Histogram, σ = 5.00 kernel 101
Figure 90. 0013-2-2a LoG Smoothing, σ = 1.00 kernel 102
Figure 91. 0013-2-2a LoG Smoothing Noise, σ = 1.00 kernel 102
Figure 92. 0013-2-2a LoG Smoothing, σ = 2.00 kernel 103
Figure 93. 0013-2-2a LoG Smoothing Noise, σ = 2.00 kernel 103
Figure 94. 0013-2-2a LoG Smoothing, σ = 3.00 kernel 104
Figure 95. 0013-2-2a LoG Smoothing Noise, σ = 3.00 kernel 104
Figure 96. 0013-2-2a LoG Smoothing, σ = 4.00 kernel 105
Figure 97. 0013-2-2a LoG Smoothing Noise, σ = 4.00 kernel 105
Figure 98. 0013-2-2a LoG Smoothing Histogram, σ = 1.00 kernel 112
Figure 99. 0013-2-2a LoG Smoothing Histogram, σ = 2.00 kernel 112
Figure 100. 0013-2-2a LoG Smoothing Histogram, σ = 3.00 kernel 113
Figure 101. 0013-2-2a LoG Smoothing Histogram, σ = 4.00 kernel 113
Figure 102. 0013-2-2a Roberts Edge Detection, Threshold = 0.001 114
Figure 103. 0013-2-2a Roberts Edge Detection, Threshold = 0.010 114
Figure 104. 0013-2-2a Roberts Edge Detection, Threshold = 0.021 115
Figure 105. 0013-2-2a Roberts Edge Detection, Threshold = 0.030 115
Figure 106. 0013-2-2a Roberts Edge Detection Histograms 117
Figure 107. 0013-2-2a Roberts Edge Detection 90° Rotation Histograms 117
Figure 108. 0013-2-2a Sobel Edge Detection, Threshold = 0.001 118
Figure 109. 0013-2-2a Sobel Edge Detection, Threshold = 0.010 118
Figure 110. 0013-2-2a Sobel Edge Detection, Threshold = 0.021 119
Figure 111. 0013-2-2a Sobel Edge Detection, Threshold = 0.030 119
Figure 112. 0013-2-2a Sobel Edge Detection Histograms 121
Figure 113. 0013-2-2a Sobel Edge Detection 90° Rotation Histograms 121
Figure 114. 0013-2-2a Canny Edge Detection, Threshold = [0.010 0.025] 122
Figure 115. 0013-2-2a Canny Edge Detection, Threshold = [0.100 0.250] 122
Figure 116. 0013-2-2a Canny Edge Detection, Threshold = [0.210 0.525] 123
Figure 117. 0013-2-2a Canny Edge Detection, Threshold = [0.300 0.750] 123
Figure 118. 0013-2-2a Canny Edge Detection Histograms 125
Figure 119. 0013-2-2a Canny Edge Detection 90° Rotation Histograms 125
Figure 120. fiber02a 158
Figure 121. fiber02a Averaging Smoothing, 3 x 3 kernel 159
Figure 122. fiber02a Averaging Smoothing Noise, 3 x 3 kernel 159
Figure 123. fiber02a Averaging Smoothing, 5 x 5 kernel 160
Figure 124. fiber02a Averaging Smoothing Noise, 5 x 5 kernel 160
Figure 125. fiber02a Averaging Smoothing, 7 x 7 kernel 161
Figure 126. fiber02a Averaging Smoothing Noise, 7 x 7 kernel 161
Figure 127. fiber02a Averaging Smoothing, 9 x 9 kernel 162
Figure 128. fiber02a Averaging Smoothing Noise, 9 x 9 kernel 162

Figure 129. fiber02a Averaging Smoothing, 11 x 11 kernel 163
Figure 130. fiber02a Averaging Smoothing Noise, 11 x 11 kernel 163
Figure 131. fiber02a Averaging Smoothing Noise Histogram, 3 x 3 kernel 170
Figure 132. fiber02a Averaging Smoothing Noise Histogram, 5 x 5 kernel 170
Figure 133. fiber02a Averaging Smoothing Noise Histogram, 7 x 7 kernel 171
Figure 134. fiber02a Averaging Smoothing Noise Histogram, 9 x 9 kernel 171
Figure 135. fiber02a Averaging Smoothing Noise Histogram, 11 x 11 kernel 172
Figure 136. fiber02a Median Smoothing, 3 x 3 kernel 173
Figure 137. fiber02a Median Smoothing Noise, 3 x 3 kernel 173
Figure 138. fiber02a Median Smoothing, 5 x 5 kernel 174
Figure 139. fiber02a Median Smoothing Noise, 5 x 5 kernel 174
Figure 140. fiber02a Median Smoothing, 7 x 7 kernel 175
Figure 141. fiber02a Median Smoothing Noise, 7 x 7 kernel 175
Figure 142. fiber02a Median Smoothing, 9 x 9 kernel 176
Figure 143. fiber02a Median Smoothing Noise, 9 x 9 kernel 176
Figure 144. fiber02a Median Smoothing, 11 x 11 kernel 177
Figure 145. fiber02a Median Smoothing Noise, 11 x 11 kernel 177
Figure 146. fiber02a Median Smoothing Noise Histogram, 3 x 3 kernel 184
Figure 147. fiber02a Median Smoothing Noise Histogram, 5 x 5 kernel 184
Figure 148. fiber02a Median Smoothing Noise Histogram, 7 x 7 kernel 185
Figure 149. fiber02a Median Smoothing Noise Histogram, 9 x 9 kernel 185
Figure 150. fiber02a Median Smoothing Noise Histogram, 11 x 11 kernel 186
Figure 151. fiber02a Gaussian Smoothing, $\sigma = 1.00$ kernel 187
Figure 152. fiber02a Gaussian Smoothing Noise, $\sigma = 1.00$ kernel 187
Figure 153. fiber02a Gaussian Smoothing, $\sigma = 2.00$ kernel 188
Figure 154. fiber02a Gaussian Smoothing Noise, $\sigma = 2.00$ kernel 188
Figure 155. fiber02a Gaussian Smoothing, $\sigma = 3.00$ kernel 189
Figure 156. fiber02a Gaussian Smoothing Noise, $\sigma = 3.00$ kernel 189
Figure 157. fiber02a Gaussian Smoothing, $\sigma = 4.00$ kernel 190
Figure 158. fiber02a Gaussian Smoothing Noise, $\sigma = 4.00$ kernel 190
Figure 159. fiber02a Gaussian Smoothing, $\sigma = 5.00$ kernel 191
Figure 160. fiber02a Gaussian Smoothing Noise, $\sigma = 5.00$ kernel 191
Figure 161. fiber02a Gaussian Smoothing Histogram, $\sigma = 1.00$ kernel 198
Figure 162. fiber02a Gaussian Smoothing Histogram, $\sigma = 2.00$ kernel 198
Figure 163. fiber02a Gaussian Smoothing Histogram, $\sigma = 3.00$ kernel 199
Figure 164. fiber02a Gaussian Smoothing Histogram, $\sigma = 4.00$ kernel 199
Figure 165. fiber02a Gaussian Smoothing Histogram, $\sigma = 5.00$ kernel 200
Figure 166. fiber02a LoG Smoothing, $\sigma = 1.00$ kernel 201
Figure 167. fiber02a LoG Smoothing Noise, $\sigma = 1.00$ kernel 201
Figure 168. fiber02a LoG Smoothing, $\sigma = 2.00$ kernel 202
Figure 169. fiber02a LoG Smoothing Noise, $\sigma = 2.00$ kernel 202
Figure 170. fiber02a LoG Smoothing, $\sigma = 3.00$ kernel 203
Figure 171. fiber02a LoG Smoothing Noise, $\sigma = 3.00$ kernel 203

Figure 172. fiber02a LoG Smoothing, σ = 4.00 kernel 204
Figure 173. fiber02a LoG Smoothing Noise, σ = 4.00 kernel 204
Figure 174. fiber02a LoG Smoothing Histogram, σ = 1.00 kernel 211
Figure 175. fiber02a LoG Smoothing Histogram, σ = 2.00 kernel 211
Figure 176. fiber02a LoG Smoothing Histogram, σ = 3.00 kernel 212
Figure 177. fiber02a LoG Smoothing Histogram, σ = 4.00 kernel 212
Figure 178. fiber2a Roberts Edge Detection, Threshold = 0.001 213
Figure 179. fiber2a Roberts Edge Detection, Threshold = 0.010 213
Figure 180. fiber2a Roberts Edge Detection, Threshold = 0.021 214
Figure 181. fiber02a Roberts Edge Detection, Threshold = 0.030 214
Figure 182. fiber02a Roberts Edge Detection Histograms 216
Figure 183. fiber02a Roberts Edge Detection 90° Rotation Histograms 216
Figure 184. fiber2a Sobel Edge Detection, Threshold = 0.001 217
Figure 185. fiber2a Sobel Edge Detection, Threshold = 0.010 217
Figure 186. fiber2a Sobel Edge Detection, Threshold = 0.021 218
Figure 187. fiber2a Sobel Edge Detection, Threshold = 0.030 218
Figure 188. fiber02a Sobel Edge Detection Histograms 220
Figure 189. fiber02a Sobel Edge Detection 90° Rotation Histograms 220
Figure 190. fiber02a Canny Edge Detection, Threshold = [0.010 0.025] 221
Figure 191. fiber02a Canny Edge Detection, Threshold = [0.100 0.250] 221
Figure 192. fiber02a Canny Edge Detection, Threshold = [0.210 0.525] 222
Figure 193. fiber02a Canny Edge Detection, Threshold = [0.300 0.750] 222
Figure 194. fiber02a Canny Edge Detection Histograms 224
Figure 195. fiber02a Canny Edge Detection 90° Rotation Histograms 224

NOMENCLATURE

f	Random function
g	Image
t	Random variable; time (seconds); Student-t value
τ	Random variable
a	Integration end point
b	Integration end point
h	Convolution kernel
n	Sample size
∇	Del operator
∂^2	2^{nd} partial differential
σ	Standard deviation, Gaussian
π	Pi
x	Independent horizontal variable; arithmetic mean, Student-t
y	Independent vertical variable
μ	Mean, Gaussian
s	Standard deviation, Student-t
Max	Sample maximum; Maximum histogram frequency
Min	Sample minimum; Minimum histogram frequency
Gray	Grayscale percentage
H	Hough Transform matrix
ρ	Minimum directed distance parameter, Hough Transform
Θ	Inclination angle, Hough Transform
θ	Line/edge angle
L	Line length

CHAPTER 1
INTRODUCTION

1.1 UTSI High Performance Carbon Fibers

The University of Tennessee Space Institute is currently pursuing research into the manufacture of low cost pitch-based carbon fibers. UTSI's carbon fiber manufacturing equipment was received as a gift from ConocoPhillips in 2004. Since then, the University has made significant progress in carbon fiber production methods and composite manufacturing techniques.

High performance carbon fibers are traditionally made from two sources: polyacrylonitrile (PAN) and pitch. PAN fibers generally produce fibers with higher tensile strength and elastic moduli due to their higher carbon content, while pitch fibers often have higher thermal and electrical conductivity coefficients. Pitch-based fibers have many possible applications in composite materials, electronic equipment, and reinforced concrete.

1.2 Manufacturing Process

As stated above, the precursor material for the carbon fibers produced at UTSI is (mesophase) pitch. In order to "spin" the pitch into carbon fiber, it must first be heated to melting. Due to the highly viscous nature of pitch, the temperature must be very accurately controlled. Once the pitch has melted, it is extruded through a *spinnerette*, which is typically a block with extremely small holes. As the extruded fibers flow from the *spinnerette,* high-velocity airflow is used to cool, continue extruding, and direct the fibers to the collection media below. Many methods can be used to collect the fibers; UTSI generally collects them in the form of an unwoven mat on a converyor belt or spooled onto a bobbin.

Fibers that have been extruded are referred to as "green." These green fibers must then be dried in low heat to remove a solvent used to aid manufacture. After the fibers have been dried (stabilized), they are then heat treated at high temperature in a non-oxidative environment, typically pure nitrogen. This process, conducted around 1500 °C is known as pyrolization, usually yields a high performance fiber of at least 95% carbon. Additionally, properties can be increased further by heat treating at higher temperatures (+2000 °C) in a process known as carbonization.

1.3 Need For Alignment Evaluation / Measurement

In the previous section, it was stated that fibers manufactured at UTSI are usually produced in an unwoven mat. The term “unwoven” can be somewhat misleading – these mats generally exhibit a certain level of alignment due to the mechanics of airflow-driven fiber laydown. Quantification of this alignment is extremely helpful when fabricating carbon fiber reinforced composites; fiber alignment is critical in determination of composite strength.

Given this need, and knowing that exact characterization of fiber alignment is beyond the scope of this exercise, digital image processing and analytical techniques are well-suited for this approach. A variety of noise attenuation methods and edge detection algorithms are explored, as well as variations of the Hough Transform for line detection.

CHAPTER 2
CONCEPTS AND LITERATURE REVIEW

2.1 Mechanical Evaluation

Mechanical evaluation of fibers can be conducted on individual fibers, or on collections of fibers (bundles, rovings, or mats). Tensile testing determines both the break strength of the fibers, as well as the accompanying strain. From that data, the modulus of elasticity can be determined using Hooke's Law.

Similarly, composites can be tested through various means to find break strength as well. The matrix properties are known before hand, and testing can be used to evaluate fiber properties, such as strength, elastic modulus, and critical fiber length. In composite testing, the alignment of the fibers is extremely critical because fiber geometry greatly influences the directional strength of the material.

2.2 Optical Evaluation

Optical evaluation on the nano-scale is accomplished with scanning electron microscopy. From this method, diameter of the fiber can be measured visually, and surface characteristics of the fiber can be easily distinguished. Other methods can be used to quantify porosity of the fiber, as well as surface characteristics.

On the micro-scale, fiber diameter can be measured using a laser micrometer. The interference of the fiber in the path of a laser beam can be quantified in order to determine the diameter of said fiber. If the measurement is taken at different angles along the same axial location, the shape of the fiber at that point can be analyzed; fibers are generally not true circles but are instead elliptical or "dog-boned."

2.3 Image Analysis

Image analysis, similar to the methods used in facial recognition software and computerized axial tomography (CAT scanning), can be a useful tool in analyzing carbon fiber alignment. Digital images can be manipulated via smoothing algorithms to lessen the effects of noise, and edges can be detected through a number of gradient approximations. Once the edges in an image are identified, they can then be interpreted as lines to be characterized. Through the use of computational software such as Matlab™, these operations can be done quickly and on a relatively large scale.

2.3.1 Digital Images

Digital images, also known as raster images, are stored as rectangular arrays of values that are discrete portions of the image. Each value in the array, also known as a pixel, stores values that represent the coloring at that point. Typically, three bits represent the values for red, blue, and green, but can range up to eight bits depending on the encoding. Black-and-white images also referred to as grayscale, only need to store one bit that represents intensity, and therefore have smaller memory requirements.

In digital images, the origin is considered to be the upper left corner, with the positive horizontal axis moving from left to right, and the positive vertical axis pointing downward. This convention will be adhered to for the analyses presented here.

As stated above, digital images are represented by arrays of values, and can be treated mathematically as matrices. In order for edge detection algorithms to function properly, however, colored digital images must be converted into grayscale. This essentially results in a matrix of values ranging from zero (black) to 1 (white) – greatly simplifying an image while still conveying its detail.

Different methods can be used to convert colored images to grayscale, such as intensity averaging, de-saturation, or a combination of the two. Various algorithms use different techniques to weight the colors, however these will not be discussed here. Matlab uses a technique that filters out the hue & saturation information of an image, leaving only an array of luminance.

Many image processing methods involve the convolution of the image matrix with a filter or mask. This operation, while similar to matrix multiplication, can be conducted with arrays of different dimensions (e.g. a 640 x 480 matrix and a 3 x 3 matrix). Convolution can be defined by Equation 1.

$$(f * g)(t) = \int_a^b f(\tau)g(t-\tau)\,d\tau \quad \textbf{(1)}$$

Each value in matrix f is evaluated according to matrix g, producing a new matrix h. Convolution can be used for many different operations including image smoothing, blurring, edge enhancement, edge detection.

2.3.2 Image Smoothing

Digital photographs, like any other measurement, are accompanied by noise. Image noise can come from a number of sources such as lighting, lens imperfections, background noise, and even data corruption. In order to reduce the likelihood of error in later steps of image analysis, a smoothing operation should take place beforehand. A small amount of

error will be induced from smoothing, but this is mitigates the larger errors generated by noise. Several methods can be used to smooth the image such as pixel averaging, pixel median, and Gaussian smoothing.

2.3.2.1 Averaging Smoothing

The averaging method is performed by convolving the grayscale image *A* with an averaging mask *h*, as shown below in Equation 2.

$$h = \frac{1}{9}\begin{bmatrix} 1 & 1 & 1 \\ 1 & 1 & 1 \\ 1 & 1 & 1 \end{bmatrix} \quad \textbf{(2)}$$

Larger masks can also be utilized, if desired. This operation results in a new matrix *B* having the same dimensions of *A*, with each value b_{ij} being the average of a_{ij} and its immediately surrounding values. Other masks, with the emphasis on the center value can be applied, such as in Equation 3.

$$h = \frac{1}{10}\begin{bmatrix} 1 & 1 & 1 \\ 1 & 2 & 1 \\ 1 & 1 & 1 \end{bmatrix} \quad \textbf{(3)}$$

Many variations of averaging are possible, types that use criteria to limit the evaluation of certain pixels or rotate the convolution mask and evaluate the image multiple times. These methods are generally very effective, but only if the noise is smaller than the points of interest in the image. Edge blurring can also become a concern.

2.3.2.2 Median Smoothing

Median smoothing replaces a point in an image with the median of brightness in the surrounding area. The median method does not blur edges as much as the averaging method, is not affected by random spikes, and reduces impulsive noise well. However, in a rectangular area, thin lines and corners can be inadvertently deemphasized. This can be avoided through the use of different area geometries, which can become increasingly complicated and will not be explored here.

Median smoothing in Matlab™ is not accomplished via convolution; instead it uses a base function *ordfilt2* to accomplish the same goal. This function is a logical operator that uses dimensional input (similar to matrix dimensional notation) to determine the kernel size. The median operator is named *medfilt2*.

2.3.2.3 Gaussian Smoothing

Gaussian smoothing is a more versatile method than those described above, because both the size of the smoothing mask can be varied, as well as the standard deviation of the distribution. However, as the standard deviation of the distribution is increased, the size of the convolution mask may have to grow in order to provide the desired resolution. This can become prohibitive in certain situations.

The Gaussian kernel is created using the same function that is used to create the averaging filter, *fspecial*. Both a standard deviation and matrix dimensions are required. Equation 4 shows a 5 x 5 smoothing kernel with standard deviation σ, of 1.

$$h_{5x5} = \begin{bmatrix} 0.0030 & 0.0133 & 0.0219 & 0.0133 & 0.0030 \\ 0.0133 & 0.0596 & 0.0983 & 0.0596 & 0.0133 \\ 0.0219 & 0.0983 & 0.1621 & 0.0983 & 0.0219 \\ 0.0133 & 0.0596 & 0.0983 & 0.0596 & 0.0133 \\ 0.0030 & 0.0133 & 0.0219 & 0.0133 & 0.0030 \end{bmatrix} \quad \textbf{(4)}$$

2.3.2.4 Laplacian of Gaussian (LoG) Smoothing

The fourth smoothing method explored in this exercise is Laplacian of Gaussian (LoG) smoothing. This combination of the Gaussian function and the Laplacian operator (Equation 5) was explored because it emphasizes edge enhancement. This is accomplished due to the use of zero crossings of the second derivative – a clear indicator of edges in image analysis.

$$LoG(x,y) = -\frac{1}{\pi\sigma^4}\left[1 - \frac{x^2+y^2}{2\sigma^2}\right]e^{-\frac{x^2+y^2}{2\sigma^2}} \quad \textbf{(5)}$$

Once again, *fspecial* is used to create the LoG kernel. Equation 6 demonstrates a 5 x 5 kernel with standard deviation σ of 1. An obvious difference between this kernel and a Gaussian kernel of equal dimension and s is the presence of negative values near the center. This phenomena helps to approximate the second derivative of the point of interest.

$$h_{5x5} = \begin{bmatrix} 0.0239 & 0.0460 & 0.0499 & 0.0460 & 0.0239 \\ 0.0460 & 0.0061 & -0.0923 & 0.0061 & 0.0460 \\ 0.0499 & -0.0923 & -0.3182 & -0.0923 & 0.0499 \\ 0.0460 & 0.0061 & -0.0923 & 0.0061 & 0.0460 \\ 0.0239 & 0.0460 & 0.0499 & 0.0460 & 0.0239 \end{bmatrix} \quad \textbf{(6)}$$

2.3.3 Edge Detection

Edge detection uses various algorithms to determine shapes in grayscale images by locating sharp changes in intensity gradients. Through the use of matrix manipulation, trends can be found on the local and global scale. Edge detection is the basis for more complicated software applications such as fingerprint identification, facial recognition, and computational tomography ("CAT scanning"). Various forms of these methods are commercially available; this exercise utilizes built-in functions in Matlab™.

Basic edge detector algorithms are broken into to groups: first order, and second order. First order edge detecting algorithms sense only that a sharp change in the intensity gradient and make these evaluations based on differences. Roberts and Sobel algorithms are classic examples of first order edge detectors. Second order algorithms are able to determine both the gradient and the direction, and base their evaluations on approximations of the second derivative. The Canny algorithm is the leading second order detectors.

2.3.3.1 Roberts Operator

The earliest form of edge detection in digital images is known as the Roberts or Roberts-Cross method. The Roberts operator is defined by the convolution masks shown below in Equation 7. And the magnitude of the edge is then calculated according to Figure 8.

$$h_1 = \begin{bmatrix} 1 & 0 \\ 0 & -1 \end{bmatrix} \quad , \quad h_2 = \begin{bmatrix} 0 & 1 \\ -1 & 0 \end{bmatrix} \qquad \textbf{(7)}$$

$$g = \left|g(i,j) - g(i+1,j+1)\right| + \left|g(i,j+1) - g(i+1,j)\right| \qquad \textbf{(8)}$$

The horizontal intensity gradient is found using h_1; the vertical intensity gradient is calculated using h_2. If either intensity gradient is above the desired threshold, that point is considered an edge. The Roberts operator is computes very quickly, because only 4 points are required to estimate the intensity gradient. However, this method is highly susceptible to noise because so few points are considered.

2.3.3.2 Sobel Operator

The Sobel operator is given by the three convolution masks shown in Equation 9; h_3 corresponds to the horizontal and h_1 corresponds to the vertical. The intermediary kernel h_2 measures the diagonal intensity gradient.

$$h_1 = \begin{bmatrix} 1 & 2 & 1 \\ 0 & 0 & 0 \\ -1 & -2 & -1 \end{bmatrix}, \quad h_2 = \begin{bmatrix} 0 & 1 & 2 \\ -1 & 0 & 1 \\ -2 & -1 & 0 \end{bmatrix}, \quad h_3 = \begin{bmatrix} -1 & 0 & 1 \\ -2 & 0 & 2 \\ -1 & 0 & 1 \end{bmatrix} \quad \textbf{(9)}$$

The Sobel operator is less sensitive to noise than the Roberts operator, because more points are evaluated and weighting is used to a limited degree. In turn, this accuracy also comes with additional computation time due to the larger mask.

2.3.3.3 Canny Method

The Canny algorithm was developed in 1986 by John Canny while performing research at the University of California. Canny edge detection is similar in nature to the Laplacian of Gaussian smoothing operator, with a few notable differences. First, the normal direction **n** of the gradient can be approximated by the relationship seen in Equation 10, where *G* is the two-dimensional Gaussian distribution and *g* is the image. Local maxima are defined by Equation 11, and intensity gradient magnitude is calculated according to Equation 12.

$$n = \frac{\nabla(G * g)}{|\nabla(G * g)|} \quad \textbf{(10)}$$

$$\frac{\partial^2}{\partial n^2} G * g = 0 \quad \textbf{(11)}$$

$$|G_n * g| = |\nabla(G * g)| \quad \textbf{(12)}$$

Having defined these relationships, the algrorithm is as follows: First, convolve the image *g* with a Gaussian filter of standard deviation σ. Next, estimate the local edge normal directions **n**. Find the location of edges using the second-order partial differential equation, and suppress the non-maxima. Then, determine the magnitude of the edges using the relationship above. Finally, use thresholding with hysteresis to eliminate false edges from the image.

2.3.3.4 Demonstration

A brief demonstration shows the differing results that the three methods return. Given a 10 x 10 matrix T (Equation 13) of random intensity values ranging between 0 and 1, all

three edge detection methods are applied using identical threshold values of 0.05. The standard deviation σ for the Canny method is one.

$$T = \begin{bmatrix} 0.40 & 0.31 & 0.02 & 0.20 & 0.09 & 0.57 & 0.73 & 0.57 & 0.58 & 0.48 \\ 0.99 & 0.97 & 0.79 & 0.04 & 0.99 & 0.54 & 0.18 & 0.25 & 0.84 & 0.78 \\ 0.42 & 0.80 & 0.05 & 0.46 & 0.46 & 0.13 & 0.24 & 0.92 & 0.15 & 0.55 \\ 0.13 & 0.81 & 0.48 & 0.79 & 0.52 & 0.44 & 0.50 & 0.21 & 0.70 & 0.64 \\ 0.59 & 0.39 & 0.15 & 0.33 & 0.90 & 0.30 & 0.33 & 0.29 & 0.43 & 0.93 \\ 0.97 & 0.18 & 0.31 & 0.76 & 0.11 & 0.79 & 0.61 & 0.18 & 0.85 & 0.15 \\ 0.13 & 1.00 & 0.75 & 0.02 & 0.47 & 0.76 & 0.08 & 0.03 & 0.80 & 0.07 \\ 0.10 & 0.55 & 0.27 & 0.99 & 0.01 & 0.79 & 0.43 & 0.44 & 0.96 & 0.59 \\ 0.09 & 0.14 & 0.11 & 0.48 & 0.53 & 0.39 & 0.93 & 0.00 & 0.89 & 0.26 \\ 0.45 & 0.49 & 0.80 & 0.17 & 0.75 & 0.08 & 0.92 & 0.05 & 0.22 & 0.93 \end{bmatrix} \quad \textbf{(13)}$$

Each of the resultant matrices, (Equations 14 – 16) R, S, and C are binary in composition; zero values represent the black background, and 1 values represent detected "edges". These example matrices are somewhat indicative of what is to be seen in future testing, and will be addressed later on in the paper.

$$R = \begin{bmatrix} 1 & 1 & 0 & 0 & 1 & 0 & 1 & 0 & 1 & 1 \\ 0 & 1 & 0 & 0 & 1 & 0 & 1 & 0 & 1 & 0 \\ 0 & 1 & 0 & 0 & 1 & 0 & 1 & 0 & 1 & 0 \\ 1 & 0 & 1 & 0 & 1 & 0 & 0 & 0 & 0 & 1 \\ 1 & 0 & 0 & 0 & 0 & 0 & 0 & 0 & 0 & 1 \\ 0 & 0 & 0 & 0 & 0 & 1 & 0 & 1 & 1 & 0 \\ 1 & 0 & 0 & 0 & 1 & 1 & 0 & 1 & 0 & 0 \\ 0 & 0 & 1 & 0 & 0 & 0 & 0 & 0 & 0 & 1 \\ 1 & 0 & 0 & 0 & 0 & 1 & 1 & 0 & 0 & 1 \\ 0 & 1 & 1 & 1 & 1 & 1 & 1 & 1 & 1 & 0 \end{bmatrix} \quad \textbf{(14)}$$

$$S = \begin{bmatrix} 1 & 1 & 0 & 1 & 1 & 0 & 1 & 0 & 0 & 1 \\ 0 & 0 & 1 & 0 & 0 & 1 & 0 & 0 & 0 & 0 \\ 1 & 1 & 1 & 0 & 0 & 1 & 0 & 0 & 0 & 1 \\ 1 & 0 & 0 & 0 & 1 & 0 & 0 & 1 & 0 & 1 \\ 1 & 0 & 0 & 1 & 0 & 0 & 1 & 0 & 1 & 0 \\ 0 & 1 & 1 & 0 & 1 & 0 & 1 & 0 & 0 & 0 \\ 1 & 0 & 0 & 0 & 1 & 0 & 1 & 0 & 1 & 1 \\ 0 & 1 & 1 & 0 & 0 & 0 & 1 & 0 & 0 & 1 \\ 0 & 0 & 0 & 0 & 0 & 1 & 0 & 0 & 1 & 0 \\ 1 & 1 & 1 & 0 & 0 & 1 & 0 & 0 & 1 & 0 \end{bmatrix} \quad \textbf{(15)}$$

$$C = \begin{bmatrix} 0 & 0 & 0 & 0 & 0 & 0 & 0 & 0 & 0 & 0 \\ 0 & 0 & 1 & 1 & 0 & 0 & 1 & 0 & 0 & 0 \\ 0 & 1 & 0 & 0 & 0 & 0 & 0 & 1 & 0 & 0 \\ 0 & 0 & 0 & 0 & 1 & 0 & 0 & 0 & 1 & 0 \\ 0 & 1 & 0 & 0 & 0 & 1 & 0 & 0 & 1 & 0 \\ 0 & 0 & 0 & 0 & 0 & 1 & 0 & 0 & 0 & 0 \\ 0 & 0 & 0 & 0 & 0 & 0 & 1 & 0 & 0 & 0 \\ 0 & 1 & 0 & 0 & 0 & 0 & 0 & 0 & 0 & 0 \\ 0 & 1 & 0 & 0 & 0 & 0 & 0 & 0 & 0 & 0 \\ 0 & 0 & 0 & 0 & 0 & 0 & 0 & 0 & 0 & 0 \end{bmatrix} \quad \textbf{(16)}$$

2.3.4 The Hough Transform

A literature search was performed to determine possible methods for line detection / feature extraction. The Hough transform, was found to be the only practical method for this type of analysis. Other methods, such as Fast Fourier Transforms and Radon Transforms were explored, but ultimately deemed ill-suited. Both methods are quite effective in signal processing; the Radon Transform is used in CAT scanning.

The Hough Transform was patented by IBM in 1962, and based upon earlier work by Paul Hough. Hough's algorithm requires the image to already be in a binary format, preferably pre-edge detected. Such edge detected images are simply arrays of 1s and 0s, exactly what is required for this process. In order to define a line, 2 points are necessary; for n points, one could define $n(n\text{-}1)/2$ pairs of points in the image and checking how many other points fall on each line. This method would require approximately $n^3/2$ computations, which becomes prohibitive very quickly. Therefore, some other set of parameters might be more suitable. Slope and intercept would not work very well here, as

specific conditions may involve no intercept and/or infinite slope. Instead, the Hough algorithm records unique parameters ρ and Θ. The minimal directed distance from the origin is defined as ρ. The parameter Θ defines the inclination angle of the line with respect to the horizontal axis.

Once all the (ρ,Θ) parameters have been determined, a scatter plot is made in Hough space, with ρ forming the horizontal axis and θ forming the vertical. Lines in the original image will appear as clusters of points in Hough space. To mathematically determine the existence of these lines in Hough space, a two-dimensional histogram needs to be constructed. From this, peaks can be found; if peaks are above a specified threshold, a line is confirmed.

Three Matlab™ functions are needed to complete this analysis: *hough*, *houghpeaks*, and *houghlines*. The *hough* function requires a binary image; the user may specify the precision of both ρ and Θ (both default to 1). A matrix H is generated from *hough*, which has Θ columns and ρ rows. Then, *houghpeaks* which requires the input matrix H along with either a specified quantity of peaks (numpeaks) or a threshold, and returns a Q x 2 matrix (peaks) of peak coordinates. Finally, *houghlines* requires the following inputs: the binary image, ρ, Θ, and peaks. This function locates line segments as specified by the inputs and returns an array of endpoints with their associated Hough parameters ρ and Θ.

2.3.5 Benchmark Evaluation

Initial benchmarking of the three edge detection methods as well as the Hough transform validates the methods prior to large-scale testing. In each case, the same artificial test image (Figure 1) is analyzed over same grid size using the same threshold values. If figure 1 is divided into 4 even sections (each section is 240 x 240), each grid will have two edges of length 240 (total of 480); the top two regions have horizontal edges and the bottom two areas have vertical lines.Table 1 shows the three methods show reasonable accuracy in both the θ_{mean} and L_{total} parameters, which will be discussed further in Chapter 3.

Table 1. Averaging Smoothing Results

	θ_{mean}		L_{total}	
Roberts	0	0	479	479
	90	90	480	480
Sobel	0	0	479	479
	90	90	478	478
Canny	0	0	477	477
	90	90	472	472

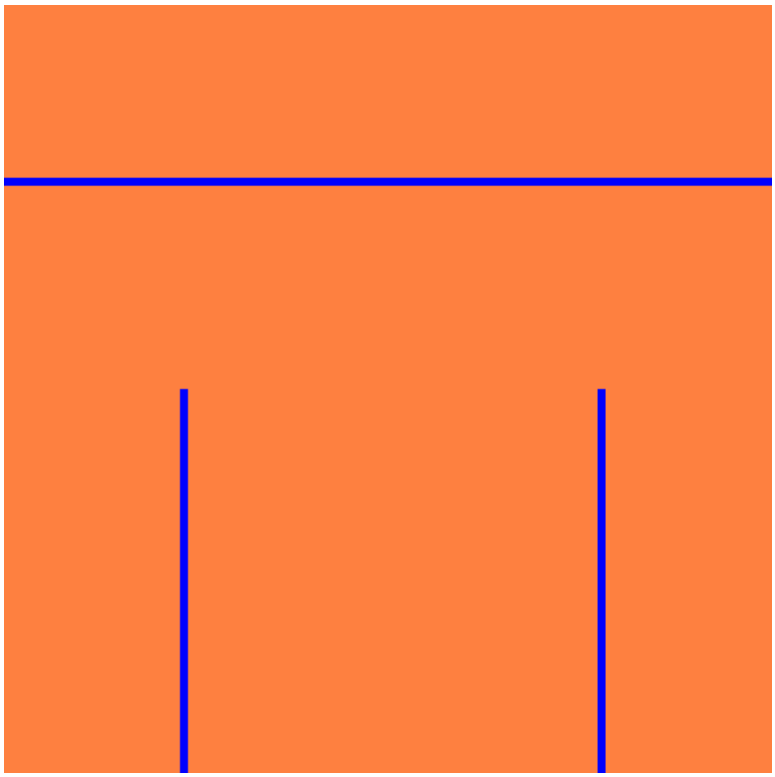


Figure 1. Fiber Image 0013-2-1a

CHAPTER 3
METHODS AND ANALYSIS

In this analysis, 21 images were processed. Twelve of these images, denoted "0013-2-#a" images taken of carbon fibers produced at UTSI. The remaining nine images, also an unwoven mat, is a typical dryer sheet.

In order to obtain statistically significant results, a Student-t distribution with 99% confidence is used. This distribution serves as a good approximation to the Gaussian distribution, especially as $n \to \infty$. The relation ship between sample mean (x) of a Student-t distribution, the t-value, and mean (μ) is given in Equation 17. The value t in Equation 18 is found in any statistical look-up table; a t-value exists for any combination of sample size n and confidence interval α. For a sample size of $n = 21$, and $\alpha = 0.01$ (99% confidence) the t-value is $t_{0.01} = 2.518$. If n, x, s, and t are known, μ can be easily found through algebraic manipulation.

$$t = \frac{x - \mu}{s / \sqrt{n}} \quad \textbf{(17)}$$

Because of the discrete nature of the 8-bit noise images, each of the 21 samples had 256 bins to populate the study. These distributions were then used to create a "composite" noise images for each method, making meaningful comparisons possible. The methodologies for each analysis are described here in Chapter 3, with some figures to help illustrate. For more detailed results, refer to Chapter 4 and the Appendix.

3.1 Preprocessing / Smoothing

Four preprocessing techniques were used in developing this method: averaging, median, Gaussian, and Laplacian of Gaussian. The criteria for evaluation of these techniques are a qualitative and quantitative analysis of noise histograms and processing speed. Metrics relevant to the histogram analysis include: maximum, median, mean grayscale value; standard deviation of grayscale value, and percentage of gray pixels.

The evaluation schemes for averaging and median smoothing were similar, with n x n smoothing kernels ranging from $n = 3$ to $n = 11$. Gaussian and Laplacian of Gaussian (LoG) kernels were fixed to a 5 x 5 square, with standard deviations ranging from 0.25 to 6.25 at intervals of 0.25 (a total of 25 iterations).The examples provided in this section are results from the smoothing techniques applied to image 0013-2-1a (Figure 2).

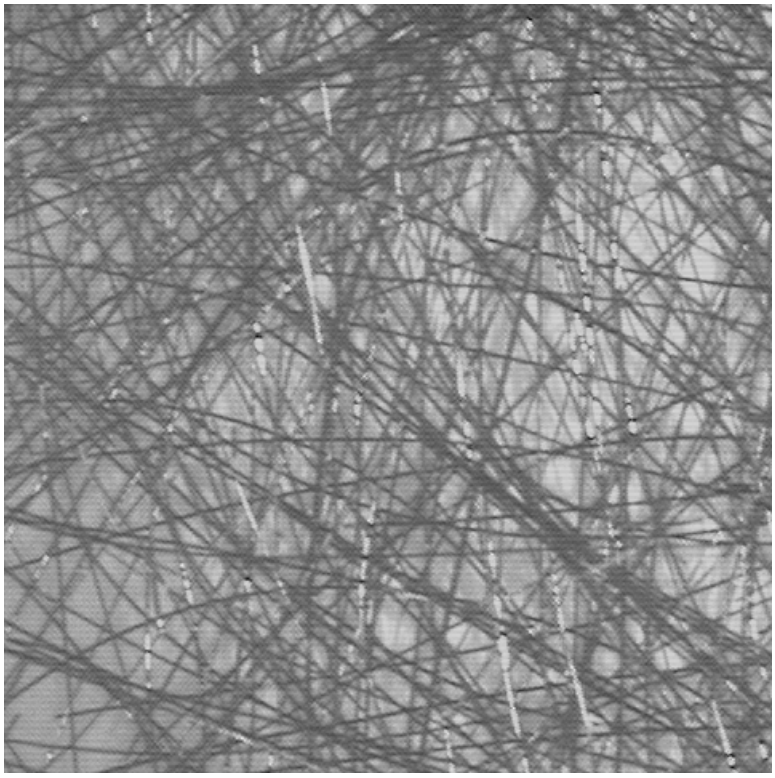


Figure 2. Fiber Image 0013-2-1a

3.1.1 Average Smoothing

As was explained in Chapter 2, the averaging technique replaces the value of a pixel with the average intensity value in the surrounding specified area. Therefore the controlling factor in averaging smoothing is the size of the area. For the purposes of this analysis, only square *n* x *n* kernels were considered.

Once the kernel is convolved with initial image, a smoothed image is produced (Figure 3). The noise in the original image can then be determined by subtracting the new image from the original (Figure 4).

Histograms can then be constructed based on the intensity values (ranging from 0 to 255) from the noise image. As the size of the averaging kernel is increased from 3 to 11, it becomes apparent that the larger kernel size increases effectiveness. More figures of typical results are shown in Chapter 4.

The recorded 0 value, which corresponds to pure black in the noise image is omitted for clarity from the histograms. Generally, the number of black pixels is multiple orders of magnitude greater than the next highest value. This is largely due to the nature of the images in this study; depth-of-field, lighting, and focus of the camera are all possible variables that effect the quality of a digital image.

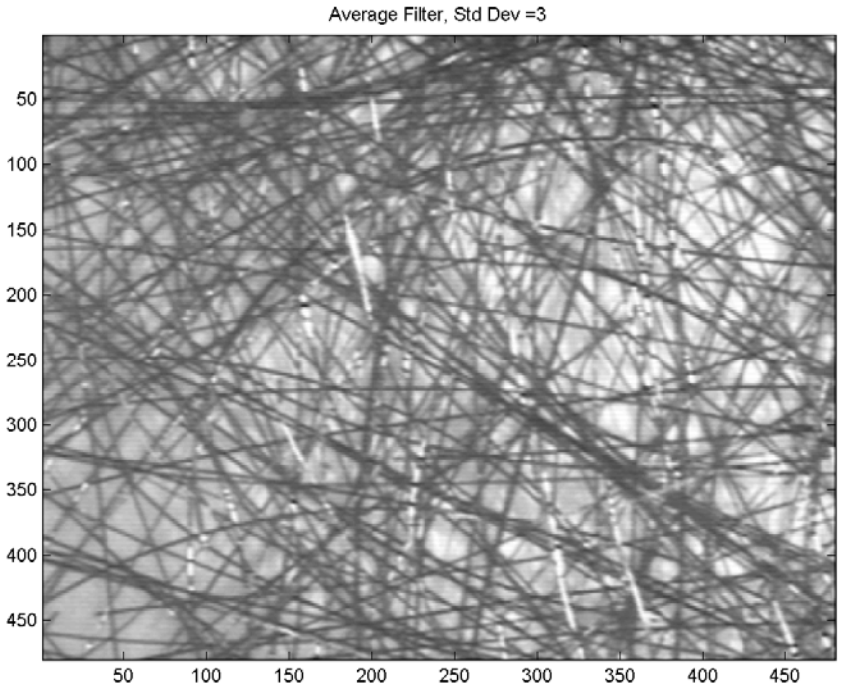


Figure 3. Average Smoothing, Image 0013-2-1a, 3 x 3 kernel

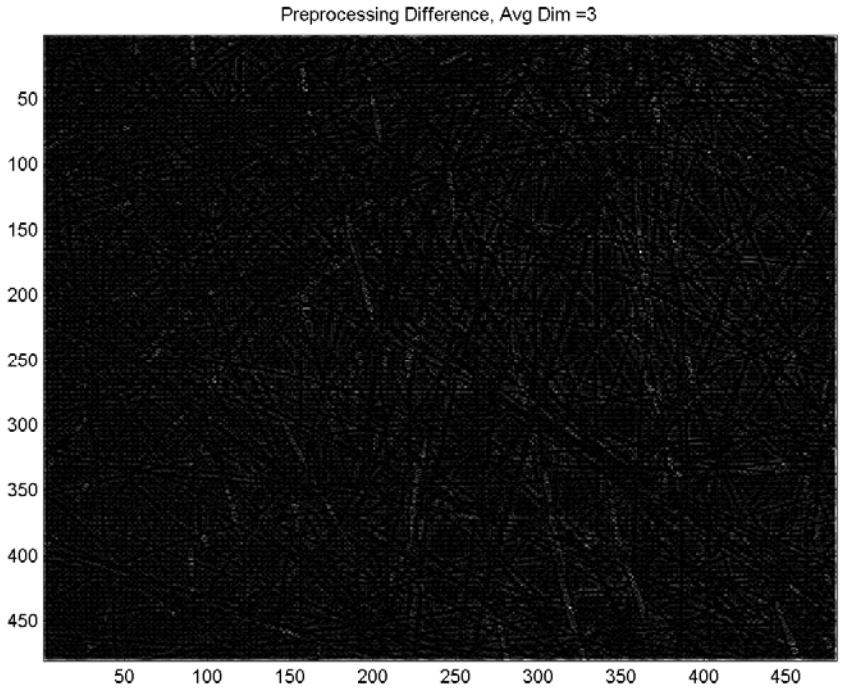


Figure 4. Noise from Original Image using Averaging Smoothing

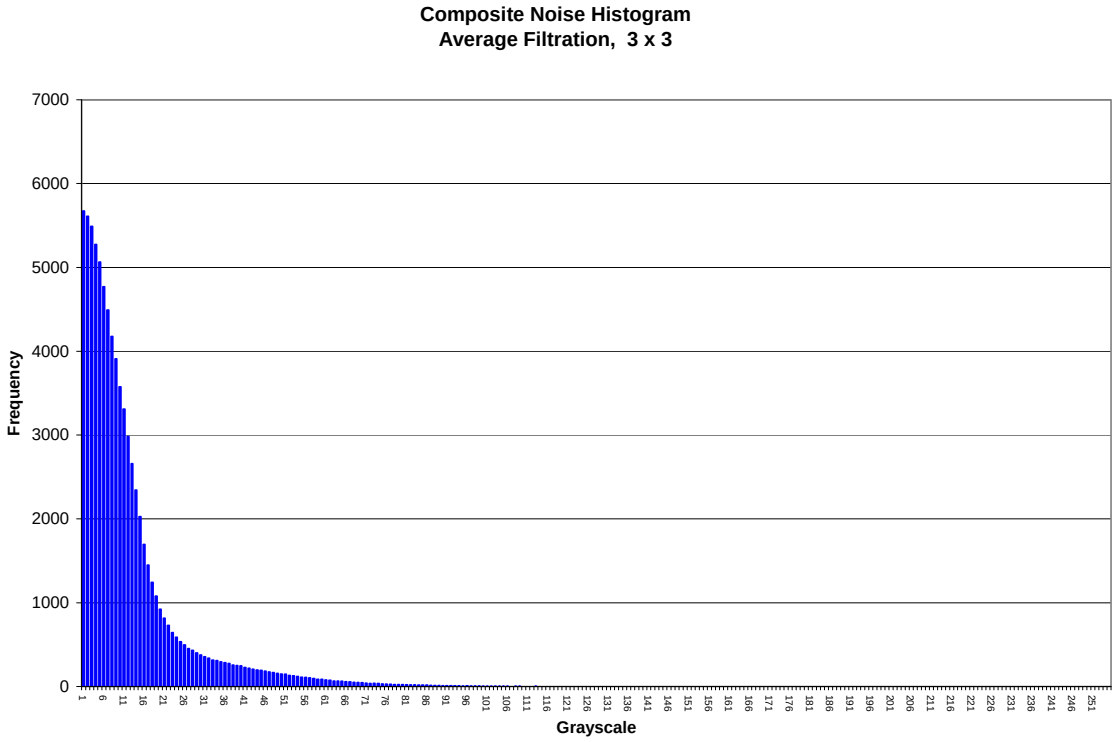


Figure 5. Averaging Noise Histogram, 3 x 3 kernel

3.1.2 Median Smoothing

Median smoothing in Matlab™ uses a different function than the other methods described in this paper, medfilt2. In this instance, the original image and dimensions kernel. For the purposes in this paper, only square kernels were used. Another distinguishing characteristic of this method is that it is not a convolution operation. For this analysis, median kernels ranged from 3 x 3 to 11 x 11.

The noise isolated from the original image is shown below (Figure 6), and is obtained via the same subtraction method in the above section. Histograms are generated again (see Chapter 4), to illustrate and quantify the effectiveness of the different kernel sizes.

3.1.3 Gaussian Smoothing

As described in Chapter 2, Gaussian smoothing convolves a *n* x *n* kernel with the original image to attenuate noise. For this analysis, each kernel was a square 5 x 5, with standard deviations ranging from 0.25 to 6.25.

As the standard deviation of the distribution increases, the smoothing effect can become very noticeable in the resultant images. This can often result in a general dimming of the image, as the lower-intensities of the carbon fibers in the foreground are blurred with the lighter background.

An analysis of the histograms generated from the Gaussian smoothing reveals that the effectiveness of increasing standard deviations is asymptotic A scatter plot of Non-zero percentage vs. standard deviation was also generated to illustrate this (Figure3.1.3.1); this percentage approaches 47.6% non-zero pixels.

3.1.4 LoG Smoothing

For the purpose of this investigation, Laplacian of Gaussian (LoG) smoothing utilizes a 5 x 5 convolution kernel with standard deviations ranging from 0.25 to 6.25 (the same parameters as Gaussian smoothing described above). The difference lies in the algorithms that determine the kernels, as shown in Chapter 2.

LoG smoothing appears to converge even more rapidly and noticeably than Gaussian smoothing, as seen in the noise image shown below (Figure 7). At $\sigma = 4.00$, only 3 "specs" of noise have been isolated from the original image. For $\sigma > 4.00$, there is no difference between the original and resultant images.

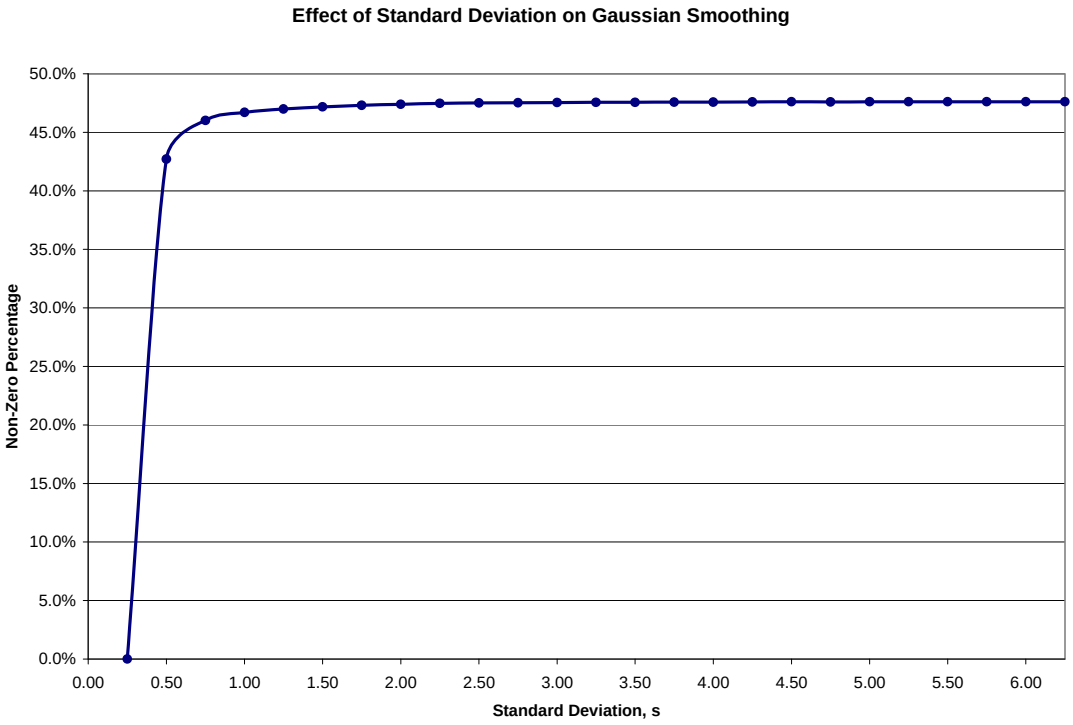


Figure 6. Effect of standard deviation on Gaussian Smoothing

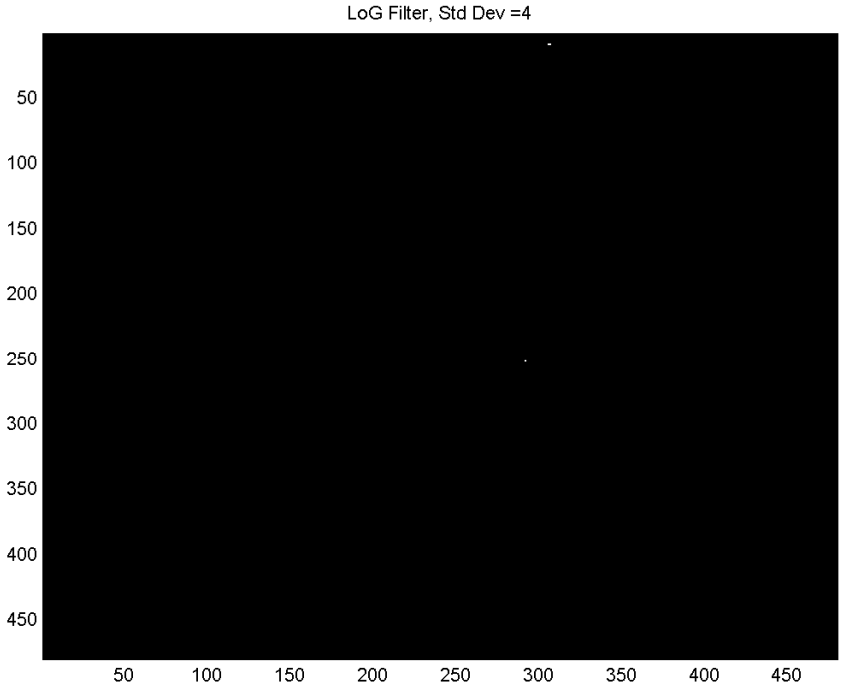


Figure 7. Noise from 0013-2-1a, LoG Smoothing, $\sigma = 4$

Another notable difference seen in LoG smoothing when compared to the other methods used in this analysis is the distribution of the histogram data. Averaging, Median, and Gaussian smoothing all appear to be variants of the positive half of a normal distribution, with the mean centered on zero. The distribution of the LoG data, however, appears to be a normal distribution, and in fact converges to the distribution of the original image. In fact, for $\sigma > 0.25$, this trend is already evident. For this reason, and the observation stated above, it is determined that the Laplacian of Gaussian method is not well-suited for this application.

3.1.5 Comparison and Method Selection

An evaluation matrix was constructed to compare the three smoothing methods remaining in this report. Using the metrics listed previously, as well as qualitative analysis, one method was to be chosen to move forward to the edge-detection phase of the analysis. The relative best of each of the three methods was selected to be compared against the other two options. Table 2 and Table 3 demonstrate the in-method variations of Averaging and Median methods.

Results from the averaging method are largely unaffected by kernel size, as seen by the minimal data spread of Gray %. Other properties show similar lack of response, as seen above. The 5 x 5 kernel was selected from this set because of its size; this kernel is large enough to significantly reduce noise while causing minimal image distortion and has a non-zero median.

Here, and in the data presented for Median and Gaussian smoothing, the parameter s represents the sample standard deviation of the frequencies in each composite histogram

Table 2. Averaging Smoothing Results

dim	μ	Max	Median	s	Gray	Time
3	766	115694	0	7282	40.97%	0.002507
5	799	114491	1	7195	44.02%	0.007142
7	799	113895	2	7145	44.29%	0.010876
9	791	113405	5	7107	43.97%	0.014867
11	786	112871	8	7069	43.92%	0.020940

Table 3. Median Smoothing Results

dim	□	Max	Median	s	Gray	Time
3	783	133492	0	8370	33.41%	0.056312
5	803	122374	1	7681	40.50%	0.158446
7	808	118723	2	7450	42.58%	0.057735
9	804	117296	5	7355	42.98%	0.063448
11	801	116254	7	7286	43.32%	0.073159

data set. This data set also includes the frequencies for 0-bin grayscale values, which are typically 2 orders of magnitude larger than the next largest frequency. That fact significantly increases the size of the standard deviation. This was done prior to the exclusion of the LoG method, which as seen above had minimal 0-bin frequencies.

The median smoothing method is more responsive to smaller kernel size than averaging, but appears to level off at the 7x7 size. This method out-performs the other two methods in non-zero median values, which implies that more values closer to white are being eliminated from the image. While the 7x7 kernel has a slightly higher μ value, the other parameters are in the middle of their respective ranges.

Due to the sample size of the Gaussian method, a more rigorous statistical analysis is used to select an appropriate candidate. Cutting off the data below $\sigma = 1.25$, as shown in the previous section regarding the asymptotic nature of the method, leaves a sample size of $n = 21$. The full data set is shown in Table 4. With a confidence level of 99%, the same t-value is used to knock down the average Gray % to 41.24%. The σ value with the closest corresponding value is 2.75.

Table 4. Gaussian Smoothing Results

σ_{input}	μ	Max	Median	s	Gray	Time
0.25	900	230400	0	14400	0.00%	0.006278
0.50	763	124222	0	7882	36.44%	0.007976
0.75	769	120941	0	7614	38.61%	0.007420
1.00	778	120322	0	7562	39.58%	0.007751
1.25	784	119937	0	7533	40.24%	0.008871
1.50	787	119642	0	7512	40.64%	0.008455
1.75	789	119485	0	7501	40.87%	0.007975
2.00	791	119376	0	7493	41.02%	0.008763
2.25	792	119297	0	7488	41.13%	0.008658
2.50	792	119243	0	7484	41.20%	0.007809
2.75	793	119199	0	7481	41.25%	0.007745
3.00	793	119164	0	7478	41.29%	0.007974
3.25	793	119145	0	7477	41.32%	0.007797
3.50	793	119115	0	7475	41.35%	0.008119
3.75	794	119094	0	7474	41.37%	0.008322
4.00	794	119084	0	7473	41.39%	0.008409
4.25	794	119070	0	7472	41.40%	0.008277
4.50	794	119058	0	7471	41.41%	0.009250
4.75	794	119051	0	7471	41.42%	0.008535
5.00	794	119039	0	7470	41.43%	0.008972
5.25	794	119037	0	7470	41.44%	0.008336
5.50	794	119032	0	7469	41.44%	0.008394
5.75	794	119033	0	7469	41.45%	0.008511
6.00	794	119028	0	7469	41.45%	0.008160
6.25	794	119025	0	7469	41.46%	0.008449

Table 5. Smoothing Method Evaluation

Method	Parameter	μ	Max	Median	s	Gray	Time
Averaging	5	799	114491	1	7195	44.02%	0.007142
Median	7	808	118723	2	7450	42.58%	0.057735
Gaussian	2.75	793	119199	0	7481	41.25%	0.007745

As stated before, the desired smoothing method should reduce a large amount of noise from the image while minimizing distortion of the original image. Indications of positive noise reduction are: small μ, non-zero m, low maximum, and relatively large s. Distortion is minimized by using a kernel with the lowest impact (for Averaging and Median methods, this equates to small kernel size; for Gaussian and LoG, this means smaller σ).

As seen in Table 5, the selected Averaging, Median, and Gaussian smoothing methods are reasonably comparable. The deciding factor then becomes the lowest maximum value, which is provided by the Averaging method. The relative difference in standard deviations of the methods ranges no more than 5%, and processing times are comparable. This technique is the method used for the rest of this investigation.

3.2 Edge Detection

Following image smoothing, three methods for edge detection were examined: Roberts, Sobel, and Canny. Each method was evaluated according the following criteria: edges detected (percentage of image), 90° image rotation sensitivity, thresholding sensitivity, and processing time.

When preparing images for line-extraction, computations can be minimized by limiting the number of edges, as well as reducing error. Because all three methods return binary images as their final product, image histograms are less telling than those presented in the previous section. However, these histograms do demonstrate the overall percentage of edge pixels (white) in each processed image. If the fibers in the images are continuous and have no discernable porosity, it is reasonable to assume that the edges in a fiber-matt image should represent a small portion of the image. This, small portion, however, should not be so small as to nullify the number of edges.

Sensitivity to image orientation can also be a concern when detecting edges, especially when basic edge (two-direction) is used. More complicated methods that examine multiple directions are generally less sensitive. For this exercise each image was rotated clockwise 90°, processed via the specified edge detection, rotated back to the initial orientation and compared with the non-rotated edge image.

The effects of thresholding on edge detection techniques can have a significant impact on the final edge image. This is especially evident in the Canny method, because both a high and low threshold are used. It is assumed that the higher thresholds return only strong edges; however, this must be weighed along with the amount of edges returned.

3.2.1 Roberts Method

As stated in Chapter 2, the Roberts method uses two convolution kernels to locate potential edges by approximating horizontal and vertical derivatives. This method is the least complex of the three techniques examined, and has the shortest processing time. A positive response from either convolution process results in a detected edge, which allows this technique to identify both strong and weak edges. Both types of edges are returned as white (1) in the binary image (Figure 8).

The Roberts method was applied to each image; the threshold value was varied from 0.001 to 0.030. Understandably, as the threshold value was increased, the percentage of white pixels decreases. For the Roberts method, this decay is approximately 0.75% per 0.001 threshold value.

Another parameter of concern for this study is the sensitivity of the method to image orientation. Because this method only detects horizontal and vertical intensity gradients and has small kernel size, sensitivity to mat orientation should be explored. However, the statistical analysis of the data shows this error is on the scale of 0.003%.

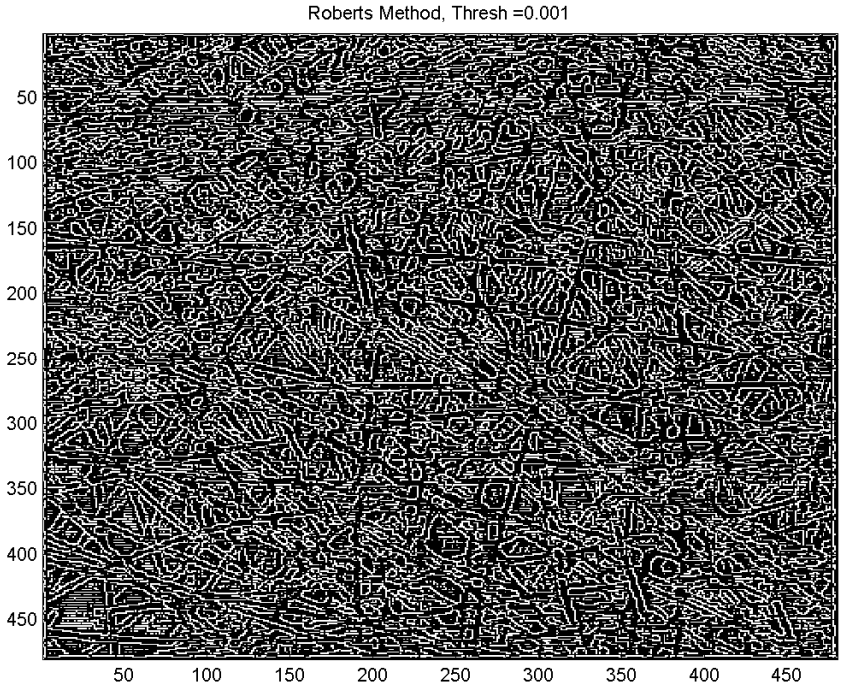


Figure 8. Image 0013-2-1a, Roberts Edge Detection, Threshold = 0.001

The final parameter evaluated in this study is processing time. The values are at least an order of magnitude greater than the smoothing operations, but still less than one second. As can be seen for the composite image, processing time for different threshold values remains somewhat constant near an average of 0.187 seconds.

3.2.2 Sobel Method

The second method studied is the Sobel Method. This method uses three weighted edge detection kernels, which are also 3 x 3 instead of 2 x 2. As expected, this increases the accuracy of the algorithm but may sacrifice processing time. For the same threshold value of 0.001, a slightly more sparse edge image is produced (Figure 9).

The Sobel Method was evaluated over the same range of thresholds as the Roberts Method, and consistently yields fewer edges for thresholds below 0.014 (See discussion in Section 3.2.4). Also, as expected, the same trend seen can be seen regarding the general decrease of edge pixels with the increase of threshold values.

The Sobel method also shows similar results to the Roberts method regarding image orientation; very little sensitivity can be seen by rotating the image 90°. The Sobel method has approximately 1/3 the sensitivity of Roberts to rotation (average error of 0.00149%).

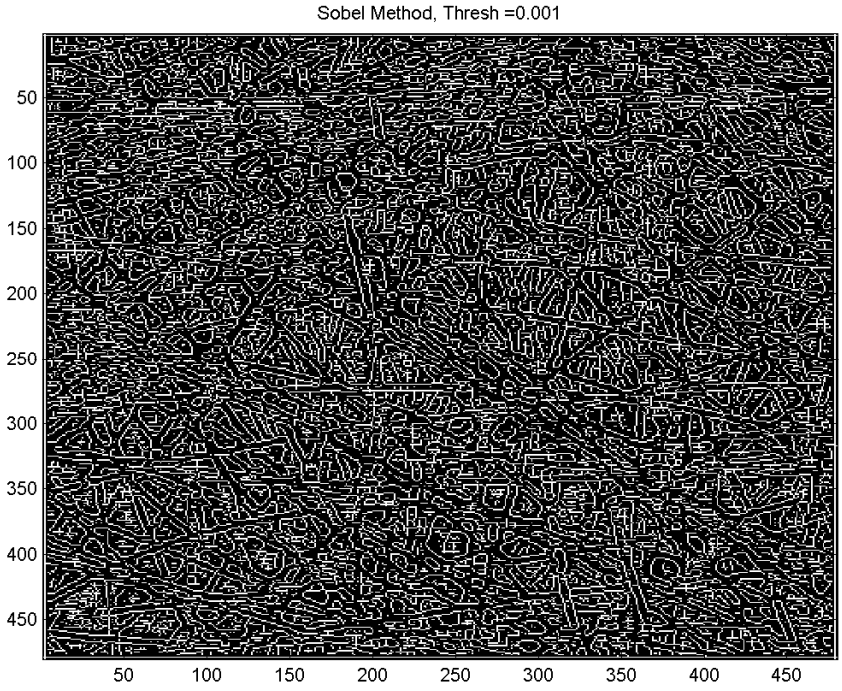


Figure 9. Image 0013-2-1a, Sobel Edge Detection, Threshold = 0.001

Processing times are on the order of 0.20 seconds. While comparable to Roberts, there is more variation over the range of threshold values. This will be discussed in greater detail in Section 3.2.4.

3.2.3 Canny Method

The Canny method is by far the most complicated of the three methods evaluated here. More convolution kernels, non-maxima suppression, and thresholding with hysteresis all equate to greater processing times. This increase in processing time is traded for an assumed increase in accuracy.

As was shown in Chapter 2 example involving a random 10 x 10 matrix of values, thresholding values can be much larger. In order to find meaningful variation in the process, a ranger of larger threshold values were needed.

Instead of ranging from 0.001 to 0.030, the Canny lower thresholds were varied from 0.010 to 0.300, with high thresholds equaling 2.5x the lower value (Matlab™ default). Note: this leaves only three points at which all three methods share a common threshold value over their ranges. For this range of threshold values, however, the Canny method consistently yields much smaller numbers of edge values (Figure 10).

While lower threshold values return edge counts of around 8%, as the thresholding values increase the number of edge pixels decrease to an almost insignificant amount.

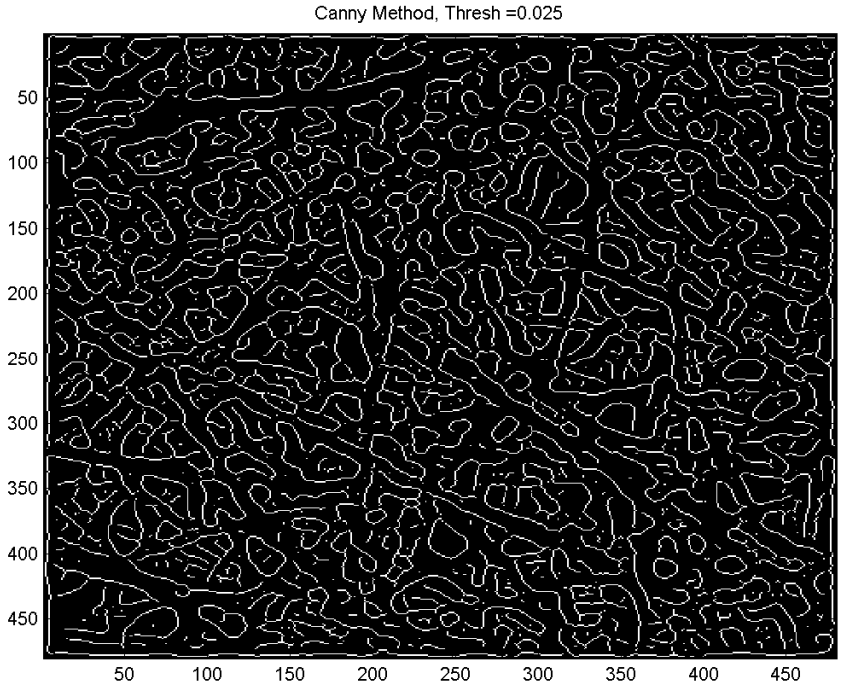


Figure 10. Image 0013-2-1a, Canny Edge Detection, Threshold = [0.010 0.025]

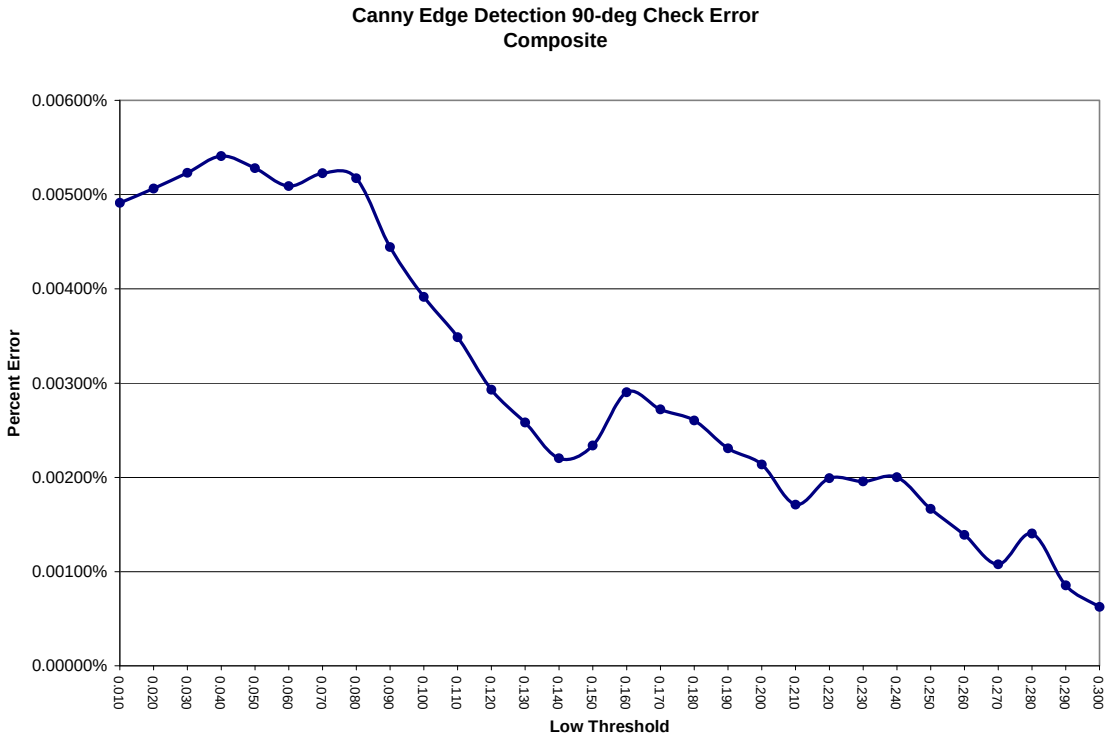


Figure 11. Composite 90° Rotation Sensitivity, Canny Method

The Canny method's sensitivity to image rotation was also explored. More variation was observed in the error values and greater values were observed, but the error greatly decreases as threshold value increases (Figure 11). This can be explained by the fact that as threshold values increase, especially for Canny, the number of edge pixels in the image decreases significantly.

Processing times for the Canny method were significantly larger than both the Roberts and Sobel methods, as was expected. Average processing time over all images and threshold values was ~0.92 seconds.

3.2.4 Comparison and Method Selection

As stated before, the three methods were evaluated based upon detection percentage, image rotation sensitivity, thesholding effects, and processing time. Of these criteria, the most paramount is detection percentage. Plots (Figure 12, Figure 13) of all three methods of detection percentage vs. threshold clearly show the Canny method to be far superior to both Roberts and Sobel in this application.

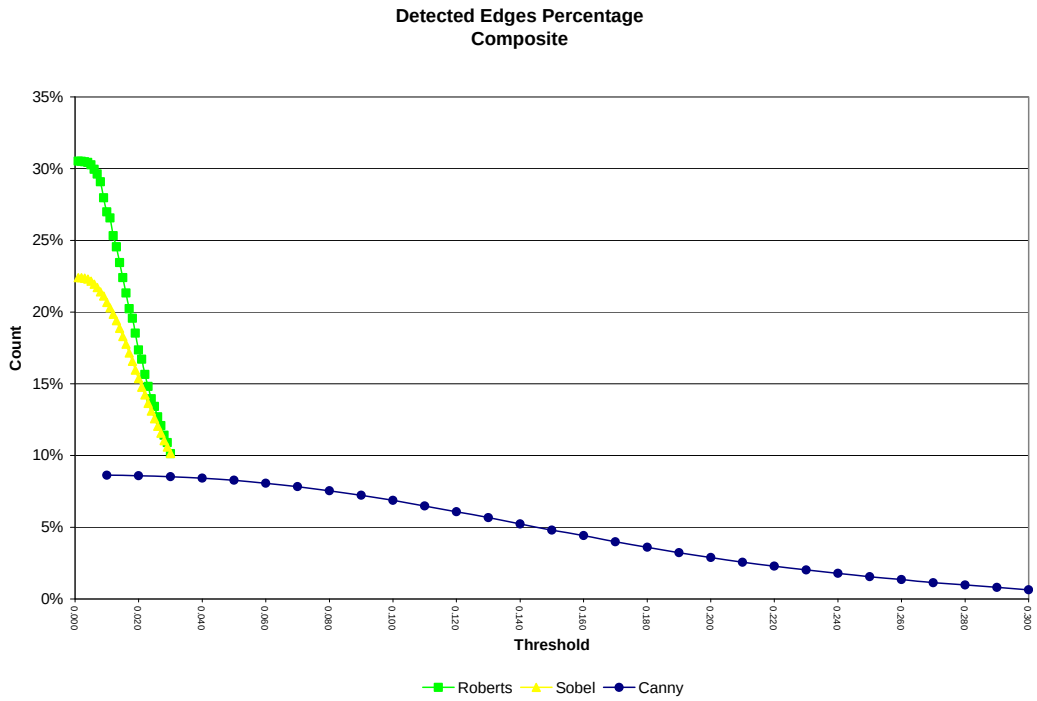


Figure 12. Composite Detection Percentages of Roberts, Sobel, and Canny

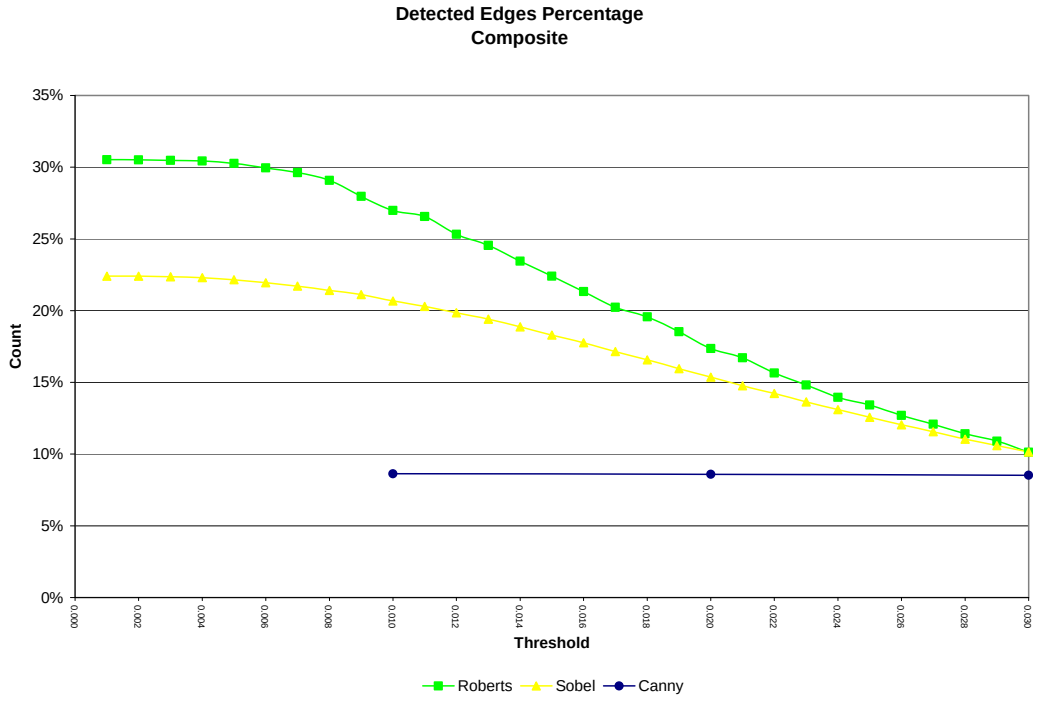


Figure 13. Composite Detection Percentages of Roberts, Sobel, and Canny (Zoom)

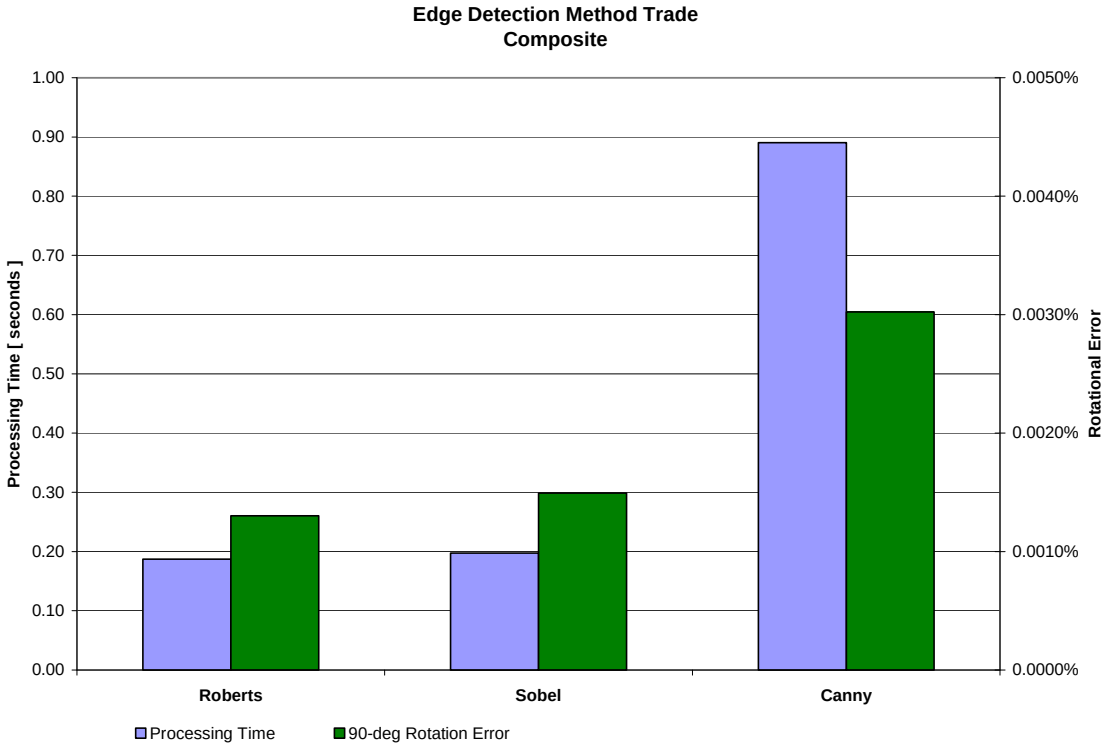


Figure 14. Processing Time, Rotational Error Study

While the ranges of thresholding values differ by an order of magnitude between both Roberts and Sobel and Canny, the overlap that does exist at 0.010, 0.020, and 0.030 shows the Canny method to be superior. This can be attributed to three major differences between Canny and the other two methods: larger number of kernels, local non-maxima suppression, and thresholding with hysteresis.

While the Canny method out-performs both Roberts and Sobel regarding edge-detection percentages, it is relatively weaker in both processing time and image orientation sensitivity (Figure 14). As expected, the Roberts method has the lowest processing time due to requiring the fewest (and smallest) kernels and therefore minimal operations needed. The Roberts method is also the least sensitive to image orientation/rotation. It should be noted, however, that the only secondary orientation that was checked was a 90° clockwise rotation; other orientations may exhibit different results.

Having seen the Canny method to outperform both Roberts and Sobel over a large range of thresholds, as well as the fact that processing times for Canny are less than 0.90 seconds and rotational error reaches a maximum of 0.00302%, it is determined that the Canny method is best suited for this exercise.

Working from the assumption that a "reasonably" low edge percentage is desirable, a relatively small lower threshold should be used. This would allow an equally small threshold, relatively maximizing the opportunity for strong edges to be detected. Having a reasonable point of comparison with Roberts and Sobel being desirable, 0.010 is selected as the threshold value for the next phase of this examination.

3.3 Line Detection via the Hough Transform

Due to the large number of parameters that could be varied for this analysis, certain assumptions were made to limit the scope. The *hough* function itself allows the user to define the resolution of both ρ and Θ; for the purposes of this study both parameters were set to their default value of 1.

The *houghpeaks* function lets the user define either the threshold value for the peaks determined or a specified count of peaks regardless of value; the suppression neighborhood surrounding a peak can also be pre-determined. For this exercise, the number of peaks was varied from 10 to 100 at intervals of 10. This was done to help ensure that no grid space returned a null value and also helps account for lower intensities in different regions. The suppression neighborhood was set to 9; the default value is the lowest odd number closest to the size of H/50.

In *houghlines*, gap spacing between two line co-linear line segments can be specified as well as the minimum length of merged lines. Default values, which were used, for each are 20 and 40 pixels respectively.

With these assumptions made, each detected image was sectioned off into grids of size 1x1, 2x2, 4x4, 5x5, 6x6, 8x8, and 10x10. The Hough Transform was then applied in each individual grid. The output returned from the *houghlines* function is an array of line endpoints. With endpoints known both length and angle can be determined.

Sensitivity to the number of peaks is one of the foremost concerns in this exercise; however, if the alignment of the fibers in the image is already homogeneous one would not expect a large amount of variation in the data. Because of this, relying purely upon angle measurements to validate the process is insufficient. Another parameter, total line length must also be considered.

The result from the twenty-one smoothed, edge-detected images are shown in Table 6. As expected, the angle measurements show little variation throughout the study. The total length measurement L, however, shows a good approximation to exponential growth (especially for lower grid sizes).

Table 6. Line Detection Results

	Composite Image			
		θ	L	t
	Peaks	[deg]	[dmls]	[sec]
Grid = 1 x 1	10	61.175	66.298	0.385
	20	60.384	77.161	0.414
	30	63.567	63.991	0.433
	40	63.259	70.85	0.457
	50	63.208	68.953	0.482
	60	62.452	64.574	0.509
	70	61.176	63.145	0.529
	80	62.032	73.386	0.557
	90	63.469	91.475	0.57
	100	61.884	64.095	0.596
Grid = 2 x 2	10	61.581	267.99	0.522
	20	62.312	280.367	0.605
	30	63.84	268.302	0.667
	40	62.947	270.434	0.733
	50	63.291	253.125	0.779
	60	62.338	251.076	0.842
	70	60.635	277.344	0.882
	80	62.123	276.384	0.93
	90	63.896	283.62	0.964
	100	62.04	271.861	1.007
Grid = 4 x 4	10	60.951	907.189	1.205
	20	63.845	908.53	1.686
	30	64.417	952.127	2.071
	40	63.719	917.642	2.453
	50	65.102	929.764	2.744
	60	64.361	905.946	3.008
	70	62.338	943.576	3.195
	80	64.073	936.335	3.4
	90	66.006	947.381	3.505
	100	64.233	948.054	3.625
Grid = 5 x 5	10	61.82	1486.382	1.626
	20	62.781	1475.2	2.349
	30	64.238	1480.068	2.949
	40	63.694	1463.912	3.395
	50	64.398	1474.164	3.794
	60	63.586	1481.79	4.09
	70	63.46	1488.902	4.398

Table 6 (Continued). Line Detection Results

	80	65.376	1495.52	4.605
	90	65.277	1464.6	4.774
	100	64.666	1489.457	4.92
Grid = 6 x 6	10	62.497	2065.877	2.137
	20	63.04	2087.23	3.165
	30	64.506	2029.554	3.942
	40	63.99	2047.4	4.506
	50	63.935	2012.006	5.04
	60	63.04	2087.23	3.165
	70	63.02	1944.85	5.672
	80	64.546	1999.376	5.876
	90	63.69	1975.075	6.053
	100	63.658	1994.011	6.221
Grid = 8 x 8	10	60.99	3662.018	3.358
	20	62.469	3707.517	5.004
	30	62.792	3677.57	6.18
	40	63.137	3645.218	6.998
	50	63.783	3626.588	7.63
	60	62.556	3619.469	8.113
	70	62.276	3549.684	8.34
	80	64.094	3556.084	8.471
	90	62.985	3549.061	8.62
	100	63.602	3502.29	8.686
Grid = 10 x 10	10	61.213	5777.99	4.827
	20	62.228	5736.679	7.18
	30	63.138	5713.062	8.738
	40	62.234	5666.717	9.784
	50	63.066	5549.078	10.37
	60	61.944	5611.403	10.659
	70	61.682	5565.343	10.802
	80	63.94	5511.326	10.942
	90	63.391	5518.343	10.876
	100	64.102	5493.264	10.861

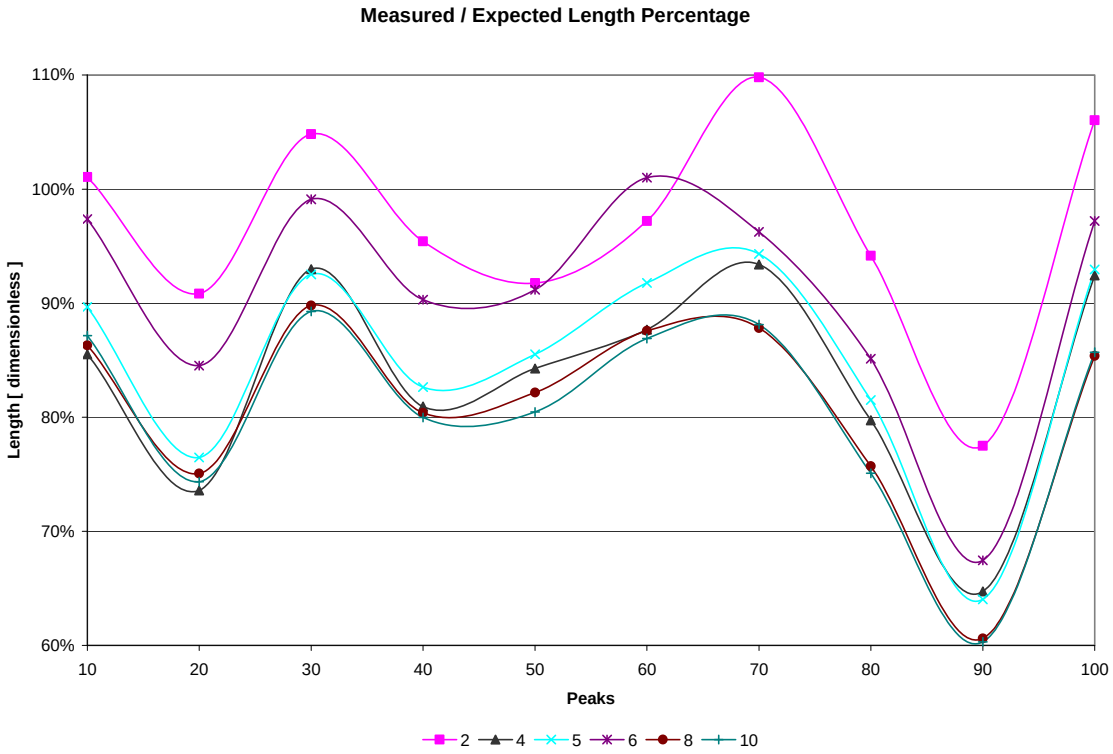


Figure 15. Percentage of Measured / Expected Length

A comparison of expected length values to measured values can easily be compiled using the power law. Figure 15 shows the measured / expected length percentage over the range of peaks.

For all grid sizes, the measured lengths are reasonably close to the expected values for that grid size. The drop in percentage at 90 peaks appears to be either anomalous or a phenomena that disproves the assumption of even distribution of lines.

Given the results in Table 6 and the observations made from Figure 15, it is determined that the number of peaks over this range has little effect on the results. Noting that the measured length values do increase at nearly the exponential rate expected from the assumption of even line distribution, it is a reasonable conclusion that most of the lines detected are of roughly equal length. This means that the range of peak values is somewhat small. More investigation is needed to truly quantify this.

CHAPTER 4
TYPICAL RESULTS

This section contains a sampling of typical results, all from analysis of image 0013-2-1a. Data presented, in both figure and tabular forms follow the typical analytical progression for this investigation: image smoothing, edge detection, and line detection. All methods are shown. More extensive examples of raw data are presented in the Appendix.

Note: the term "frequency," seen in histogram figures refers to the total count of occurrences in a data set; "frequency" and "count" are often used interchangeably in histogram analyses.

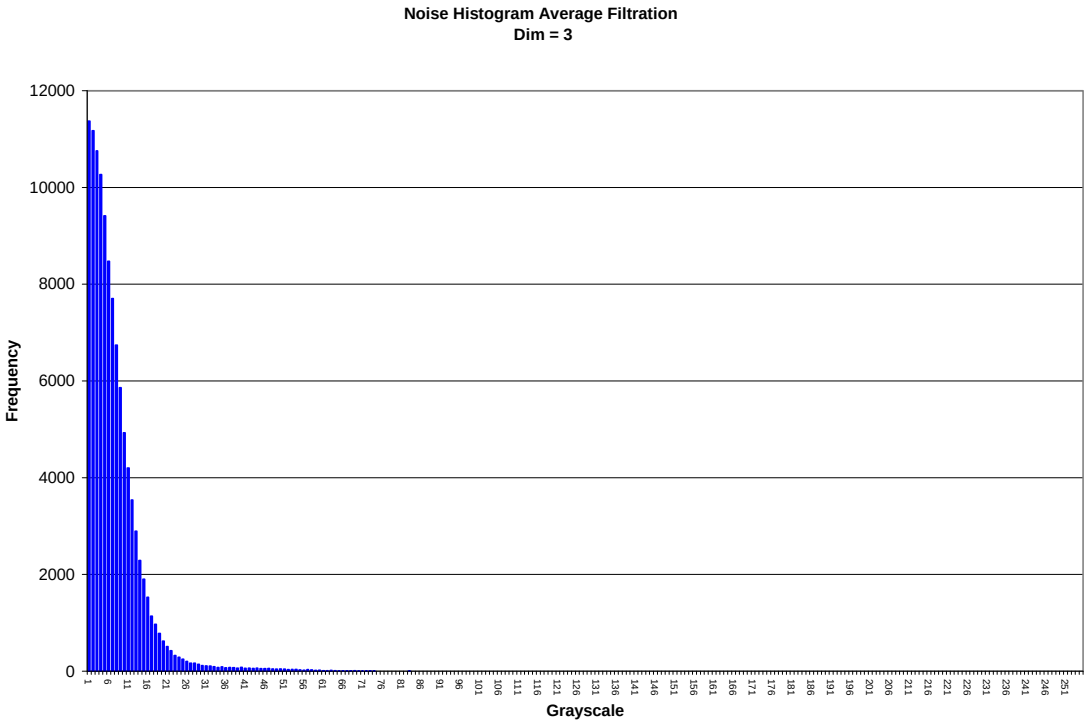


Figure 16. Averaging Smoothing, 3 x 3 kernel

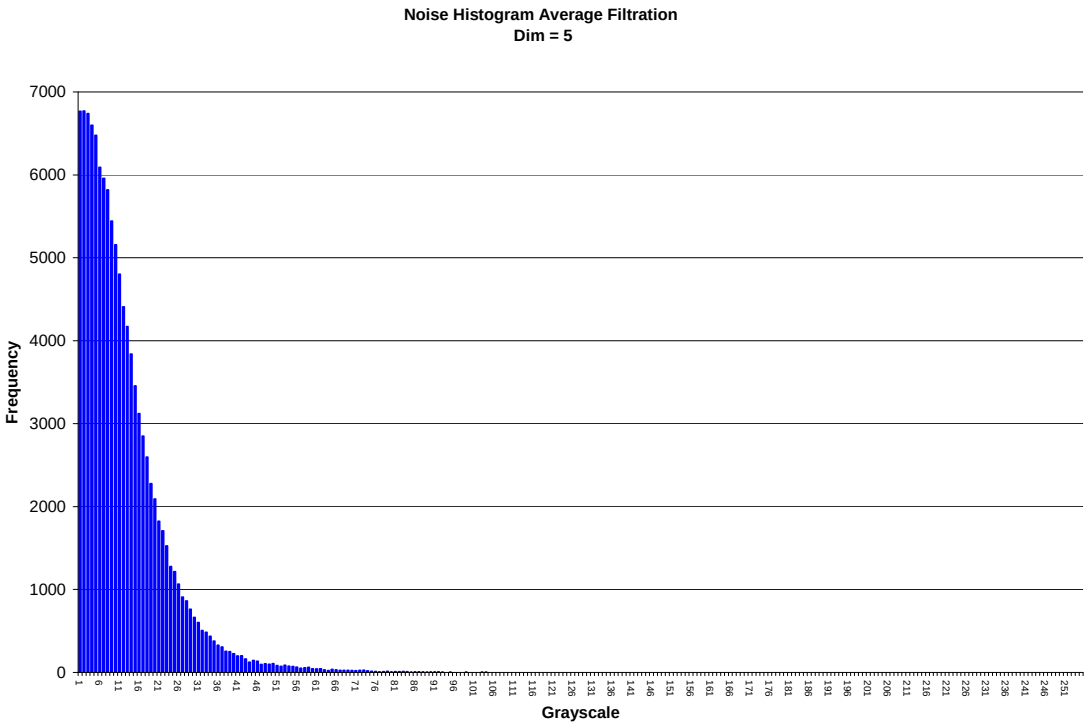


Figure 17. Averaging Smoothing, 5 x 5 kernel

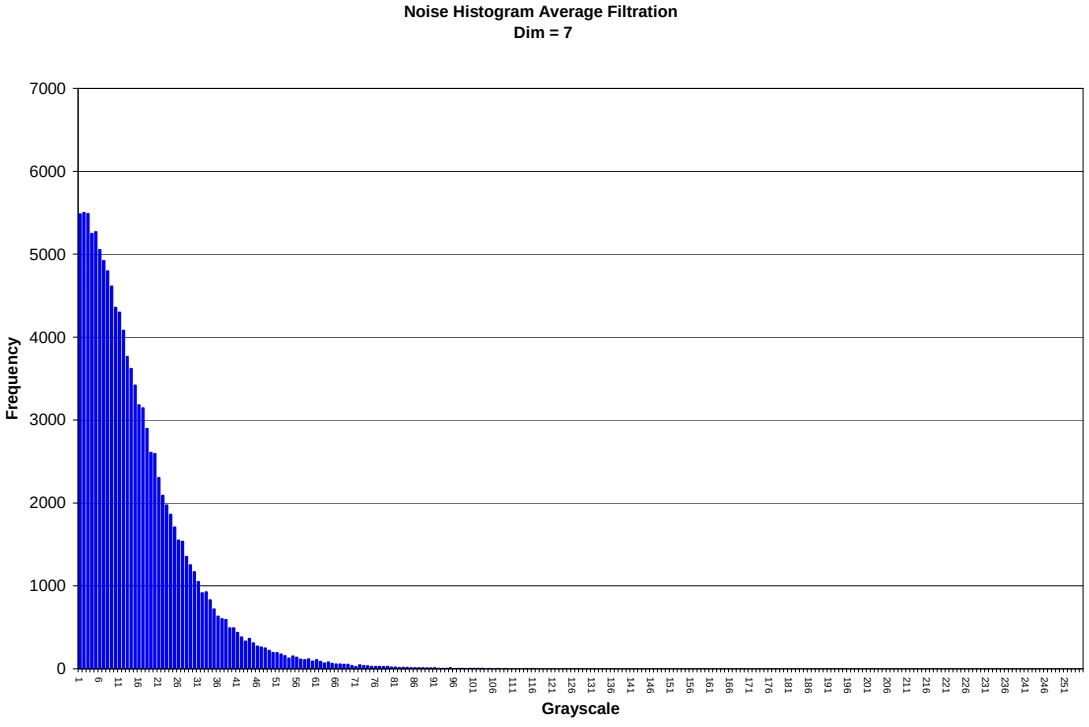


Figure 18. Averaging Smoothing, 7 x 7 kernel

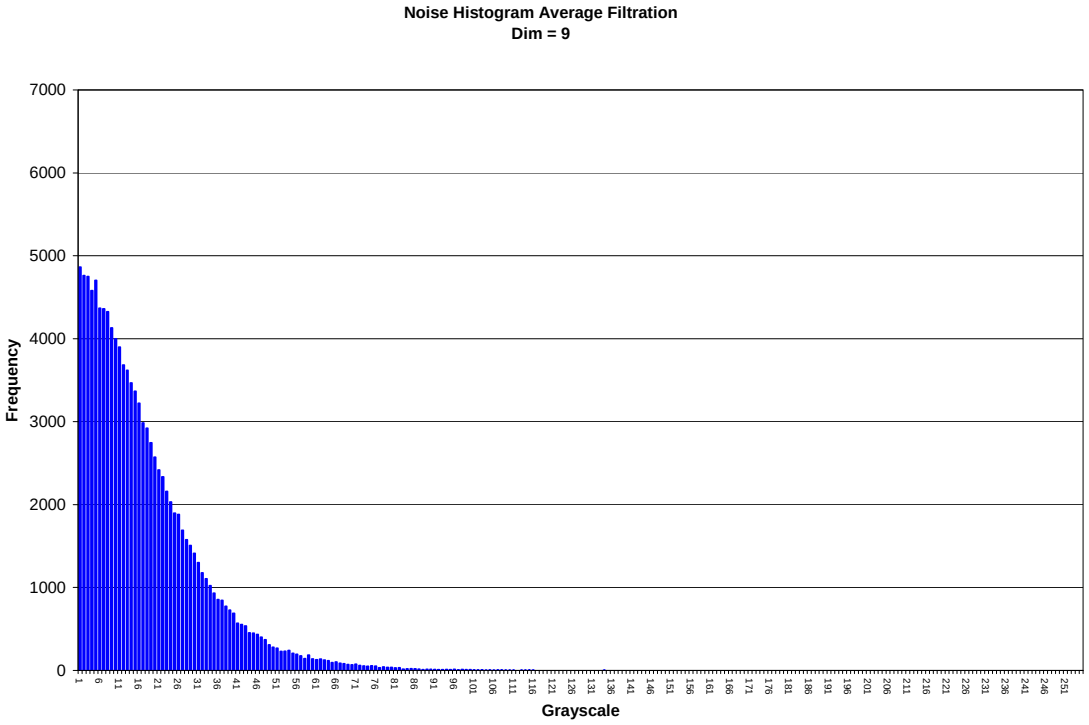


Figure 19. Averaging Smoothing, 9 x 9 kernel

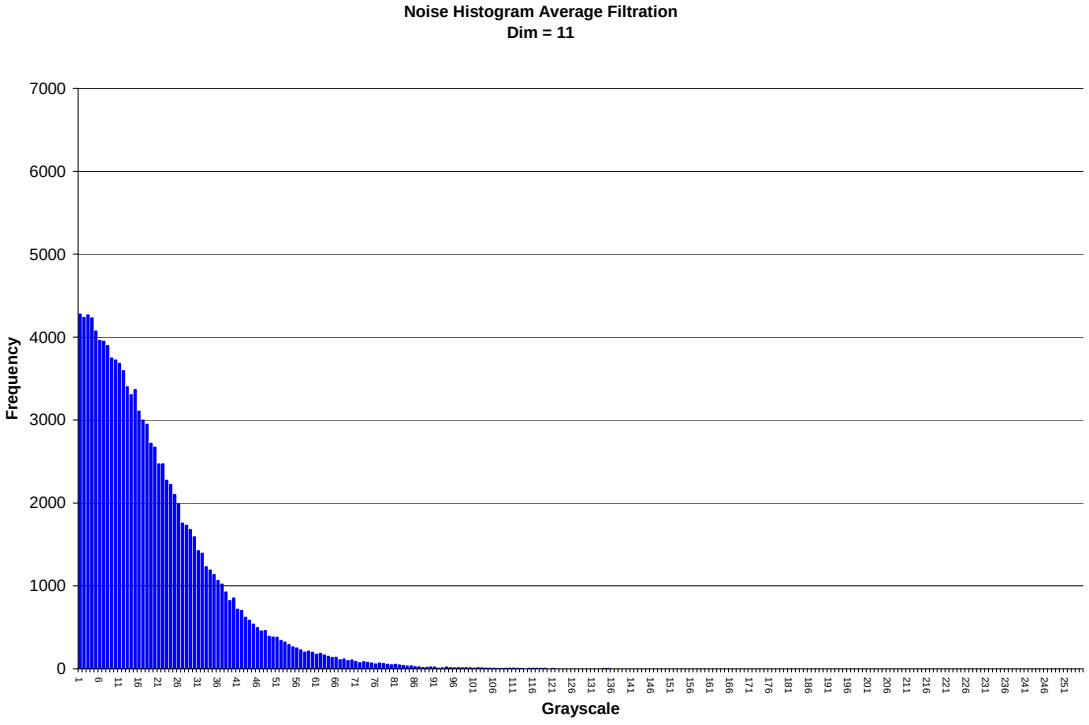


Figure 20. Averaging Smoothing, 11 x 11 kernel

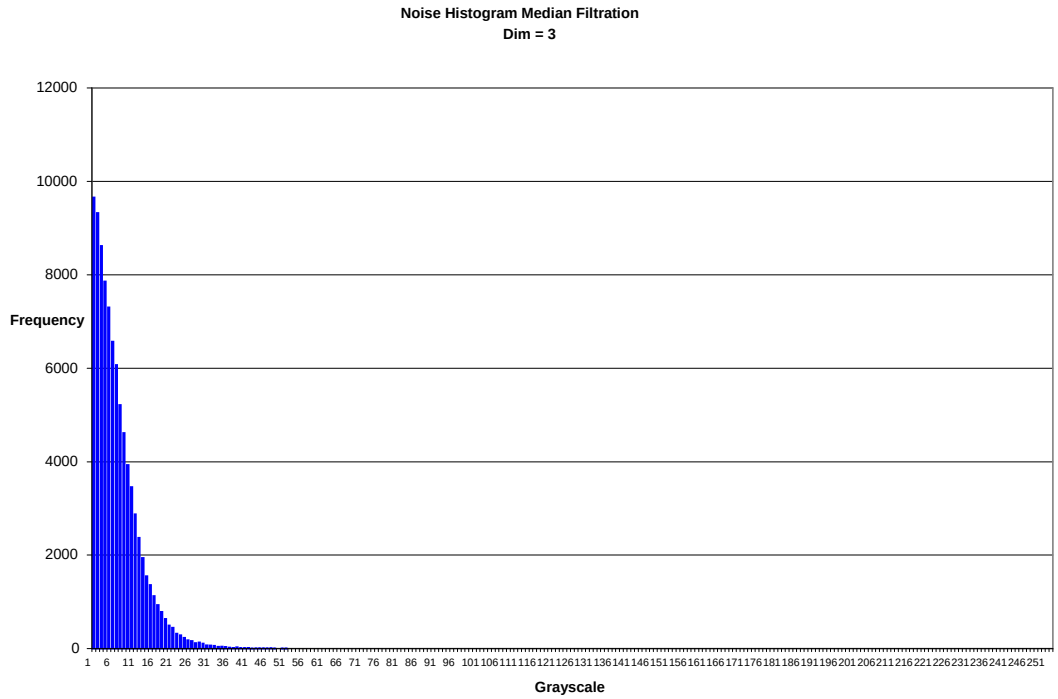


Figure 21. Median Smoothing, 3 x 3 kernel

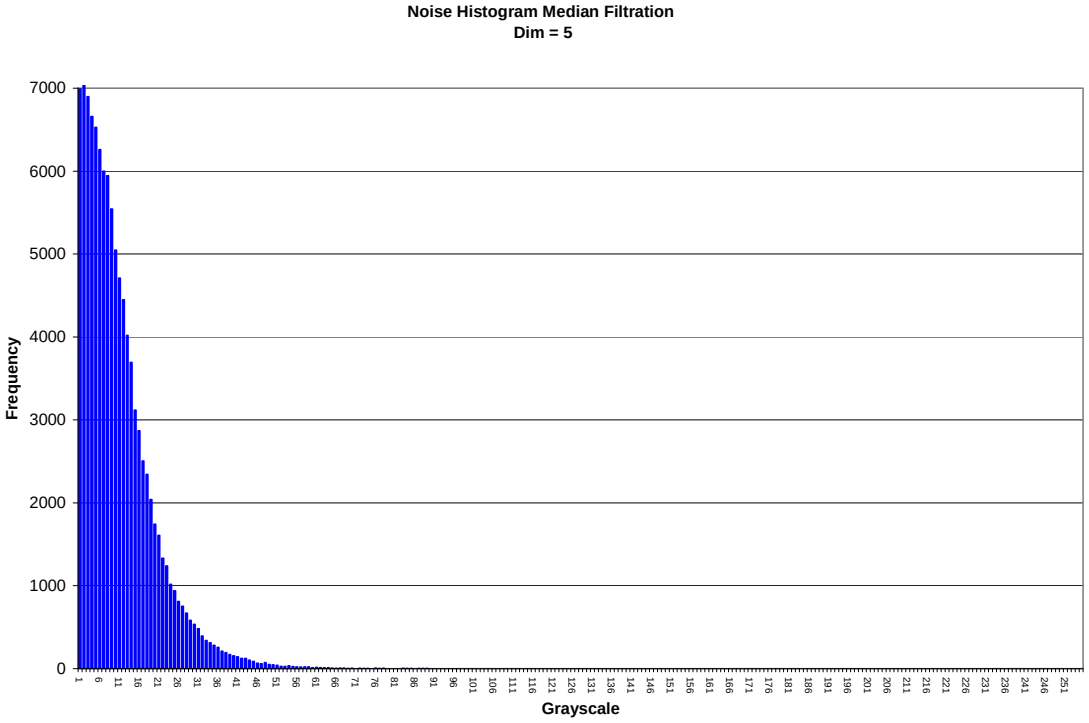


Figure 22. Median Smoothing, 5 x 5 kernel

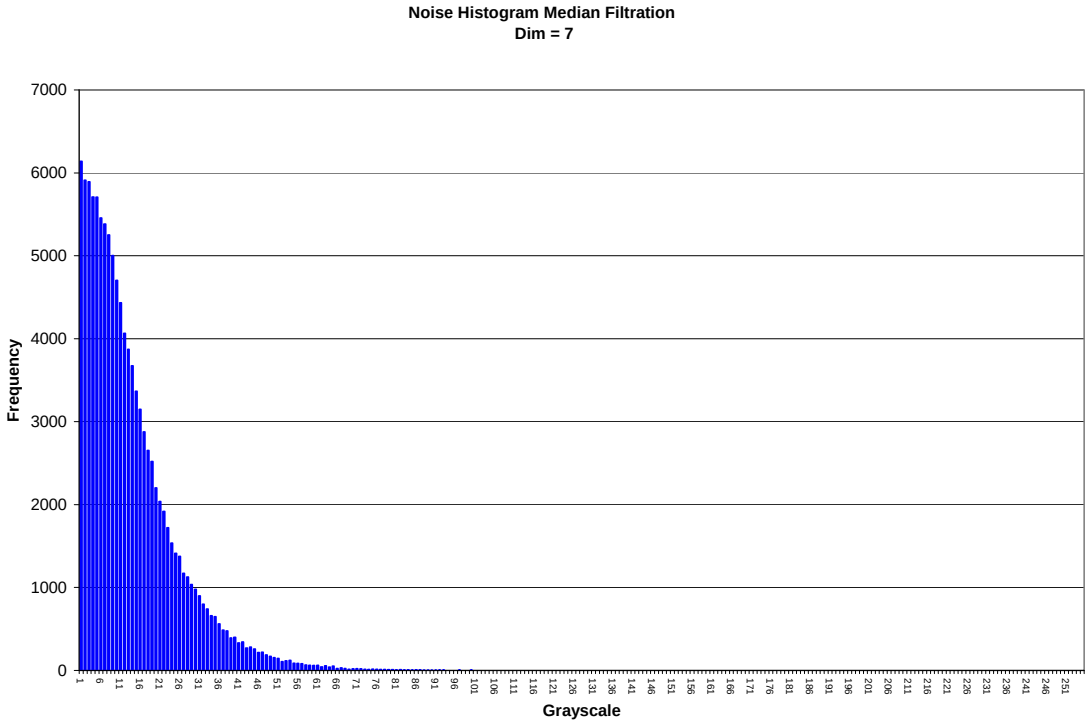


Figure 23. Median Smoothing, 7 x 7 kernel

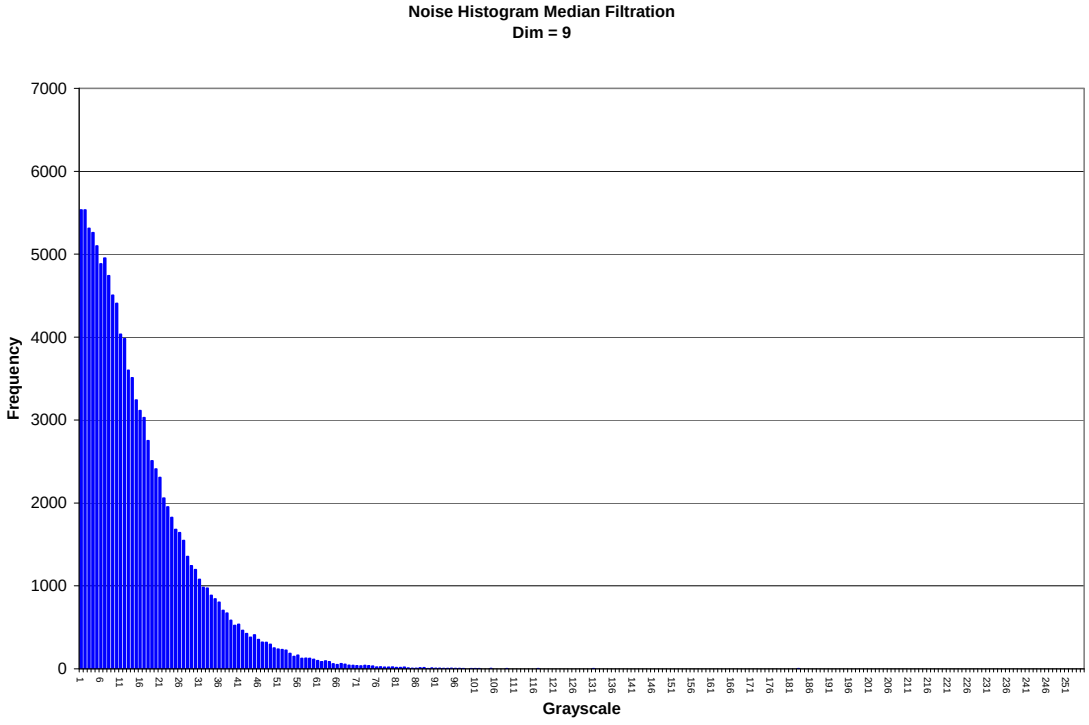


Figure 24. Median Smoothing, 9 x 9 kernel

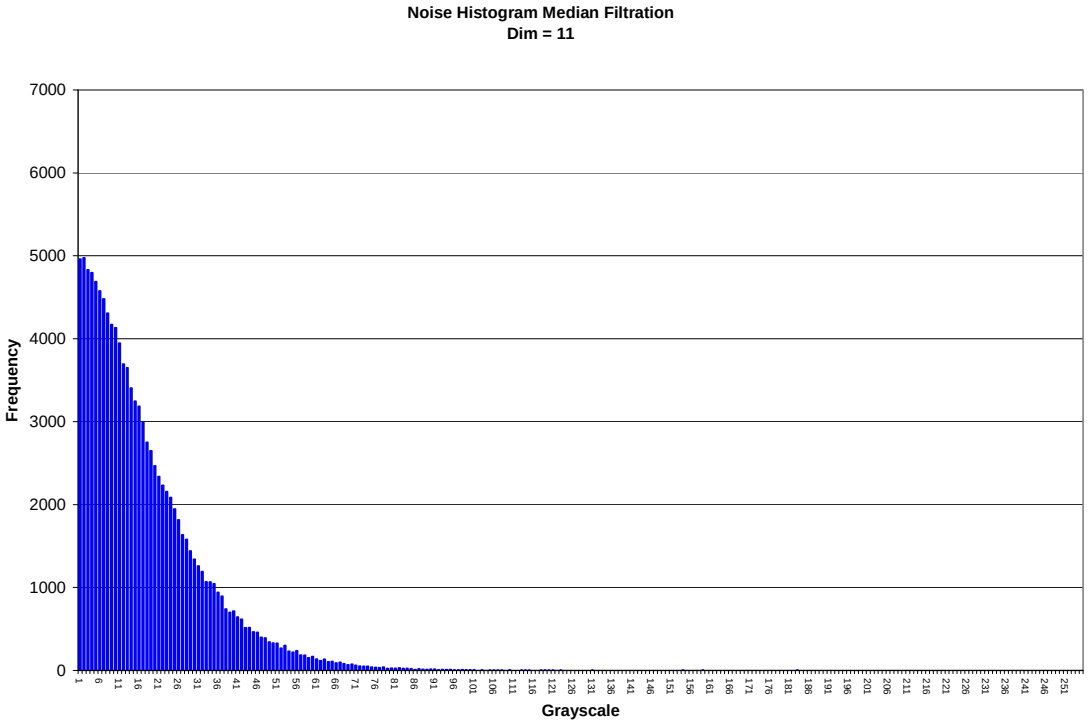


Figure 25. Median Smoothing, 11 x 11 kernel

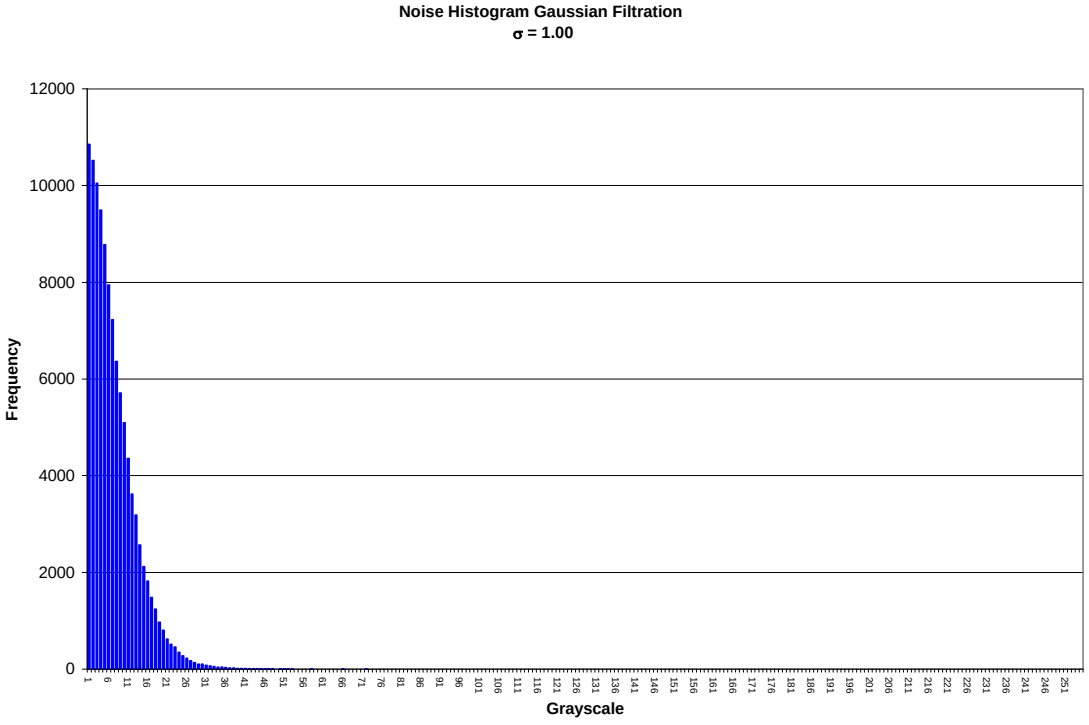


Figure 26. Gaussian Smoothing, σ = 1.00

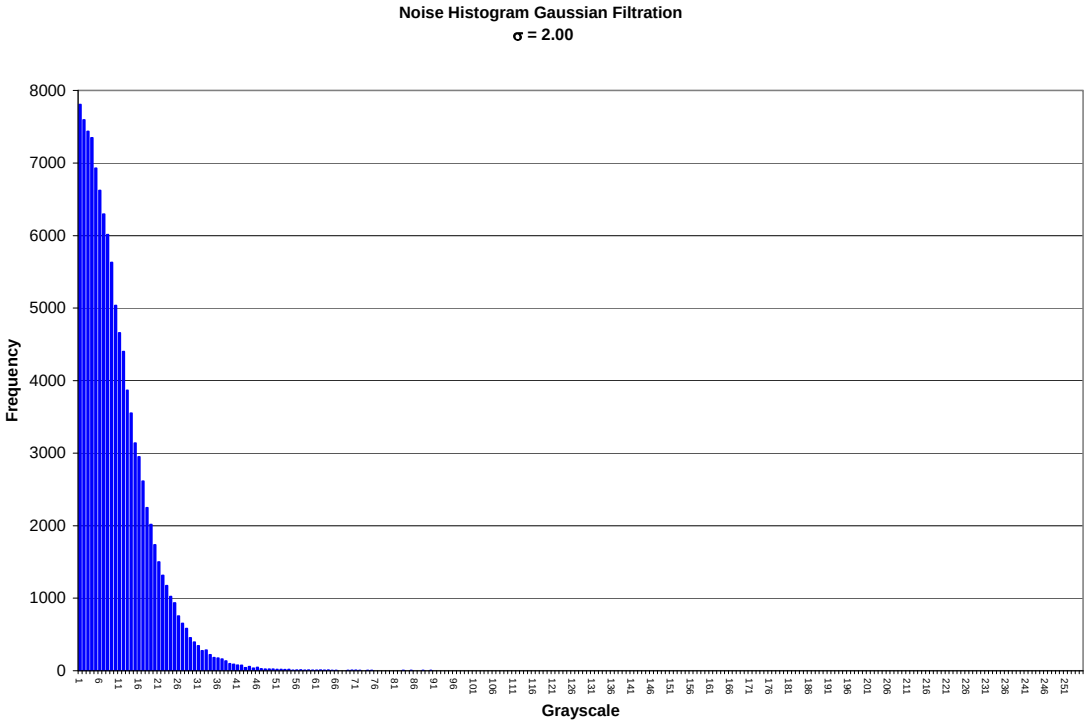


Figure 27. Gaussian Smoothing, σ = 2.00

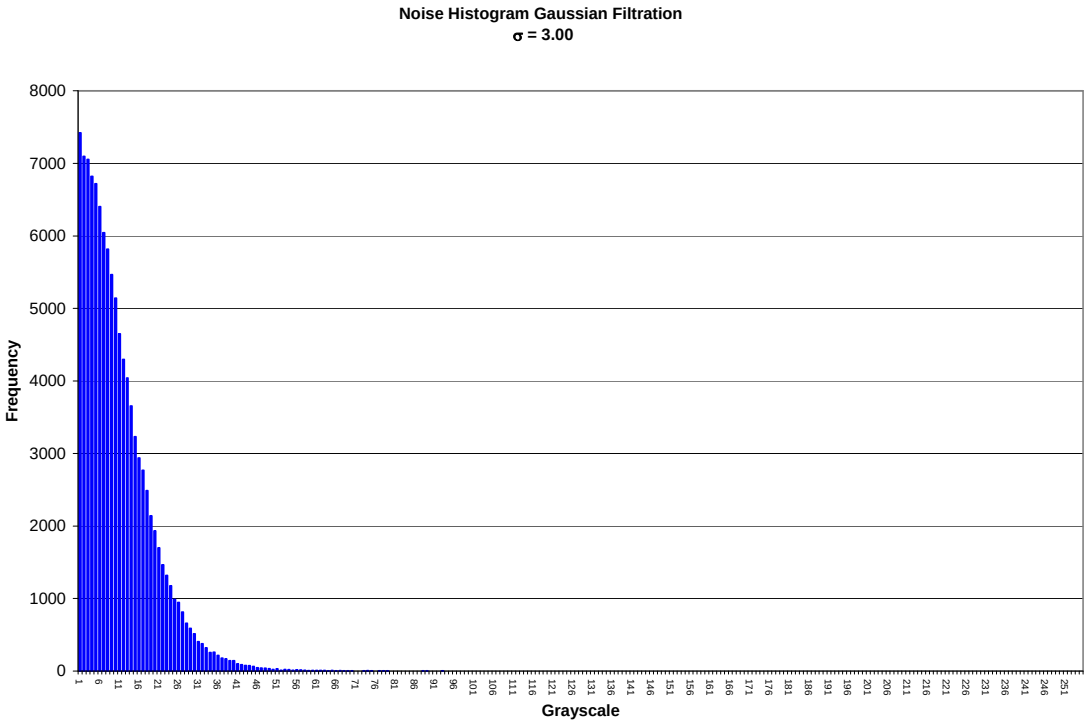


Figure 28. Gaussian Smoothing, σ = 3.00

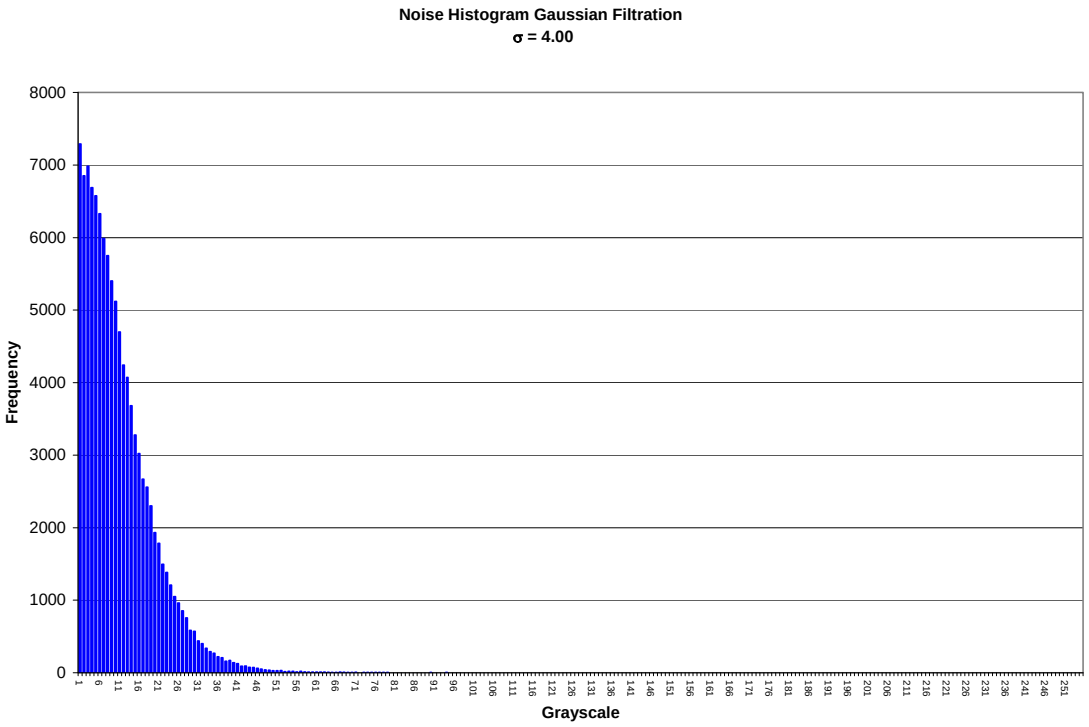


Figure 29. Gaussian Smoothing, σ = 4.00

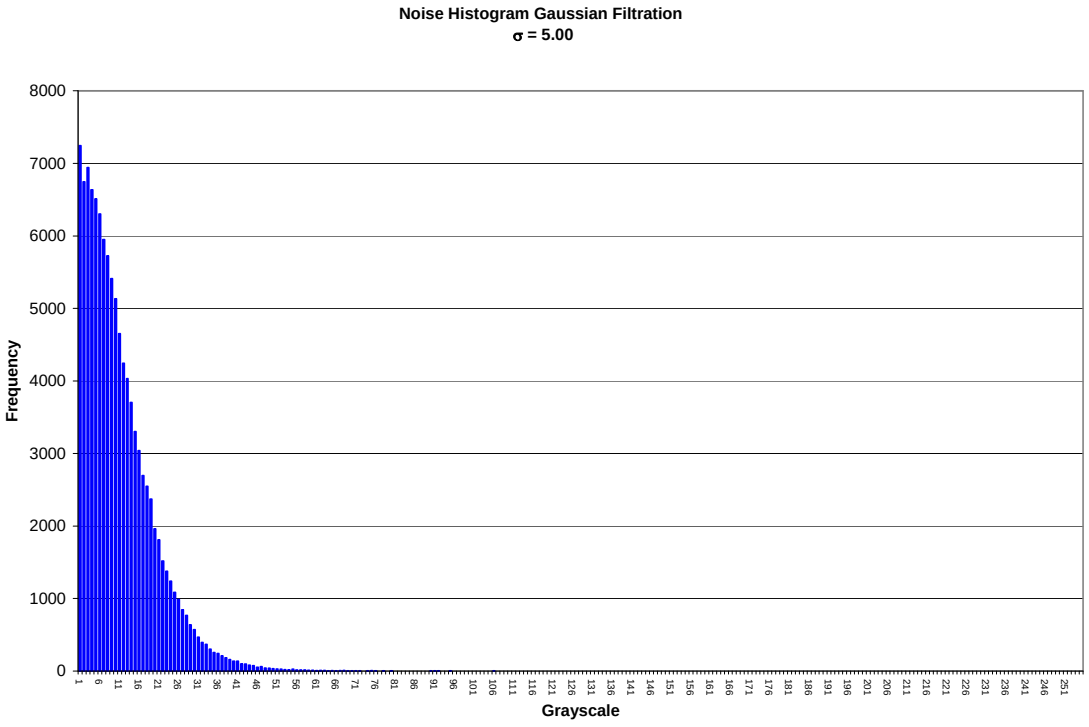


Figure 30. Gaussian Smoothing, σ = 5.00

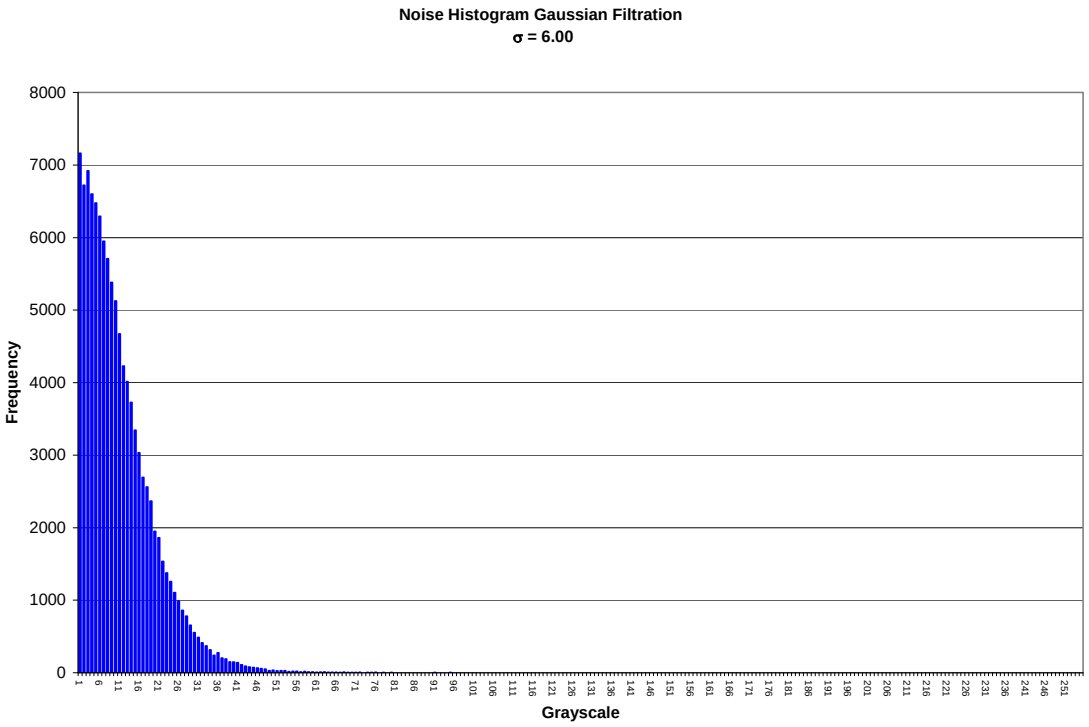


Figure 31. Gaussian Smoothing, σ = 6.00

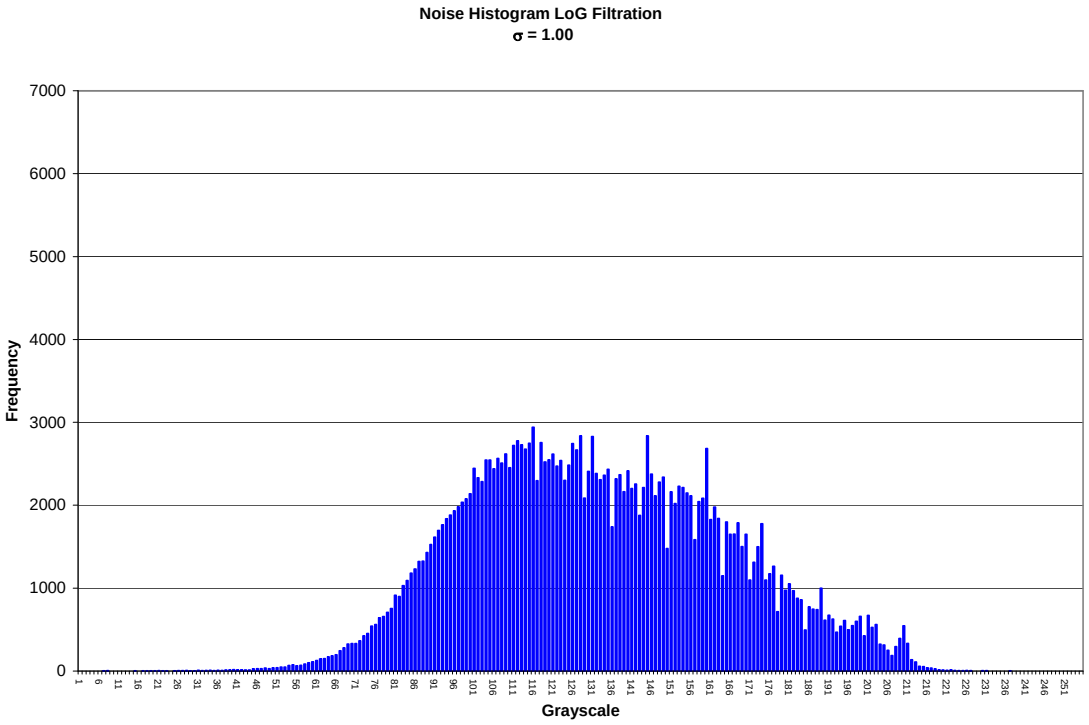


Figure 32. LoG Smoothing, σ = 1.00

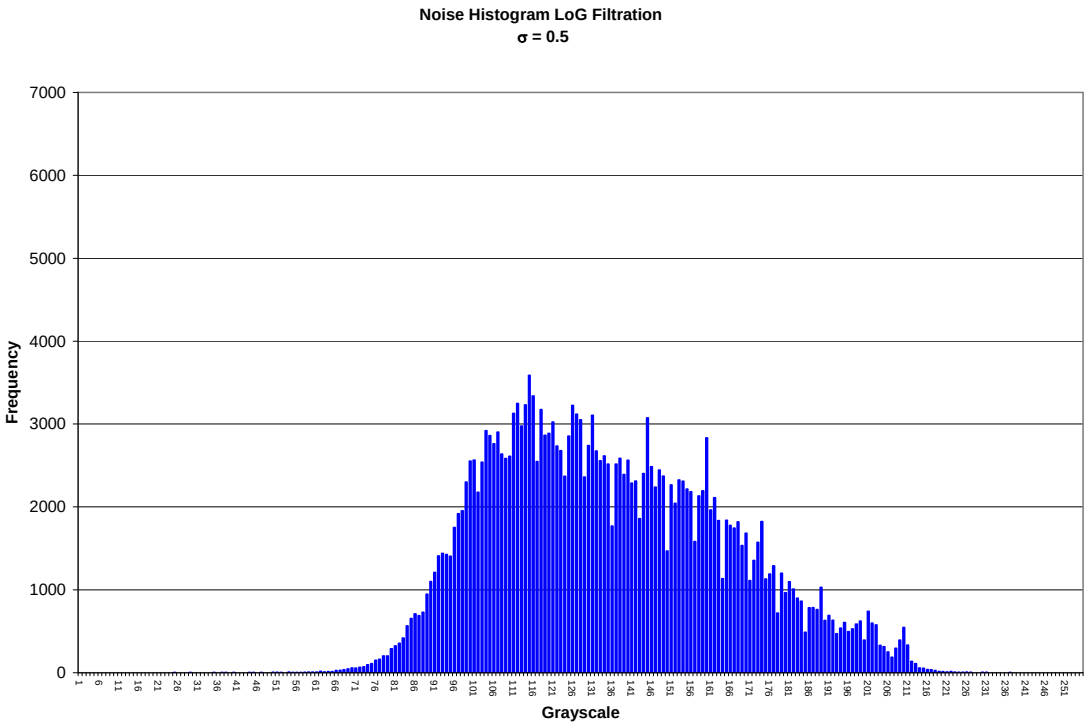


Figure 33. LoG Smoothing, σ = 2.00

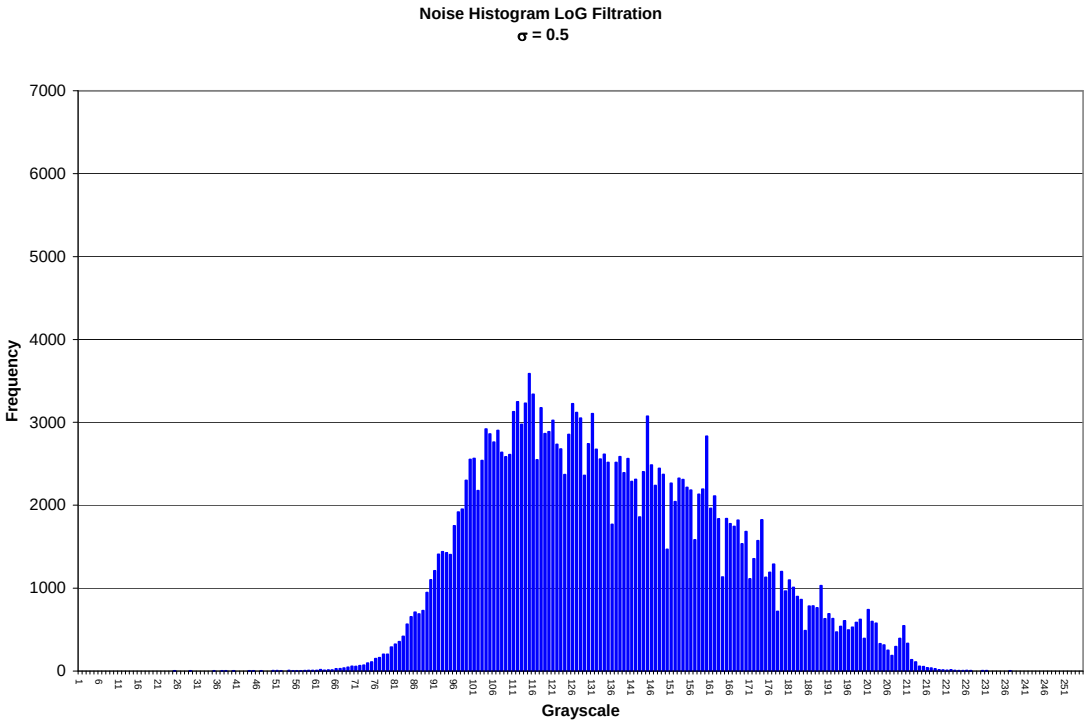


Figure 34. LoG Smoothing, σ = 3.00

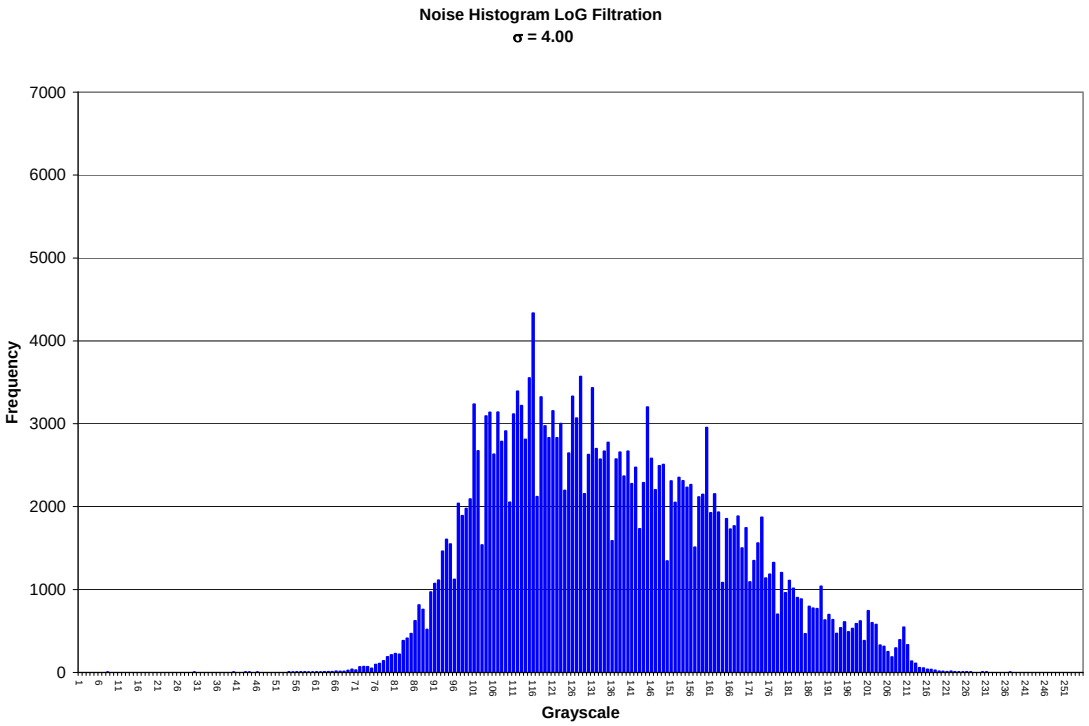


Figure 35. LoG Smoothing, σ = 4.00

Table 7. Averaging Method Summary

	3	5	7	9	11
μ:	766	799	799	791	786
Max:	115694	114491	113895	113405	112871
Median:	0	1	2	5	8
s:	7282	7195	7145	7107	7069
% Black:	59.03%	55.98%	55.71%	56.03%	56.08%
% Gray	40.97%	44.02%	44.29%	43.97%	43.92%

Table 8. Averaging Method Time Summary

	3	5	7	9	11
Min:	0.003865	0.006345	0.010033	0.013697	0.019599
x:	0.005541	0.007838	0.011638	0.015525	0.022342
Max:	0.029592	0.012245	0.015897	0.017810	0.028251
Median:	0.004245	0.007692	0.011176	0.015478	0.021707
s:	0.005522	0.001267	0.001388	0.001198	0.002553
μ:	0.002507	0.007142	0.010876	0.014867	0.020940

Table 9. Median Method Summary

	3	5	7	9	11
μ:	783	803	808	804	801
Max:	133492	122374	118723	117296	116254
Median:	0	1	2	5	7
s:	8370	7681	7450	7355	7286
% Black:	66.59%	59.50%	57.42%	57.02%	56.68%
% Gray	33.41%	40.50%	42.58%	42.98%	43.32%

Table 10. Median Method Time Summary

	3	5	7	9	11
Min:	0.053391	0.154877	0.052967	0.059954	0.068427
x:	0.057598	0.160796	0.061545	0.066368	0.076102
Max:	0.061771	0.171827	0.073464	0.079716	0.090039
Median:	0.057490	0.160166	0.058037	0.063663	0.075368
s:	0.002285	0.004276	0.006933	0.005313	0.005356
μ:	0.056312	0.158446	0.057735	0.063448	0.073159

Table 11. Gaussian Method Summary

σ:	0.25	0.50	0.75	1.00	1.25
μ:	900	763	769	778	784
Max:	230400	124222	120941	120322	119937
Median:	0	0	0	0	0
s:	14400	7882	7614	7562	7533
% Black:	100.00%	63.56%	61.39%	60.42%	59.76%
% Gray	0.00%	36.44%	38.61%	39.58%	40.24%
σ:	1.50	1.75	2.00	2.25	2.50
μ:	787	789	791	792	792
Max:	119642	119485	119376	119297	119243
Median:	0	0	0	0	0
s:	7512	7501	7493	7488	7484
% Black:	59.36%	59.13%	58.98%	58.87%	58.80%
% Gray	40.64%	40.87%	41.02%	41.13%	41.20%
σ:	2.75	3.00	3.25	3.50	3.75
μ:	793	793	793	793	794
Max:	119199	119164	119145	119115	119094
Median:	0	0	0	0	0
S:	7481	7478	7477	7475	7474
% Black:	58.75%	58.71%	58.68%	58.65%	58.63%
% Gray	41.25%	41.29%	41.32%	41.35%	41.37%
σ:	4.00	4.25	4.50	4.75	5.00
μ:	794	794	794	794	794
Max:	119084	119070	119058	119051	119039
Median:	0	0	0	0	0
s:	7473	7472	7471	7471	7470
% Black:	58.61%	58.60%	58.59%	58.58%	58.57%
% Gray	41.39%	41.40%	41.41%	41.42%	41.43%
σ:	5.25	5.50	5.75	6.00	6.25
μ:	794	794	794	794	794
Max:	119037	119032	119033	119028	119025
Median:	0	0	0	0	0
s:	7470	7469	7469	7469	7469
% Black:	58.56%	58.56%	58.55%	58.55%	58.54%
% Gray	41.44%	41.44%	41.45%	41.45%	41.46%

Table 12. Gaussian Method Time Summary

σ:	0.25	0.50	0.75	1.00	1.25
Min:	0.005837	0.006862	0.006711	0.006538	0.007039
X:	0.006562	0.008923	0.009730	0.009076	0.012254
Max:	0.007576	0.012906	0.024505	0.014220	0.036017
m:	0.006339	0.008418	0.008106	0.008205	0.011898
s:	0.000517	0.001725	0.004204	0.002412	0.006156
μ:	0.006278	0.007976	0.007420	0.007751	0.008871
σ:	1.50	1.75	2.00	2.25	2.50
Min:	0.006856	0.006710	0.006578	0.006874	0.006248
X:	0.009875	0.010350	0.010281	0.010950	0.009222
Max:	0.014698	0.025823	0.015275	0.025957	0.014311
m:	0.009458	0.009050	0.010001	0.010333	0.008436
s:	0.002586	0.004323	0.002763	0.004171	0.002573
μ:	0.008455	0.007975	0.008763	0.008658	0.007809
σ:	2.75	3.00	3.25	3.50	3.75
Min:	0.006396	0.006343	0.006441	0.006511	0.006158
x:	0.009501	0.009593	0.009657	0.009276	0.010238
Max:	0.018985	0.016064	0.021365	0.013924	0.019933
m:	0.008925	0.008520	0.009414	0.008556	0.009538
s:	0.003196	0.002946	0.003385	0.002107	0.003488
μ:	0.007745	0.007974	0.007797	0.008119	0.008322
σ:	4.00	4.25	4.50	4.75	5.00
Min:	0.006530	0.006631	0.006378	0.006614	0.006646
x:	0.010206	0.010183	0.010943	0.010036	0.010176
Max:	0.019606	0.021424	0.017567	0.015760	0.013749
m:	0.009236	0.010463	0.009777	0.009226	0.009680
s:	0.003271	0.003468	0.003080	0.002731	0.002190
μ:	0.008409	0.008277	0.009250	0.008535	0.008972
σ:	5.25	5.50	5.75	6.00	6.25
Min:	0.007017	0.006862	0.006611	0.006728	0.006230
x:	0.010071	0.010207	0.009771	0.010394	0.009997
Max:	0.019020	0.019959	0.014126	0.023274	0.015367
Median:	0.009219	0.009652	0.009561	0.009300	0.009711
s:	0.003158	0.003299	0.002293	0.004065	0.002816
μ:	0.008336	0.008394	0.008511	0.008160	0.008449

Table 13. LoG Method Summary

σ:	0.25	0.50	0.75	1.00	1.25
μ:	600	522	498	490	487
Max:	89084	15604	3951	1617	1681
Median:	153	467	324	259	226
s:	5558	1009	502	488	499
% Black:	58.01%	11.67%	3.10%	1.29%	0.66%
% Gray	41.99%	88.33%	96.90%	98.71%	99.34%
σ:	1.50	1.75	2.00	2.25	2.50
μ:	485	480	472	461	445
Max:	1732	1747	1760	1788	1794
Median:	223	207	190	171	149
s:	507	513	518	521	522
% Black:	0.39%	0.27%	0.20%	0.17%	0.15%
% Gray	99.61%	99.73%	99.80%	99.83%	99.85%
σ:	2.75	3.00	3.25	3.50	3.75
μ:	427	410	393	379	371
Max:	1800	1797	1799	1838	1864
Median:	139	125	115	110	107
s:	523	522	522	522	523
% Black:	0.14%	0.13%	0.12%	0.12%	0.12%
% Gray	99.86%	99.87%	99.88%	99.88%	99.88%
σ:	4.00	4.25	4.50	4.75	5.00
μ:	367	367	366	366	366
Max:	1873	1873	1873	1873	1873
Median:	103	103	103	103	103
s:	524	524	524	524	524
% Black:	0.12%	0.12%	0.12%	0.12%	0.12%
% Gray	99.88%	99.88%	99.88%	99.88%	99.88%
σ:	5.25	5.50	5.75	6.00	6.25
μ:	366	366	366	366	366
Max:	1873	1873	1873	1873	1873
Median:	103	103	103	103	103
s:	524	524	524	524	524
% Black:	0.12%	0.12%	0.12%	0.12%	0.12%
% Gray	99.88%	99.88%	99.88%	99.88%	99.88%

Table 14. LoG Method Time Summary

σ:	0.25	0.50	0.75	1.00	1.25
Min:	0.005790	0.006581	0.006356	0.006630	0.006973
Mean:	0.006187	0.007584	0.007701	0.008065	0.008410
Max:	0.006549	0.009011	0.009163	0.011302	0.011501
Median:	0.006218	0.007498	0.007381	0.007769	0.008075
s:	0.000190	0.000614	0.000853	0.001268	0.001364
σ:	1.50	1.75	2.00	2.25	2.50
Min:	0.006999	0.006320	0.006508	0.006404	0.006451
Mean:	0.008349	0.008637	0.007779	0.007942	0.007856
Max:	0.011158	0.012372	0.009407	0.011530	0.010878
Median:	0.008079	0.008588	0.007571	0.007715	0.007588
s:	0.001178	0.001672	0.000925	0.001181	0.001056
σ:	2.75	3.00	3.25	3.50	3.75
Min:	0.006333	0.006390	0.006467	0.006345	0.006298
Mean:	0.007824	0.008117	0.008433	0.008744	0.008446
Max:	0.010229	0.011151	0.012952	0.016596	0.012649
Median:	0.007272	0.007580	0.008164	0.007819	0.007761
s:	0.001099	0.001491	0.001770	0.002709	0.001896
σ:	4.00	4.25	4.50	4.75	5.00
Min:	0.006212	0.006357	0.006161	0.005985	0.006257
Mean:	0.009216	0.008626	0.008000	0.007982	0.008258
Max:	0.026257	0.012589	0.012469	0.011108	0.014775
Median:	0.007978	0.008101	0.007631	0.007460	0.007434
s:	0.004408	0.001772	0.001590	0.001422	0.002043
σ:	5.25	5.50	5.75	6.00	6.25
Min:	0.006432	0.006376	0.006290	0.006342	0.006781
Mean:	0.008376	0.008330	0.008873	0.008918	0.008709
Max:	0.011797	0.014962	0.013042	0.020471	0.015900
Median:	0.008158	0.007597	0.008560	0.008512	0.008092
s:	0.001545	0.002099	0.002290	0.003020	0.002260

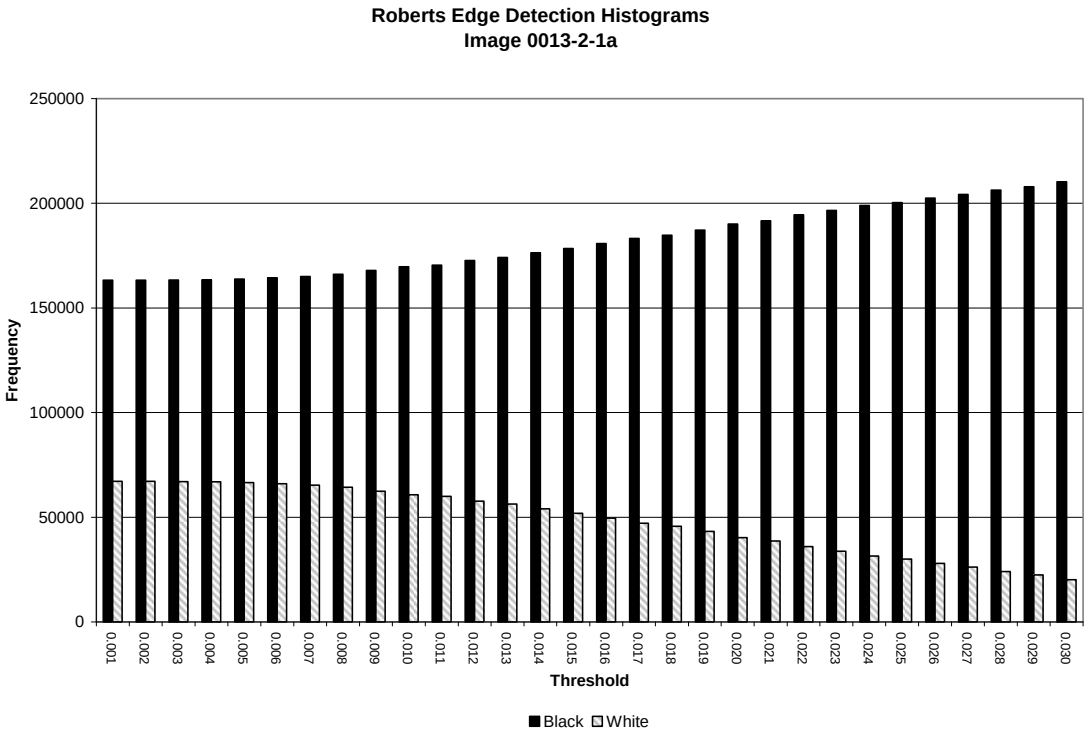


Figure 36. Roberts Histograms

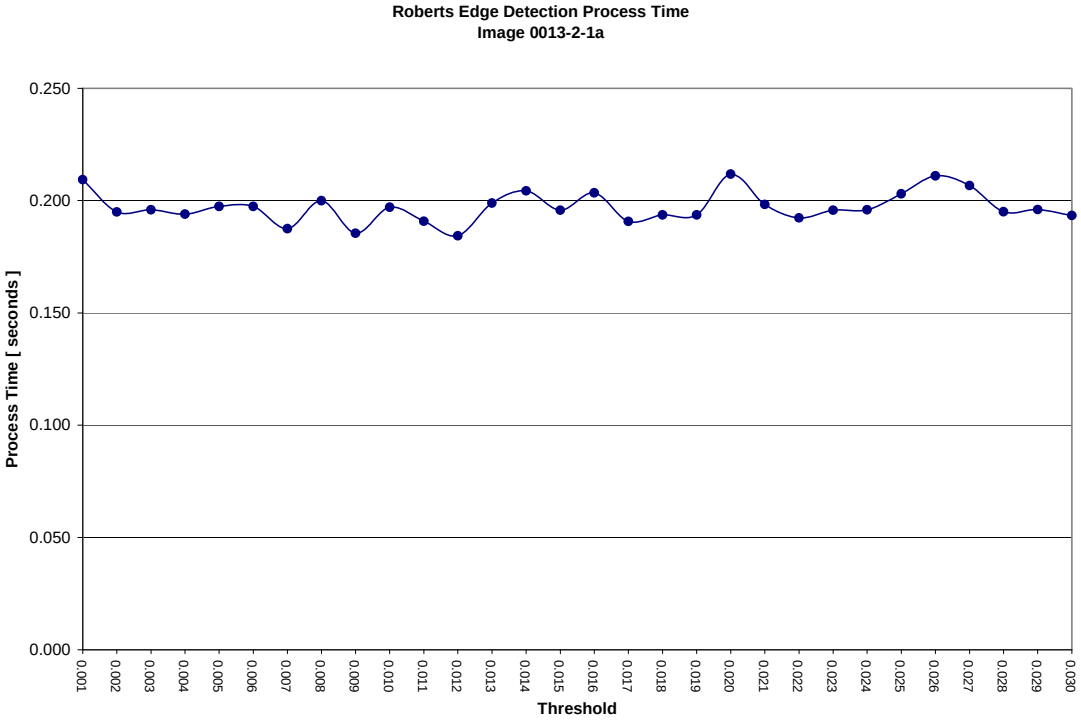


Figure 37. Roberts Processing Time

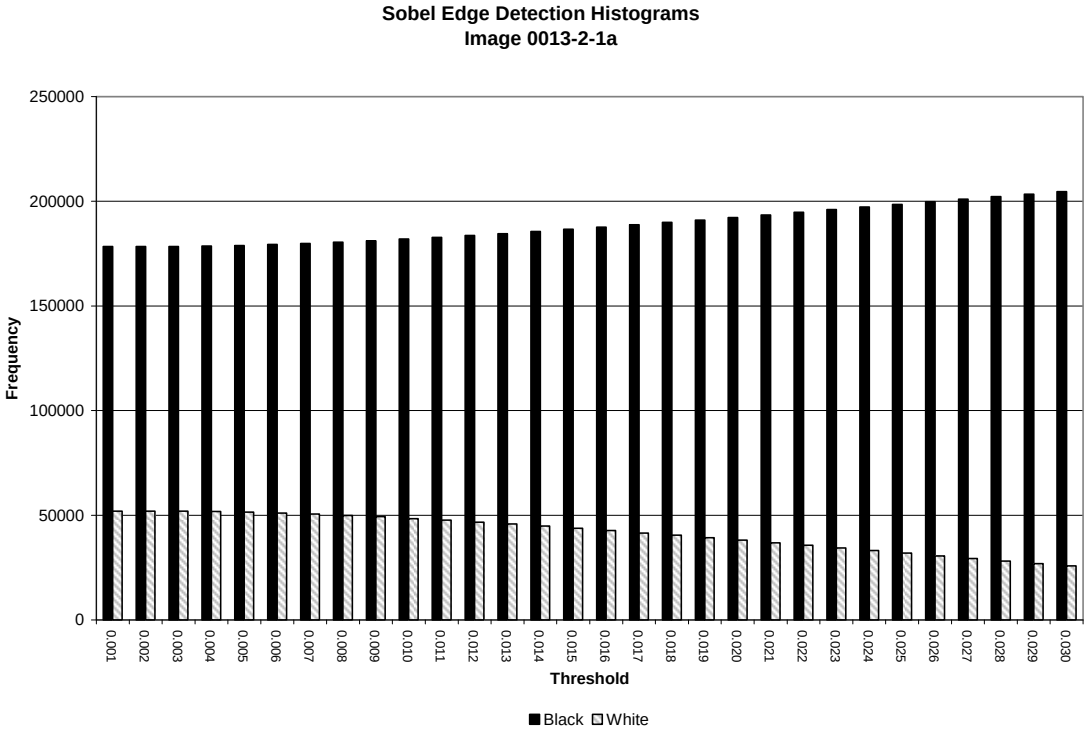


Figure 38. Sobel Histograms

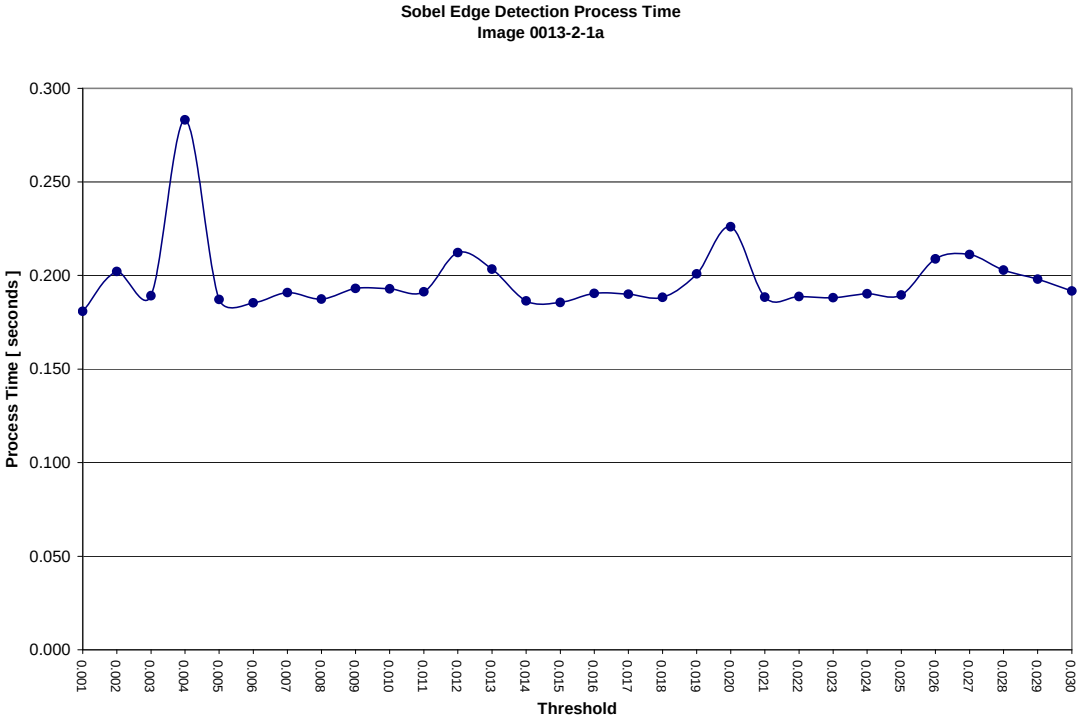


Figure 39. Sobel Processing Time

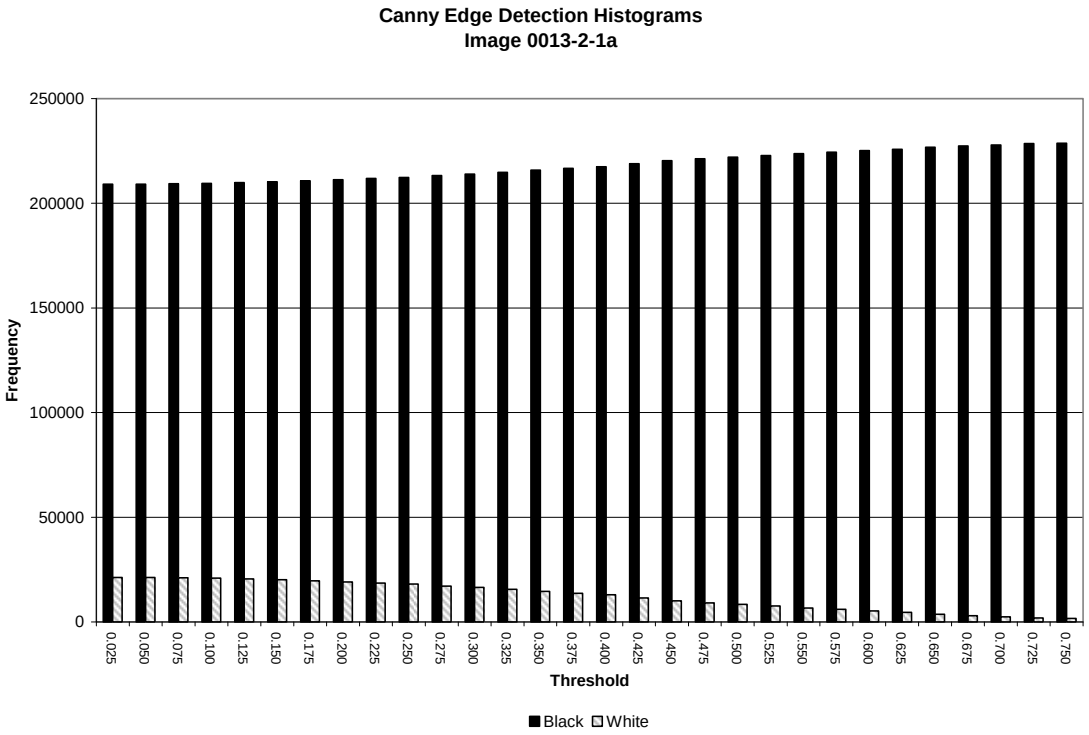


Figure 40. Canny Histograms

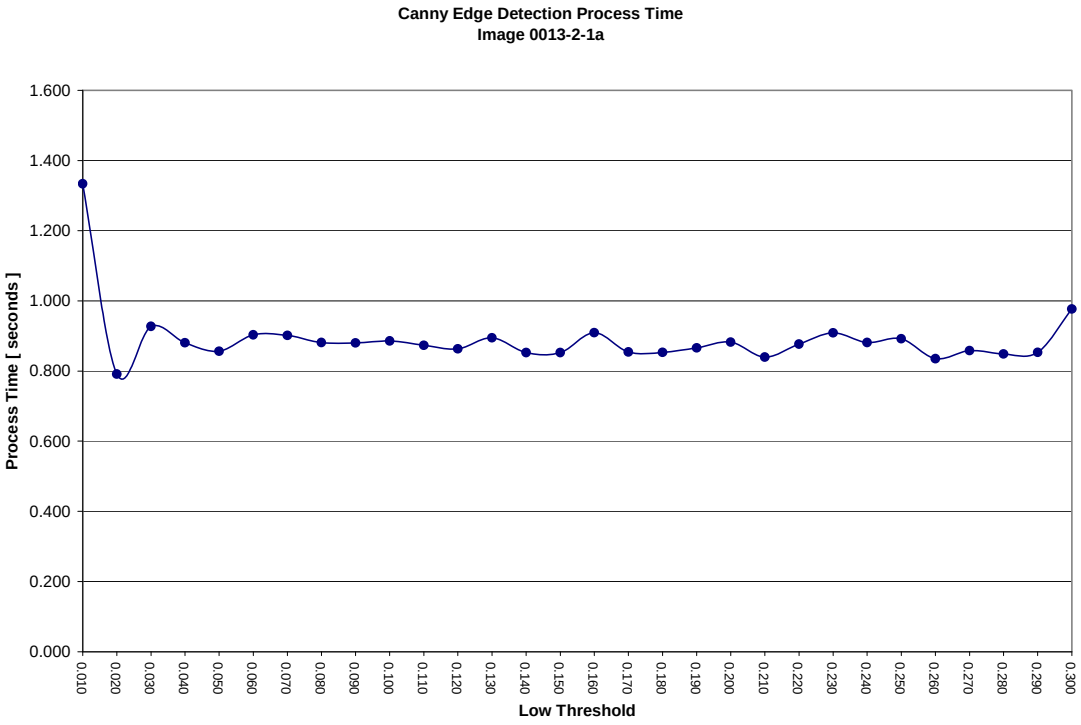


Figure 41. Canny Processing Time

CHAPTER 5
CONCLUSIONS AND RECOMMENDATIONS

5.1 Conclusions

A digital image processing method was developed and evaluated in this thesis consisting of three steps: preprocessing using image smoothing, edge detection based upon local intensity gradients, and line detection via the Hough Transform. This method was applied to digital photographs taken from two sources: a carbon fiber mat produced by the University and a generic anti-static dryer sheet.

Four digital preprocessing approaches are considered: Averaging, Median, Gaussian, and LoG smoothing. Each method was evaluated based upon the noise reduction from the original image. After preprocessing, three edge detection methods were evaluated: Roberts, Sobel, and Canny. Edge detection methods were judged over a range of threshold values to determine the appropriate technique. Finally, the Hough Transform is used to detect lines in the edge image over various grid sizes. Mean angle θ, total length L and processing time are considered as the number of grids is increased.

The final method presented in this paper uses three image processing techniques: noise-reducing Averaging smoothing with a 5 x 5 kernel, Canny edge detection with a standard deviation $\sigma = 2.75$ and threshold interval (0.010, 0.250), and line detection via the Hough Transform with ρ and Θ resolutions of 1, respectively. As the line detection grid size decreases (more grids overall), this method provides a reasonable approximation of the relative alignment of nonwoven fiber mats.

5.2 Recommendations

The most obvious use for the line detection code is to analyze carbon fiber mats after production. However, a camera could be placed directly above the conveyor belt (or bobbin) and used to periodically examine the mats as fibers are being spun. If the image size is small and the processor fast enough, "real-time" data could be approximated as a quality control tool. A general alignment characteristic could be derived from output from the Hough transform itself. In industry, many times a fiber mat is quoted to have a general alignment of XX%. Using the Hough parameterization value Θ, which represents the inclination angle in Hough-space, a statistical analysis of the returned values could help to quantify this alignment.

One important factor that has been omitted for this study is the three dimensional nature of the fiber mat. This was done strictly for convenience. More complicated methods could be developed to help quantify fiber alignment above and below the plane being examined; this would necessitate a model of the fiber lay down itself – no small task.

Another area that could be improved is the quality of the original image. This can be done through: carefully tuning of light sources, proper use of zoom and depth-of-field, and use of high-resolution cameras. This exercise was not concerned with this issue, but it should be considered when using this tool in the future.

The only method of image preprocessing explored in this paper is smoothing, however, there exists a wide variety of techniques that can be used to enhance digital images. Matlab™ has other built-in functions that could be used, such as sharpening. Other operations could be performed on a more basic level, such as bit-shifting. This can be used to increase the contrast in an image or brighten it.

As with preprocessing methods, there is a wide range of edge detection techniques that are available; many are built-in to Matlab™. A more productive exercise, however, would be to determine a better low-high relationship between Canny thresholds (currently, fixed ratio of 2.5).

Many assumptions were made when analyzing the Hough transform in this study in order to minimize the amount of data to be analyzed. Parameters such as Θ and ρ resolution, peaks threshold, neighborhood size, fill gap length, and minimum merged length all have the potential to greatly effect the outcome of the analysis. As mentioned in Section 3.3, any future work should include an in-depth exploration of the effects of peak thresholding vs. peak counting.

A graphical user interface would be very useful when analyzing large quantities of images. Matlab™ has a built-in toolbox known as GUIDE (graphical user interface development environment) that makes the procedure largely automatic.

LIST OF REFERENCES

LIST OF REFERENCES

Galbiati, Jr. Louis J. *Machine Vision and Digital Image Processing Fundamentals*. New Jersey: Prentice-Hall, 1990.

Gonzalez, Rafael C. and Paul Wintz. Digital Image Processing, 2nd Ed. Massachusetts: Addison-Wesley Publishing, 1987.

Pearson, Don, ed. Image Processing. New York: McGraw-Hill, 1991.

Pratt, William K. Digital Image Processing. New York: John Wiley & Sons, 1978.

APPENDIX

Appendix A: Analysis of Image 0013-2-2a

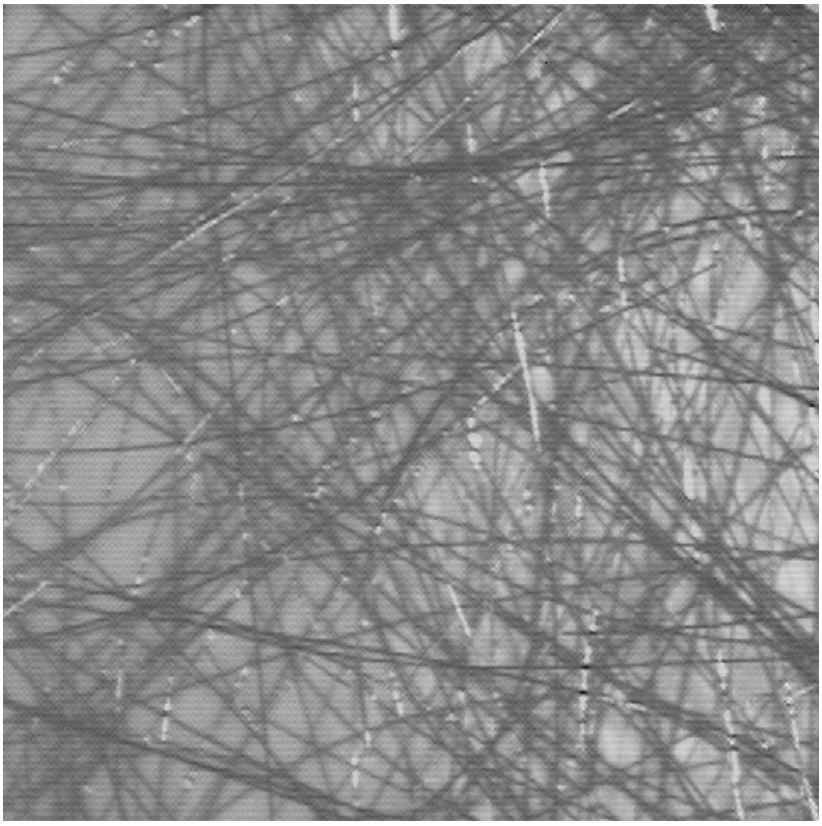


Figure 42. 0013-2-2a

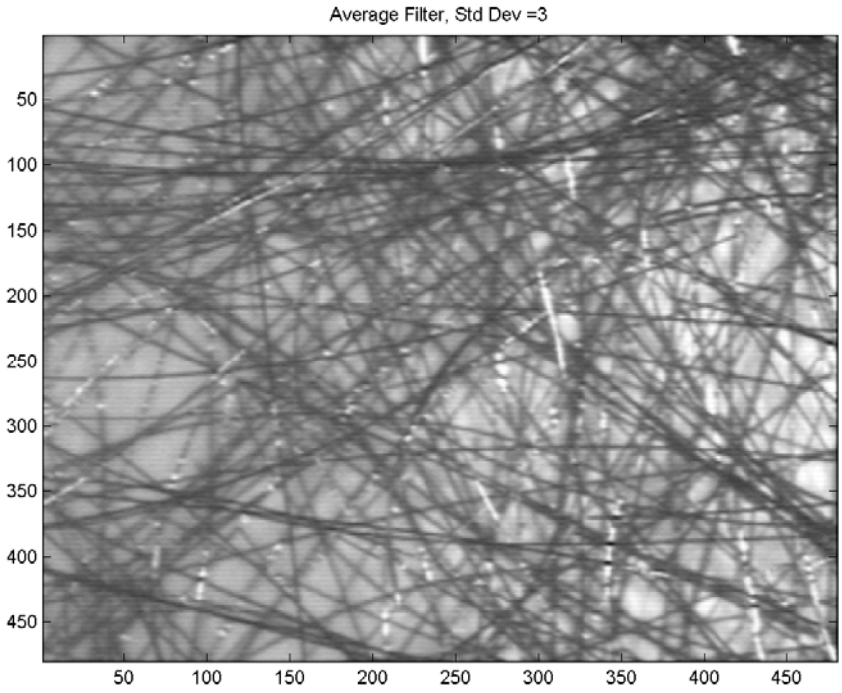


Figure 43. 0013-2-2a Averaging Smoothing, 3 x 3 kernel

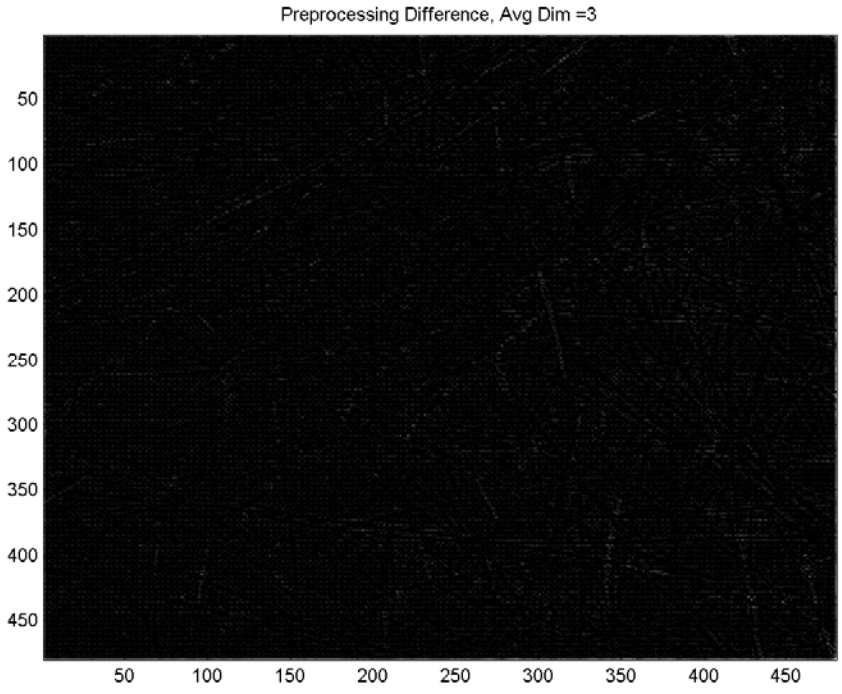


Figure 44. 0013-2-2a Averaging Smoothing Noise, 3 x 3 kernel

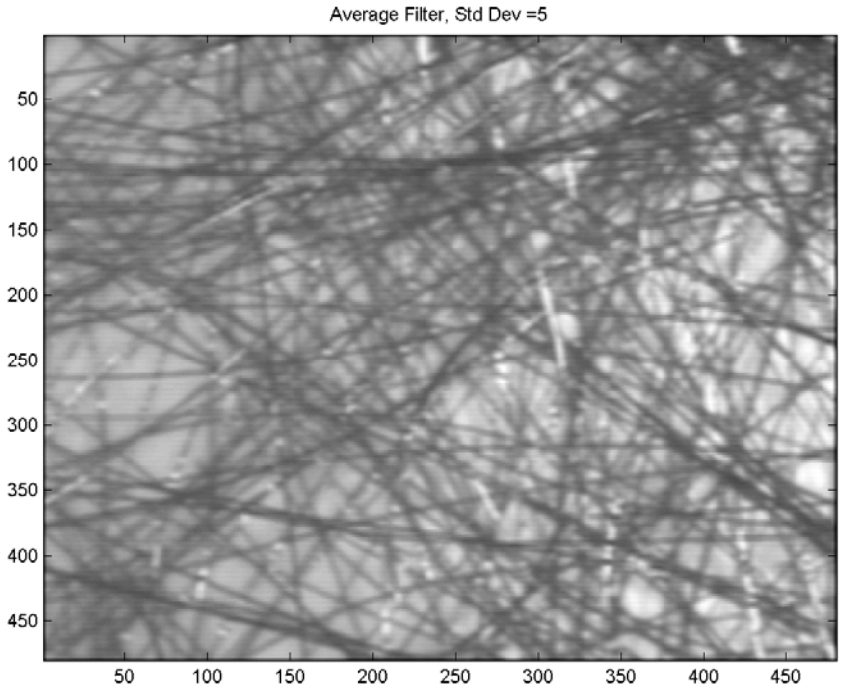


Figure 45. 0013-2-2a Averaging Smoothing, 5 x 5 kernel

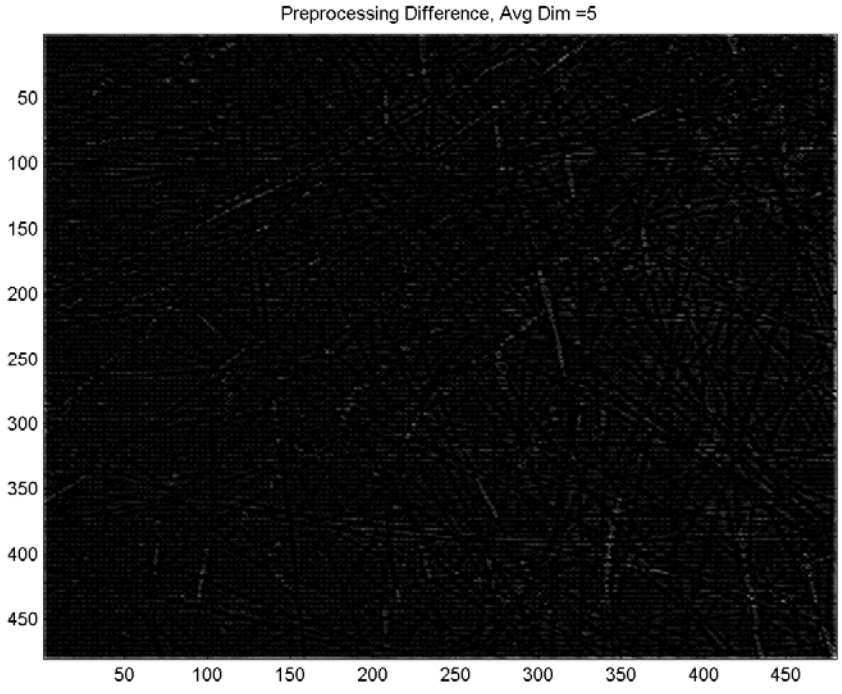


Figure 46. 0013-2-2a Averaging Smoothing Noise, 5 x 5 kernel

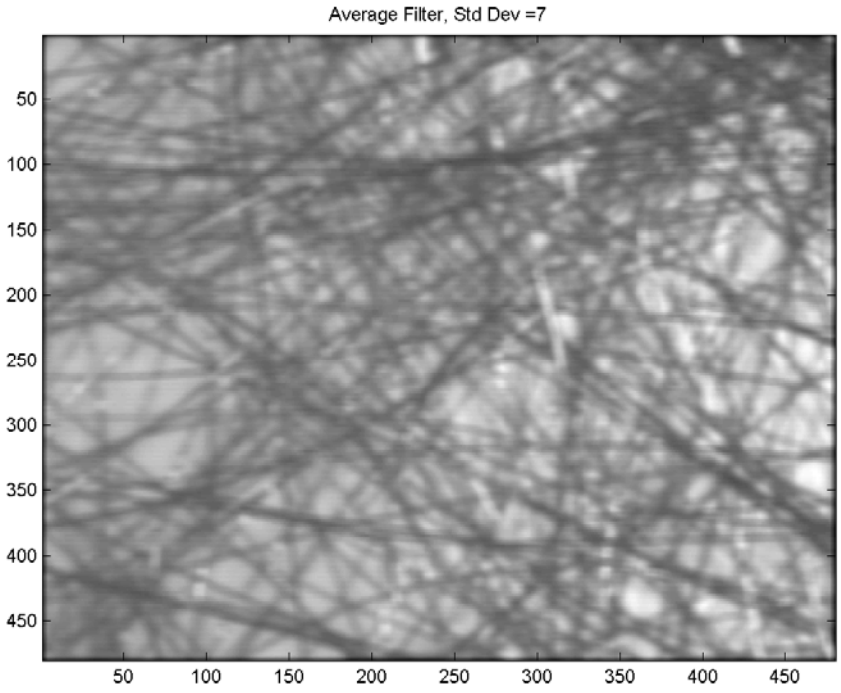


Figure 47. 0013-2-2a Averaging Smoothing, 5 x 5 kernel

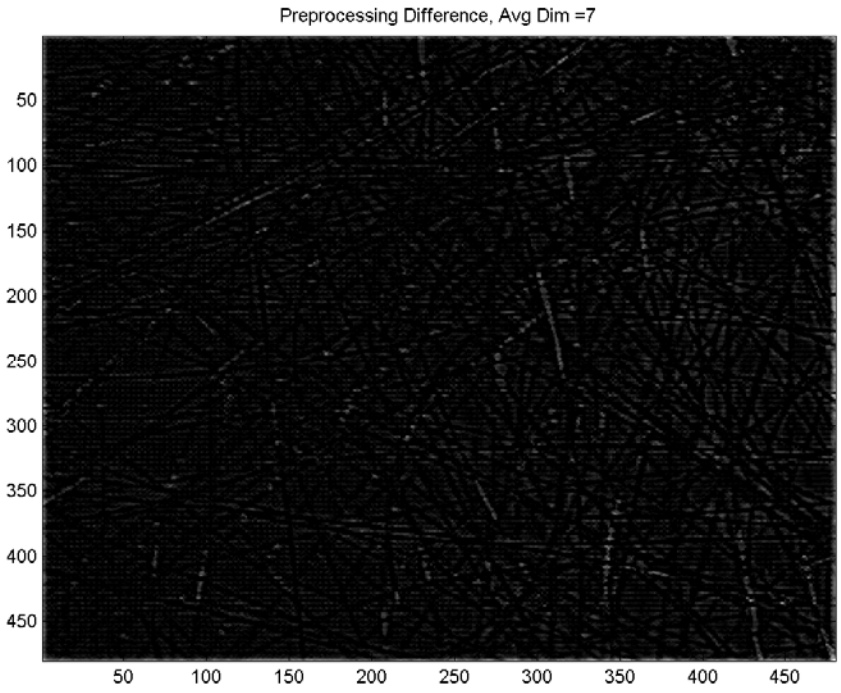


Figure 48. 0013-2-2a Averaging Smoothing Noise, 5 x 5 kernel

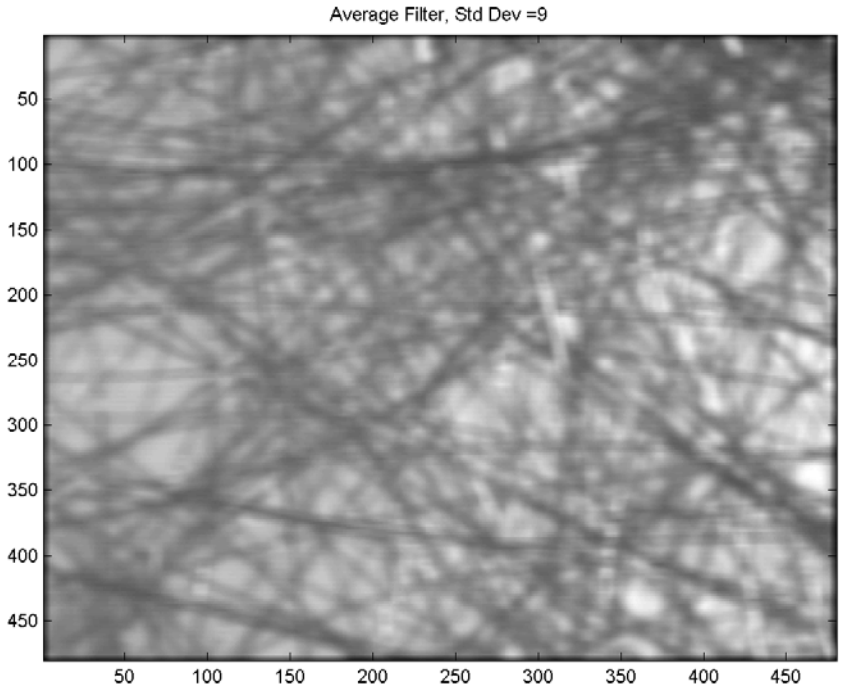


Figure 49. 0013-2-2a Averaging Smoothing, 7 x 7 kernel

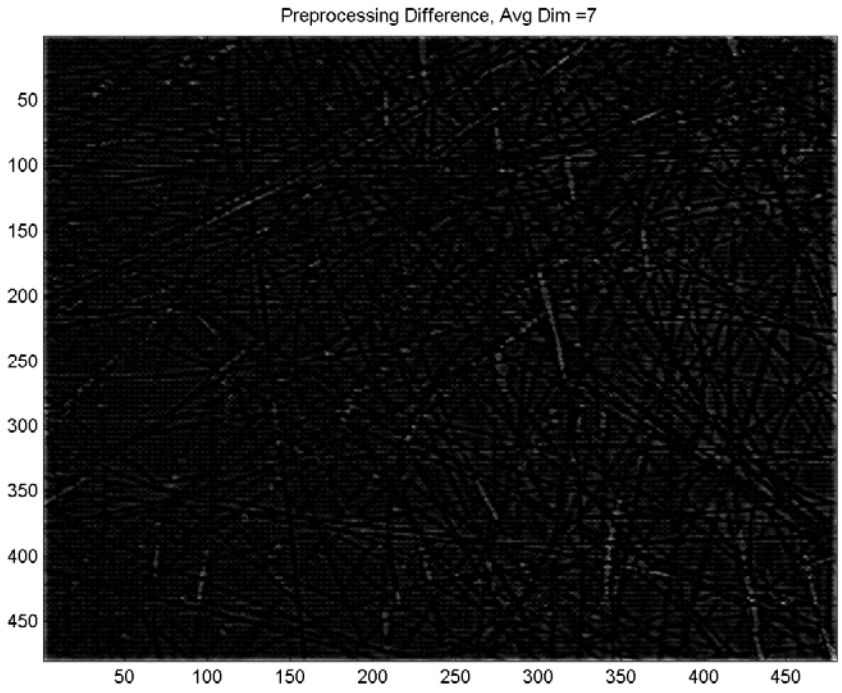


Figure 50. 0013-2-2a Averaging Smoothing Noise, 7 x 7 kernel

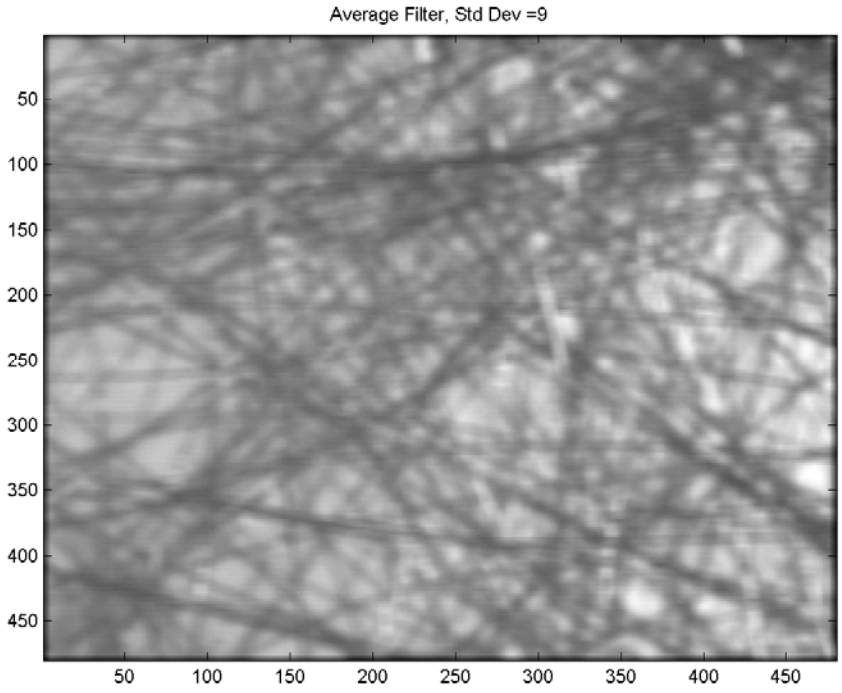


Figure 51. 0013-2-2a Averaging Smoothing, 9 x 9 kernel

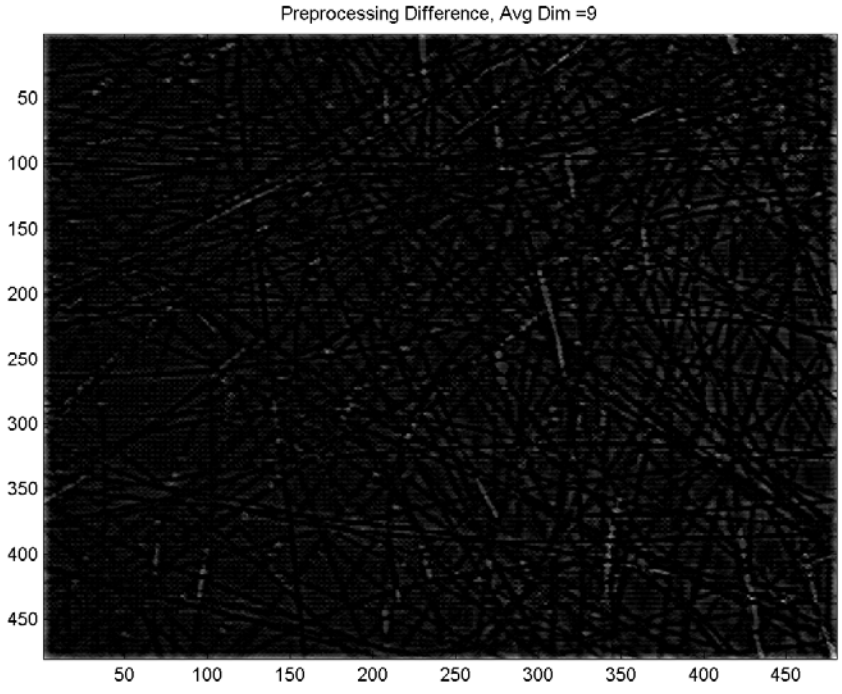


Figure 52. 0013-2-2a Averaging Smoothing Noise, 9 x 9 kernel

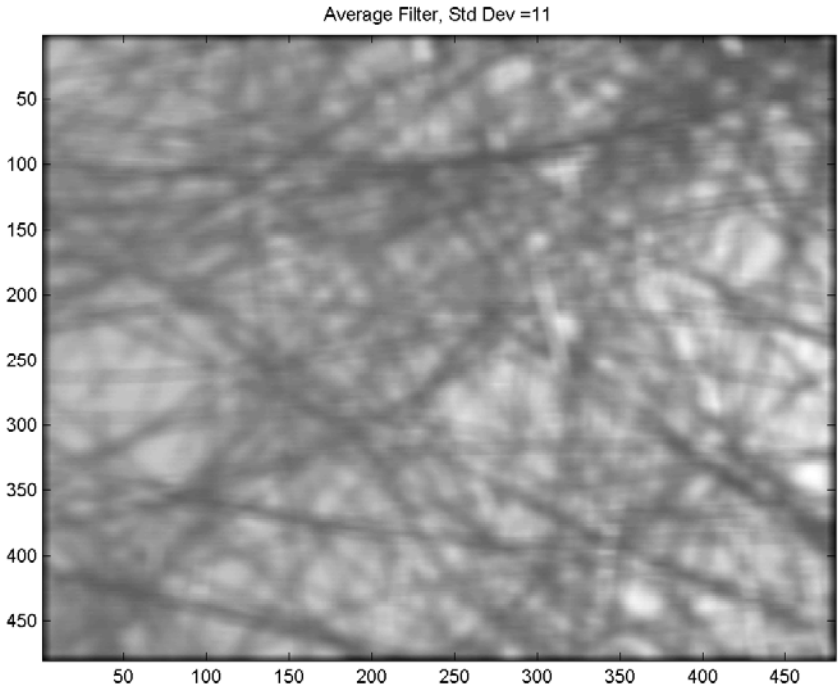


Figure 53. 0013-2-2a Averaging Smoothing, 11 x 11 kernel

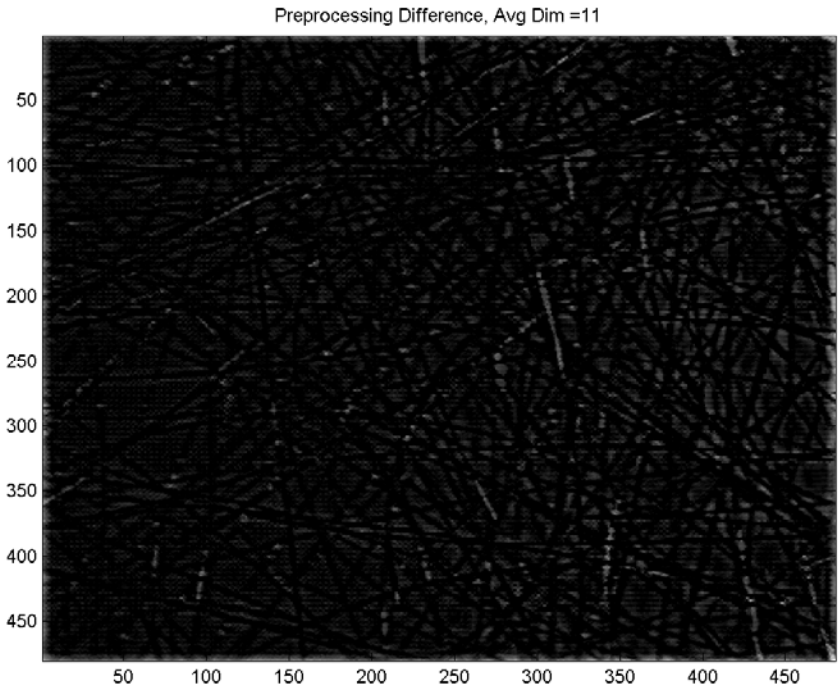


Figure 54. 0013-2-2a Averaging Smoothing Noise, 11 x 11 kernel

Table 15. 0013-2-2a Averaging Smoothing Histogram Data

Grayscale	3	5	7	9	11
0	120794	117420	116644	116589	116281
1	13107	8441	7562	7021	6234
2	12978	8139	7232	6816	6124
3	12179	8304	7332	6791	6054
4	11301	8090	7012	6559	5896
5	10221	7716	6960	6298	5748
6	9072	7571	6389	6203	5657
7	8013	7143	6389	5853	5563
8	6626	6554	6070	5353	5035
9	5535	6163	5648	5368	4949
10	4480	5698	5257	4980	4781
11	3522	5208	4923	4672	4415
12	2646	4532	4444	4241	4139
13	1946	3987	4112	3884	3921
14	1502	3545	3598	3633	3662
15	1147	2960	3209	3239	3386
16	792	2491	3020	2897	3145
17	646	2155	2568	2748	2884
18	432	1814	2196	2390	2596
19	353	1542	2002	2111	2391
20	249	1309	1801	1993	2232
21	204	1076	1600	1858	2020
22	162	952	1323	1511	1808
23	137	779	1234	1441	1676
24	103	666	1038	1197	1475
25	79	548	998	1152	1339
26	63	506	818	1033	1157
27	65	419	739	1007	1113
28	56	360	656	889	980
29	58	324	587	752	950
30	45	288	511	698	861
31	49	233	447	686	826
32	49	211	372	582	743
33	57	209	386	479	672
34	57	190	366	496	611
35	48	137	329	461	573
36	47	131	268	417	557
37	70	136	261	371	453
38	68	120	241	342	451
39	56	117	217	335	463
40	70	98	218	302	409
41	73	91	210	278	358
42	72	95	184	259	317
43	45	86	190	254	362

Table 15 (Continued). 0013-2-2a Averaging Smoothing Histogram Data

Grayscale	3	5	7	9	11
44	60	81	155	229	312
45	86	86	161	217	283
46	70	87	135	203	268
47	73	61	130	197	270
48	67	76	128	175	238
49	80	72	109	183	213
50	56	56	118	165	211
51	67	63	104	155	206
52	60	70	109	145	171
53	46	57	83	136	175
54	44	57	80	115	176
55	43	80	94	102	162
56	47	68	94	124	138
57	46	53	85	116	148
58	36	68	82	124	130
59	39	59	72	93	115
60	36	47	66	99	126
61	18	52	79	93	107
62	22	56	61	89	130
63	13	53	45	84	101
64	17	46	61	68	106
65	12	35	56	79	93
66	8	40	62	71	85
67	8	43	38	50	76
68	9	36	65	59	62
69	7	40	40	53	59
70	6	35	42	64	74
71	7	29	53	59	72
72	3	27	40	39	67
73	6	28	36	52	49
74	6	17	26	42	53
75	3	23	31	38	55
76	3	12	21	32	47
77	2	13	27	42	40
78	2	13	26	31	38
79	6	11	23	23	42
80	3	7	16	24	38
81	1	10	17	23	25
82	3	4	16	26	17
83	0	4	10	20	26
84	0	7	12	22	26
85	1	3	11	13	35
86	0	1	11	14	22
87	1	7	7	17	18

Table 15 (Continued). 0013-2-2a Averaging Smoothing Histogram Data

Grayscale	3	5	7	9	11
88	0	4	10	10	12
89	0	5	4	9	21
90	0	6	8	5	15
91	0	3	2	6	9
92	1	5	4	11	12
93	0	5	9	5	9
94	0	4	4	9	7
95	0	3	6	12	12
96	0	3	5	6	5
97	0	0	3	5	10
98	0	1	4	1	6
99	0	3	4	8	9
100	0	0	2	10	5
101	0	1	5	6	5
102	1	2	3	2	8
103	0	0	3	1	1
104	0	1	2	4	17
105	0	1	4	0	2
106	0	2	2	4	5
107	0	0	3	6	4
108	0	0	4	4	4
109	0	0	0	3	1
110	0	1	0	3	6
111	0	0	2	3	8
112	0	0	0	4	1
113	0	0	3	3	1
114	0	0	1	1	2
115	0	0	1	0	2
116	0	0	0	4	1
117	0	0	0	2	3
118	0	0	1	1	8
119	0	0	0	1	2
120	0	0	0	2	0
121	0	0	0	0	3
122	0	2	0	0	1
123	0	0	0	0	0
124	0	0	0	1	2
125	0	0	0	0	0
126	1	0	0	1	1
127	0	0	0	0	1
128	0	0	0	0	1
129	0	0	1	0	1
130	0	0	0	0	1
131	0	0	0	0	0

Table 15 (Continued). 0013-2-2a Averaging Smoothing Histogram Data

Grayscale	3	5	7	9	11
132	0	0	0	1	0
133	0	0	0	0	0
134	0	0	0	0	0
135	0	0	0	0	1
136	0	0	0	0	0
137	0	0	0	0	0
138	0	0	0	0	0
139	0	0	1	0	0
140	0	0	0	0	1
141	0	0	0	0	0
142	0	0	0	0	0
143	0	0	0	0	0
144	0	0	0	0	0
145	0	1	0	0	0
146	0	0	0	0	0
147	0	0	0	0	0
148	0	0	0	0	0
149	0	0	0	1	0
150	0	0	0	0	0
151	0	0	0	0	0
152	0	0	0	0	0
153	0	0	0	0	0
154	0	0	1	0	0
155	0	0	0	0	1
156	0	0	0	0	0
157	0	0	0	0	0
158	0	0	0	0	0
159	0	0	0	0	0
160	0	0	0	0	0
161	0	0	0	1	0
162	0	0	0	0	0
163	0	0	0	0	0
164	0	0	0	0	0
165	0	0	0	0	0
166	0	0	0	0	1
167	0	0	0	0	0
168	0	0	0	0	0
169	0	0	0	0	0
170	0	0	0	0	0
171	0	0	0	0	0
172	0	0	0	0	0
173	0	0	0	0	0
174	0	0	0	0	0
175	0	0	0	0	0

Table 15 (Continued). 0013-2-2a Averaging Smoothing Histogram Data

Grayscale	3	5	7	9	11
176	0	0	0	0	0
177	0	0	0	0	0
178	0	0	0	0	0
179	0	0	0	0	0
180	0	0	0	0	0
181	0	0	0	0	0
182	0	0	0	0	0
183	0	0	0	0	0
184	0	0	0	0	0
185	0	0	0	0	0
186	0	0	0	0	0
187	0	0	0	0	0
188	0	0	0	0	0
189	0	0	0	0	0
190	0	0	0	0	0
191	0	0	0	0	0
192	0	0	0	0	0
193	0	0	0	0	0
194	0	0	0	0	0
195	0	0	0	0	0
196	0	0	0	0	0
197	0	0	0	0	0
198	0	0	0	0	0
199	0	0	0	0	0
200	0	0	0	0	0
201	0	0	0	0	0
202	0	0	0	0	0
203	0	0	0	0	0
204	0	0	0	0	0
205	0	0	0	0	0
206	0	0	0	0	0
207	0	0	0	0	0
208	0	0	0	0	0
209	0	0	0	0	0
210	0	0	0	0	0
211	0	0	0	0	0
212	0	0	0	0	0
213	0	0	0	0	0
214	0	0	0	0	0
215	0	0	0	0	0
216	0	0	0	0	0
217	0	0	0	0	0
218	0	0	0	0	0
219	0	0	0	0	0

Table 15 (Continued). 0013-2-2a Averaging Smoothing Histogram Data

Grayscale	3	5	7	9	11
220	0	0	0	0	0
221	0	0	0	0	0
222	0	0	0	0	0
223	0	0	0	0	0
224	0	0	0	0	0
225	0	0	0	0	0
226	0	0	0	0	0
227	0	0	0	0	0
228	0	0	0	0	0
229	0	0	0	0	0
230	0	0	0	0	0
231	0	0	0	0	0
232	0	0	0	0	0
233	0	0	0	0	0
234	0	0	0	0	0
235	0	0	0	0	0
236	0	0	0	0	0
237	0	0	0	0	0
238	0	0	0	0	0
239	0	0	0	0	0
240	0	0	0	0	0
241	0	0	0	0	0
242	0	0	0	0	0
243	0	0	0	0	0
244	0	0	0	0	0
245	0	0	0	0	0
246	0	0	0	0	0
247	0	0	0	0	0
248	0	0	0	0	0
249	0	0	0	0	0
250	0	0	0	0	0
251	0	0	0	0	0
252	0	0	0	0	0
253	0	0	0	0	0
254	0	0	0	0	0
255	0	0	0	0	0
Min:	0	0	0	0	0
μ:	900	900	900	900	900
Max:	120794	117420	116644	116589	116281
Median:	0	0	0	0	1
σ:	7764.7	7473.1	7399.2	7380.7	7347.6
% Black:	52.43%	50.96%	50.63%	50.60%	50.47%
% Gray:	47.57%	49.04%	49.37%	49.40%	49.53%

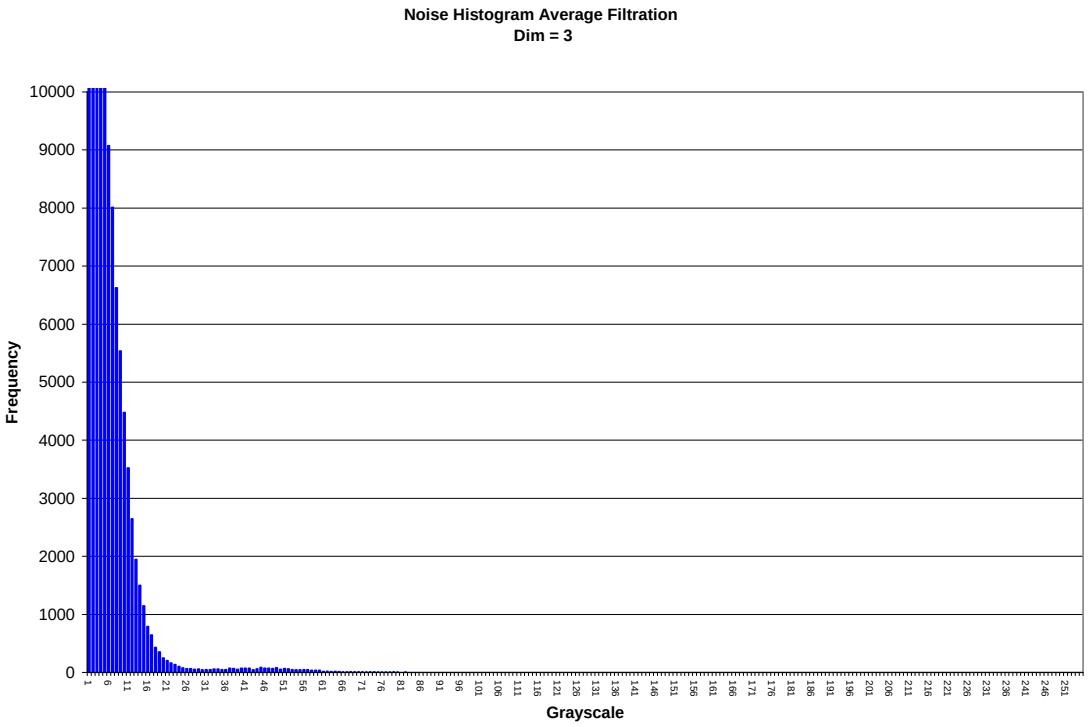


Figure 55. 0013-2-2a Averaging Smoothing Histogram, 3 x 3 kernel

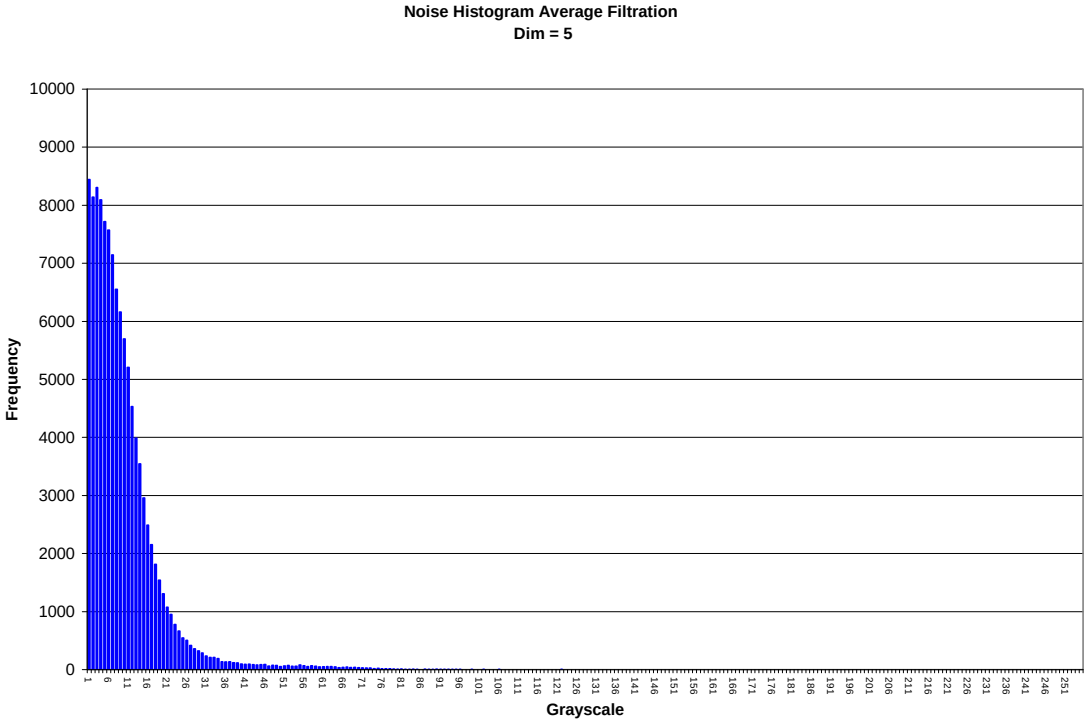


Figure 56. 0013-2-2a Averaging Smoothing Histogram, 5 x 5 kernel

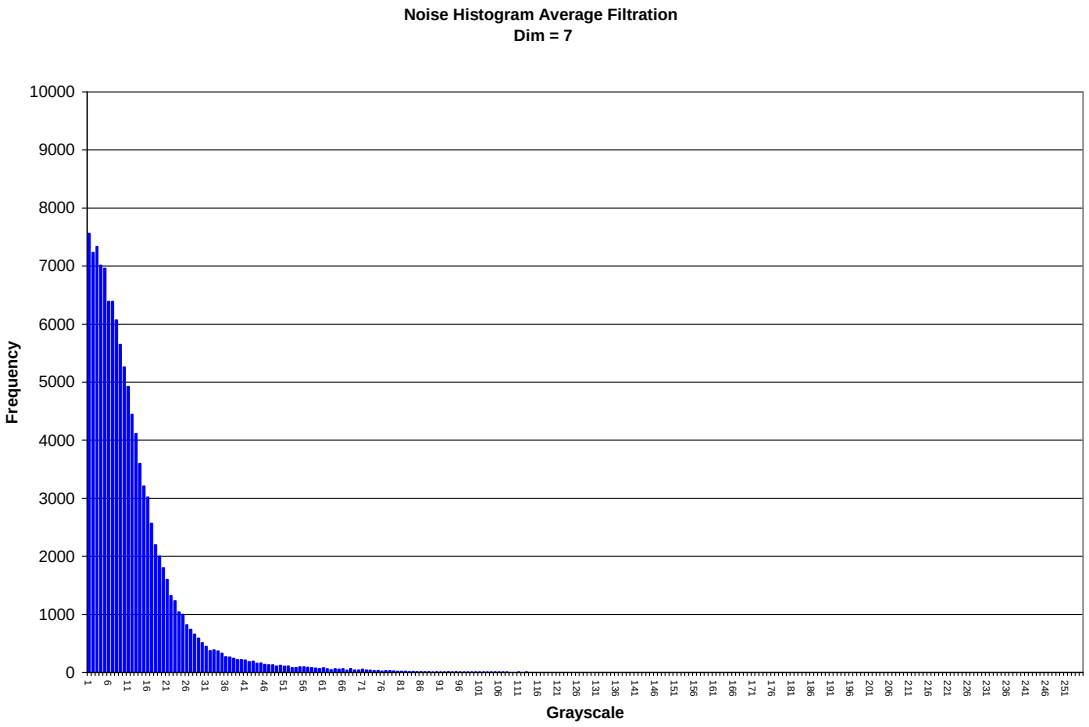


Figure 57. 0013-2-2a Averaging Smoothing Histogram, 7 x 7 kernel

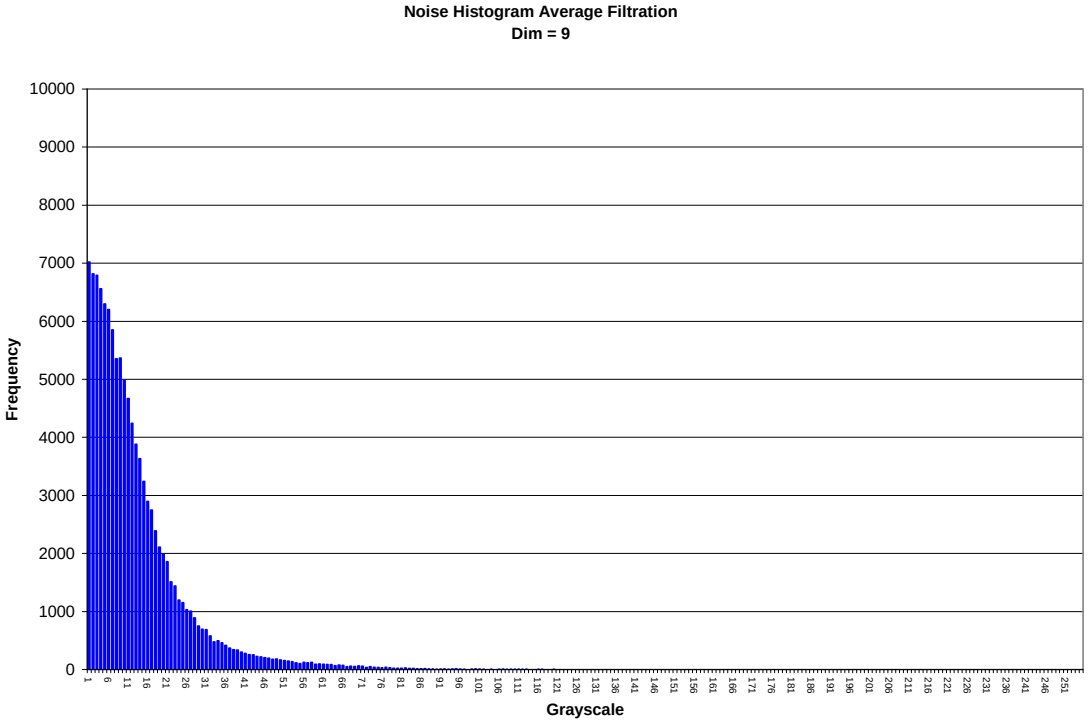


Figure 58. 0013-2-2a Averaging Smoothing Histogram, 9 x 9 kernel

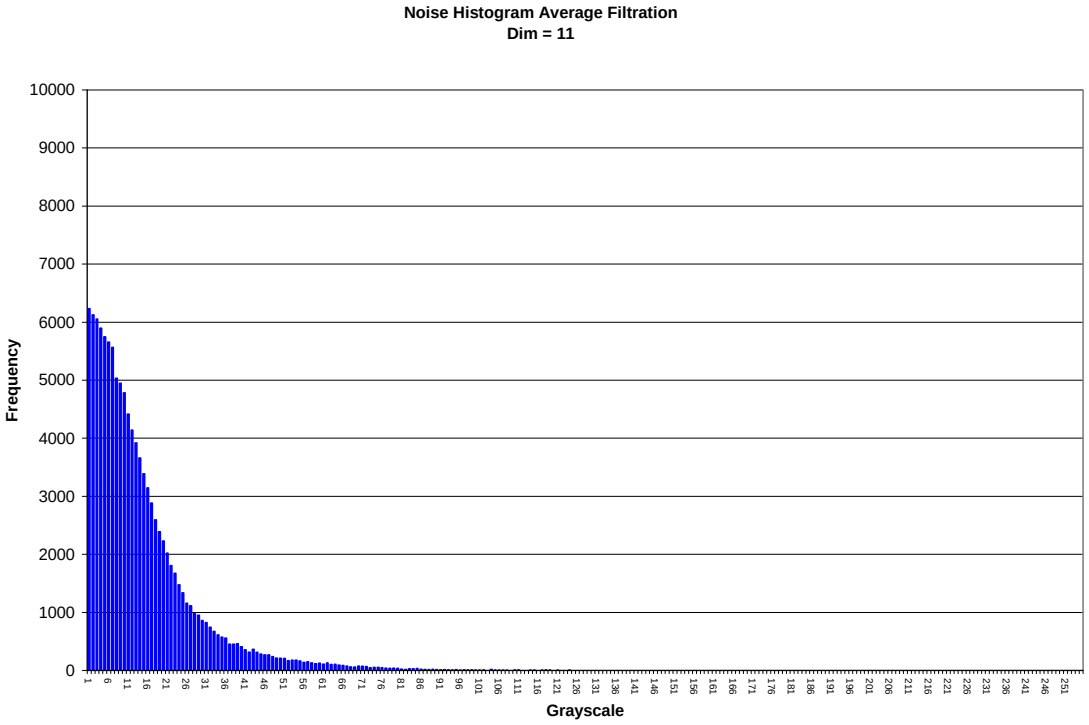


Figure 59. 0013-2-2a Averaging Smoothing Histogram, 11 x 11 kernel

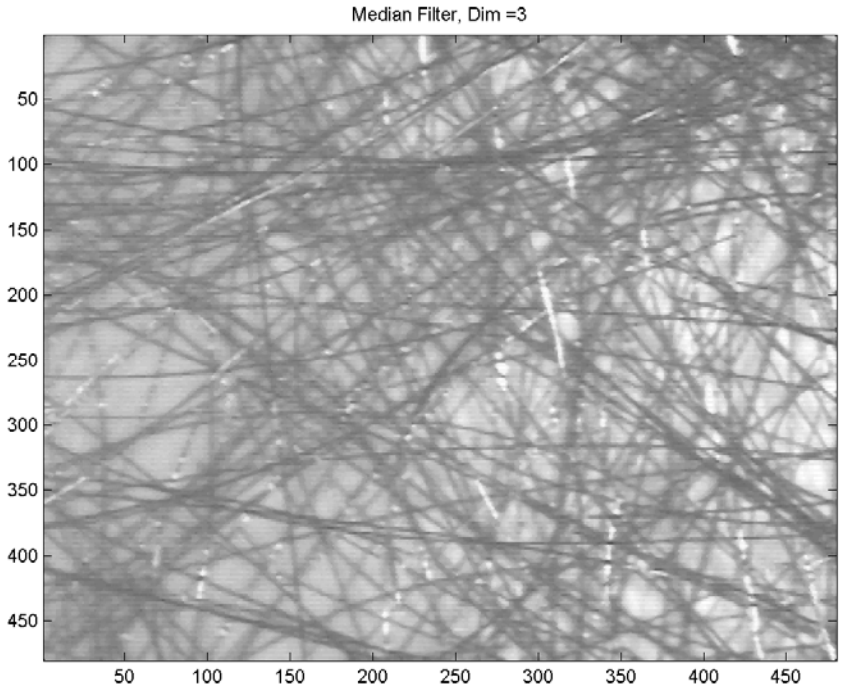


Figure 60. 0013-2-2a Median Smoothing, 3 x 3 kernel

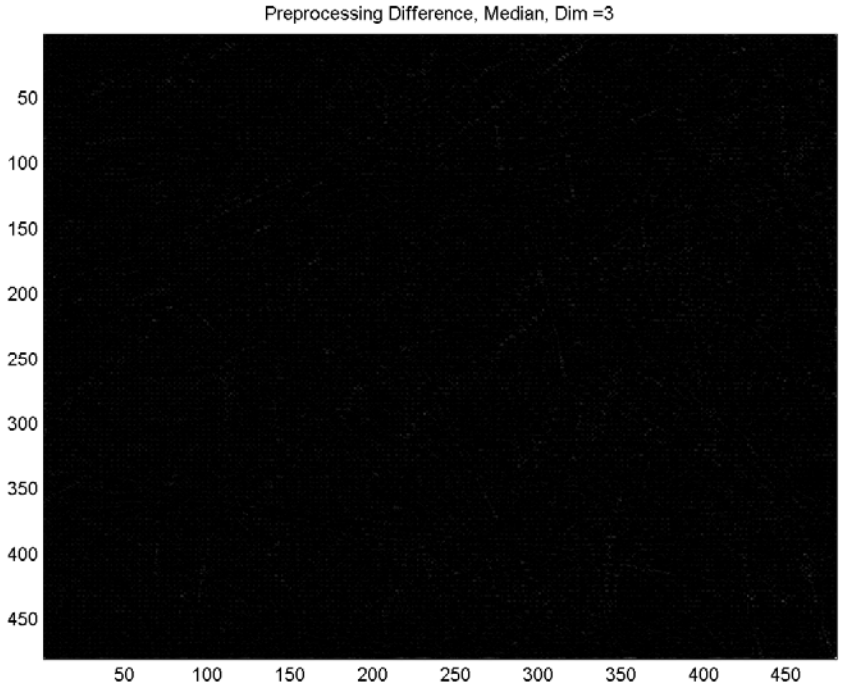


Figure 61. 0013-2-2a Median Smoothing Noise, 3 x 3 kernel

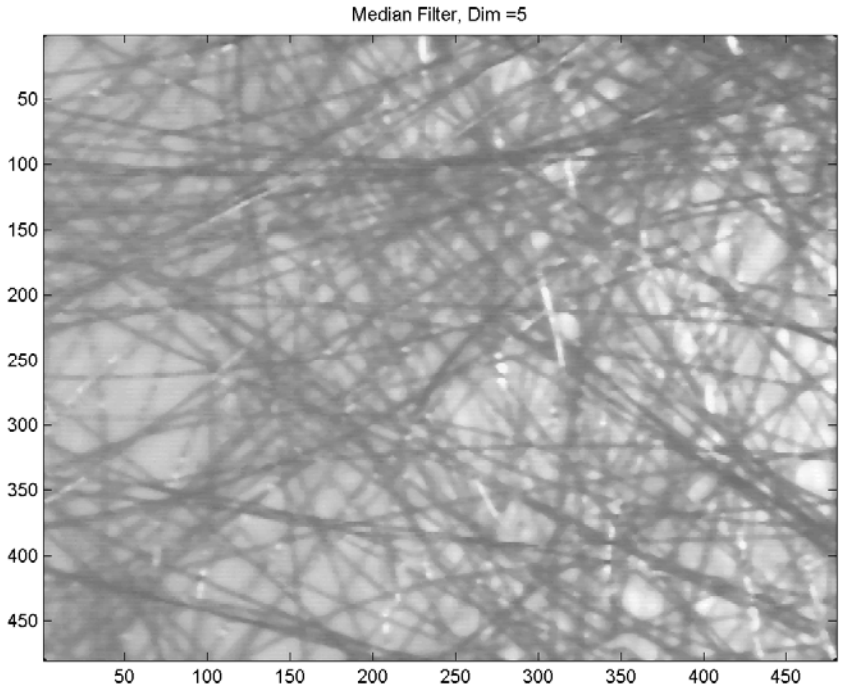


Figure 62. 0013-2-2a Median Smoothing, 5 x 5 kernel

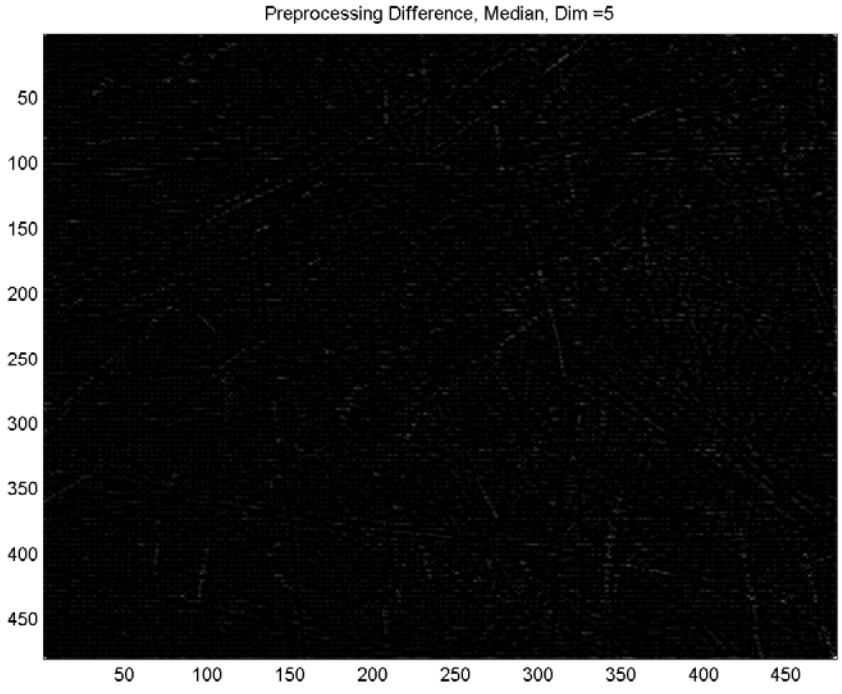


Figure 63. 0013-2-2a Median Smoothing Noise, 5 x 5 kernel

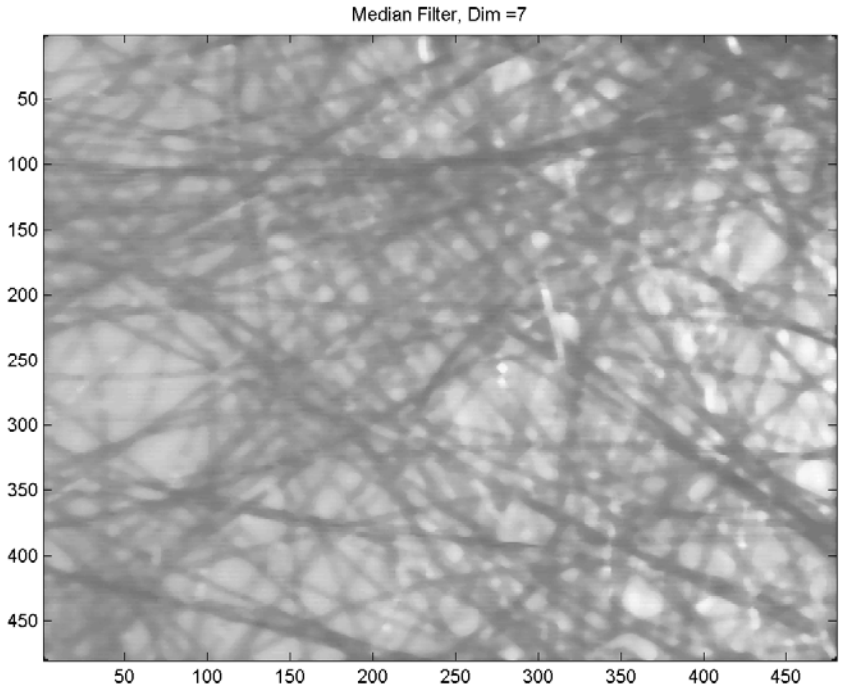


Figure 64. 0013-2-2a Median Smoothing, 7 x 7 kernel

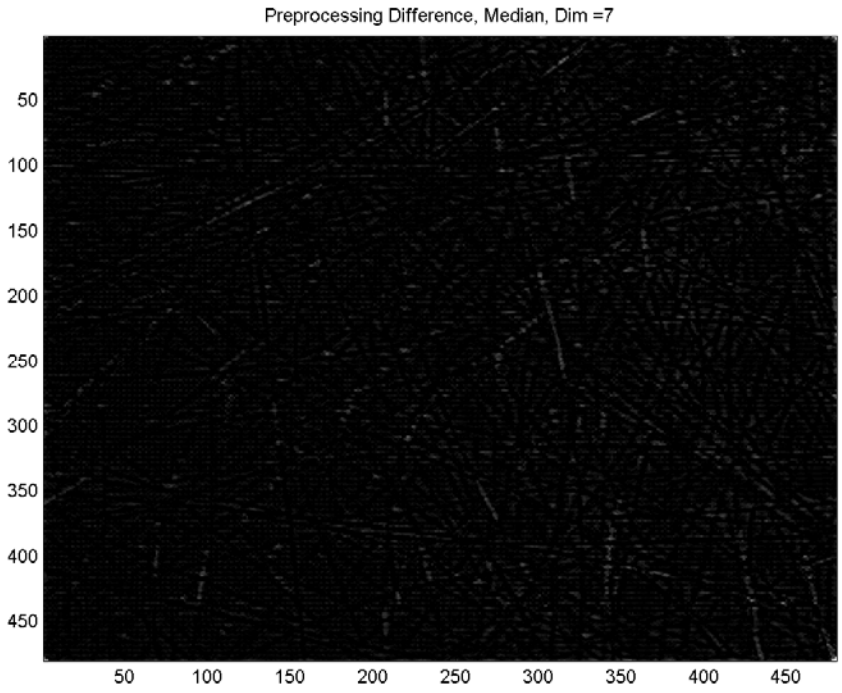


Figure 65. 0013-2-2a Median Smoothing Noise, 7 x 7 kernel

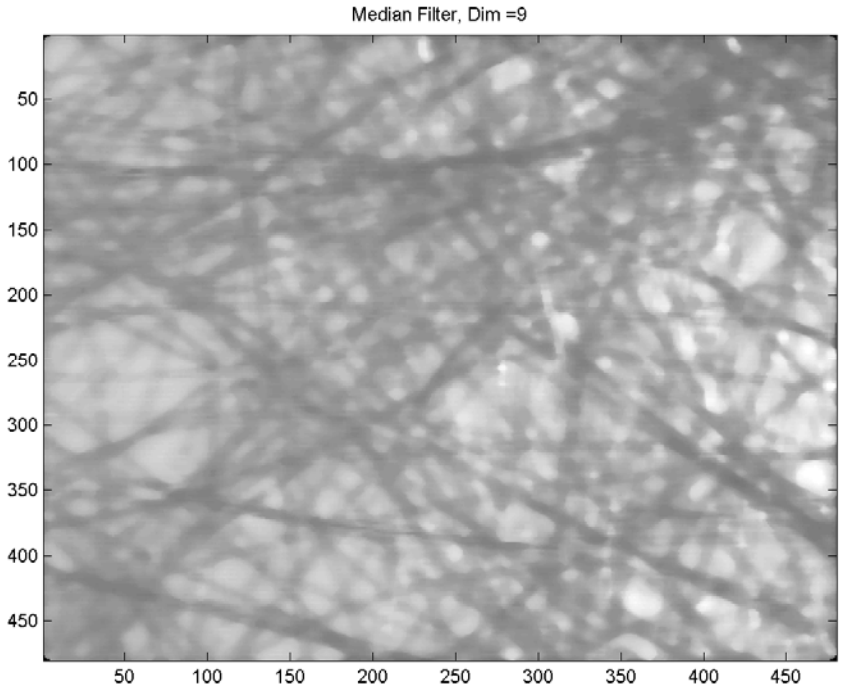


Figure 66. 0013-2-2a Median Smoothing, 9 x 9 kernel

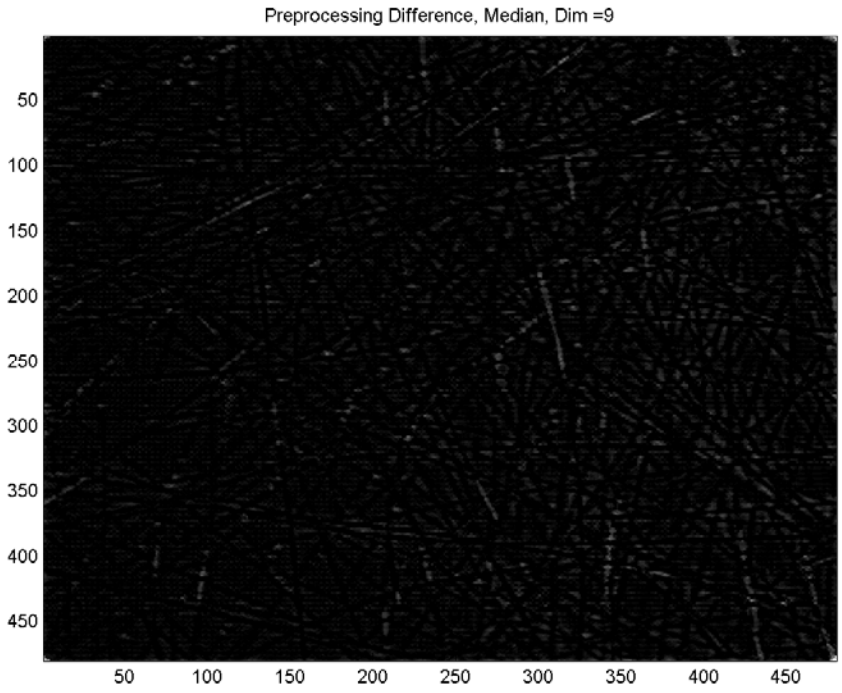


Figure 67. 0013-2-2a Median Smoothing Noise, 9 x 9 kernel

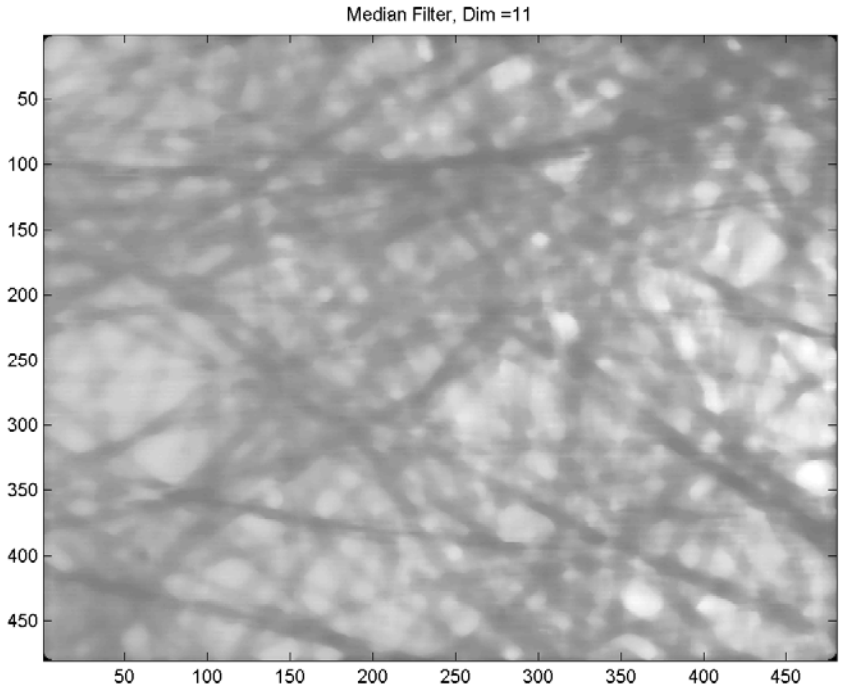


Figure 68. 0013-2-2a Median Smoothing, 11 x 11 kernel

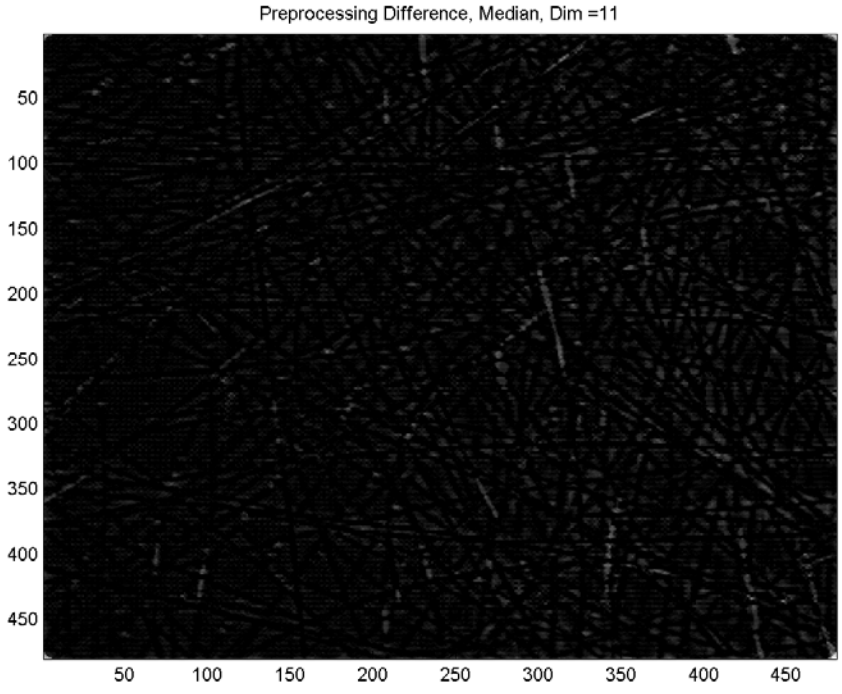


Figure 69. 0013-2-2a Median Smoothing Noise, 11 x 11 kernel

Table 16. 0013-2-2a Median Smoothing Histogram Data

Grayscale	3	5	7	9	11
0	139867	122735	118937	117443	116563
1	11531	8334	7861	7567	6749
2	10971	8274	7659	7524	6742
3	10278	8329	7573	7190	6678
4	9396	8090	7432	7177	6469
5	8388	7776	7200	6839	6245
6	7371	7423	6875	6535	6231
7	6454	7136	6642	6393	5980
8	5228	6436	6218	5762	5499
9	4413	6109	5771	5478	5262
10	3582	5509	5332	5053	4943
11	2932	4894	4936	4737	4755
12	2342	4378	4519	4366	4281
13	1697	3789	3844	3924	3911
14	1309	3240	3579	3642	3769
15	1040	2748	3061	3069	3355
16	743	2283	2728	2801	3076
17	571	2009	2446	2485	2745
18	432	1584	2059	2280	2532
19	325	1382	1777	2034	2251
20	285	1137	1602	1799	1988
21	213	957	1417	1586	1899
22	165	855	1248	1444	1701
23	123	702	1039	1267	1442
24	122	538	936	1148	1337
25	91	462	814	1020	1259
26	90	432	765	913	1115
27	65	337	633	796	999
28	64	320	578	763	910
29	49	272	491	652	862
30	30	243	421	596	725
31	32	185	398	546	638
32	27	191	371	502	630
33	18	130	279	448	545
34	13	134	290	428	578
35	21	131	232	354	451
36	11	98	233	327	423
37	17	88	210	280	385
38	9	75	187	259	337
39	15	63	169	259	353
40	9	66	151	226	282
41	5	51	124	204	264
42	5	66	113	183	275
43	8	50	107	174	237

Table 16 (Continued). 0013-2-2a Median Smoothing Histogram Data

Grayscale	3	5	7	9	11
44	2	34	124	174	217
45	2	41	104	156	181
46	2	23	86	161	183
47	3	28	72	114	175
48	2	18	66	103	178
49	0	20	69	107	145
50	4	19	53	86	136
51	1	16	61	83	123
52	2	17	45	67	120
53	2	10	33	65	103
54	2	16	30	81	82
55	2	7	36	54	89
56	1	9	37	51	85
57	2	3	34	63	55
58	3	15	22	39	64
59	2	11	20	39	62
60	2	5	20	40	47
61	0	5	18	39	45
62	2	3	24	38	54
63	0	5	16	31	43
64	1	5	23	27	47
65	0	2	9	28	39
66	0	2	12	20	44
67	0	0	10	22	21
68	0	2	5	17	37
69	0	6	10	14	25
70	0	2	8	15	26
71	1	4	9	19	22
72	0	0	6	18	17
73	0	2	3	11	19
74	0	1	6	12	20
75	0	3	4	12	19
76	1	1	5	8	16
77	0	0	5	4	15
78	0	0	3	11	15
79	0	0	4	5	13
80	0	2	2	3	15
81	0	1	2	6	8
82	0	3	0	4	12
83	0	1	2	4	5
84	0	1	2	5	3
85	0	0	1	1	3
86	0	0	5	2	5
87	0	0	2	3	4

Table 16 (Continued). 0013-2-2a Median Smoothing Histogram Data

Grayscale	3	5	7	9	11
88	0	1	1	4	2
89	0	0	1	1	2
90	0	2	2	2	8
91	0	0	1	2	2
92	0	0	2	1	2
93	0	0	0	1	2
94	0	0	1	1	0
95	0	0	1	2	0
96	0	0	0	3	5
97	0	0	0	2	2
98	0	1	0	0	0
99	0	0	2	0	1
100	0	0	0	1	2
101	0	1	1	1	3
102	0	0	0	1	0
103	0	0	0	3	2
104	0	0	0	1	1
105	0	0	0	2	1
106	0	0	1	0	2
107	0	0	0	1	0
108	0	0	1	1	2
109	0	0	0	0	0
110	0	0	0	0	0
111	1	1	2	4	3
112	0	0	1	1	1
113	0	0	0	1	1
114	0	0	1	0	1
115	0	0	0	0	0
116	0	0	0	0	2
117	0	0	0	0	1
118	0	0	0	1	1
119	0	0	0	0	0
120	0	0	0	0	0
121	0	0	0	0	0
122	0	0	0	0	1
123	0	0	0	0	0
124	0	0	0	0	1
125	0	0	0	0	0
126	0	0	0	0	0
127	0	0	0	1	1
128	0	0	0	0	0
129	0	0	1	1	2
130	0	0	0	0	0
131	0	0	0	0	0

Table 16 (Continued). 0013-2-2a Median Smoothing Histogram Data

Grayscale	3	5	7	9	11
132	0	0	1	2	2
133	0	0	0	1	2
134	0	1	1	2	2
135	0	0	0	0	0
136	0	1	1	1	1
137	0	0	0	0	1
138	0	0	0	0	1
139	0	0	0	1	1
140	0	0	0	0	1
141	0	0	0	0	0
142	0	0	0	0	0
143	1	1	1	1	1
144	0	0	0	0	0
145	0	0	0	0	0
146	0	1	1	1	1
147	0	0	1	2	3
148	0	0	0	0	1
149	0	0	0	0	0
150	0	0	0	0	0
151	1	1	1	1	1
152	0	0	0	0	1
153	0	0	0	0	0
154	0	0	0	0	0
155	0	0	0	0	0
156	0	0	0	0	0
157	0	0	0	1	1
158	0	0	0	0	0
159	0	0	1	2	3
160	0	0	0	0	0
161	0	0	0	0	0
162	0	0	0	0	0
163	0	0	0	0	0
164	0	0	0	0	0
165	0	1	1	1	2
166	0	0	0	0	0
167	0	0	0	0	0
168	0	0	0	0	0
169	0	0	0	1	1
170	0	0	0	0	0
171	0	0	0	0	0
172	0	0	1	1	1
173	0	0	0	0	0
174	0	0	0	0	0
175	0	0	1	1	1

Table 16 (Continued). 0013-2-2a Median Smoothing Histogram Data

Grayscale	3	5	7	9	11
176	0	0	1	2	2
177	0	1	1	1	1
178	0	0	0	0	0
179	0	0	0	0	0
180	0	0	0	0	0
181	0	1	1	1	1
182	0	0	0	0	0
183	0	0	0	0	0
184	0	0	0	0	0
185	0	0	0	0	0
186	0	0	0	0	0
187	0	0	0	0	0
188	0	0	0	0	0
189	0	0	0	0	1
190	0	0	0	0	0
191	0	0	0	1	1
192	0	0	0	0	0
193	0	0	0	0	0
194	0	0	0	0	1
195	0	0	0	0	0
196	0	0	0	0	0
197	0	0	0	0	0
198	0	0	0	0	1
199	0	0	0	0	0
200	0	0	0	0	0
201	0	0	0	0	0
202	0	0	0	0	0
203	0	0	0	0	0
204	0	0	0	0	0
205	0	0	0	0	0
206	0	0	0	0	0
207	0	0	0	0	0
208	0	0	0	0	0
209	0	0	0	0	0
210	0	1	1	1	1
211	0	0	0	0	0
212	0	0	0	0	0
213	0	0	0	0	0
214	0	0	0	0	0
215	1	1	1	1	1
216	0	0	0	0	0
217	0	0	0	0	0
218	0	0	0	0	0
219	0	0	0	0	0

Table 16 (Continued). 0013-2-2a Median Smoothing Histogram Data

Grayscale	3	5	7	9	11
220	0	0	0	0	0
221	0	0	0	0	0
222	0	0	0	0	0
223	0	0	0	0	0
224	0	0	0	0	0
225	0	0	0	0	0
226	0	0	0	0	0
227	0	0	0	0	0
228	0	0	0	0	0
229	0	0	0	0	0
230	0	0	0	0	0
231	0	0	0	0	0
232	0	0	0	0	0
233	0	0	0	0	0
234	0	0	0	0	0
235	0	0	0	0	0
236	0	0	0	0	0
237	0	0	0	0	0
238	0	0	0	0	0
239	0	0	0	0	0
240	0	0	0	0	0
241	0	0	0	0	0
242	0	0	0	0	0
243	0	0	0	0	0
244	0	0	0	0	0
245	0	0	0	0	0
246	0	0	0	0	0
247	0	0	0	0	0
248	0	0	0	0	0
249	0	0	0	0	0
250	0	0	0	0	0
251	0	0	0	0	0
252	0	0	0	0	0
253	0	0	0	0	0
254	0	0	0	0	0
255	0	0	0	0	0
Min:	0	0	0	0	0
μ:	900	900	900	900	900
Max:	139867	122735	118937	117443	116563
Median:	0	0	0	1	1
σ:	8867.166	7796.095	7548.319	7446.788	7379.402
% Black:	60.71%	53.27%	51.62%	50.97%	50.59%
% Gray:	39.29%	46.73%	48.38%	49.03%	49.41%

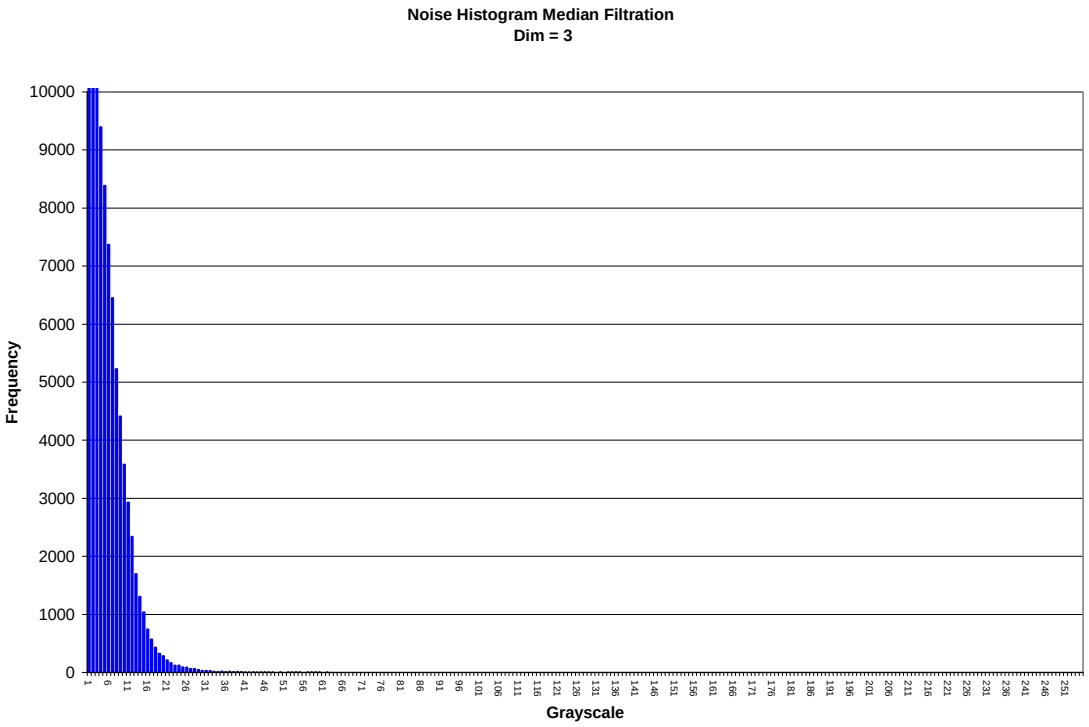


Figure 70. 0013-2-2a Median Smoothing Histogram, 3 x 3 kernel

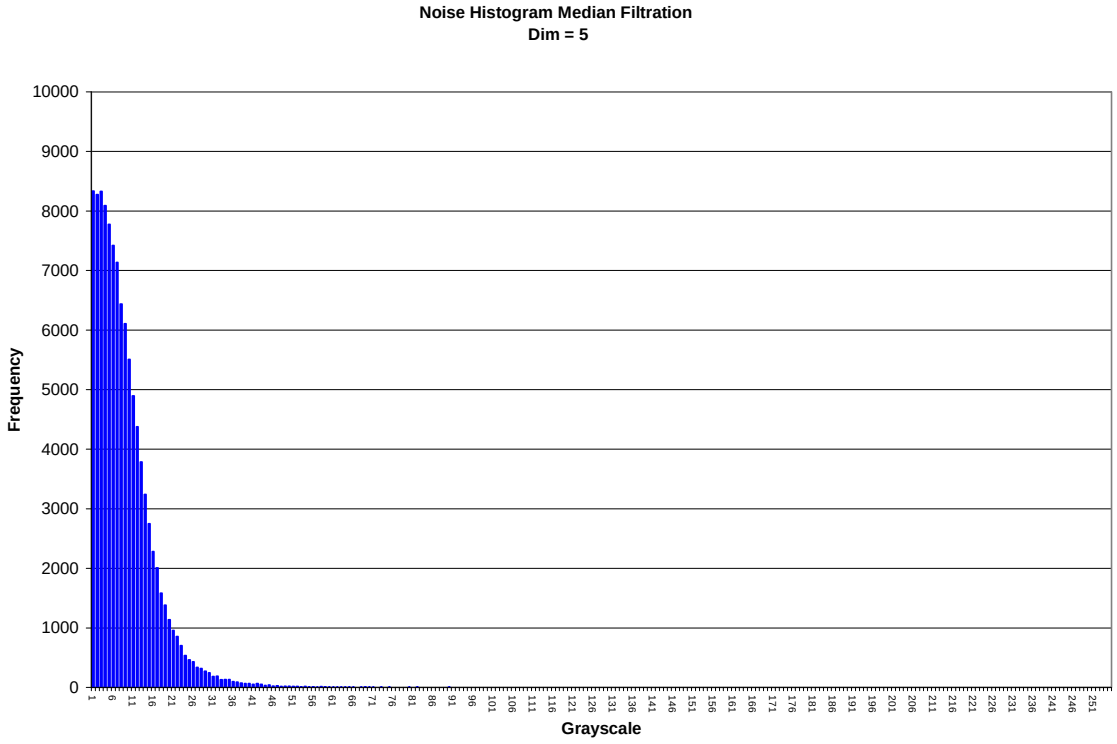


Figure 71. 0013-2-2a Median Smoothing Histogram, 5 x 5 kernel

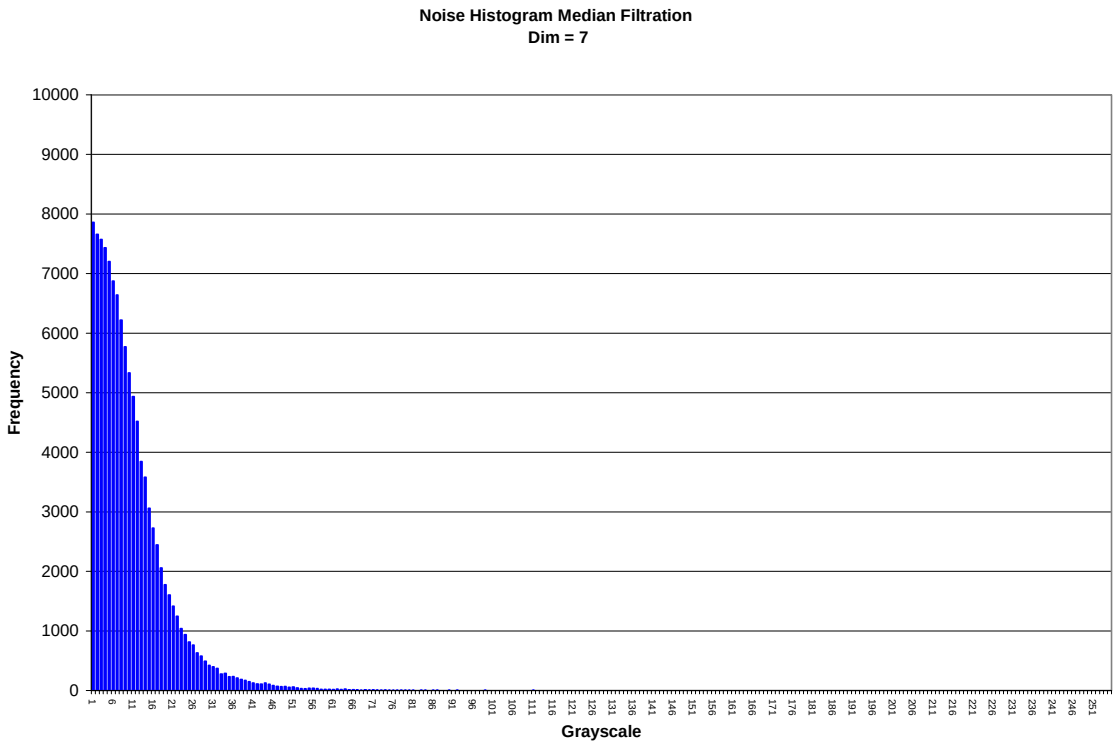


Figure 72. 0013-2-2a Median Smoothing Histogram, 7 x 7 kernel

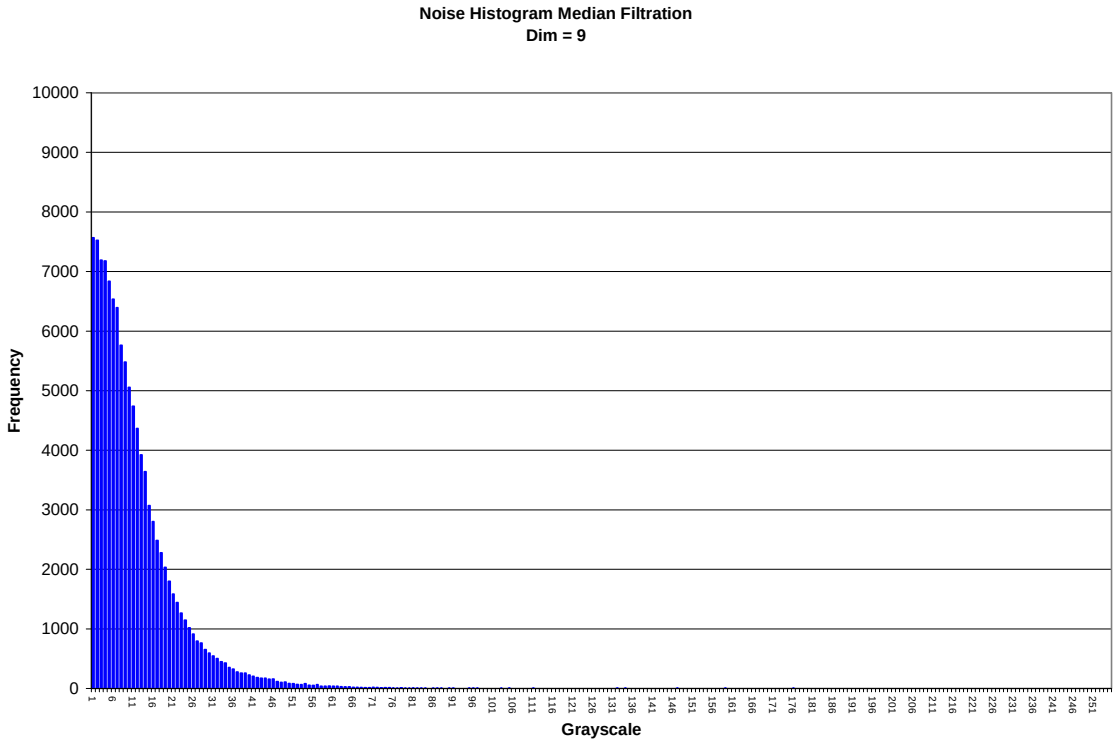


Figure 73. 0013-2-2a Median Smoothing Histogram, 9 x 9 kernel

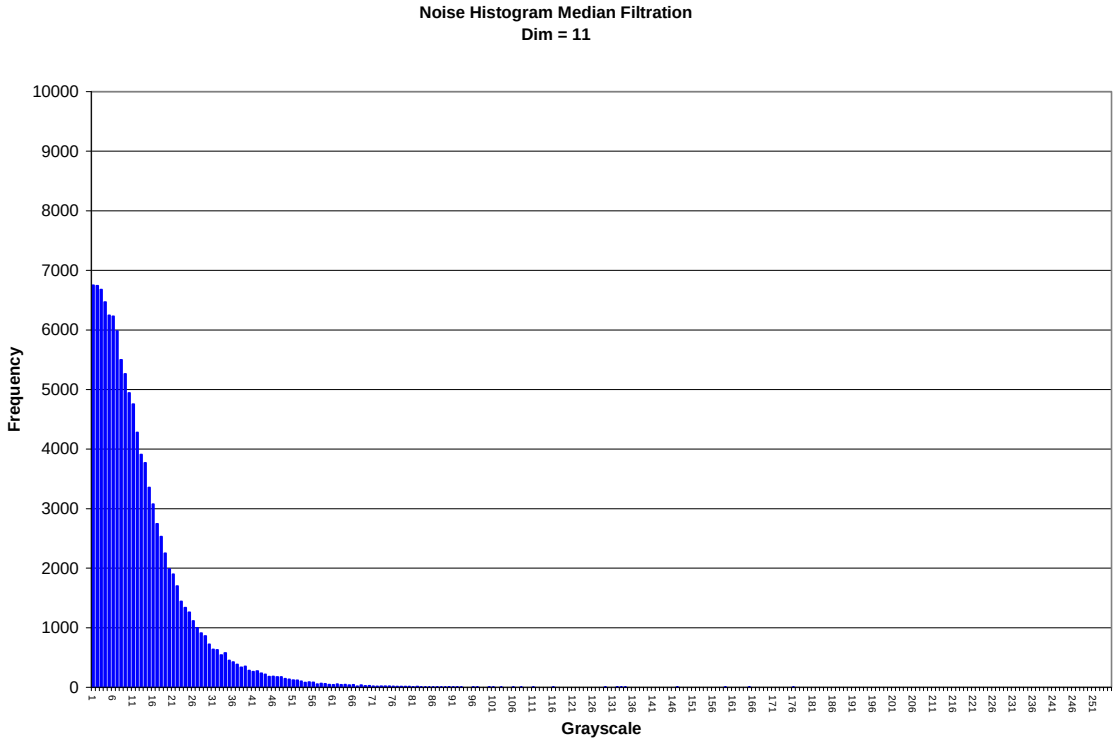


Figure 74. 0013-2-2a Median Smoothing Histogram, 11 x 11 kernel

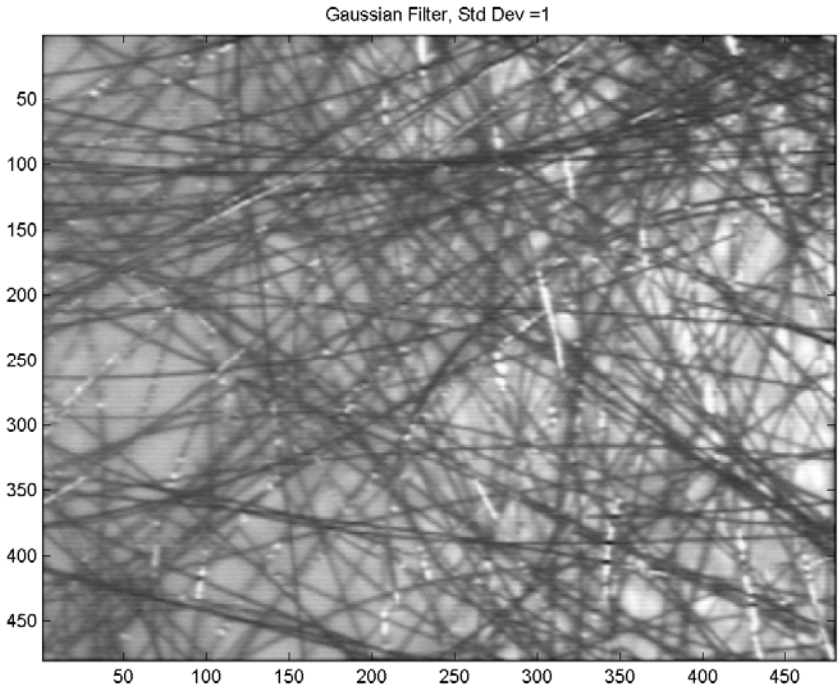


Figure 75. 0013-2-2a Gaussian Smoothing, σ = 1.00 kernel

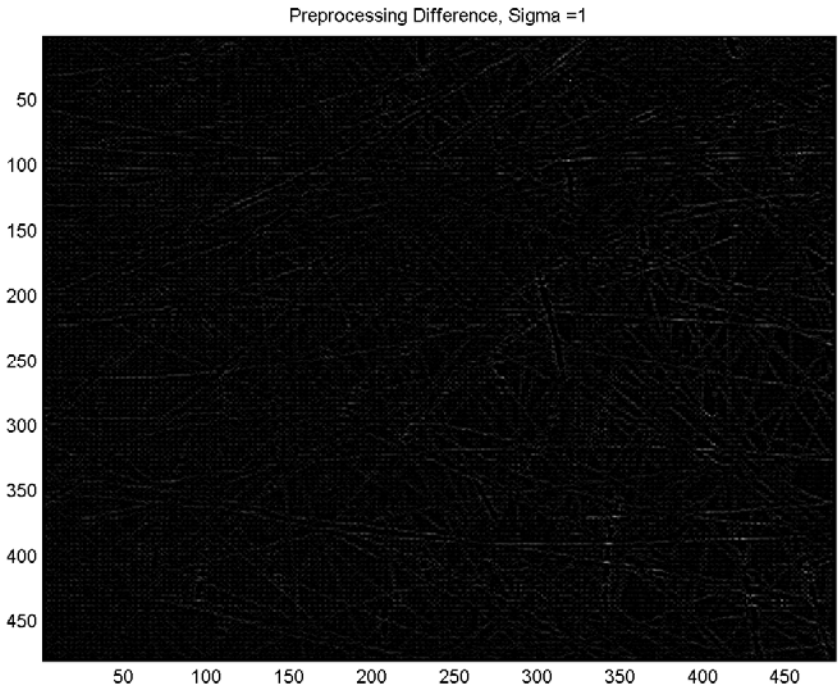


Figure 76. 0013-2-2a Gaussian Smoothing Noise, σ = 1.00 kernel

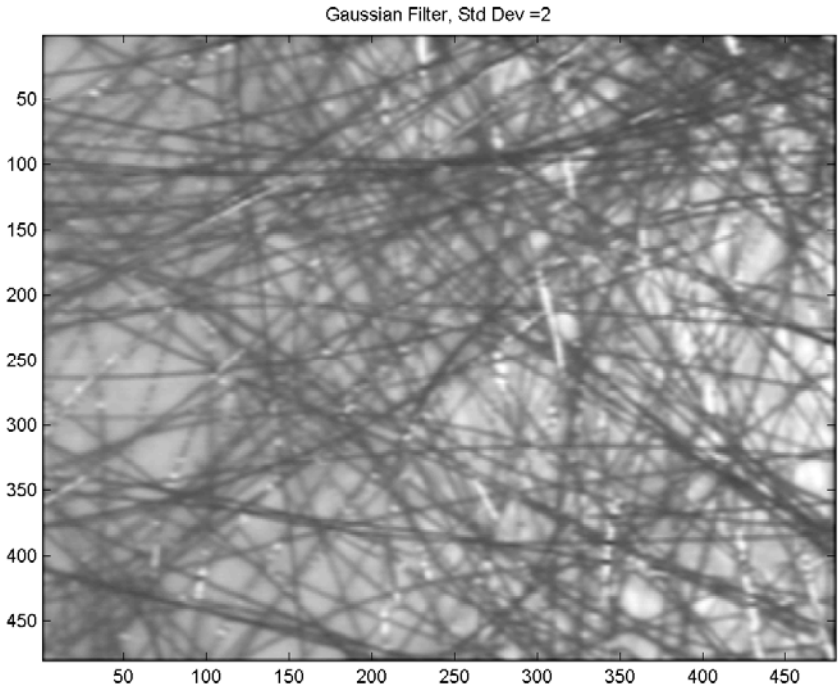


Figure 77. 0013-2-2a Gaussian Smoothing, σ = 2.00 kernel

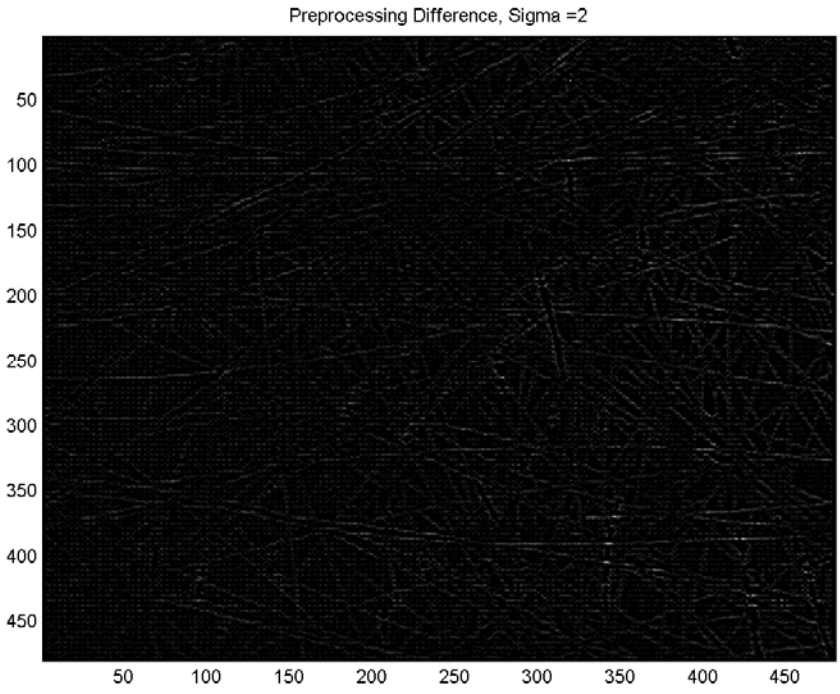


Figure 78. 0013-2-2a Gaussian Smoothing Noise, σ = 2.00 kernel

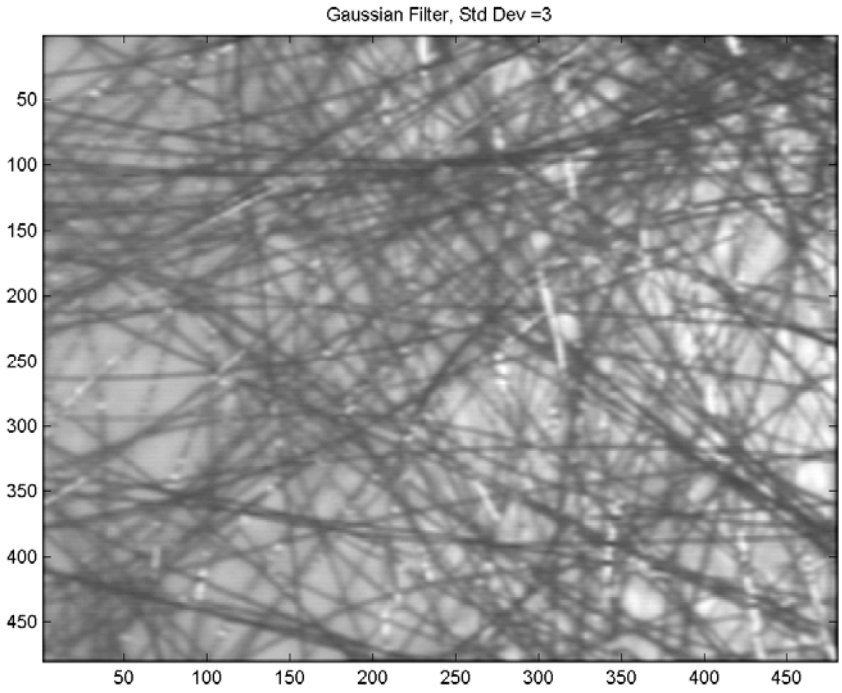


Figure 79. 0013-2-2a Gaussian Smoothing, σ = 3.00 kernel

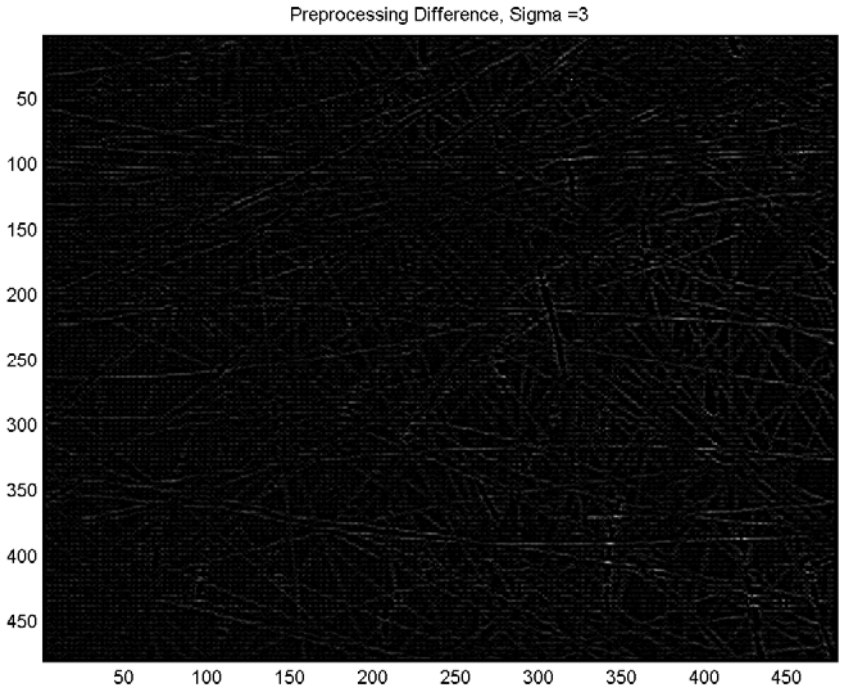


Figure 80. 0013-2-2a Gaussian Smoothing Noise, σ = 3.00 kernel

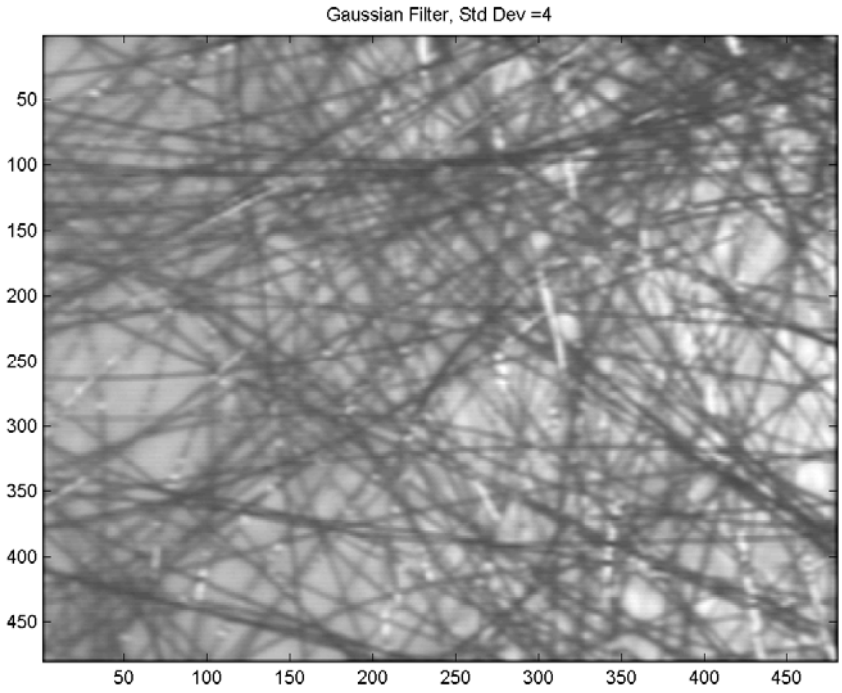


Figure 81. 0013-2-2a Gaussian Smoothing, σ = 4.00 kernel

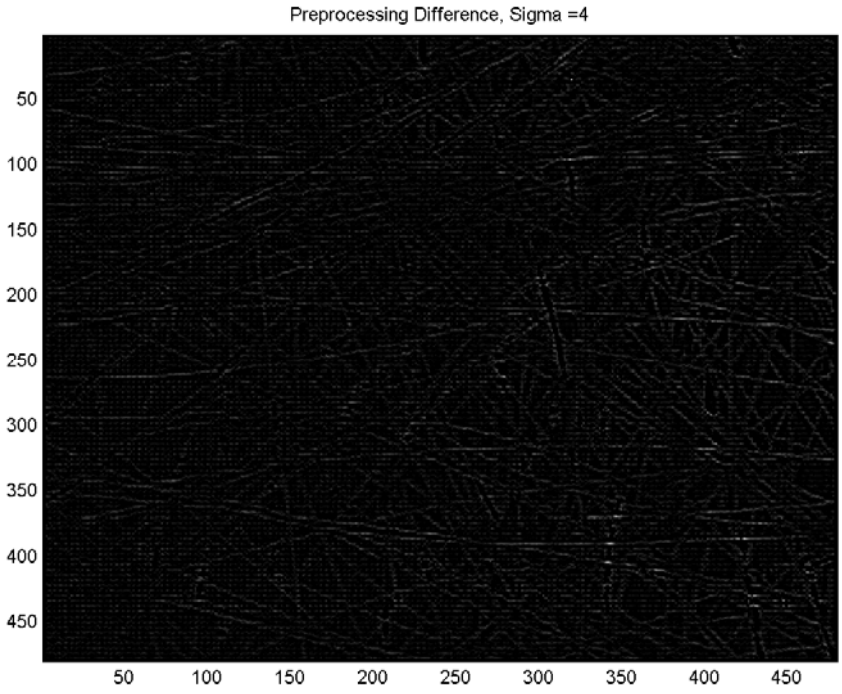


Figure 82. 0013-2-2a Gaussian Smoothing Noise, σ = 4.00 kernel

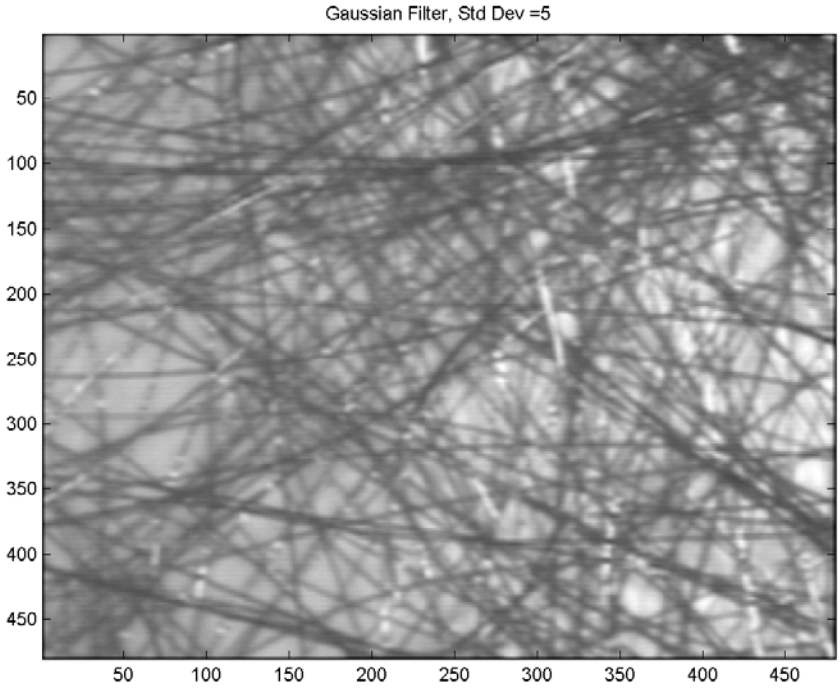


Figure 83. 0013-2-2a Gaussian Smoothing, σ = 5.00 kernel

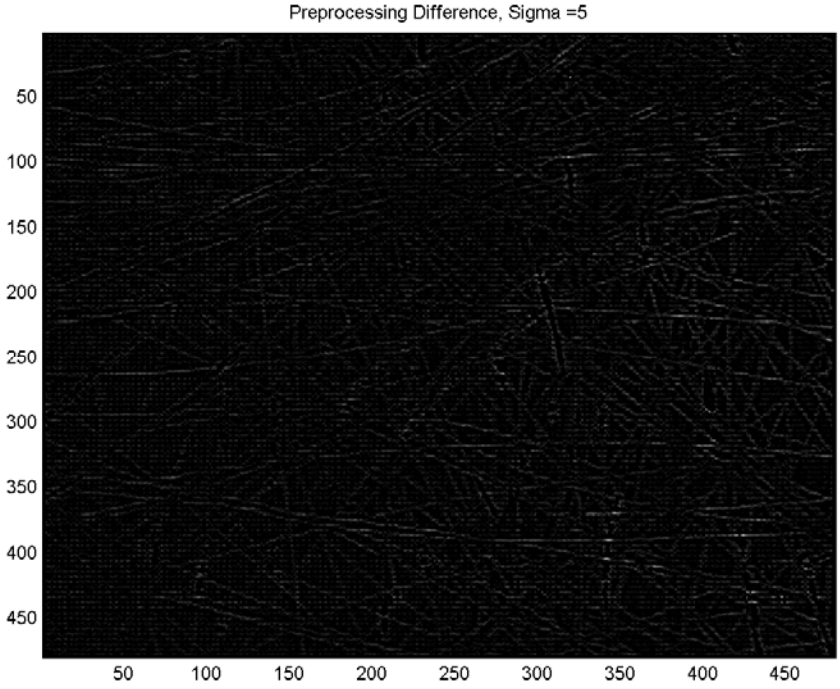


Figure 84. 0013-2-2a Gaussian Smoothing Noise, σ = 5.00 kernel

Table 17. 0013-2-2a Gaussian Smoothing Histogram Data

Grayscale	1	2	3	4	5
0	123465	121824	121528	121386	121344
1	12672	9297	8758	8662	8588
2	12295	9261	8697	8515	8417
3	11693	8877	8542	8365	8306
4	10814	8636	8228	8063	7969
5	9811	8463	8018	7860	7806
6	8927	7942	7639	7591	7592
7	7639	7113	7235	7234	7226
8	6656	6794	6571	6553	6586
9	5576	6075	6131	6116	6024
10	4536	5398	5470	5492	5508
11	3843	4870	4930	4928	4983
12	2930	4230	4425	4492	4496
13	2314	3581	3767	3838	3836
14	1675	3073	3292	3324	3369
15	1342	2640	2791	2895	2898
16	1084	2218	2417	2457	2523
17	777	1764	2010	2137	2130
18	559	1472	1618	1672	1736
19	439	1264	1434	1453	1454
20	300	1032	1191	1240	1262
21	216	833	1027	1059	1107
22	196	758	808	890	891
23	143	549	677	732	780
24	116	422	590	602	610
25	77	360	462	491	505
26	66	290	347	403	421
27	43	210	291	319	327
28	38	218	251	258	254
29	27	149	188	201	237
30	25	149	175	194	192
31	16	101	152	138	153
32	12	91	132	163	144
33	9	73	84	104	127
34	8	57	92	80	77
35	5	53	61	84	96
36	8	36	58	62	60
37	9	38	51	52	49
38	6	25	27	40	53
39	2	27	45	32	27
40	2	22	21	39	41
41	3	15	24	21	24
42	1	14	22	23	24
43	4	6	18	23	23

Table 17 (Continued). 0013-2-2a Gaussian Smoothing Histogram Data

Grayscale	3	5	7	9	11
44	3	6	18	13	16
45	2	5	6	19	20
46	1	9	4	4	6
47	2	6	3	5	5
48	0	6	13	4	3
49	0	7	6	10	9
50	1	2	7	8	11
51	4	1	2	6	4
52	0	4	5	2	5
53	0	3	2	4	2
54	1	3	3	4	6
55	1	3	3	2	2
56	0	2	2	2	2
57	2	1	1	3	1
58	0	1	4	1	3
59	1	1	3	4	1
60	0	0	3	4	5
61	0	3	0	2	4
62	0	2	0	0	0
63	1	0	1	0	0
64	0	0	1	1	1
65	0	2	3	1	0
66	1	1	1	3	1
67	0	1	0	1	4
68	0	0	0	0	0
69	0	1	1	0	0
70	0	3	0	1	0
71	0	0	1	0	1
72	0	0	3	0	0
73	0	1	1	4	1
74	0	0	0	1	3
75	0	1	1	0	1
76	0	0	0	0	0
77	0	0	1	1	1
78	0	1	0	1	0
79	0	0	0	0	1
80	0	1	0	0	0
81	0	0	1	0	0
82	0	0	1	0	0
83	0	0	0	2	0
84	0	0	0	0	2
85	0	0	1	0	0
86	0	0	0	1	0
87	0	0	0	0	1

Table 17 (Continued). 0013-2-2a Gaussian Smoothing Histogram Data

Grayscale	3	5	7	9	11
88	0	0	0	0	0
89	0	0	0	0	0
90	0	0	0	0	0
91	0	0	0	0	0
92	0	1	0	0	0
93	0	1	0	0	0
94	0	0	0	0	0
95	0	0	0	0	0
96	0	0	0	0	0
97	0	0	0	0	0
98	0	0	1	0	0
99	0	0	1	0	0
100	1	0	0	1	0
101	0	0	0	1	1
102	0	0	0	0	1
103	0	0	0	0	0
104	0	0	0	0	0
105	0	0	0	0	0
106	0	0	0	0	0
107	0	0	0	0	0
108	0	0	0	0	0
109	0	0	0	0	0
110	0	0	0	0	0
111	0	0	0	0	0
112	0	0	0	0	0
113	0	0	0	0	0
114	0	0	0	0	0
115	0	1	0	0	0
116	0	0	0	0	0
117	0	0	1	0	0
118	0	0	0	1	1
119	0	0	0	0	0
120	0	0	0	0	0
121	0	0	0	0	0
122	0	0	0	0	0
123	0	0	0	0	0
124	0	0	0	0	0
125	0	0	0	0	0
126	0	0	0	0	0
127	0	0	0	0	0
128	0	0	0	0	0
129	0	0	0	0	0
130	0	0	0	0	0
131	0	0	0	0	0

Table 17 (Continued). 0013-2-2a Gaussian Smoothing Histogram Data

Grayscale	3	5	7	9	11
132	0	0	0	0	0
133	0	0	0	0	0
134	0	0	0	0	0
135	0	0	0	0	0
136	0	0	0	0	0
137	0	0	0	0	0
138	0	0	0	0	0
139	0	0	0	0	0
140	0	0	0	0	0
141	0	0	0	0	0
142	0	0	0	0	0
143	0	0	0	0	0
144	0	0	0	0	0
145	0	0	0	0	0
146	0	0	0	0	0
147	0	0	0	0	0
148	0	0	0	0	0
149	0	0	0	0	0
150	0	0	0	0	0
151	0	0	0	0	0
152	0	0	0	0	0
153	0	0	0	0	0
154	0	0	0	0	0
155	0	0	0	0	0
156	0	0	0	0	0
157	0	0	0	0	0
158	0	0	0	0	0
159	0	0	0	0	0
160	0	0	0	0	0
161	0	0	0	0	0
162	0	0	0	0	0
163	0	0	0	0	0
164	0	0	0	0	0
165	0	0	0	0	0
166	0	0	0	0	0
167	0	0	0	0	0
168	0	0	0	0	0
169	0	0	0	0	0
170	0	0	0	0	0
171	0	0	0	0	0
172	0	0	0	0	0
173	0	0	0	0	0
174	0	0	0	0	0
175	0	0	0	0	0

Table 17 (Continued). 0013-2-2a Gaussian Smoothing Histogram Data

Grayscale	3	5	7	9	11
176	0	0	0	0	0
177	0	0	0	0	0
178	0	0	0	0	0
179	0	0	0	0	0
180	0	0	0	0	0
181	0	0	0	0	0
182	0	0	0	0	0
183	0	0	0	0	0
184	0	0	0	0	0
185	0	0	0	0	0
186	0	0	0	0	0
187	0	0	0	0	0
188	0	0	0	0	0
189	0	0	0	0	0
190	0	0	0	0	0
191	0	0	0	0	0
192	0	0	0	0	0
193	0	0	0	0	0
194	0	0	0	0	0
195	0	0	0	0	0
196	0	0	0	0	0
197	0	0	0	0	0
198	0	0	0	0	0
199	0	0	0	0	0
200	0	0	0	0	0
201	0	0	0	0	0
202	0	0	0	0	0
203	0	0	0	0	0
204	0	0	0	0	0
205	0	0	0	0	0
206	0	0	0	0	0
207	0	0	0	0	0
208	0	0	0	0	0
209	0	0	0	0	0
210	0	0	0	0	0
211	0	0	0	0	0
212	0	0	0	0	0
213	0	0	0	0	0
214	0	0	0	0	0
215	0	0	0	0	0
216	0	0	0	0	0
217	0	0	0	0	0
218	0	0	0	0	0
219	0	0	0	0	0

Table 17 (Continued). 0013-2-2a Gaussian Smoothing Histogram Data

Grayscale	3	5	7	9	11
220	0	0	0	0	0
221	0	0	0	0	0
222	0	0	0	0	0
223	0	0	0	0	0
224	0	0	0	0	0
225	0	0	0	0	0
226	0	0	0	0	0
227	0	0	0	0	0
228	0	0	0	0	0
229	0	0	0	0	0
230	0	0	0	0	0
231	0	0	0	0	0
232	0	0	0	0	0
233	0	0	0	0	0
234	0	0	0	0	0
235	0	0	0	0	0
236	0	0	0	0	0
237	0	0	0	0	0
238	0	0	0	0	0
239	0	0	0	0	0
240	0	0	0	0	0
241	0	0	0	0	0
242	0	0	0	0	0
243	0	0	0	0	0
244	0	0	0	0	0
245	0	0	0	0	0
246	0	0	0	0	0
247	0	0	0	0	0
248	0	0	0	0	0
249	0	0	0	0	0
250	0	0	0	0	0
251	0	0	0	0	0
252	0	0	0	0	0
253	0	0	0	0	0
254	0	0	0	0	0
255	0	0	0	0	0
Min:	0	0	0	0	0
μ:	900	900	900	900	900
Max:	123465	121824	121528	121386	121344
Median:	0	0	0	0	0
σ:	7913.195	7756.754	7729.796	7718.371	7714.465
% Black:	53.59%	52.88%	52.75%	52.68%	52.67%
% Gray:	46.41%	47.13%	47.25%	47.32%	47.33%

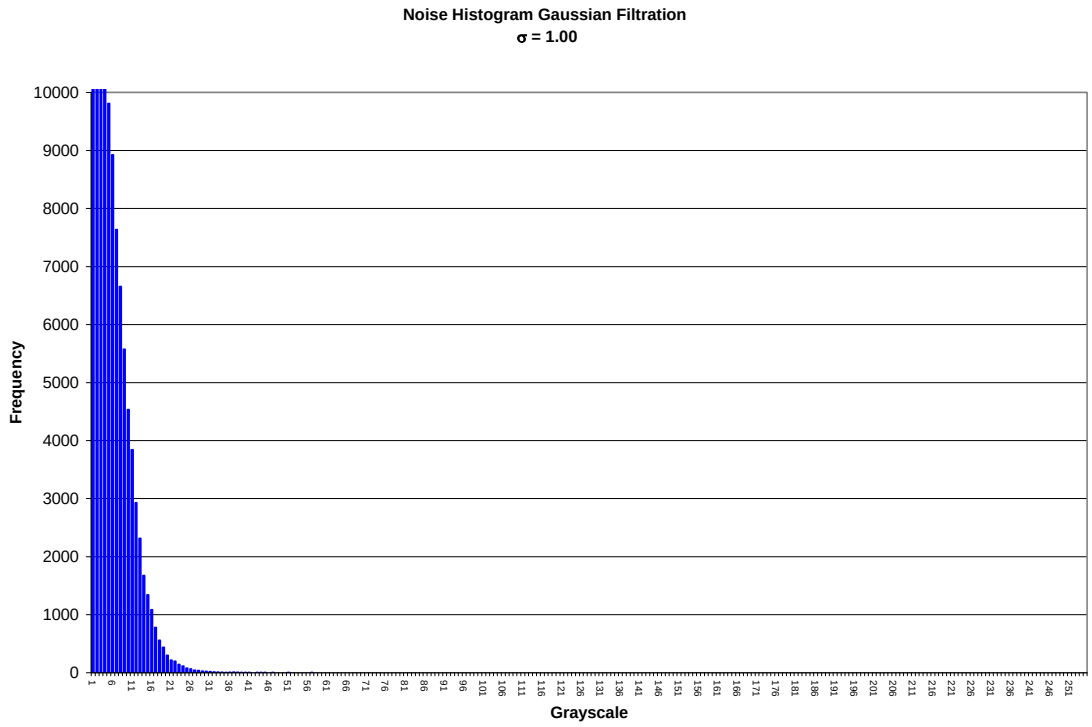


Figure 85. 0013-2-2a Gaussian Smoothing Histogram, σ = 1.00 kernel

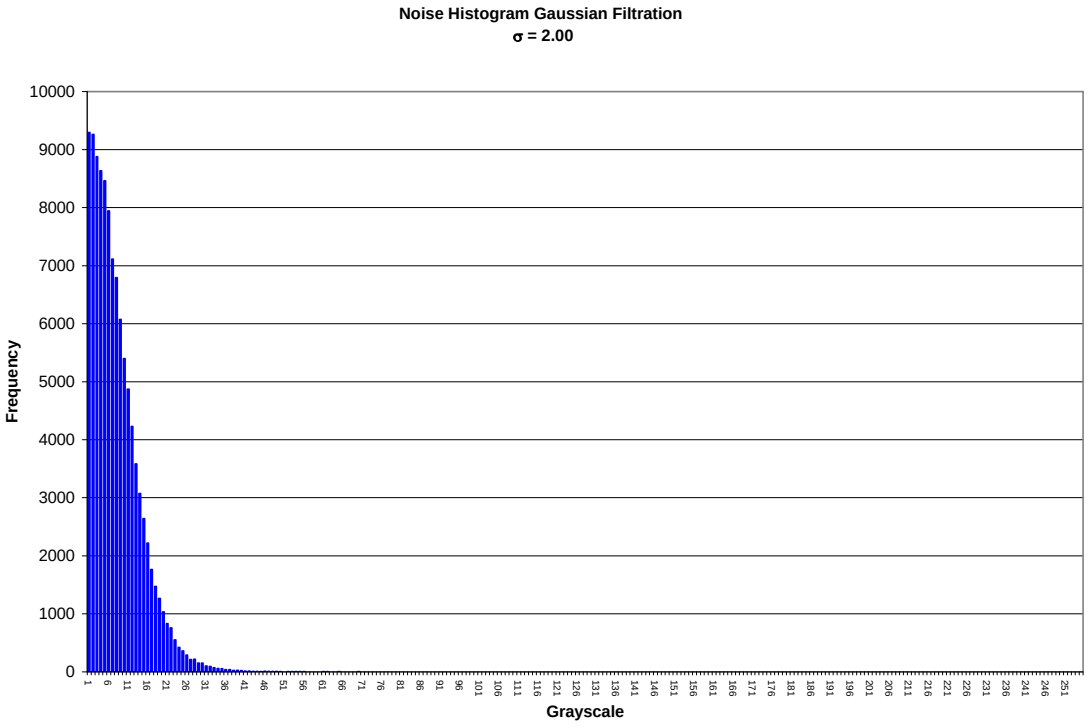


Figure 86. 0013-2-2a Gaussian Smoothing Histogram, σ = 2.00 kernel

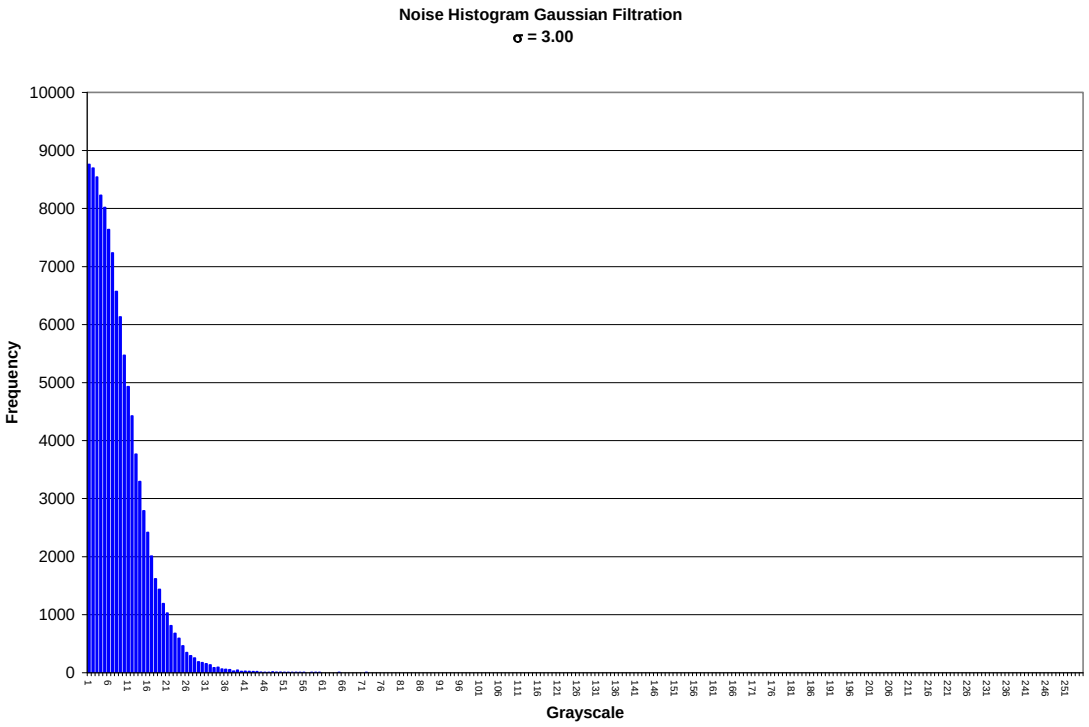


Figure 87. 0013-2-2a Gaussian Smoothing Histogram, σ = 3.00 kernel

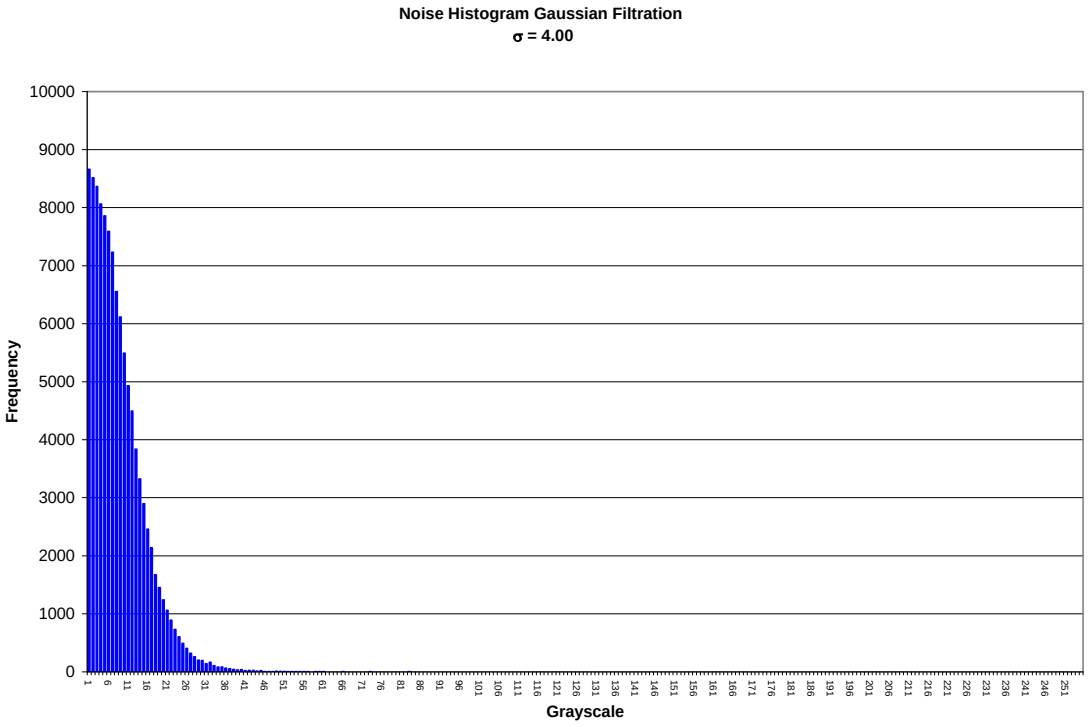


Figure 88. 0013-2-2a Gaussian Smoothing Histogram, σ = 4.00 kernel

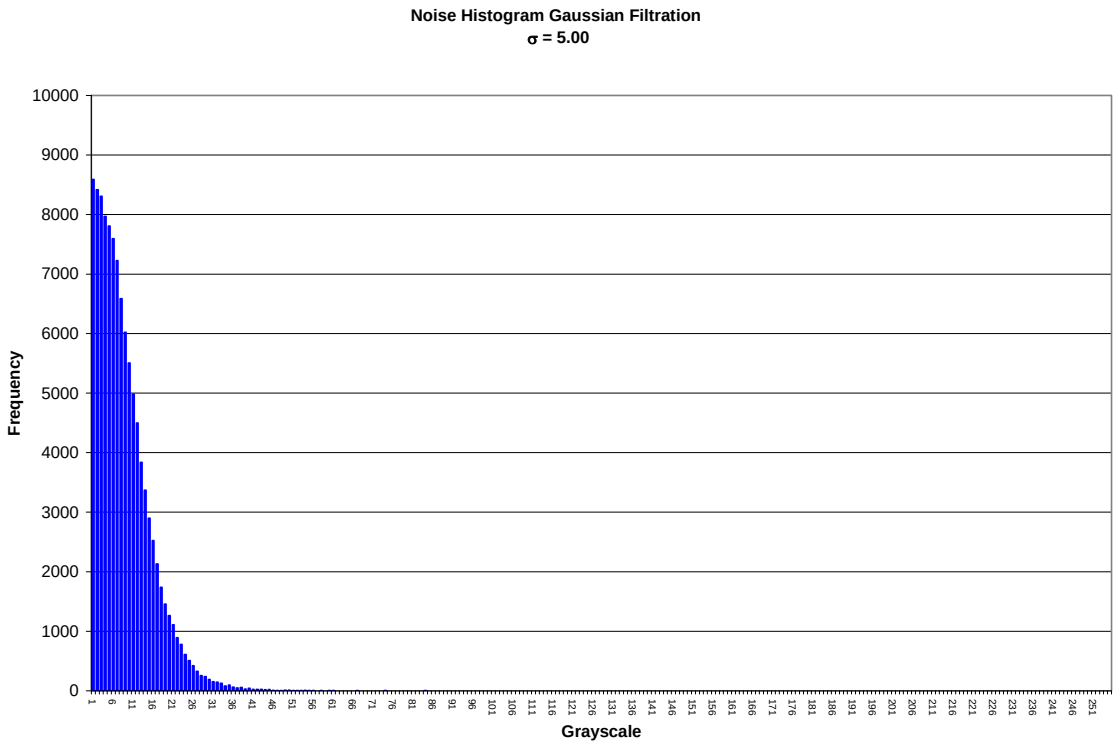


Figure 89. 0013-2-2a Gaussian Smoothing Histogram, σ = 5.00 kernel

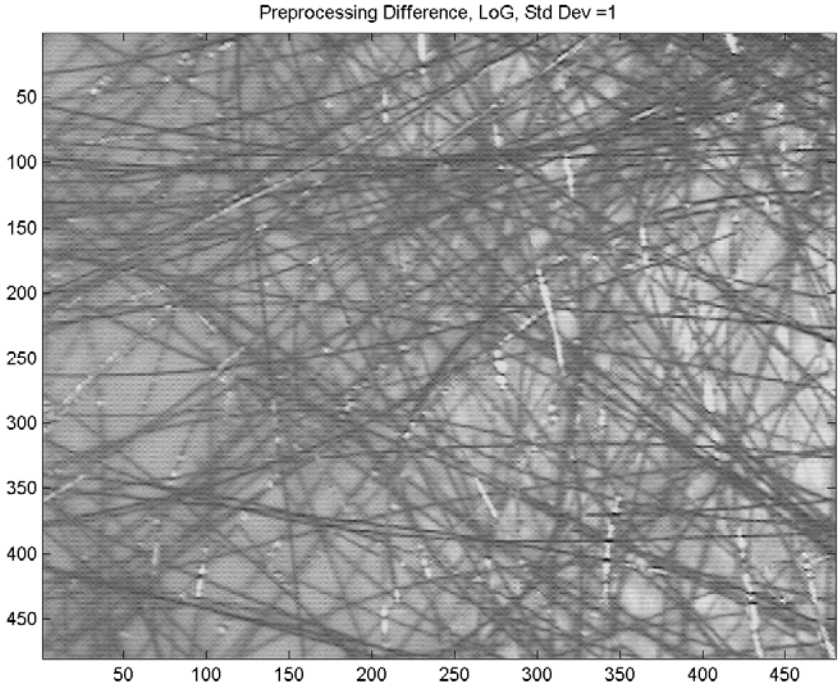


Figure 90. 0013-2-2a LoG Smoothing, σ = 1.00 kernel

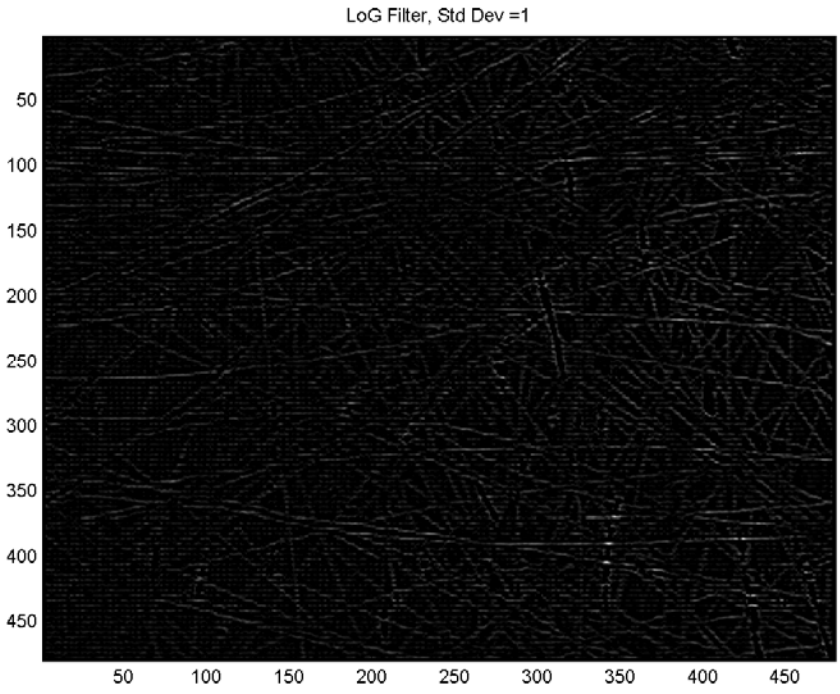


Figure 91. 0013-2-2a LoG Smoothing Noise, σ = 1.00 kernel

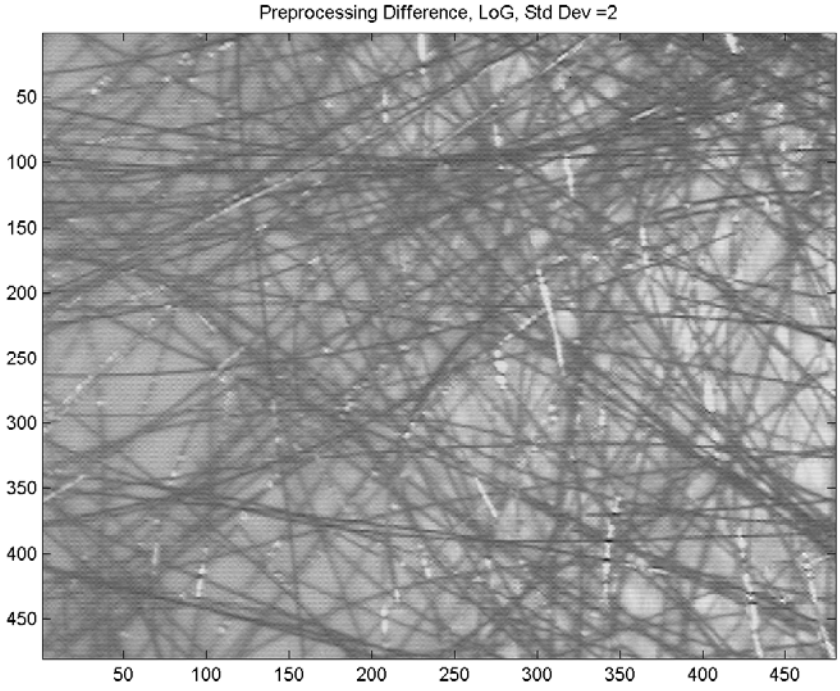


Figure 92. 0013-2-2a LoG Smoothing, σ = 2.00 kernel

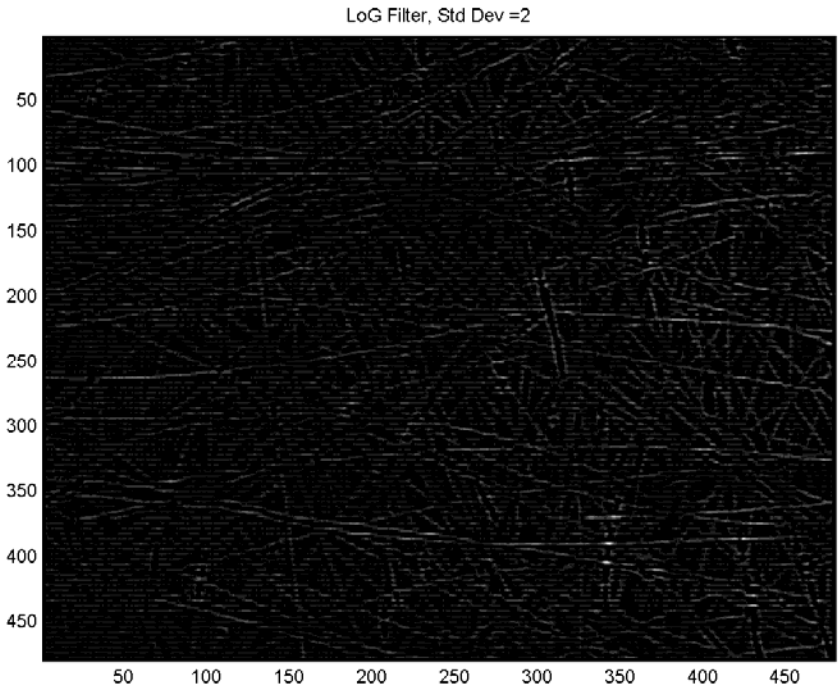


Figure 93. 0013-2-2a LoG Smoothing Noise, σ = 2.00 kernel

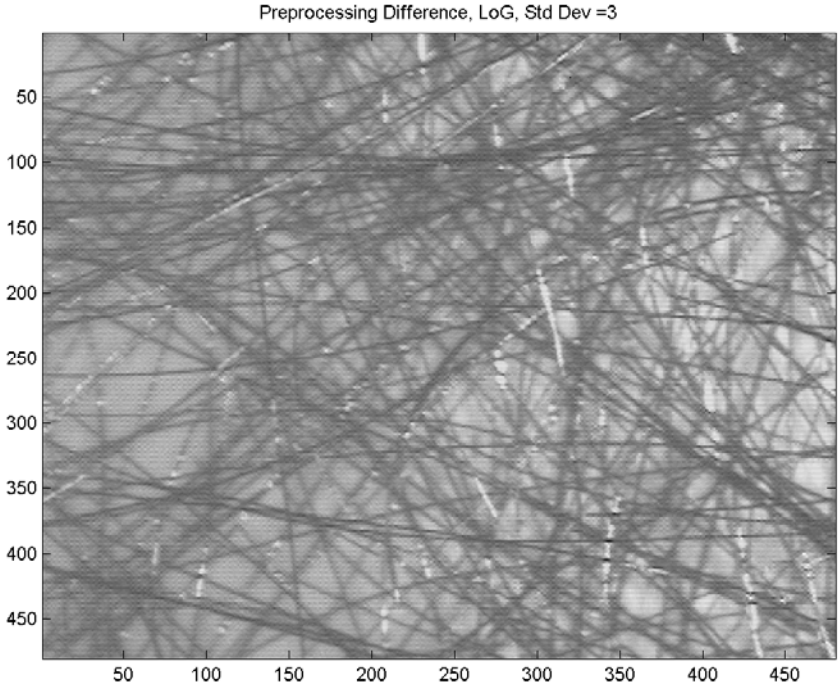


Figure 94. 0013-2-2a LoG Smoothing, σ = 3.00 kernel

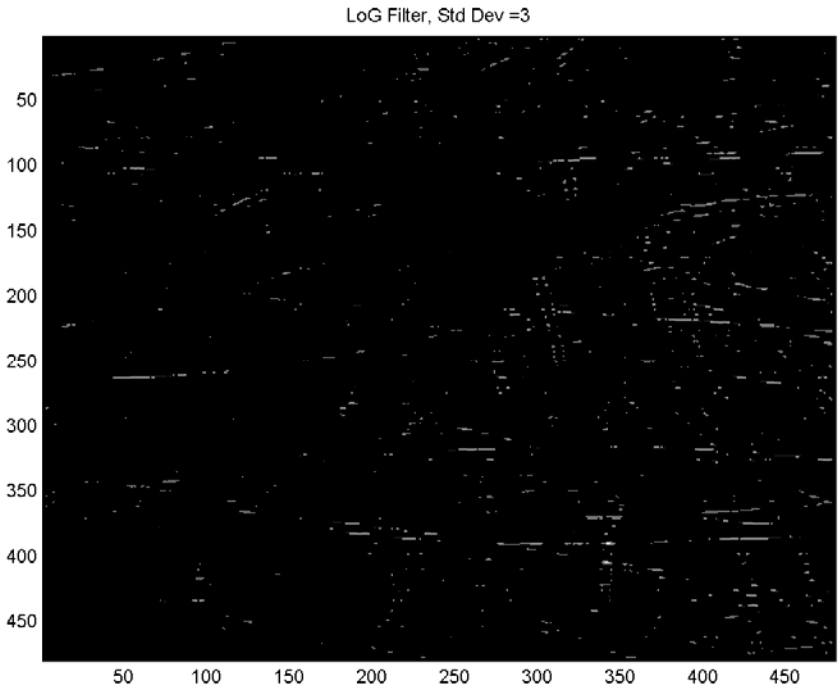


Figure 95. 0013-2-2a LoG Smoothing Noise, σ = 3.00 kernel

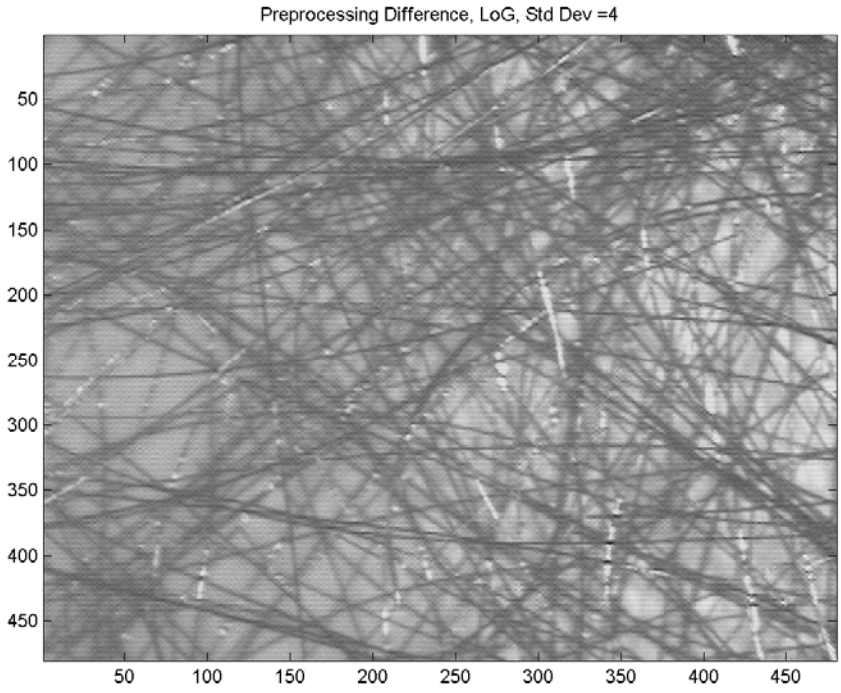


Figure 96. 0013-2-2a LoG Smoothing, σ = 4.00 kernel

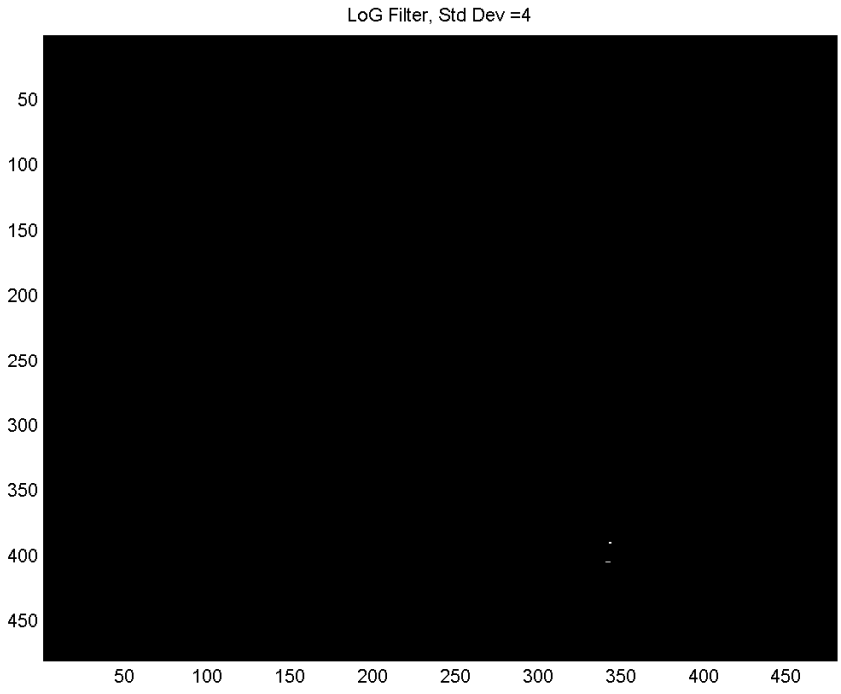


Figure 97. 0013-2-2a LoG Smoothing Noise, σ = 4.00 kernel

Table 18. 0013-2-2a LoG Smoothing Histogram Data

Grayscale	1	2	3	4	5
0	11	3	1	1	1
1	0	0	0	0	0
2	1	0	0	0	0
3	0	0	0	0	0
4	0	0	1	0	0
5	0	0	1	1	0
6	0	0	0	1	1
7	0	0	0	0	1
8	0	0	0	0	0
9	1	1	0	0	0
10	0	0	0	0	0
11	0	0	0	0	0
12	1	0	0	0	0
13	1	1	0	0	0
14	0	1	0	0	0
15	0	0	1	0	0
16	0	0	0	1	0
17	0	0	0	0	1
18	0	0	1	0	0
19	0	0	1	1	1
20	0	0	0	1	0
21	0	0	0	0	1
22	0	1	0	0	0
23	0	0	0	0	0
24	3	1	0	0	0
25	1	0	0	0	0
26	0	0	0	0	0
27	1	0	1	0	0
28	0	0	0	0	0
29	4	1	1	1	1
30	0	1	0	1	1
31	1	0	0	0	0
32	1	0	0	0	0
33	3	1	0	0	0
34	1	0	1	0	0
35	0	0	1	1	0
36	6	0	0	1	2
37	1	0	0	0	0
38	4	0	1	0	0
39	2	0	0	1	1
40	1	0	0	0	0
41	1	0	0	0	0
42	5	1	0	0	0
43	3	0	0	0	0

Table 18 (Continued). 0013-2-2a LoG Smoothing Histogram Data

Grayscale	1	2	3	4	5
44	6	0	0	0	0
45	5	1	0	0	0
46	4	1	1	0	0
47	2	0	0	1	1
48	3	1	0	0	0
49	7	0	0	0	0
50	7	0	2	0	0
51	10	0	0	2	2
52	16	0	0	0	0
53	10	1	1	0	0
54	9	2	1	2	2
55	20	0	0	0	0
56	9	1	1	1	1
57	14	1	2	0	0
58	21	1	0	2	2
59	27	1	0	0	0
60	21	1	1	0	0
61	28	5	0	1	1
62	17	3	2	1	1
63	50	8	4	3	3
64	48	5	4	5	5
65	53	4	9	3	3
66	58	7	5	9	9
67	77	14	7	9	9
68	71	8	8	4	4
69	83	9	10	9	9
70	84	8	5	8	8
71	114	17	15	9	9
72	133	26	18	24	24
73	159	15	14	11	11
74	177	34	27	22	22
75	202	34	19	22	22
76	249	42	33	30	30
77	255	40	44	37	37
78	283	61	44	42	42
79	302	68	52	61	61
80	382	72	61	54	54
81	423	100	71	75	75
82	448	129	73	61	61
83	493	193	155	156	156
84	570	196	157	150	150
85	645	257	217	200	200
86	700	306	235	240	240
87	778	286	313	326	326

Table 18 (Continued). 0013-2-2a LoG Smoothing Histogram Data

Grayscale	1	2	3	4	5
88	826	323	319	325	325
89	854	490	241	219	219
90	994	537	527	512	512
91	1111	591	553	555	555
92	1174	727	565	558	558
93	1275	790	802	810	810
94	1391	809	789	788	788
95	1530	815	855	876	876
96	1557	1113	736	696	696
97	1702	1230	1243	1258	1258
98	1674	1342	1269	1276	1276
99	1868	1572	1295	1288	1288
100	1875	2000	1610	1569	1569
101	2107	1995	2330	2348	2348
102	2101	1641	2046	2065	2065
103	2034	2034	1241	1224	1224
104	2310	2431	2578	2579	2579
105	2422	2510	2497	2511	2511
106	2460	2576	2469	2442	2442
107	2658	2668	2871	2891	2891
108	2613	2512	2556	2563	2563
109	2717	2318	2661	2696	2696
110	2684	2497	1973	1934	1934
111	3025	3241	3025	3038	3038
112	3128	3424	3562	3548	3548
113	3193	3244	3449	3468	3468
114	3051	3422	3000	3001	3001
115	3323	4131	3943	3917	3917
116	3712	3978	5041	5094	5094
117	2811	3099	2537	2516	2516
118	3336	3778	3941	3936	3936
119	3122	3383	3511	3522	3522
120	3258	3610	3488	3491	3491
121	3408	3755	3888	3888	3888
122	3350	3676	3718	3722	3722
123	3522	3537	3923	3935	3935
124	3018	3027	2823	2823	2823
125	3327	3578	3392	3377	3377
126	3750	4165	4305	4320	4320
127	3665	4173	4051	4039	4039
128	3873	4176	4756	4771	4771
129	2985	3031	2926	2920	2920
130	3342	3688	3375	3382	3382
131	3728	4207	4565	4569	4569

Table 18 (Continued). 0013-2-2a LoG Smoothing Histogram Data

Grayscale	1	2	3	4	5
132	3278	3506	3527	3526	3526
133	3250	3508	3553	3554	3554
134	3180	3588	3597	3598	3598
135	3323	3444	3773	3781	3781
136	2365	2346	2127	2124	2124
137	3209	3444	3433	3440	3440
138	3220	3409	3564	3553	3553
139	2842	3058	2975	2979	2979
140	3231	3394	3523	3519	3519
141	2802	2897	2914	2919	2919
142	2917	2979	3148	3151	3151
143	2389	2278	2164	2161	2161
144	2845	3138	2955	2953	2953
145	3650	3963	4144	4147	4147
146	2970	3075	3133	3137	3137
147	2635	2800	2749	2745	2745
148	2693	2983	3026	3028	3028
149	2748	2871	3083	3087	3087
150	1788	1745	1616	1611	1611
151	2668	2785	2819	2820	2820
152	2388	2513	2471	2473	2473
153	2416	2544	2597	2597	2597
154	2383	2496	2525	2527	2527
155	2206	2345	2345	2345	2345
156	2295	2321	2436	2436	2436
157	1675	1688	1633	1635	1635
158	2042	2137	2141	2138	2138
159	2167	2311	2223	2226	2226
160	2634	2837	2943	2941	2941
161	1818	1968	1948	1949	1949
162	1898	2045	2102	2103	2103
163	1589	1609	1674	1674	1674
164	1111	1066	1028	1027	1027
165	1605	1679	1681	1682	1682
166	1488	1583	1588	1588	1588
167	1431	1535	1547	1547	1547
168	1443	1495	1538	1538	1538
169	1199	1212	1210	1210	1210
170	1301	1338	1372	1372	1372
171	905	879	863	863	863
172	1096	1105	1115	1115	1115
173	1174	1207	1196	1196	1196
174	1306	1359	1388	1388	1388
175	805	834	838	838	838

Table 18 (Continued). 0013-2-2a LoG Smoothing Histogram Data

Grayscale	1	2	3	4	5
176	895	905	896	896	896
177	854	885	913	913	913
178	513	505	493	493	493
179	758	784	792	792	792
180	620	638	631	631	631
181	731	747	752	752	752
182	651	669	686	686	686
183	525	534	519	519	519
184	559	566	585	585	585
185	303	287	283	283	283
186	479	493	483	483	483
187	448	461	464	464	464
188	399	405	408	408	408
189	541	564	570	570	570
190	319	315	314	314	314
191	362	380	380	380	380
192	292	299	299	299	299
193	198	206	204	204	204
194	265	272	280	280	280
195	258	263	261	261	261
196	248	245	248	248	248
197	248	244	244	244	244
198	239	240	238	238	238
199	267	252	255	255	255
200	164	148	144	144	144
201	305	336	340	340	340
202	174	199	199	199	199
203	219	229	229	229	229
204	141	141	141	141	141
205	115	115	115	115	115
206	93	93	93	93	93
207	71	71	71	71	71
208	99	99	99	99	99
209	132	132	132	132	132
210	167	167	167	167	167
211	150	150	150	150	150
212	73	73	73	73	73
213	41	41	41	41	41
214	24	24	24	24	24
215	24	24	24	24	24
216	14	14	14	14	14
217	12	12	12	12	12
218	7	7	7	7	7
219	3	3	3	3	3

Table 18 (Continued). 0013-2-2a LoG Smoothing Histogram Data

Grayscale	1	2	3	4	5
220	3	3	3	3	3
221	1	1	1	1	1
222	2	2	2	2	2
223	2	2	2	2	2
224	3	3	3	3	3
225	3	3	3	3	3
226	1	1	1	1	1
227	4	4	4	4	4
228	1	1	1	1	1
229	3	3	3	3	3
230	1	1	1	1	1
231	3	3	3	3	3
232	1	1	1	1	1
233	1	1	1	1	1
234	0	0	0	0	0
235	0	0	0	0	0
236	2	2	2	2	2
237	0	0	0	0	0
238	0	0	0	0	0
239	0	0	0	0	0
240	1	1	1	1	1
241	0	0	0	0	0
242	0	0	0	0	0
243	0	0	0	0	0
244	0	0	0	0	0
245	0	0	0	0	0
246	0	0	0	0	0
247	0	0	0	0	0
248	0	0	0	0	0
249	0	0	0	0	0
250	0	0	0	0	0
251	0	0	0	0	0
252	0	0	0	0	0
253	0	0	0	0	0
254	0	0	0	0	0
255	0	0	0	0	0
Min:	0	0	0	0	0
μ:	900	900	900	900	900
Max:	3873	4207	5041	5094	5094
Median:	175.5	99.5	83	84	84
σ:	1200.334	1288.528	1313.592	1314.92	1314.92
% Black:	0.00%	0.00%	0.00%	0.00%	0.00%
% Gray:	100.00%	100.00%	100.00%	100.00%	100.00%

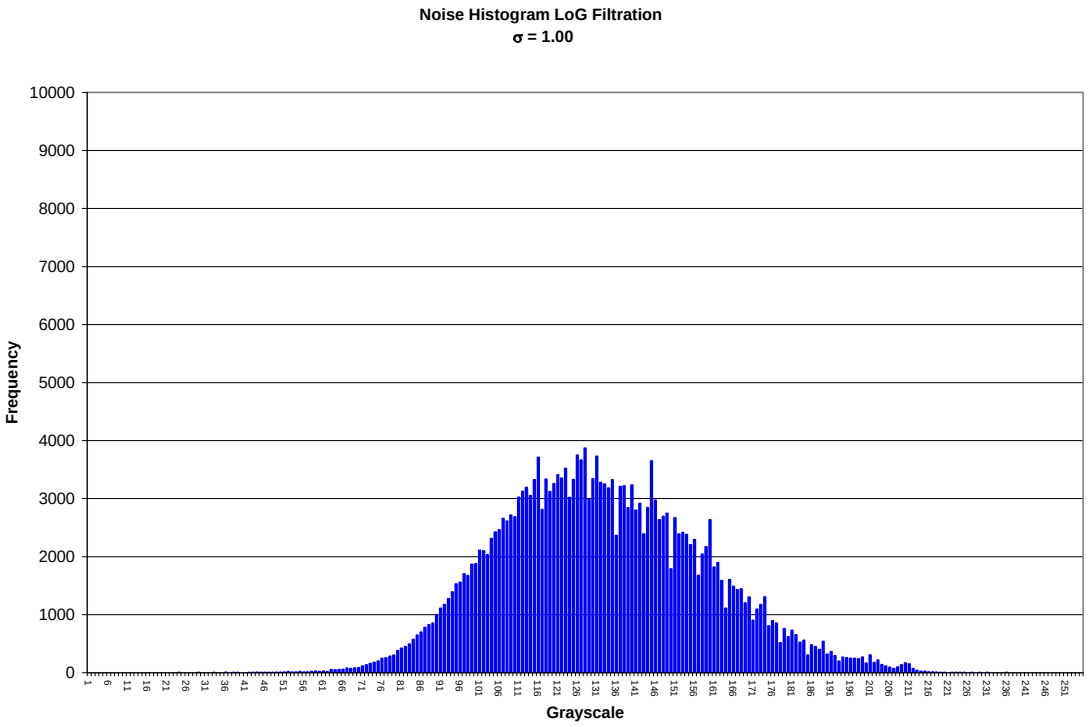


Figure 98. 0013-2-2a LoG Smoothing Histogram, σ = 1.00 kernel

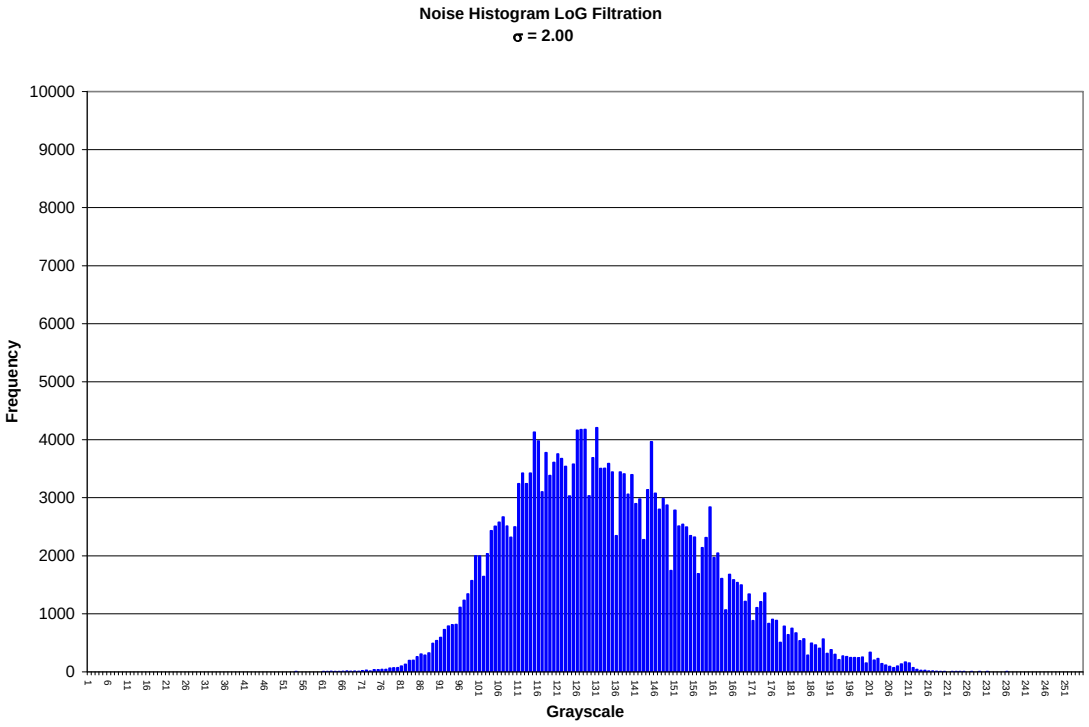


Figure 99. 0013-2-2a LoG Smoothing Histogram, σ = 2.00 kernel

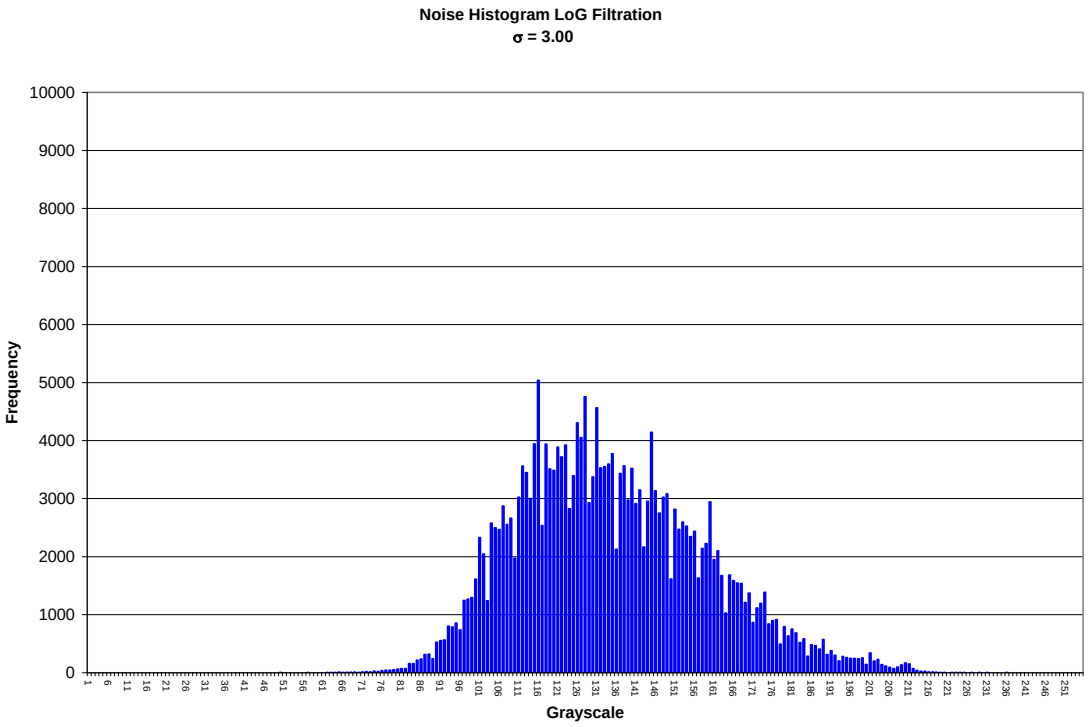


Figure 100. 0013-2-2a LoG Smoothing Histogram, σ = 3.00 kernel

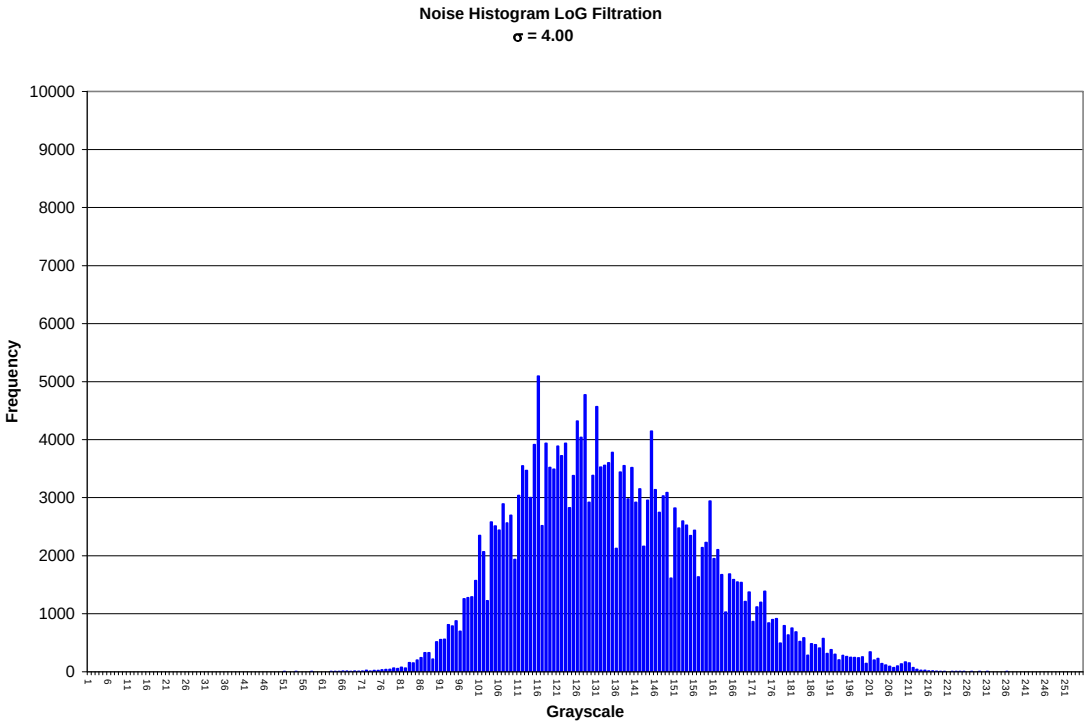


Figure 101. 0013-2-2a LoG Smoothing Histogram, σ = 4.00 kernel

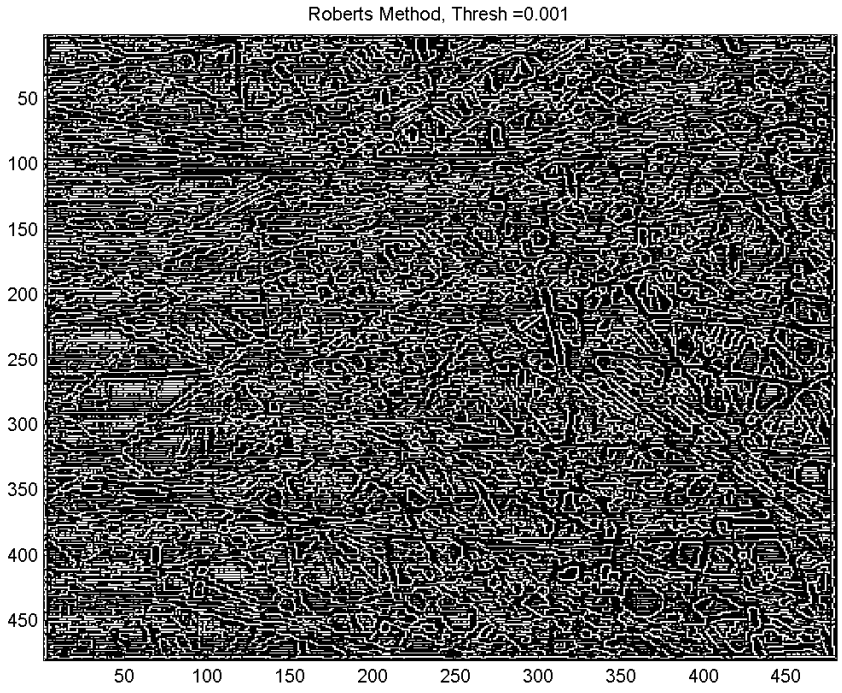


Figure 102. 0013-2-2a Roberts Edge Detection, Threshold = 0.001

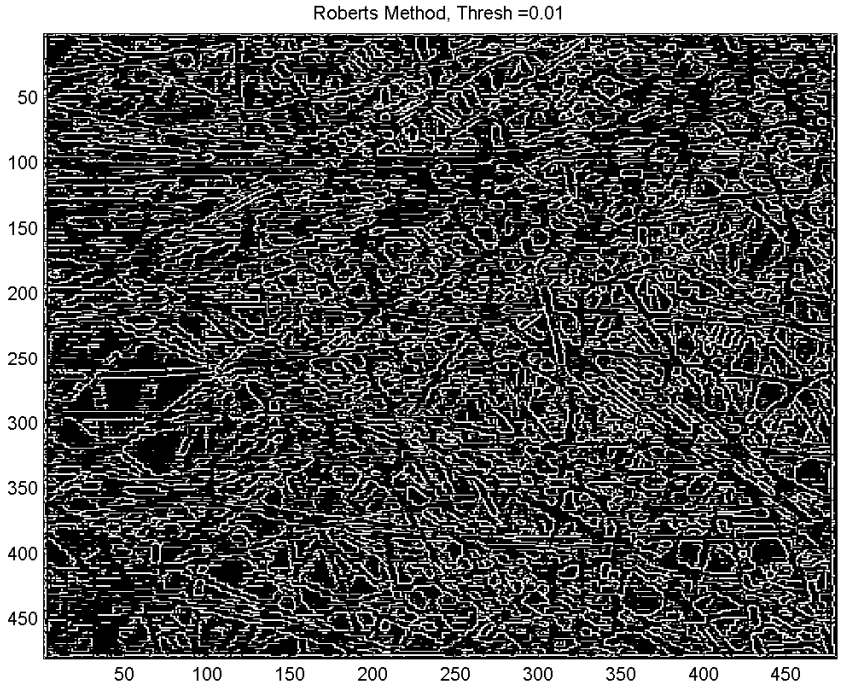


Figure 103. 0013-2-2a Roberts Edge Detection, Threshold = 0.010

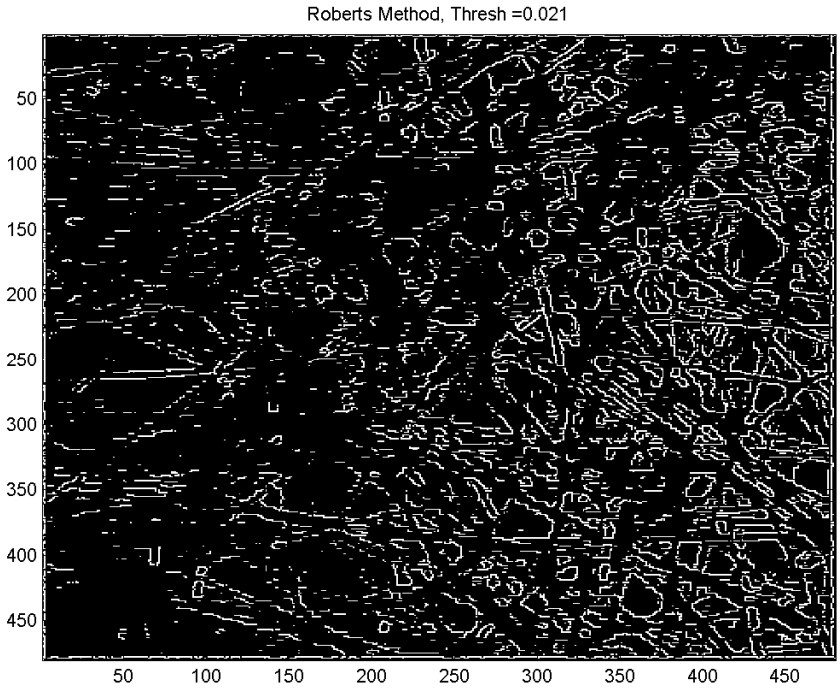


Figure 104. 0013-2-2a Roberts Edge Detection, Threshold = 0.021

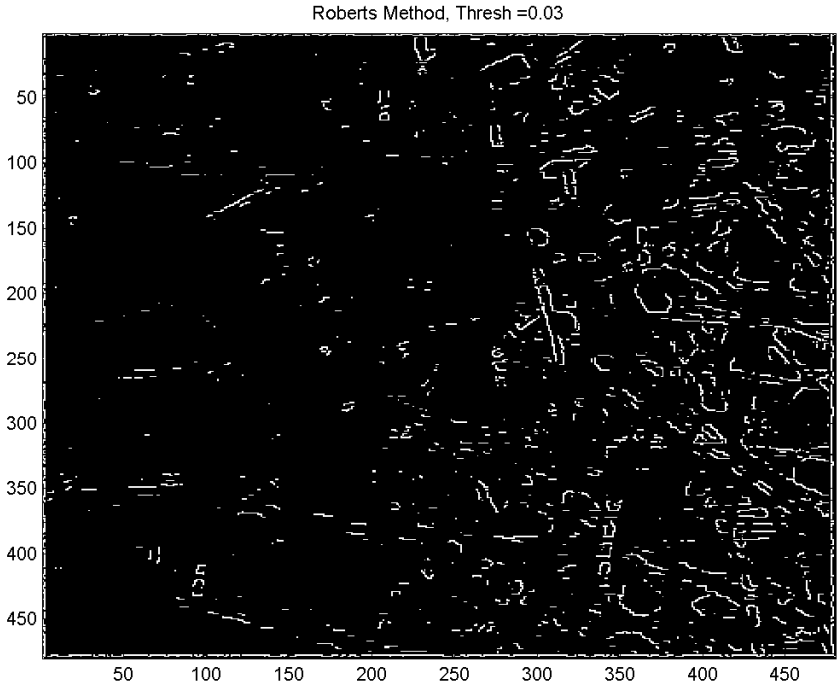


Figure 105. 0013-2-2a Roberts Edge Detection, Threshold = 0.030

Table 19. 0013-2-2a Roberts Edge Detection Histogram Data

	Edge Hist		90 Rotation		Difference		
Thresh	**0**	**1**	**0**	**1**	**0**	**1**	**Percent**
0.001	162747	67653	162684	67716	-63	63	0.02734%
0.002	162765	67635	162698	67702	-67	67	0.02908%
0.003	163038	67362	162938	67462	-100	100	0.04340%
0.004	163247	67153	163157	67243	-90	90	0.03906%
0.005	164096	66304	164015	66385	-81	81	0.03516%
0.006	165493	64907	165411	64989	-82	82	0.03559%
0.007	166830	63570	166762	63638	-68	68	0.02951%
0.008	168976	61424	168931	61469	-45	45	0.01953%
0.009	173049	57351	173018	57382	-31	31	0.01345%
0.010	176484	53916	176464	53936	-20	20	0.00868%
0.011	177915	52485	177899	52501	-16	16	0.00694%
0.012	182142	48258	182137	48263	-5	5	0.00217%
0.013	184697	45703	184701	45699	4	-4	0.00174%
0.014	188131	42269	188143	42257	12	-12	0.00521%
0.015	191364	39036	191373	39027	9	-9	0.00391%
0.016	194611	35789	194612	35788	1	-1	0.00043%
0.017	197825	32575	197825	32575	0	0	0.00000%
0.018	199707	30693	199707	30693	0	0	0.00000%
0.019	202529	27871	202522	27878	-7	7	0.00304%
0.020	205677	24723	205668	24732	-9	9	0.00391%
0.021	207317	23083	207312	23088	-5	5	0.00217%
0.022	209945	20455	209940	20460	-5	5	0.00217%
0.023	211944	18456	211944	18456	0	0	0.00000%
0.024	213905	16495	213905	16495	0	0	0.00000%
0.025	215081	15319	215082	15318	1	-1	0.00043%
0.026	216629	13771	216629	13771	0	0	0.00000%
0.027	217899	12501	217899	12501	0	0	0.00000%
0.028	219219	11181	219220	11180	1	-1	0.00043%
0.029	220178	10222	220180	10220	2	-2	0.00087%
0.030	221478	8922	221479	8921	1	-1	0.00043%

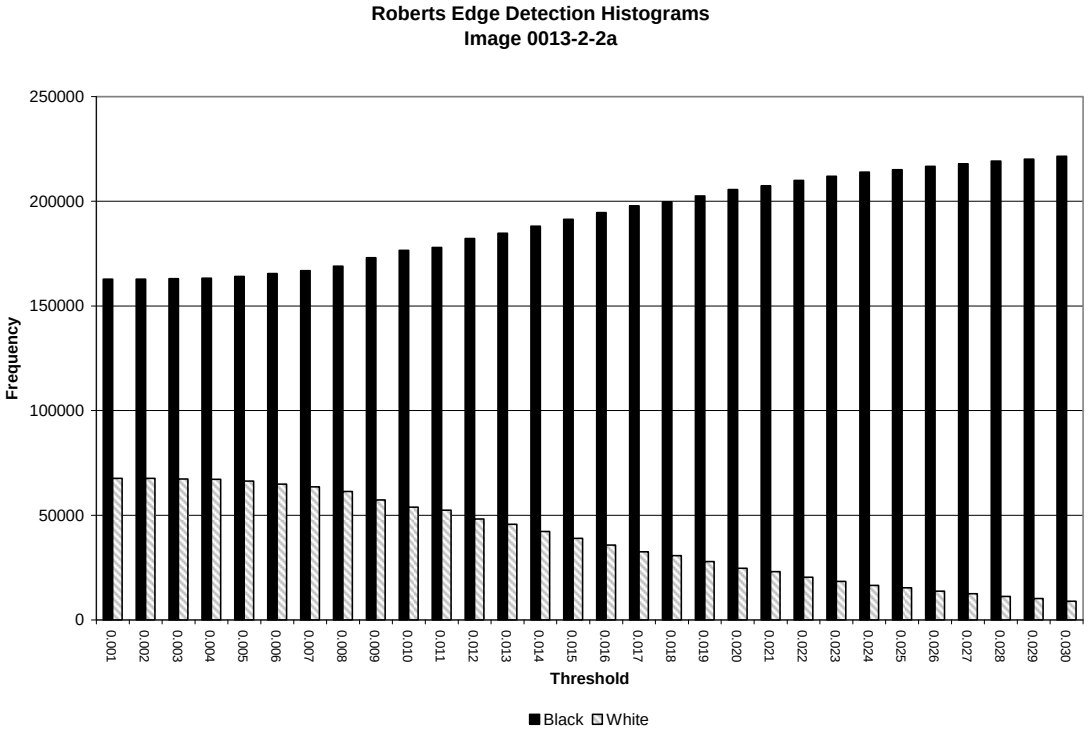


Figure 106. 0013-2-2a Roberts Edge Detection Histograms

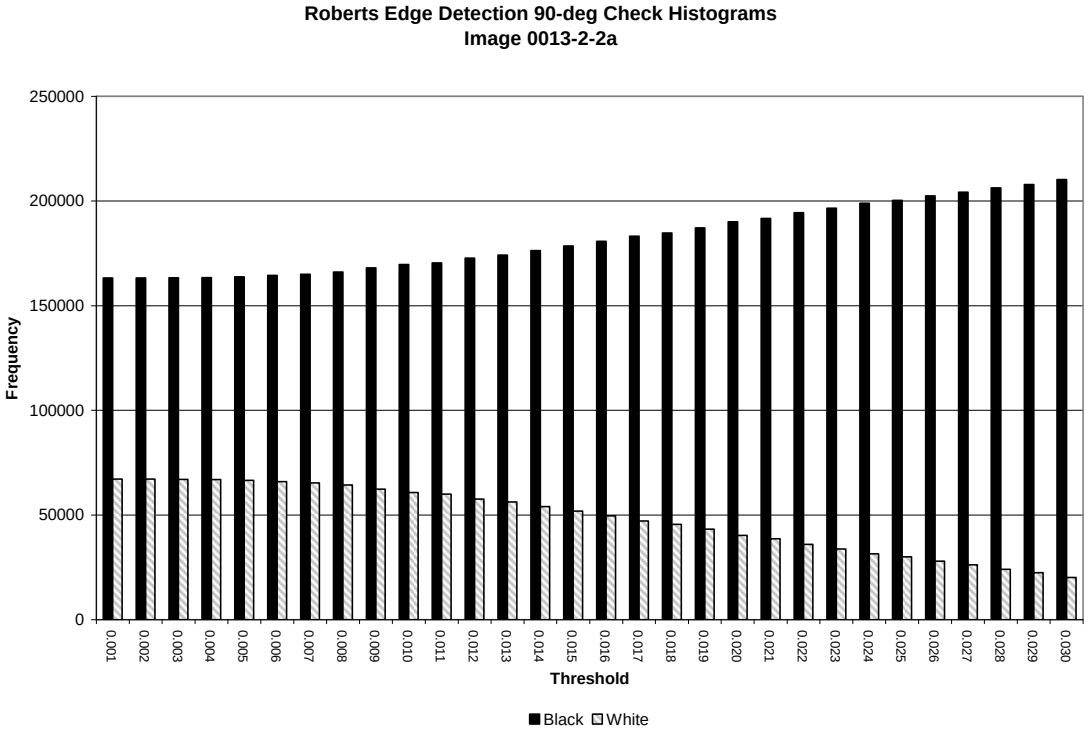


Figure 107. 0013-2-2a Roberts Edge Detection 90° Rotation Histograms

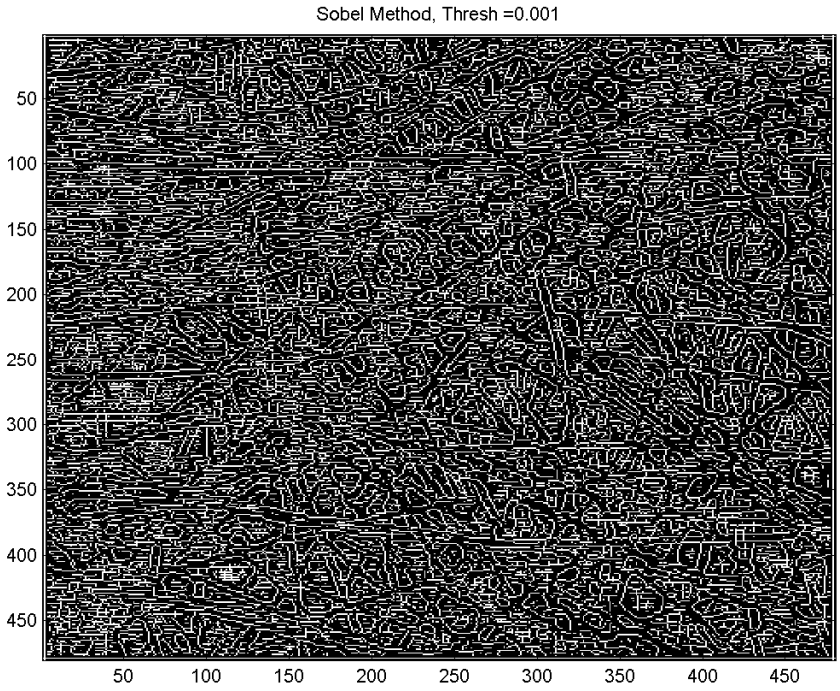


Figure 108. 0013-2-2a Sobel Edge Detection, Threshold = 0.001

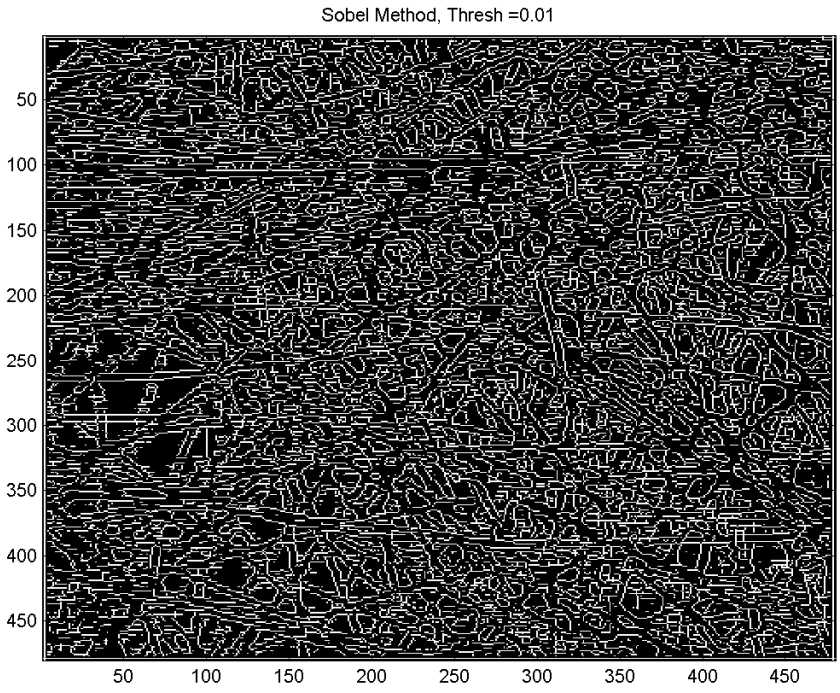


Figure 109. 0013-2-2a Sobel Edge Detection, Threshold = 0.010

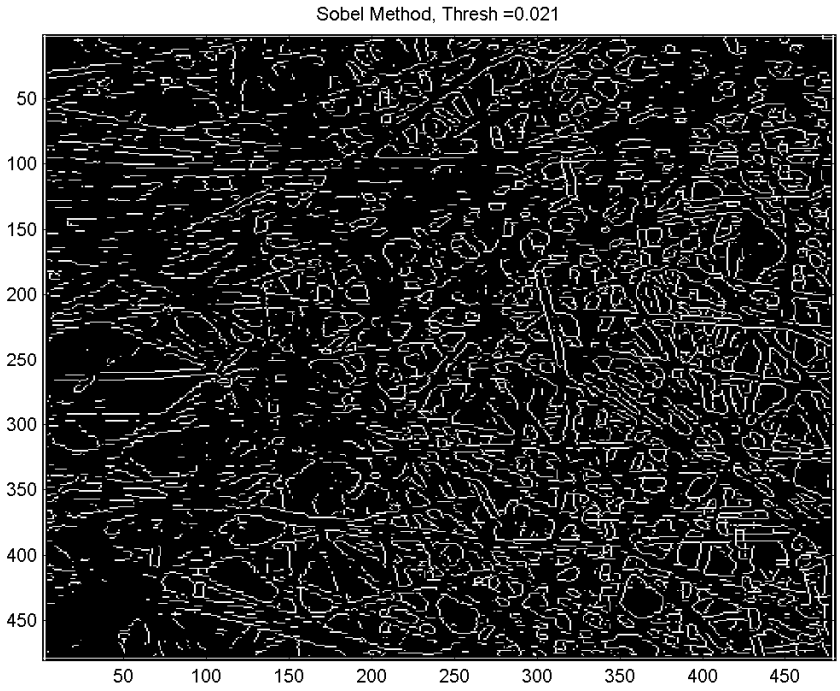


Figure 110. 0013-2-2a Sobel Edge Detection, Threshold = 0.021

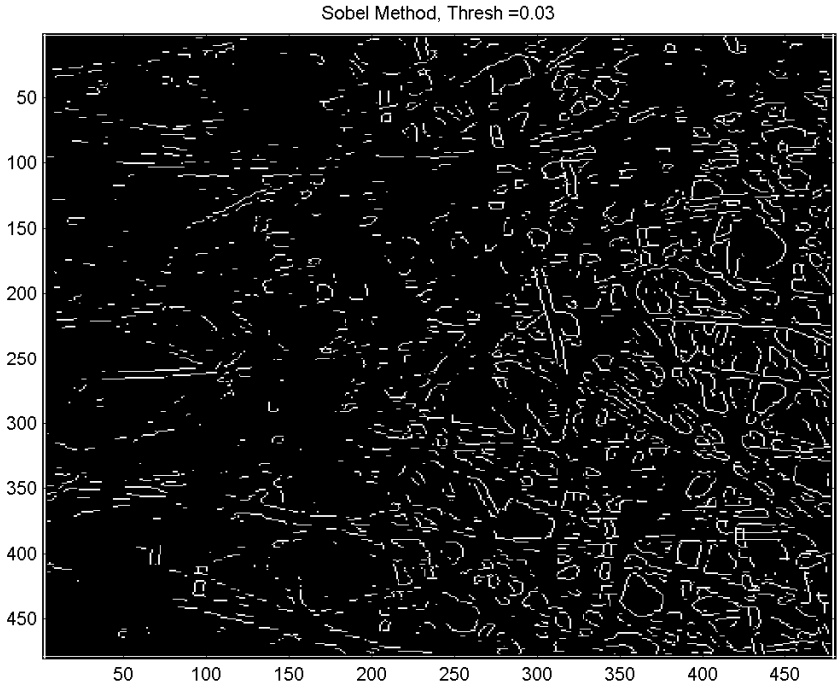


Figure 111. 0013-2-2a Sobel Edge Detection, Threshold = 0.030

Table 20. 0013-2-2a Sobel Edge Detection Histogram Data

	Edge Hist		90 Rotation		Difference		
Thresh	**0**	**1**	**0**	**1**	**0**	**1**	**Percent**
0.001	174851	55549	174845	55555	-6	6	0.00260%
0.002	174881	55519	174875	55525	-6	6	0.00260%
0.003	175057	55343	175053	55347	-4	4	0.00174%
0.004	175403	54997	175387	55013	-16	16	0.00694%
0.005	176128	54272	176107	54293	-21	21	0.00911%
0.006	177179	53221	177150	53250	-29	29	0.01259%
0.007	178385	52015	178374	52026	-11	11	0.00477%
0.008	179780	50620	179780	50620	0	0	0.00000%
0.009	181212	49188	181211	49189	-1	1	0.00043%
0.010	183198	47202	183201	47199	3	-3	0.00130%
0.011	184790	45610	184794	45606	4	-4	0.00174%
0.012	186607	43793	186612	43788	5	-5	0.00217%
0.013	188327	42073	188343	42057	16	-16	0.00694%
0.014	190206	40194	190220	40180	14	-14	0.00608%
0.015	192207	38193	192220	38180	13	-13	0.00564%
0.016	193956	36444	193976	36424	20	-20	0.00868%
0.017	195883	34517	195894	34506	11	-11	0.00477%
0.018	197638	32762	197659	32741	21	-21	0.00911%
0.019	199525	30875	199543	30857	18	-18	0.00781%
0.020	201278	29122	201289	29111	11	-11	0.00477%
0.021	202969	27431	202979	27421	10	-10	0.00434%
0.022	204597	25803	204604	25796	7	-7	0.00304%
0.023	206252	24148	206262	24138	10	-10	0.00434%
0.024	207807	22593	207818	22582	11	-11	0.00477%
0.025	209289	21111	209307	21093	18	-18	0.00781%
0.026	210710	19690	210722	19678	12	-12	0.00521%
0.027	212001	18399	212011	18389	10	-10	0.00434%
0.028	213311	17089	213317	17083	6	-6	0.00260%
0.029	214453	15947	214458	15942	5	-5	0.00217%
0.030	215576	14824	215578	14822	2	-2	0.00087%

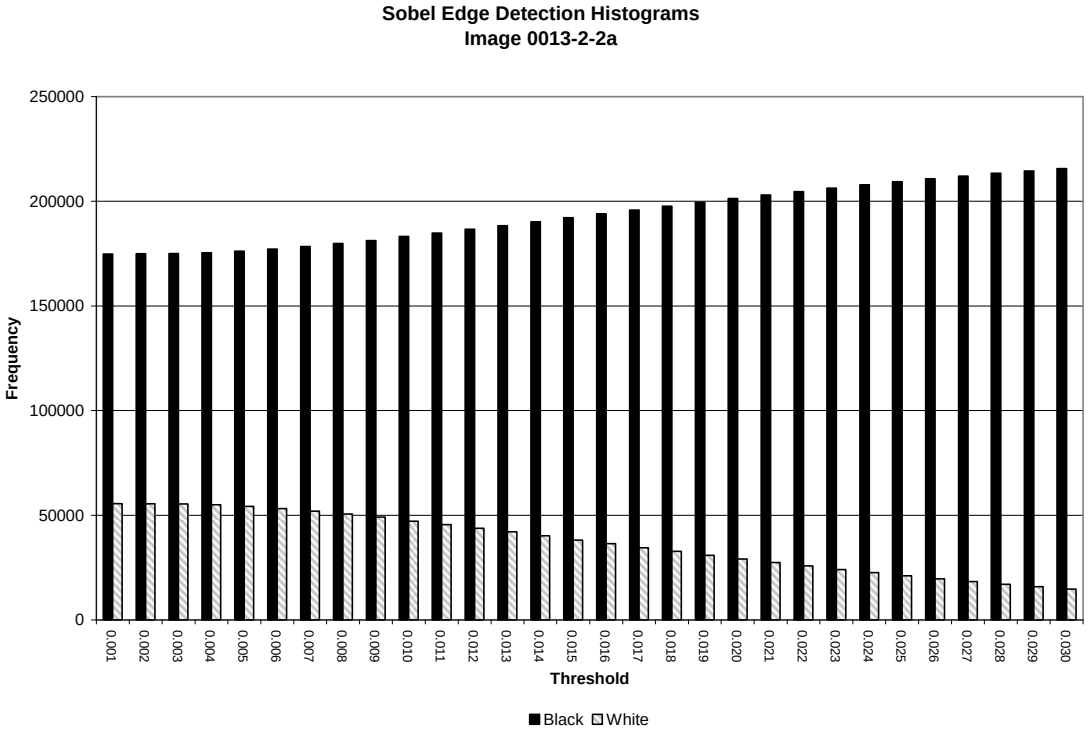


Figure 112. 0013-2-2a Sobel Edge Detection Histograms

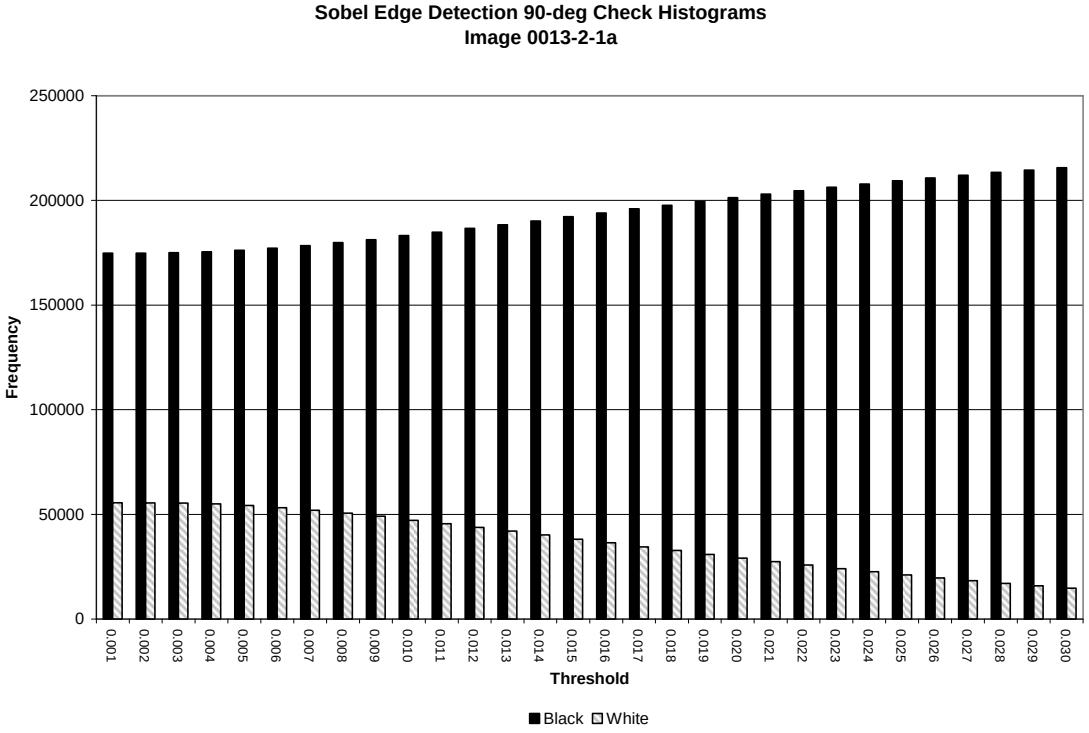


Figure 113. 0013-2-2a Sobel Edge Detection 90° Rotation Histograms

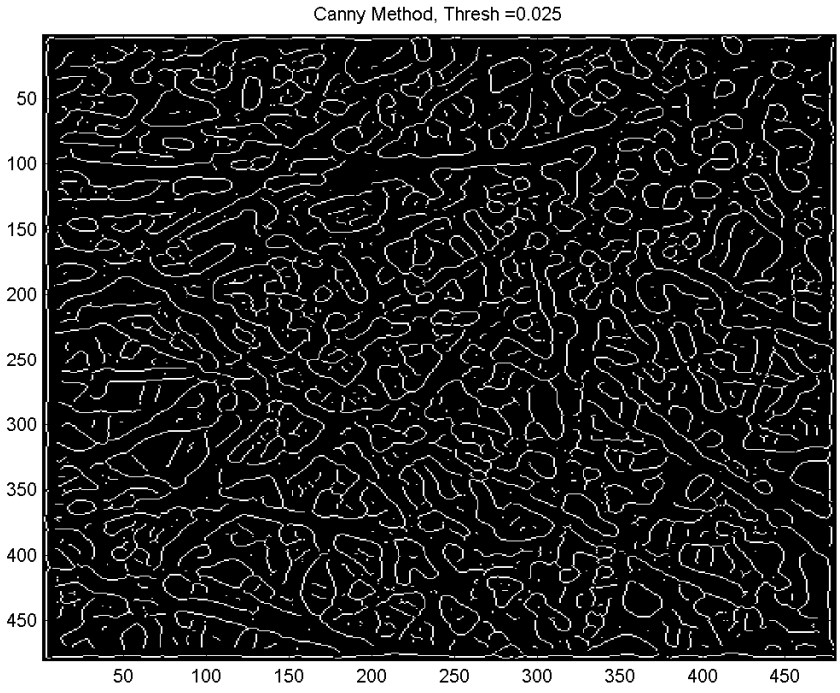


Figure 114. 0013-2-2a Canny Edge Detection, Threshold = [0.010 0.025]

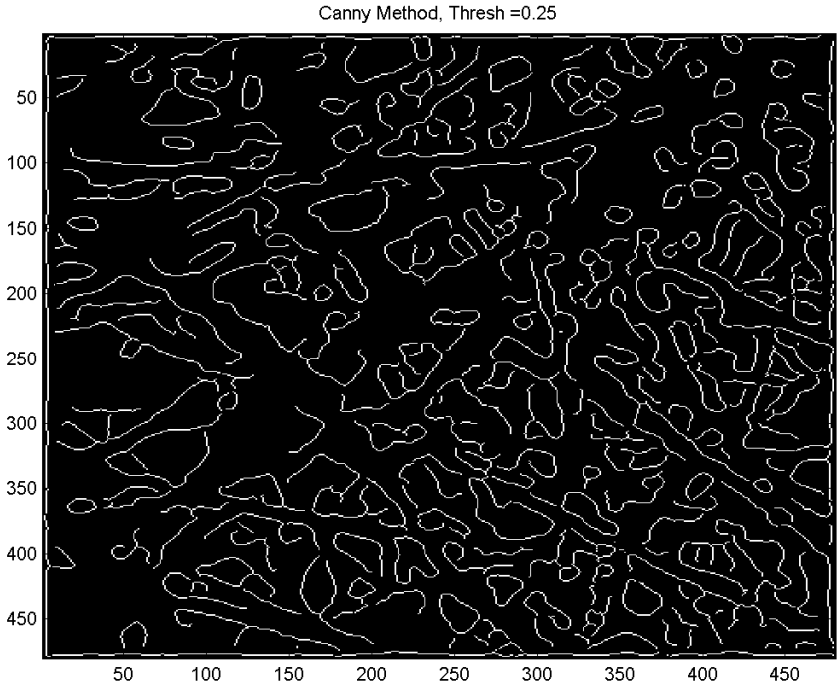


Figure 115. 0013-2-2a Canny Edge Detection, Threshold = [0.100 0.250]

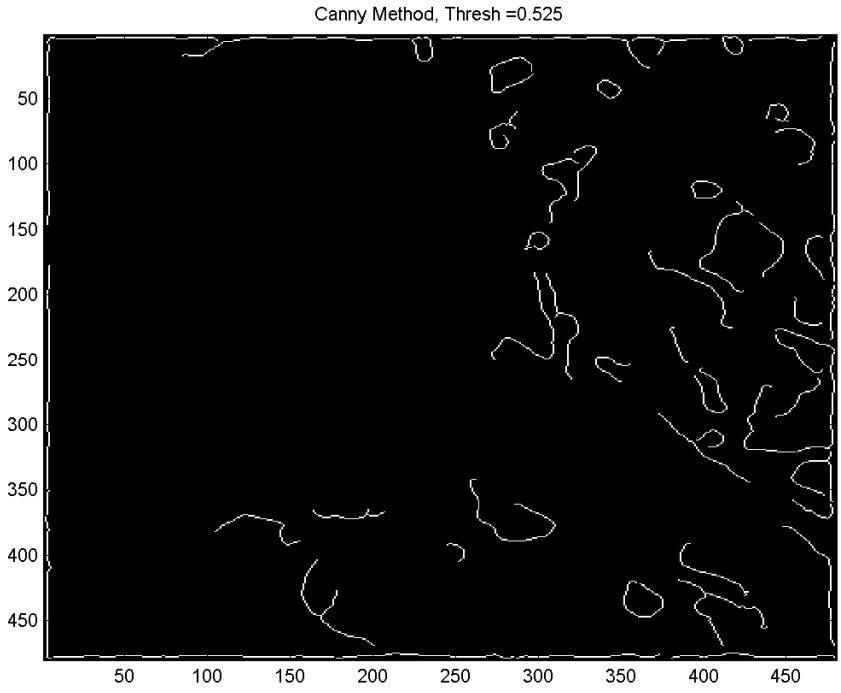


Figure 116. 0013-2-2a Canny Edge Detection, Threshold = [0.210 0.525]

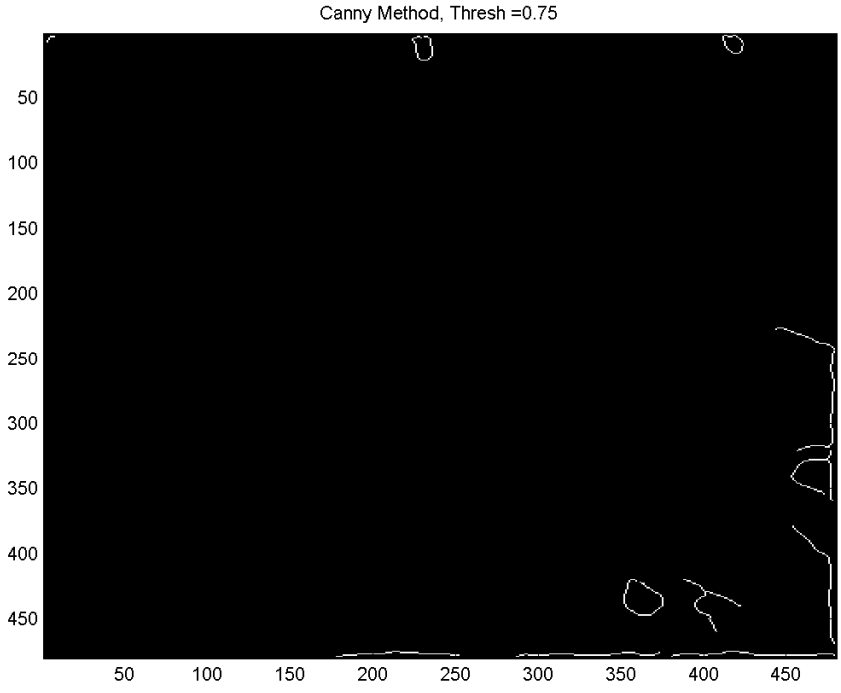


Figure 117. 0013-2-2a Canny Edge Detection, Threshold = [0.300 0.750]

Table 21. 0013-2-2a Canny Edge Detection Histogram Data

		Edge Hist		90 Rotation		Difference		
$Thresh_L$	**$Thresh_H$**	**0**	**1**	**0**	**1**	**0**	**1**	**Percent**
0.010	0.025	210095	20305	210115	20285	20	-20	9.65515%
0.020	0.050	210254	20146	210275	20125	21	-21	9.57175%
0.030	0.075	210572	19828	210594	19806	22	-22	9.40580%
0.040	0.100	210894	19506	210915	19485	21	-21	9.23923%
0.050	0.125	211472	18928	211495	18905	23	-23	8.93971%
0.060	0.150	212176	18224	212193	18207	17	-17	8.58108%
0.070	0.175	212878	17522	212890	17510	12	-12	8.22536%
0.080	0.200	213589	16811	213598	16802	9	-9	7.86650%
0.090	0.225	214694	15706	214701	15699	7	-7	7.31226%
0.100	0.250	215962	14438	215970	14430	8	-8	6.68172%
0.110	0.275	217419	12981	217424	12976	5	-5	5.96819%
0.120	0.300	218589	11811	218599	11801	10	-10	5.39871%
0.130	0.325	219699	10701	219702	10698	3	-3	4.86938%
0.140	0.350	220884	9516	220888	9512	4	-4	4.30632%
0.150	0.375	222348	8052	222349	8051	1	-1	3.62089%
0.160	0.400	223425	6975	223421	6979	-4	4	3.12364%
0.170	0.425	223917	6483	223909	6491	-8	8	2.89883%
0.180	0.450	224840	5560	224838	5562	-2	2	2.47375%
0.190	0.475	225544	4856	225540	4860	-4	4	2.15478%
0.200	0.500	225996	4404	225994	4406	-2	2	1.94959%
0.210	0.525	226436	3964	226435	3965	-1	1	1.75104%
0.220	0.550	227080	3320	227076	3324	-4	4	1.46380%
0.230	0.575	227743	2657	227739	2661	-4	4	1.16842%
0.240	0.600	227864	2536	227857	2543	-7	7	1.11601%
0.250	0.625	228242	2158	228240	2160	-2	2	0.94636%
0.260	0.650	228614	1786	228614	1786	0	0	0.78123%
0.270	0.675	229155	1245	229153	1247	-2	2	0.54417%
0.280	0.700	229387	1013	229384	1016	-3	3	0.44292%
0.290	0.725	229556	844	229554	846	-2	2	0.36854%
0.300	0.750	229601	799	229600	800	-1	1	0.34843%

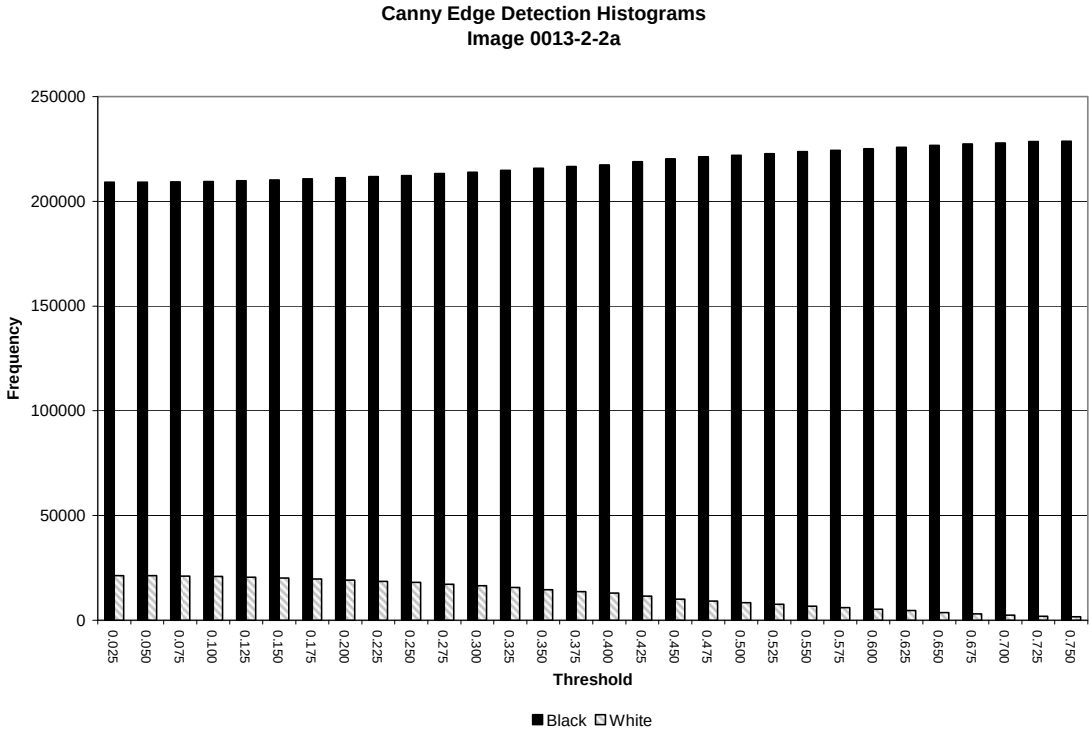


Figure 118. 0013-2-2a Canny Edge Detection Histograms

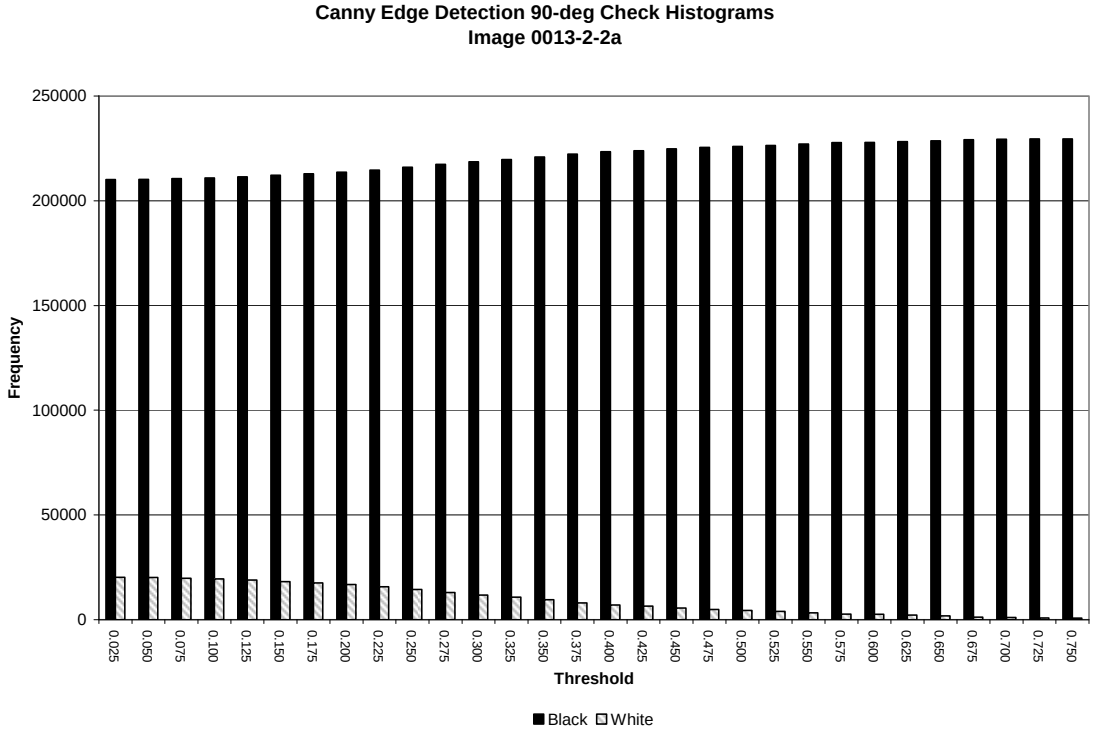


Figure 119. 0013-2-2a Canny Edge Detection 90° Rotation Histograms

Table 22. 0013-2-2a Line Detection θ_{mean}, Grid = 1 x 1

Peaks	θ_{mean}
10	72.039
20	68.860
30	68.470
40	68.582
50	70.550
60	69.773
70	64.911
80	62.973
90	61.551
100	64.221

Table 23. 0013-2-2a Line Detection θ_{mean}, Grid = 2 x 2

Peaks	θ_{mean}	
10	72.039	72.039
10	72.039	70.819
20	68.860	68.860
20	68.860	68.686
30	68.470	68.470
30	68.470	68.297
40	68.582	68.582
40	68.582	68.409
50	70.550	70.550
50	70.550	70.377
60	69.773	69.773
60	69.773	69.599
70	64.911	64.911
70	64.911	64.738
80	62.973	62.973
80	62.973	62.800
90	61.551	61.551
90	61.551	61.378
100	64.221	64.221
100	64.221	64.048

Table 24. 0013-2-2a Line Detection θ_{mean}, Grid = 4 x 4

Peaks	θ_{mean}			
10	70.247	71.237	71.237	74.288
10	74.288	73.032	71.758	73.092
10	76.392	72.693	70.891	72.543
10	73.164	73.740	72.112	71.260
20	68.310	69.300	69.300	71.896
20	71.896	72.941	70.809	70.553
20	73.853	70.477	69.386	71.039
20	71.659	72.235	70.607	71.590
30	67.920	68.911	68.911	71.507
30	71.507	75.749	72.167	70.698
30	73.998	70.205	68.731	70.384
30	71.004	71.580	69.952	70.936
40	68.032	69.023	69.023	71.619
40	71.619	76.040	75.934	73.990
40	77.291	70.664	69.434	71.086
40	71.706	72.283	70.655	71.638
50	70.000	70.991	70.991	73.587
50	73.587	79.265	78.529	76.585
50	79.885	73.803	70.328	71.981
50	72.601	73.177	71.549	72.532
60	69.223	70.213	70.213	72.809
60	72.809	78.951	77.778	75.835
60	79.135	72.419	69.255	70.907
60	71.527	72.103	70.476	71.459
70	64.361	65.352	65.352	67.948
70	67.948	77.823	75.452	73.508
70	76.809	69.577	65.669	67.321
70	67.941	68.518	66.890	67.873
80	62.423	63.414	63.414	66.010
80	66.010	74.031	70.833	68.889
80	72.190	65.796	63.865	65.518
80	66.138	66.714	65.086	66.070
90	61.001	61.991	61.991	64.588
90	64.588	73.594	71.806	69.863
90	73.163	69.094	64.705	66.357
90	66.977	67.554	65.926	66.909
100	63.671	64.662	64.662	67.258
100	67.258	73.494	74.155	72.212
100	75.512	67.305	63.736	65.389
100	66.009	66.585	64.957	65.941

Table 25. 0013-2-2a Line Detection θ_{mean}, Grid = 5 x 5

Peaks	θ_{mean}				
10	72.03	71.96	71.96	74.02	73.82
10	73.50	74.67	73.71	75.11	75.36
10	75.37	73.18	72.35	73.51	71.98
10	71.98	71.10	70.61	73.56	68.37
10	68.37	67.50	68.02	68.06	68.59
20	72.36	73.67	73.67	74.81	74.62
20	74.29	74.23	75.06	71.17	71.42
20	71.43	72.17	71.11	72.75	68.78
20	68.78	69.37	67.19	69.48	67.52
20	67.52	66.64	67.17	67.20	67.74
30	71.70	73.69	73.69	74.84	74.64
30	74.32	71.53	74.44	68.87	69.12
30	69.13	70.65	70.92	72.24	67.91
30	67.91	70.08	68.75	72.64	70.68
30	70.68	69.80	70.33	70.36	70.90
40	72.40	76.89	76.89	78.03	77.84
40	77.51	74.51	78.41	70.00	70.25
40	70.25	73.04	73.15	73.74	69.40
40	69.40	73.29	70.95	72.75	70.79
40	70.79	69.91	70.44	70.47	71.01
50	73.30	77.78	77.78	78.93	78.73
50	78.41	77.89	79.41	72.14	72.39
50	72.40	74.56	74.85	75.23	70.90
50	70.90	72.82	70.37	72.86	70.90
50	70.90	70.02	70.55	70.58	71.12
60	72.23	76.71	76.71	77.85	77.66
60	77.33	80.26	81.82	71.06	71.32
60	71.32	74.46	73.65	73.11	68.77
60	68.77	70.65	65.49	66.46	64.50
60	64.50	63.62	64.15	64.18	64.72
70	68.64	73.12	73.12	74.27	74.07
70	73.75	71.63	75.14	70.38	70.63
70	70.63	69.36	69.20	71.19	66.85
70	66.85	72.50	61.72	64.41	62.45
70	62.45	61.57	62.10	62.13	62.67
80	66.84	71.32	71.32	72.46	72.27
80	71.94	72.22	78.12	70.13	70.38
80	70.39	69.52	72.96	68.22	63.89
80	63.89	71.67	57.13	61.58	59.62
80	59.62	58.74	59.27	59.30	59.84
90	67.68	72.16	72.16	73.30	73.11
90	72.78	74.44	77.92	69.72	69.97
90	69.98	63.91	67.35	65.79	61.45

Table 25 (Continued). 0013-2-2a Line Detection θ_{mean}, Grid = 5 x 5

Peaks	θ_{mean}				
90	61.45	70.15	57.55	64.42	62.46
90	62.46	61.58	62.11	62.14	62.68
100	66.71	71.19	71.19	72.33	72.14
100	71.81	73.47	78.40	67.25	67.50
100	67.51	64.61	68.05	64.72	60.38
100	60.38	69.07	60.39	69.87	67.91
100	67.91	67.03	67.56	67.59	68.13

Table 26. 0013-2-2a Line Detection θ_{mean}, Grid = 6 x 6

P	θ_{mean}					
10	69.33	71.71	70.84	70.84	70.15	69.85
10	66.73	68.62	68.83	69.67	71.11	70.81
10	71.70	71.23	73.08	71.82	71.23	70.28
10	71.15	70.81	70.14	70.10	69.76	70.15
10	70.15	67.85	68.77	68.46	69.53	69.97
10	69.61	68.94	70.04	71.50	71.19	71.17
20	68.48	73.22	72.35	72.35	71.49	71.19
20	67.66	72.41	72.03	68.92	71.68	71.38
20	72.28	70.74	71.82	71.24	68.91	67.38
20	68.26	68.27	68.20	70.00	69.33	69.41
20	69.41	70.00	67.17	66.59	69.16	69.61
20	69.24	68.58	67.95	69.41	69.38	69.07
30	71.64	75.64	74.77	74.77	72.18	71.88
30	68.35	74.10	73.28	71.65	75.08	74.78
30	75.68	71.88	72.11	72.75	73.30	73.15
30	74.03	72.34	70.29	72.64	71.08	71.16
30	71.16	71.21	68.86	68.85	71.24	71.69
30	71.32	70.66	70.03	71.49	71.46	71.15
40	71.75	75.75	74.88	74.88	69.74	69.44
40	65.91	71.08	71.33	70.13	75.01	74.71
40	75.60	71.80	72.21	73.19	73.38	73.69
40	74.56	70.95	72.77	74.60	70.99	71.07
40	71.07	73.76	70.60	72.04	72.95	73.40
40	73.03	72.37	71.75	73.20	73.17	72.86
50	71.86	75.86	74.99	74.99	72.27	71.97
50	68.43	73.60	73.86	73.32	77.30	77.00
50	77.89	73.74	78.66	79.91	76.33	77.03
50	77.91	74.15	74.88	74.35	68.76	68.84
50	68.84	71.53	73.87	75.32	74.80	75.24
50	74.88	74.21	73.59	75.05	75.01	74.71
60	65.46	69.46	68.59	68.59	65.87	65.57
60	62.04	67.21	67.46	67.48	72.94	72.64
60	73.53	66.40	67.62	70.68	66.69	67.68
60	68.55	65.75	68.55	68.86	64.73	64.81
60	64.81	67.50	69.57	71.01	73.18	73.63
60	73.26	72.60	71.98	73.43	73.40	73.09
70	63.41	67.41	66.54	66.54	63.82	63.52
70	59.98	65.15	65.40	66.51	72.81	72.51
70	73.41	64.83	72.41	75.48	65.01	67.05
70	67.92	65.14	68.12	68.79	65.32	65.40
70	65.40	68.08	67.91	69.35	67.11	67.55
70	67.19	66.52	65.90	67.36	67.32	67.02
80	60.58	64.58	63.71	63.71	60.99	60.69

Table 26 (Continued). 0013-2-2a Line Detection θ_{mean}, Grid = 6 x 6

P	θ_{mean}					
80	57.16	62.32	62.58	63.68	71.37	71.07
80	71.97	59.01	65.58	68.65	60.09	62.13
80	63.00	62.08	60.32	61.97	58.39	58.47
80	58.47	61.16	62.93	64.38	61.14	61.59
80	61.22	60.56	59.94	61.39	61.36	61.06
90	63.42	67.42	66.55	66.55	63.83	63.53
90	60.00	65.17	65.42	66.52	73.84	73.54
90	74.43	59.55	68.40	71.47	63.30	65.34
90	66.22	65.72	64.86	67.25	65.85	65.93
90	65.93	68.62	70.39	71.84	65.06	65.50
90	65.14	64.47	63.85	65.31	65.27	64.97
100	68.86	72.87	72.00	72.00	69.27	68.97
100	65.44	70.61	70.86	71.97	79.56	79.26
100	80.15	64.59	75.81	78.87	70.09	72.13
100	73.00	73.36	68.24	71.51	67.84	67.93
100	67.93	70.61	72.38	73.83	70.78	71.22
100	70.86	70.19	69.57	71.02	70.99	70.69

Table 27. 0013-2-2a Line Detection θ_{mean}, Grid = 8 x 8

P	θ_{mean}							
10	70.79	68.61	68.61	71.93	71.19	70.3	70.04	72.26
10	71.57	71.06	71.02	71.57	70.32	69.71	71.73	72.05
10	71.31	73.39	73.15	72.41	70.89	69.79	71.38	71.8
10	73.13	69.67	70.49	72.37	70.11	71.96	71.42	71.75
10	71.61	70.87	69.04	70.19	70.31	71.2	70.58	70.38
10	70.38	70.84	71.71	69.6	69.55	69.15	69.53	70.52
10	70.52	71.12	69.93	69.41	68.49	69.86	69.23	70.58
10	71.51	71.58	70.76	72.68	70.32	72.16	70.95	70.87
20	68.7	66.51	66.51	69.84	69.09	68.2	67.95	70.16
20	69.48	69.26	68.62	70.26	68.64	68.53	70.19	70.5
20	69.77	72.16	70.25	70.78	68.78	70.3	74.19	72.77
20	74.1	67.91	68.84	72.24	68.65	72.42	71.28	71.68
20	71.54	69.36	67.55	70.67	71.54	69.89	70.94	69.75
20	69.75	70.56	72.11	70.58	69.55	68.38	69.55	70.54
20	70.54	71.79	70.95	69.41	68.66	69.01	68.17	68.19
20	69.12	69.19	68.37	70.3	67.93	69.77	70.4	70.32
30	70.78	68.59	68.59	71.92	71.17	70.28	70.03	72.24
30	71.56	70.88	72.4	74.22	71.15	72.04	70.31	70.63
30	69.89	72.28	70.51	69.71	69.19	70.24	71.96	70.55
30	71.88	69.78	69.73	73.03	71.01	73.75	72.53	72.93
30	72.8	70.62	65.6	69.88	73.52	71.46	70.71	69.85
30	69.85	70.66	71.45	72.37	71.07	68.09	68.59	69.58
30	69.58	72.32	71.07	69.92	68.99	70.25	69.45	69.94
30	70.87	70.94	70.12	72.04	69.68	71.52	72.14	72.06
40	72.49	70.3	70.3	73.63	72.89	72	71.74	73.96
40	73.27	72.59	72.2	77.05	74.56	75.44	72.21	72.53
40	71.79	74.18	72.02	73.64	73.34	74.74	78.3	76.89
40	78.22	70.71	70.91	74.37	72.97	74.95	75.28	75.68
40	75.55	73.37	68.67	72.11	74.74	74	73.71	72.85
40	72.85	73.66	75.99	74.05	73.89	68.93	70.34	71.32
40	71.32	74.07	72.82	70.37	67.17	71.46	68.55	69.04
40	69.97	70.04	69.22	71.14	68.78	70.62	71.24	71.16
50	74.34	72.15	72.15	75.47	74.73	73.84	73.58	75.8
50	75.12	74.44	75.25	80.34	77.84	78.73	72.06	72.38
50	71.64	74.03	73.16	74.78	75.27	74.24	76.62	75.2
50	76.53	70.28	72.86	78.52	77.81	74.83	72.62	73.02
50	72.89	70.71	66.83	70.46	73.1	72.37	69.22	68.36
50	68.36	69.17	70.98	69.89	70.75	69.23	67.93	68.92
50	68.92	71.66	70.41	70.38	68.1	72.55	69.62	70.11
50	71.04	71.11	70.29	72.21	69.85	71.69	72.31	72.23
60	72.72	70.53	70.53	73.86	73.12	72.23	71.97	74.19
60	73.5	72.82	73.64	78.72	76.23	77.11	66.41	66.72
60	65.99	68.38	66.47	68.09	68.58	69.44	71.82	70.4

Table 27 (Continued). 0013-2-2a Line Detection θ_{mean}, Grid = 8 x 8

P	θ_{mean}							
60	71.74	64.28	67.61	74.31	68.79	69.62	69.16	69.56
60	69.43	67.25	64.29	68.10	70.19	69.46	67.12	66.25
60	66.25	67.07	70.86	63.01	65.59	63.53	63.94	64.93
60	64.93	67.67	66.42	63.76	62.51	68.01	64.34	64.83
60	65.76	65.83	65.01	66.93	64.57	66.41	67.03	66.95
70	66.65	64.46	64.46	67.78	67.04	66.15	65.89	68.11
70	67.43	66.75	67.56	72.65	70.15	71.04	62.67	62.99
70	62.25	64.64	65.53	67.15	67.64	63.65	64.33	62.91
70	64.24	59.50	66.34	73.04	67.12	66.43	61.26	61.66
70	61.52	59.34	58.12	62.22	59.66	58.93	56.69	55.83
70	55.83	56.64	60.43	58.03	61.95	60.85	62.53	63.52
70	63.52	66.26	65.01	61.07	58.68	64.94	59.57	60.06
70	60.99	61.06	60.24	62.17	59.80	61.64	62.27	62.19
80	60.68	58.50	58.50	61.82	61.08	60.19	59.93	62.15
80	61.46	60.78	61.60	66.69	64.19	65.07	59.12	59.44
80	58.70	61.09	59.07	60.69	61.18	60.94	62.20	60.78
80	62.11	54.12	61.82	68.53	62.61	61.84	59.00	59.40
80	59.26	57.08	56.06	60.16	61.37	60.64	57.35	56.49
80	56.49	57.30	61.10	58.01	58.99	61.16	62.84	63.83
80	63.83	66.57	65.32	61.39	57.57	64.65	59.71	60.20
80	61.13	61.20	60.38	62.30	59.94	61.78	62.41	62.33
90	64.60	62.41	62.41	65.74	64.99	64.10	63.84	66.06
90	65.38	64.70	65.51	70.60	68.10	68.99	63.95	64.27
90	63.53	65.92	64.19	65.81	66.30	67.11	65.69	64.27
90	65.60	59.13	63.65	70.36	64.44	63.67	61.11	61.51
90	61.38	59.20	60.95	65.05	66.26	65.53	63.99	63.12
90	63.12	63.93	67.73	64.64	63.59	63.87	65.55	66.54
90	66.54	69.28	68.03	64.09	61.38	67.82	62.88	63.37
90	64.30	64.37	63.55	65.48	63.11	64.95	65.58	65.50
100	70.32	68.13	68.13	71.45	70.71	69.82	69.56	71.78
100	71.10	70.41	71.23	76.32	73.82	74.71	71.15	71.47
100	70.73	73.12	71.96	73.58	74.07	69.37	69.49	68.08
100	69.41	64.08	66.01	72.71	66.80	66.03	65.15	65.55
100	65.42	63.24	62.99	67.09	68.31	67.57	66.18	65.32
100	65.32	66.13	69.93	66.84	68.13	67.54	69.23	70.21
100	70.21	72.96	71.71	67.77	65.06	72.75	67.82	68.30
100	69.24	69.30	68.49	70.41	68.04	69.88	70.51	70.43

Table 28. 0013-2-2a Line Detection θ_{mean}, Grid = 10 x 10

P	θ_{mean}									
10	71.99	70.87	70.18	70.18	71.81	71.81	67.57	68.90	70.28	69.92
10	69.34	69.31	67.73	68.53	70.71	70.65	70.65	69.41	68.83	68.59
10	67.67	69.20	68.97	69.10	69.23	68.70	69.52	69.23	68.22	68.58
10	68.58	71.62	70.33	68.68	70.11	70.30	70.07	70.60	69.36	69.42
10	69.43	68.95	70.48	68.99	68.88	70.25	70.84	70.50	69.72	69.20
10	69.47	68.83	70.00	68.54	70.40	69.04	70.19	70.71	71.59	72.19
10	71.95	73.01	72.37	70.00	71.20	68.04	71.76	69.31	70.16	68.95
10	68.96	69.00	69.49	69.56	71.56	71.32	67.92	68.53	68.20	68.90
10	68.91	69.92	69.70	71.14	72.99	67.84	68.22	68.67	69.04	71.60
10	70.22	70.25	69.57	68.27	69.85	69.98	68.97	69.81	70.39	70.34
20	71.43	70.32	68.16	69.08	70.71	70.71	67.65	68.07	69.09	68.73
20	68.14	68.12	67.48	67.95	69.73	72.40	72.40	69.70	67.69	67.45
20	66.54	68.06	67.21	67.42	70.21	69.32	69.05	69.24	66.38	66.74
20	66.74	70.13	68.28	68.34	70.03	69.98	69.79	69.05	68.74	68.80
20	68.80	68.02	69.78	68.90	68.20	69.84	72.70	70.77	67.44	66.72
20	66.99	66.34	67.72	65.85	67.59	68.24	69.13	68.25	68.87	68.89
20	68.66	69.01	68.84	65.69	67.68	64.31	69.13	65.89	65.90	65.50
20	65.51	64.42	64.20	65.85	69.01	69.61	65.47	68.67	67.97	68.67
20	68.68	68.05	67.93	70.53	71.23	66.25	68.73	68.60	67.78	70.34
20	68.95	68.98	68.30	67.00	68.72	68.59	67.58	67.78	70.00	69.95
30	73.18	72.06	71.73	72.20	73.83	73.83	71.12	69.69	71.67	71.31
30	70.72	69.61	68.97	69.44	72.33	75.70	75.70	73.36	70.35	70.11
30	69.19	70.72	70.13	68.54	71.38	70.50	72.39	72.16	68.72	69.07
30	69.07	73.84	71.99	69.40	71.35	72.19	71.72	71.07	72.74	72.81
30	72.81	68.52	70.30	70.26	69.59	70.33	73.49	71.37	68.88	68.16
30	68.43	67.78	69.40	66.10	68.66	67.60	71.14	68.38	70.01	70.03
30	69.80	70.15	70.83	65.14	67.50	66.41	70.69	69.02	67.90	68.45
30	68.46	66.63	66.41	68.06	71.37	69.55	65.41	69.62	68.44	69.15
30	69.16	68.90	67.73	69.84	71.98	68.33	67.89	68.43	67.53	70.09
30	68.71	68.74	68.06	66.75	68.47	68.34	67.33	68.13	70.11	70.07
40	72.28	71.16	71.18	71.66	73.28	73.28	70.10	70.38	72.35	71.99
40	71.40	70.29	69.65	70.12	73.16	76.50	76.50	70.29	70.19	69.96
40	69.04	70.57	69.11	67.52	72.18	71.29	72.24	72.57	67.20	67.55
40	67.55	71.48	69.63	68.60	72.69	73.68	72.37	69.24	72.05	72.11
40	72.12	68.07	72.38	70.64	69.00	71.65	74.81	71.59	69.02	68.30
40	68.57	67.92	70.80	67.67	71.47	71.15	74.12	67.45	73.76	73.78
40	73.55	73.90	75.73	68.98	70.21	67.02	71.05	70.33	68.91	69.46
40	69.47	65.40	65.18	66.83	72.47	71.61	67.48	72.04	70.86	71.57
40	71.58	72.31	70.81	72.93	73.98	71.44	72.76	73.31	70.51	73.07
40	71.69	71.72	71.04	69.73	71.46	71.33	70.31	70.10	72.08	72.03
50	73.35	72.23	72.61	73.08	74.71	74.71	71.17	71.45	73.42	73.06
50	72.47	71.36	70.72	71.19	74.08	76.61	76.61	72.36	69.50	69.26
50	68.34	69.87	68.41	66.82	72.64	71.76	72.70	72.19	67.77	68.12
50	68.13	71.04	69.18	67.35	73.94	74.93	73.31	69.42	73.01	73.08
50	73.08	68.12	70.26	69.64	69.18	70.98	74.15	69.90	64.52	63.80

Table 28 (Continued). 0013-2-2a Line Detection θ_{mean}, Grid = 10 x 10

P	θ_{mean}									
50	64.07	63.42	66.75	61.82	67.37	64.54	68.65	66.71	73.65	73.67
50	73.44	73.79	75.62	69.09	71.66	67.70	69.91	72.18	70.76	71.31
50	71.32	67.13	66.91	68.56	75.27	73.13	68.99	73.62	72.78	73.49
50	73.50	74.76	73.26	75.38	73.41	69.86	70.08	70.63	69.73	72.29
50	70.91	70.94	70.26	68.96	70.68	70.55	69.54	69.32	71.30	71.26
60	68.07	66.95	67.33	67.80	69.43	69.43	65.89	66.17	68.14	67.78
60	67.19	66.08	65.44	65.91	70.97	71.66	71.66	66.14	61.16	60.93
60	60.01	61.53	60.07	58.49	65.86	64.97	65.91	63.45	59.54	59.89
60	59.89	63.57	61.71	59.87	64.82	65.82	64.37	59.35	62.94	63.01
60	63.01	60.34	64.52	63.90	61.85	65.05	68.21	65.27	60.16	59.45
60	59.72	59.07	64.10	60.46	66.21	62.67	66.78	60.88	67.83	67.85
60	67.62	67.97	69.80	63.27	64.96	61.89	65.50	64.72	63.30	63.85
60	63.86	60.26	60.03	61.68	68.61	62.38	58.24	64.27	63.44	64.14
60	64.15	63.58	62.08	64.20	66.43	62.96	64.72	65.26	64.87	67.43
60	66.05	66.08	65.40	64.09	65.82	65.69	64.68	64.46	66.44	66.40
70	63.30	62.19	62.56	63.03	64.66	64.66	61.13	61.40	63.38	63.01
70	62.43	61.31	60.68	61.14	66.20	65.52	65.52	61.73	59.88	59.64
70	58.73	60.25	58.79	57.20	62.92	62.04	62.98	62.89	58.98	59.34
70	59.34	59.76	57.90	56.07	63.86	64.85	63.41	59.06	62.66	62.72
70	62.72	59.31	58.14	57.53	55.62	58.82	61.98	58.62	54.05	53.34
70	53.61	52.96	58.87	53.03	58.78	55.44	59.54	57.36	64.31	64.33
70	64.10	64.45	66.28	59.75	61.45	58.36	61.17	63.88	62.46	63.01
70	63.02	59.42	59.20	60.85	67.78	58.77	54.63	62.47	61.64	62.35
70	62.35	60.85	59.34	61.46	62.82	59.35	62.78	63.32	62.93	65.49
70	64.11	64.14	63.46	62.16	63.88	63.75	62.74	62.52	64.50	64.46
80	63.44	62.33	62.70	63.17	64.80	64.80	61.26	61.54	63.52	63.15
80	62.57	61.45	60.82	61.28	66.34	62.99	62.99	60.32	57.42	57.18
80	56.26	57.79	56.33	54.74	60.87	59.98	60.93	58.93	55.02	55.38
80	55.38	59.72	57.86	56.03	66.99	67.99	66.55	62.53	66.12	66.18
80	66.19	62.07	57.24	56.63	55.02	58.22	61.38	58.02	54.76	54.04
80	54.31	53.67	59.58	54.93	60.68	56.08	60.18	58.12	65.06	65.09
80	64.86	65.21	67.04	60.51	62.13	59.12	62.15	64.85	63.44	63.98
80	64.00	60.39	60.17	61.82	68.75	57.35	53.21	61.05	60.22	60.92
80	60.93	59.42	57.91	60.04	61.40	57.92	61.36	61.90	61.51	64.07
80	62.69	62.72	62.04	60.73	62.46	62.33	61.31	61.10	63.08	63.03
90	66.61	65.50	65.87	66.34	67.97	67.97	64.44	64.71	66.69	66.33
90	65.74	64.63	63.99	64.46	69.52	67.33	67.33	64.66	61.75	61.52
90	60.60	62.13	60.67	59.08	65.44	64.55	65.50	64.41	60.50	60.85
90	60.85	64.06	62.20	60.36	71.33	72.33	70.89	66.86	70.46	70.52
90	70.53	66.41	60.96	60.35	61.55	64.75	67.91	64.55	61.29	60.57
90	60.84	60.19	66.10	60.69	66.44	61.47	65.58	61.56	68.51	68.53
90	68.30	68.65	70.48	63.95	65.57	62.56	65.59	68.30	66.88	67.43
90	67.44	63.83	63.61	65.26	72.19	60.02	55.88	63.72	62.89	63.59
90	63.60	62.09	60.59	62.71	64.07	60.59	64.03	64.57	64.18	66.74
90	65.36	65.39	64.71	63.40	65.13	65.00	63.98	63.77	65.75	65.70
100	71.55	70.43	70.80	71.28	72.90	72.90	69.37	69.64	71.62	71.26
100	70.67	69.56	68.92	69.39	74.45	72.77	72.77	70.10	67.20	66.96
100	66.05	67.57	66.11	64.52	70.88	70.00	70.94	70.33	66.42	66.78

Table 28 (Continued). 0013-2-2a Line Detection θ_{mean}, Grid = 10 x 10

P	θ_{mean}									
100	66.78	69.50	67.64	65.81	76.77	77.77	76.33	72.31	75.90	75.96
100	75.97	71.85	65.89	65.28	66.66	69.86	73.02	69.66	66.40	65.68
100	65.95	65.31	71.22	65.81	71.55	69.31	73.42	66.49	73.44	73.46
100	73.23	73.58	75.41	68.88	70.50	67.50	70.52	73.23	71.81	72.36
100	72.37	68.77	68.54	70.19	77.12	66.44	62.30	70.15	69.31	70.02
100	70.03	68.52	67.01	69.13	70.49	67.02	70.45	71.00	70.61	73.17
100	71.79	71.81	71.13	69.83	71.55	71.42	70.41	70.19	72.18	72.13

Table 29. 0013-2-2a Line Detection L_{total}, Grid = 1 x 1

P	L_{total}
10	398.000
20	398.000
30	398.000
40	398.000
50	398.000
60	398.000
70	398.000
80	398.000
90	398.000
100	398.000

Table 30. 0013-2-2a Line Detection L_{total}, Grid = 2 x 2

P	L_{total}	
10	57.000	42.000
10	172.000	60.299
20	57.000	42.000
20	172.000	60.299
30	57.000	42.000
30	172.000	60.299
40	57.000	42.000
40	172.000	60.299
50	57.000	42.000
50	172.000	60.299
60	57.000	42.000
60	172.000	60.299
70	57.000	42.000
70	172.000	60.299
80	57.000	42.000
80	172.000	60.299
90	57.000	42.000
90	172.000	60.299
100	57.000	42.000
100	172.000	60.299

Table 31. 0013-2-2a Line Detection L_{total}, Grid = 4 x 4

P	L_{total}			
10	151.080	104.690	104.690	130.180
10	104.000	86.833	44.654	61.522
10	43.012	91.241	119.200	44.102
10	71.028	206.000	220.200	198.700
20	151.080	104.690	104.690	130.180
20	104.000	53.151	102.300	44.721
20	43.012	154.830	64.008	44.102
20	71.028	206.000	220.200	49.092
30	151.080	104.690	104.690	130.180
30	104.000	62.073	40.311	66.910
30	43.012	51.313	94.032	44.102
30	71.028	206.000	220.200	49.092
40	151.080	104.690	104.690	130.180
40	104.000	47.424	44.553	66.910
40	43.012	47.170	44.643	44.102
40	71.028	206.000	220.200	49.092
50	151.080	104.690	104.690	130.180
50	104.000	74.250	65.031	66.910
50	43.012	49.649	57.689	44.102
50	71.028	206.000	220.200	49.092
60	151.080	104.690	104.690	130.180
60	104.000	50.537	61.400	66.910
60	43.012	53.339	50.000	44.102
60	71.028	206.000	220.200	49.092
70	151.080	104.690	104.690	130.180
70	104.000	61.522	94.810	66.910
70	43.012	102.620	100.570	44.102
70	71.028	206.000	220.200	49.092
80	151.080	104.690	104.690	130.180
80	104.000	65.299	45.453	66.910
80	43.012	66.573	93.005	44.102
80	71.028	206.000	220.200	49.092
90	151.080	104.690	104.690	130.180
90	104.000	137.710	216.830	66.910
90	43.012	46.325	70.264	44.102
90	71.028	206.000	220.200	49.092
100	151.080	104.690	104.690	130.180
100	104.000	104.240	55.973	66.910
100	43.012	40.249	149.250	44.102
100	71.028	206.000	220.200	49.092

Table 32. 0013-2-2a Line Detection L_{total}, Grid = 5 x 5

P	L_{total}				
10	87.21	54.45	54.45	41.77	53.09
10	104.17	147.80	94.03	64.48	171.12
10	104.00	49.74	45.97	114.93	103.31
10	115.00	65.77	46.07	76.24	47.63
10	195.00	68.88	103.48	182.32	159.51
20	87.21	58.69	58.69	50.33	53.09
20	104.17	80.31	41.04	157.15	171.12
20	104.00	40.71	81.32	103.08	164.05
20	115.00	40.00	73.35	79.31	47.63
20	195.00	68.88	103.48	182.32	159.51
30	87.21	42.05	42.05	50.33	53.09
30	104.17	98.08	45.79	209.70	171.12
30	104.00	109.02	121.00	76.32	164.61
30	115.00	62.13	61.98	67.48	47.63
30	195.00	68.88	103.48	182.32	159.51
40	87.21	74.43	74.43	50.33	53.09
40	104.17	82.10	111.02	40.61	171.12
40	104.00	43.83	43.14	104.69	164.61
40	115.00	92.05	92.05	111.40	47.63
40	195.00	68.88	103.48	182.32	159.51
50	87.21	74.43	74.43	50.33	53.09
50	104.17	49.93	52.39	41.15	171.12
50	104.00	49.73	90.80	85.21	164.61
50	115.00	42.72	86.05	47.00	47.63
50	195.00	68.88	103.48	182.32	159.51
60	87.21	74.43	74.43	50.33	53.09
60	104.17	83.65	40.31	69.64	171.12
60	104.00	88.24	53.23	174.61	164.61
60	115.00	93.81	49.93	119.08	47.63
60	195.00	68.88	103.48	182.32	159.51
70	87.21	74.43	74.43	50.33	53.09
70	104.17	56.22	86.65	46.17	171.12
70	104.00	169.50	53.85	44.15	164.61
70	115.00	91.42	76.24	54.08	47.63
70	195.00	68.88	103.48	182.32	159.51
80	87.21	74.43	74.43	50.33	53.09
80	104.17	48.88	40.00	51.55	171.12
80	104.00	71.31	44.72	50.12	164.61
80	115.00	75.93	79.08	100.58	47.63
80	195.00	68.88	103.48	182.32	159.51
90	87.21	74.43	74.43	50.33	53.09
90	104.17	44.28	148.17	55.11	171.12
90	104.00	49.65	44.72	53.67	164.61

Table 32 (Continued). 0013-2-2a Line Detection L_{total}, Grid = 5 x 5

P	L_{total}				
90	115.00	58.55	143.57	152.20	47.63
90	195.00	68.88	103.48	182.32	159.51
100	87.21	74.43	74.43	50.33	53.09
100	104.17	44.28	87.92	120.28	171.12
100	104.00	128.32	44.72	97.62	164.61
100	115.00	58.55	105.91	148.77	47.63
100	195.00	68.88	103.48	182.32	159.51

Table 33. 0013-2-2a Line Detection L_{total}, Grid = 6 x 6

P	L_{total}					
10	54.01	52.01	42.00	42.00	84.40	51.16
10	42.11	41.04	143.12	146.49	48.38	99.00
10	88.60	112.45	41.04	76.94	222.58	178.90
10	60.03	44.41	47.01	81.32	207.00	91.27
10	115.00	79.51	52.01	104.55	107.38	42.52
10	104.00	103.09	104.69	171.12	79.40	47.68
20	54.01	121.10	42.00	42.00	42.19	51.16
20	42.11	87.32	159.54	209.25	42.06	99.00
20	88.60	56.05	152.90	41.23	188.00	57.28
20	60.03	85.00	62.64	64.03	96.54	51.92
20	115.00	163.00	50.48	127.88	68.47	42.52
20	104.00	103.09	76.49	171.12	127.88	47.68
30	54.01	54.59	42.00	42.00	52.01	51.16
30	42.11	170.42	141.09	54.34	51.55	99.00
30	88.60	62.51	94.34	188.00	43.00	150.37
30	60.03	308.00	50.25	69.35	47.17	51.92
30	115.00	68.88	43.83	58.59	43.83	42.52
30	104.00	103.09	76.49	171.12	127.88	47.68
40	54.01	54.59	42.00	42.00	62.63	51.16
40	42.11	187.00	60.14	50.22	124.23	99.00
40	88.60	101.53	66.94	68.88	40.00	64.85
40	60.03	294.00	57.49	321.60	60.08	51.92
40	115.00	50.49	114.42	89.05	56.73	42.52
40	104.00	103.09	76.49	171.12	127.88	47.68
50	54.01	54.59	42.00	42.00	50.91	51.16
50	42.11	187.00	60.14	71.02	123.76	99.00
50	88.60	137.71	65.52	58.05	243.87	160.38
50	60.03	143.54	66.37	69.03	58.25	51.92
50	115.00	50.49	43.83	89.05	111.49	42.52
50	104.00	103.09	76.49	171.12	127.88	47.68
60	54.01	54.59	42.00	42.00	50.91	51.16
60	42.11	187.00	60.14	137.71	43.42	99.00
60	88.60	45.65	42.00	128.46	90.09	54.23
60	60.03	146.09	97.42	51.00	88.02	51.92
60	115.00	50.49	117.02	89.05	64.38	42.52
60	104.00	103.09	76.49	171.12	127.88	47.68
70	54.01	54.59	42.00	42.00	50.91	51.16
70	42.11	187.00	60.14	150.08	156.55	99.00
70	88.60	43.00	87.21	128.46	83.86	71.61
70	60.03	71.59	55.08	44.94	98.41	51.92
70	115.00	50.49	283.52	89.05	49.68	42.52
70	104.00	103.09	76.49	171.12	127.88	47.68
80	54.01	54.59	42.00	42.00	50.91	51.16

Table 33 (Continued). 0013-2-2a Line Detection L_{total}, Grid = 6 x 6

P	L_{total}					
80	42.11	187.00	60.14	150.08	287.39	99.00
80	88.60	57.32	73.01	128.46	209.31	71.61
80	60.03	50.70	211.70	191.38	71.59	51.92
80	115.00	50.49	99.25	89.05	202.07	42.52
80	104.00	103.09	76.49	171.12	127.88	47.68
90	54.01	54.59	42.00	42.00	50.91	51.16
90	42.11	187.00	60.14	150.08	52.33	99.00
90	88.60	132.06	42.94	128.46	301.42	71.61
90	60.03	99.49	43.60	46.86	147.09	51.92
90	115.00	50.49	99.25	89.05	146.77	42.52
90	104.00	103.09	76.49	171.12	127.88	47.68
100	54.01	54.59	42.00	42.00	50.91	51.16
100	42.11	187.00	60.14	150.08	125.02	99.00
100	88.60	86.93	52.33	128.46	40.22	71.61
100	60.03	217.83	161.70	79.10	195.44	51.92
100	115.00	50.49	99.25	89.05	50.04	42.52
100	104.00	103.09	76.49	171.12	127.88	47.68

Table 34. 0013-2-2a Line Detection L_{total}, Grid = 8 x 8

P	L_{total}							
10	54.01	61.35	61.35	49.01	398.00	77.39	51.40	210.15
10	123.18	112.79	72.67	45.22	221.18	61.27	92.54	41.11
10	80.06	108.37	66.03	106.79	92.63	122.02	47.71	59.41
10	51.16	70.24	101.79	49.77	71.85	210.05	45.54	134.08
10	60.03	71.57	68.59	122.58	44.55	69.30	273.88	55.58
10	115.00	264.49	51.42	40.00	63.89	54.45	170.42	123.86
10	115.00	48.77	243.85	45.89	265.60	177.00	118.07	87.62
10	155.08	74.33	71.00	43.42	65.86	190.52	44.69	75.24
20	54.01	61.35	61.35	49.01	398.00	77.39	51.40	210.15
20	123.18	143.17	159.83	211.15	157.28	50.09	56.22	41.11
20	80.06	130.11	72.80	206.78	58.82	83.43	49.19	59.41
20	51.16	40.52	47.00	57.25	55.04	48.09	90.52	149.09
20	60.03	51.86	41.04	104.58	82.80	166.37	382.06	151.99
20	115.00	98.37	48.47	94.02	43.14	74.73	175.86	123.86
20	115.00	43.29	100.12	174.65	124.60	76.30	47.30	79.01
20	155.08	74.33	71.00	43.42	65.86	190.52	51.62	75.24
30	54.01	61.35	61.35	49.01	398.00	77.39	51.40	210.15
30	123.18	158.49	41.15	147.14	55.00	138.24	129.20	41.11
30	80.06	130.11	74.53	87.46	50.00	130.19	48.00	59.41
30	51.16	177.00	41.59	50.12	92.35	40.50	86.28	149.09
30	60.03	51.86	51.66	95.13	56.22	48.00	49.52	54.45
30	115.00	98.37	51.40	55.15	92.18	59.06	230.14	123.86
30	115.00	54.04	59.03	74.95	42.19	41.18	159.97	41.04
30	155.08	74.33	71.00	43.42	65.86	190.52	51.62	75.24
40	54.01	61.35	61.35	49.01	398.00	77.39	51.40	210.15
40	123.18	158.49	71.45	233.24	52.33	138.24	83.86	41.11
40	80.06	130.11	245.36	81.03	91.78	148.34	96.03	59.41
40	51.16	50.45	44.00	74.95	112.45	80.78	62.77	149.09
40	60.03	51.86	45.70	54.41	51.42	50.00	50.91	54.45
40	115.00	98.37	58.18	115.52	41.11	66.29	76.69	123.86
40	115.00	54.04	59.03	73.35	152.84	161.61	46.33	41.04
40	155.08	74.33	71.00	43.42	65.86	190.52	51.62	75.24
50	54.01	61.35	61.35	49.01	398.00	77.39	51.40	210.15
50	123.18	158.49	71.06	82.30	52.33	138.24	156.63	41.11
50	80.06	130.11	43.14	81.03	70.18	181.87	59.03	59.41
50	51.16	101.71	54.45	49.98	80.23	60.75	69.26	149.09
50	60.03	51.86	62.65	53.76	51.48	50.00	205.19	54.45
50	115.00	98.37	54.33	44.01	44.92	110.15	47.51	123.86
50	115.00	54.04	59.03	60.47	222.58	89.28	219.82	41.04
50	155.08	74.33	71.00	43.42	65.86	190.52	51.62	75.24
60	54.01	61.35	61.35	49.01	398.00	77.39	51.40	210.15
60	123.18	158.49	71.06	82.30	52.33	138.24	65.86	41.11
60	80.06	130.11	177.00	81.03	70.18	54.45	56.09	59.41

Table 34 (Continued). 0013-2-2a Line Detection L_{total}, Grid = 8 x 8

P	L_{total}							
60	51.16	57.22	58.69	40.20	50.45	56.32	60.03	149.09
60	60.03	51.86	99.16	96.03	165.11	50.00	55.90	54.45
60	115.00	98.37	45.10	49.65	52.40	112.92	106.61	123.86
60	115.00	54.04	59.03	54.13	58.01	134.73	107.71	41.04
60	155.08	74.33	71.00	43.42	65.86	190.52	51.62	75.24
70	54.01	61.35	61.35	49.01	398.00	77.39	51.40	210.15
70	123.18	158.49	71.06	82.30	52.33	138.24	167.59	41.11
70	80.06	130.11	76.03	81.03	70.18	42.95	80.80	59.41
70	51.16	76.94	72.56	40.20	43.29	40.00	71.40	149.09
70	60.03	51.86	47.01	118.70	120.42	50.00	68.36	54.45
70	115.00	98.37	45.10	59.67	70.71	90.79	49.20	123.86
70	115.00	54.04	59.03	54.13	134.08	307.00	54.45	41.04
70	155.08	74.33	71.00	43.42	65.86	190.52	51.62	75.24
80	54.01	61.35	61.35	49.01	398.00	77.39	51.40	210.15
80	123.18	158.49	71.06	82.30	52.33	138.24	54.41	41.11
80	80.06	130.11	166.60	81.03	70.18	151.12	50.01	59.41
80	51.16	81.74	65.00	40.20	43.29	53.04	58.82	149.09
80	60.03	51.86	103.87	118.70	71.45	50.00	123.37	54.45
80	115.00	98.37	45.10	53.04	142.13	92.63	49.20	123.86
80	115.00	54.04	59.03	54.13	117.27	44.05	70.73	41.04
80	155.08	74.33	71.00	43.42	65.86	190.52	51.62	75.24
90	54.01	61.35	61.35	49.01	398.00	77.39	51.40	210.15
90	123.18	158.49	71.06	82.30	52.33	138.24	42.76	41.11
90	80.06	130.11	52.01	81.03	70.18	60.13	97.08	59.41
90	51.16	88.89	55.95	40.20	43.29	53.04	43.86	149.09
90	60.03	51.86	79.40	118.70	71.45	50.00	106.89	54.45
90	115.00	98.37	45.10	53.04	45.40	221.05	49.20	123.86
90	115.00	54.04	59.03	54.13	49.20	43.11	70.73	41.04
90	155.08	74.33	71.00	43.42	65.86	190.52	51.62	75.24
100	54.01	61.35	61.35	49.01	398.00	77.39	51.40	210.15
100	123.18	158.49	71.06	82.30	52.33	138.24	51.25	41.11
100	80.06	130.11	44.78	81.03	70.18	76.40	65.80	59.41
100	51.16	60.84	180.49	40.20	43.29	53.04	43.86	149.09
100	60.03	51.86	58.94	118.70	71.45	50.00	72.18	54.45
100	115.00	98.37	45.10	53.04	43.68	75.93	49.20	123.86
100	115.00	54.04	59.03	54.13	49.20	42.19	70.73	41.04
100	155.08	74.33	71.00	43.42	65.86	190.52	51.62	75.24

Table 35. 0013-2-2a Line Detection L_{total}, Grid = 10 x 10

P	t_{total}									
10	54.01	57.00	277.75	105.39	219.04	219.04	54.92	300.02	111.76	136.19
10	50.45	118.96	294.44	193.75	161.00	66.22	66.22	124.00	161.61	205.18
10	41.20	173.23	61.86	44.10	223.16	81.22	66.03	74.53	57.00	60.01
10	54.01	42.20	41.76	56.52	162.80	61.22	68.54	118.87	128.63	100.26
10	152.08	97.42	112.15	92.63	65.00	44.69	102.00	87.69	43.17	122.07
10	56.00	70.01	97.49	51.87	114.83	50.49	70.24	124.00	57.49	40.25
10	63.03	82.01	48.00	87.64	40.31	128.28	79.31	60.11	50.25	74.22
10	115.00	49.20	55.90	306.24	100.62	119.85	50.09	99.50	43.38	91.29
10	115.00	66.37	108.90	124.00	55.66	65.28	42.38	47.85	76.85	60.02
10	66.00	130.19	88.23	68.26	107.69	66.10	112.93	118.79	130.03	139.18
20	54.01	57.00	54.08	225.28	219.04	219.04	285.00	42.20	75.43	136.19
20	50.45	125.48	71.59	193.75	58.60	64.41	64.41	111.65	131.04	205.18
20	41.20	173.23	87.32	116.81	285.00	242.91	111.31	101.24	110.15	60.01
20	54.01	130.11	41.11	61.21	51.48	85.60	41.59	56.72	222.58	100.26
20	152.08	58.90	92.63	46.04	51.62	153.18	61.91	110.02	59.46	51.62
20	56.00	70.01	49.40	74.04	285.00	68.71	111.40	93.54	43.05	228.85
20	63.03	67.94	68.15	83.10	140.04	211.95	65.00	102.73	54.20	46.69
20	115.00	42.11	165.08	77.16	200.72	122.19	66.76	56.22	99.04	91.29
20	115.00	74.97	76.24	143.40	45.35	196.06	124.00	40.22	56.72	60.02
20	66.00	130.19	88.23	68.26	74.15	54.38	112.93	44.18	48.51	139.18
30	54.01	57.00	48.09	59.46	219.04	219.04	121.02	132.54	62.59	136.19
30	50.45	93.13	71.59	193.75	91.92	54.67	54.67	46.17	40.26	205.18
30	41.20	173.23	47.52	178.02	84.39	242.91	44.39	97.08	57.78	60.01
30	54.01	66.29	41.11	61.66	51.87	74.25	124.49	89.81	43.42	100.26
30	152.08	45.28	101.61	43.83	124.00	93.13	61.91	101.83	285.00	51.62
30	56.00	70.01	141.60	55.11	140.22	110.26	96.14	132.42	106.40	228.85
30	63.03	67.94	43.38	76.32	83.82	64.89	84.05	50.29	73.25	65.38
30	115.00	52.33	165.08	77.16	107.56	118.79	66.76	230.89	72.45	91.29
30	115.00	59.44	145.21	50.00	64.50	93.81	104.40	111.22	78.41	60.02
30	66.00	130.19	88.23	68.26	74.15	54.38	112.93	339.84	163.08	139.18
40	54.01	57.00	273.15	59.46	219.04	219.04	45.88	213.53	62.59	136.19
40	50.45	93.13	71.59	193.75	55.36	72.69	72.69	64.03	120.33	205.18
40	41.20	173.23	131.04	178.02	43.93	242.91	44.39	68.36	47.42	60.01
40	54.01	45.00	41.11	122.02	87.28	87.46	61.40	132.85	45.45	100.26
40	152.08	40.61	123.07	74.47	219.04	190.00	61.91	169.19	180.89	51.62
40	56.00	70.01	137.53	127.82	88.24	202.23	41.34	86.28	50.16	228.85
40	63.03	67.94	42.05	97.17	46.33	62.30	85.91	199.54	186.22	65.38
40	115.00	44.94	165.08	77.16	61.19	75.03	66.76	40.46	60.01	91.29
40	115.00	75.96	245.36	50.00	285.00	44.28	62.39	111.22	48.00	60.02
40	66.00	130.19	88.23	68.26	74.15	54.38	112.93	99.13	163.08	139.18
50	54.01	57.00	143.40	59.46	219.04	219.04	45.88	213.53	62.59	136.19
50	50.45	93.13	71.59	193.75	67.90	45.00	45.00	73.50	69.30	205.18
50	41.20	173.23	131.04	178.02	107.20	242.91	44.39	77.90	52.40	60.01
50	54.01	73.25	41.11	122.02	48.51	87.46	50.36	74.67	81.57	100.26
50	152.08	115.87	106.47	42.49	67.23	191.32	61.91	46.86	53.31	51.62

Table 35 (Continued). 0013-2-2a Line Detection L_{total}, Grid = 10 x 10

P	L_{total}									
50	56.00	70.01	81.39	41.40	214.28	80.10	41.34	45.61	51.00	228.85
50	63.03	67.94	42.05	58.80	63.06	62.65	49.37	86.93	186.22	65.38
50	115.00	106.25	165.08	77.16	43.19	104.81	66.76	92.63	70.83	91.29
50	115.00	325.44	245.36	50.00	44.41	70.21	41.73	111.22	70.35	60.02
50	66.00	130.19	88.23	68.26	74.15	54.38	112.93	99.13	163.08	139.18
60	54.01	57.00	143.40	59.46	219.04	219.04	45.88	213.53	62.59	136.19
60	50.45	93.13	71.59	193.75	43.11	40.11	40.11	69.64	74.33	205.18
60	41.20	173.23	131.04	178.02	118.83	242.91	44.39	156.35	46.10	60.01
60	54.01	187.96	41.11	122.02	95.21	87.46	50.36	53.60	81.57	100.26
60	152.08	62.00	45.35	42.49	219.15	87.73	61.91	62.13	92.54	51.62
60	56.00	70.01	78.16	163.20	102.96	42.72	41.34	102.40	51.00	228.85
60	63.03	67.94	42.05	58.80	42.45	43.14	79.08	46.82	186.22	65.38
60	115.00	44.05	165.08	77.16	43.19	69.31	66.76	54.45	70.83	91.29
60	115.00	40.36	245.36	50.00	60.88	81.58	49.40	111.22	70.35	60.02
60	66.00	130.19	88.23	68.26	74.15	54.38	112.93	99.13	163.08	139.18
70	54.01	57.00	143.40	59.46	219.04	219.04	45.88	213.53	62.59	136.19
70	50.45	93.13	71.59	193.75	43.11	143.20	143.20	42.01	183.81	205.18
70	41.20	173.23	131.04	178.02	64.89	242.91	44.39	198.58	46.10	60.01
70	54.01	55.87	41.11	122.02	88.24	87.46	50.36	68.03	81.57	100.26
70	152.08	90.27	294.04	42.49	44.91	87.73	61.91	62.13	85.49	51.62
70	56.00	70.01	127.12	154.87	102.96	97.08	41.34	62.65	51.00	228.85
70	63.03	67.94	42.05	58.80	126.70	43.14	94.13	43.11	186.22	65.38
70	115.00	44.05	165.08	77.16	43.19	62.39	66.76	43.19	70.83	91.29
70	115.00	80.36	245.36	50.00	60.88	81.58	75.80	111.22	70.35	60.02
70	66.00	130.19	88.23	68.26	74.15	54.38	112.93	99.13	163.08	139.18
80	54.01	57.00	143.40	59.46	219.04	219.04	45.88	213.53	62.59	136.19
80	50.45	93.13	71.59	193.75	43.11	42.54	42.54	50.57	183.81	205.18
80	41.20	173.23	131.04	178.02	59.03	242.91	44.39	53.25	46.10	60.01
80	54.01	102.59	41.11	122.02	44.10	87.46	50.36	47.51	81.57	100.26
80	152.08	90.27	94.76	42.49	55.66	87.73	61.91	62.13	71.06	51.62
80	56.00	70.01	127.12	80.75	102.96	105.95	41.34	50.00	51.00	228.85
80	63.03	67.94	42.05	58.80	47.41	43.14	211.27	43.11	186.22	65.38
80	115.00	44.05	165.08	77.16	43.19	152.54	66.76	43.19	70.83	91.29
80	115.00	80.36	245.36	50.00	60.88	81.58	75.80	111.22	70.35	60.02
80	66.00	130.19	88.23	68.26	74.15	54.38	112.93	99.13	163.08	139.18
90	54.01	57.00	143.40	59.46	219.04	219.04	45.88	213.53	62.59	136.19
90	50.45	93.13	71.59	193.75	43.11	109.93	109.93	50.57	183.81	205.18
90	41.20	173.23	131.04	178.02	54.45	242.91	44.39	56.85	46.10	60.01
90	54.01	102.59	41.11	122.02	44.10	87.46	50.36	47.51	81.57	100.26
90	152.08	90.27	94.76	42.49	66.85	87.73	61.91	62.13	71.06	51.62
90	56.00	70.01	127.12	80.75	102.96	54.33	41.34	82.86	51.00	228.85
90	63.03	67.94	42.05	58.80	47.41	43.14	211.27	43.11	186.22	65.38
90	115.00	44.05	165.08	77.16	43.19	233.55	66.76	43.19	70.83	91.29
90	115.00	80.36	245.36	50.00	60.88	81.58	75.80	111.22	70.35	60.02
90	66.00	130.19	88.23	68.26	74.15	54.38	112.93	99.13	163.08	139.18
100	54.01	57.00	143.40	59.46	219.04	219.04	45.88	213.53	62.59	136.19
100	50.45	93.13	71.59	193.75	43.11	54.45	54.45	50.57	183.81	205.18
100	41.20	173.23	131.04	178.02	54.45	242.91	44.39	57.20	46.10	60.01

Table 35 (Continued). 0013-2-2a Line Detection L_{total}, Grid = 10 x 10

P	t_{total}									
100	54.01	102.59	41.11	122.02	44.10	87.46	50.36	47.51	81.57	100.26
100	152.08	90.27	94.76	42.49	61.21	87.73	61.91	62.13	71.06	51.62
100	56.00	70.01	127.12	80.75	102.96	104.58	41.34	82.86	51.00	228.85
100	63.03	67.94	42.05	58.80	47.41	43.14	211.27	43.11	186.22	65.38
100	115.00	44.05	165.08	77.16	43.19	41.04	66.76	43.19	70.83	91.29
100	115.00	80.36	245.36	50.00	60.88	81.58	75.80	111.22	70.35	60.02
100	66.00	130.19	88.23	68.26	74.15	54.38	112.93	99.13	163.08	139.18

Table 36. 0013-2-2a Line Detection t_{total}, Grid = 1 x 1

P	t_{total}
10	0.316
20	0.329
30	0.350
40	0.367
50	0.339
60	0.372
70	0.345
80	0.383
90	0.347
100	0.343

Table 37. 0013-2-2a Line Detection t_{total}, Grid = 2 x 2

P	t_{total}	
10	0.113	0.114
10	0.116	0.131
20	0.112	0.114
20	0.112	0.135
30	0.116	0.113
30	0.115	0.136
40	0.149	0.128
40	0.122	0.156
50	0.115	0.116
50	0.113	0.142
60	0.121	0.123
60	0.121	0.143
70	0.120	0.121
70	0.117	0.139
80	0.124	0.125
80	0.125	0.150
90	0.121	0.118
90	0.121	0.147
100	0.119	0.121
100	0.120	0.144

Table 38. 0013-2-2a Line Detection t_{total}, Grid = 4 x 4

P	t_{total}			
10	0.089	0.091	0.048	0.206
10	0.068	0.100	0.156	0.128
10	0.086	0.096	0.096	0.075
10	0.061	0.130	0.053	0.097
20	0.087	0.092	0.046	0.202
20	0.065	0.166	0.220	0.195
20	0.087	0.167	0.165	0.075
20	0.061	0.123	0.051	0.199
30	0.088	0.094	0.045	0.225
30	0.069	0.257	0.302	0.247
30	0.094	0.233	0.251	0.085
30	0.065	0.125	0.055	0.206
40	0.106	0.103	0.049	0.246
40	0.087	0.310	0.389	0.263
40	0.094	0.333	0.370	0.103
40	0.065	0.143	0.073	0.223
50	0.093	0.095	0.050	0.208
50	0.070	0.376	0.451	0.252
50	0.089	0.422	0.431	0.093
50	0.067	0.150	0.056	0.209
60	0.118	0.099	0.047	0.219
60	0.070	0.466	0.540	0.258
60	0.092	0.498	0.469	0.079
60	0.066	0.130	0.057	0.244
70	0.093	0.092	0.048	0.219
70	0.071	0.533	0.601	0.254
70	0.092	0.553	0.533	0.075
70	0.062	0.127	0.050	0.212
80	0.106	0.103	0.058	0.232
80	0.075	0.660	0.721	0.280
80	0.104	0.688	0.661	0.087
80	0.070	0.146	0.060	0.217
90	0.101	0.099	0.051	0.214
90	0.072	0.675	0.758	0.265
90	0.094	0.711	0.675	0.080
90	0.065	0.131	0.057	0.211
100	0.097	0.111	0.049	0.212
100	0.068	0.789	0.894	0.272
100	0.096	0.829	0.778	0.096
100	0.067	0.147	0.057	0.221

Table 39. 0013-2-2a Line Detection t_{total}, Grid = 5 x 5

P	t_{total}				
10	0.06	0.163	0.032	0.077	0.097
10	0.082	0.085	0.076	0.084	0.036
10	0.076	0.079	0.085	0.083	0.118
10	0.03	0.084	0.075	0.139	0.11
10	0.057	0.037	0.056	0.049	0.087
20	0.059	0.216	0.031	0.129	0.096
20	0.082	0.145	0.125	0.151	0.036
20	0.051	0.131	0.144	0.129	0.175
20	0.031	0.159	0.224	0.145	0.108
20	0.052	0.044	0.055	0.048	0.077
30	0.061	0.294	0.033	0.143	0.102
30	0.085	0.244	0.231	0.216	0.042
30	0.054	0.195	0.223	0.187	0.219
30	0.028	0.232	0.293	0.218	0.131
30	0.053	0.049	0.071	0.055	0.091
40	0.06	0.331	0.035	0.136	0.1
40	0.094	0.305	0.29	0.295	0.046
40	0.056	0.253	0.31	0.253	0.224
40	0.033	0.404	0.351	0.282	0.117
40	0.064	0.044	0.063	0.05	0.092
50	0.061	0.337	0.039	0.157	0.105
50	0.104	0.36	0.393	0.346	0.037
50	0.054	0.317	0.372	0.331	0.256
50	0.053	0.584	0.421	0.402	0.115
50	0.057	0.045	0.059	0.05	0.083
60	0.061	0.337	0.031	0.146	0.105
60	0.083	0.413	0.445	0.412	0.037
60	0.051	0.369	0.444	0.366	0.22
60	0.032	0.538	0.463	0.463	0.114
60	0.06	0.048	0.07	0.05	0.089
70	0.062	0.368	0.034	0.154	0.105
70	0.092	0.503	0.659	0.503	0.043
70	0.06	0.46	0.552	0.455	0.25
70	0.036	0.716	0.568	0.585	0.139
70	0.066	0.046	0.079	0.049	0.119
80	0.067	0.36	0.046	0.156	0.107
80	0.089	0.596	0.752	0.638	0.043
80	0.056	0.528	0.626	0.512	0.233
80	0.034	0.771	0.646	0.614	0.122
80	0.065	0.05	0.064	0.053	0.092
90	0.063	0.334	0.031	0.145	0.103
90	0.083	0.566	0.776	0.63	0.037
90	0.054	0.548	0.608	0.538	0.225

Table 39 (Continued). 0013-2-2a Line Detection t_{total}, Grid = 5 x 5

P	t_{total}				
90	0.035	0.718	0.628	0.656	0.12
90	0.058	0.045	0.063	0.051	0.089
100	0.073	0.352	0.034	0.148	0.105
100	0.101	0.614	0.844	0.767	0.039
100	0.059	0.645	0.642	0.66	0.23
100	0.032	0.756	0.743	0.758	0.128
100	0.06	0.043	0.072	0.051	0.088

Table 40. 0013-2-2a Line Detection t_{total}, Grid = 6 x 6

P	t_{total}					
10	0.03	0.1	0.094	0.03	0.088	0.053
10	0.074	0.082	0.076	0.078	0.078	0.031
10	0.038	0.155	0.082	0.08	0.093	0.102
10	0.043	0.141	0.079	0.147	0.076	0.099
10	0.029	0.083	0.081	0.081	0.081	0.041
10	0.048	0.034	0.085	0.056	0.08	0.095
20	0.029	0.135	0.085	0.029	0.163	0.05
20	0.071	0.131	0.151	0.141	0.133	0.03
20	0.037	0.195	0.133	0.135	0.176	0.15
20	0.044	0.194	0.136	0.209	0.134	0.113
20	0.026	0.193	0.134	0.139	0.14	0.039
20	0.049	0.033	0.136	0.057	0.154	0.091
30	0.031	0.184	0.098	0.035	0.227	0.064
30	0.084	0.209	0.232	0.222	0.277	0.03
30	0.038	0.253	0.191	0.252	0.28	0.207
30	0.045	0.254	0.241	0.266	0.191	0.116
30	0.027	0.253	0.195	0.194	0.193	0.042
30	0.049	0.033	0.14	0.058	0.157	0.101
40	0.031	0.191	0.095	0.031	0.292	0.054
40	0.074	0.266	0.234	0.275	0.357	0.028
40	0.038	0.344	0.272	0.343	0.381	0.285
40	0.044	0.395	0.314	0.379	0.268	0.121
40	0.028	0.346	0.281	0.288	0.275	0.046
40	0.054	0.033	0.148	0.063	0.158	0.1
50	0.033	0.186	0.096	0.032	0.35	0.051
50	0.075	0.266	0.252	0.367	0.446	0.028
50	0.043	0.445	0.34	0.41	0.47	0.35
50	0.048	0.426	0.394	0.412	0.331	0.119
50	0.029	0.312	0.329	0.268	0.354	0.043
50	0.054	0.04	0.157	0.063	0.157	0.106
60	0.031	0.194	0.09	0.028	0.342	0.055
60	0.08	0.269	0.25	0.384	0.474	0.033
60	0.038	0.459	0.417	0.467	0.526	0.398
60	0.045	0.478	0.431	0.52	0.399	0.123
60	0.029	0.316	0.395	0.269	0.386	0.049
60	0.053	0.035	0.146	0.065	0.159	0.101
70	0.033	0.212	0.101	0.047	0.38	0.058
70	0.081	0.315	0.268	0.458	0.582	0.034
70	0.041	0.619	0.517	0.507	0.642	0.489
70	0.051	0.586	0.553	0.643	0.507	0.154
70	0.035	0.365	0.52	0.308	0.511	0.048
70	0.053	0.049	0.173	0.071	0.19	0.104
80	0.04	0.189	0.111	0.032	0.367	0.057

Table 40 (Continued). 0013-2-2a Line Detection t_{total}, Grid = 6 x 6

P	t_{total}					
80	0.086	0.28	0.262	0.441	0.648	0.033
80	0.041	0.657	0.584	0.497	0.675	0.464
80	0.046	0.625	0.595	0.688	0.535	0.127
80	0.034	0.337	0.539	0.299	0.547	0.046
80	0.057	0.041	0.154	0.068	0.172	0.103
90	0.031	0.18	0.097	0.027	0.337	0.052
90	0.082	0.266	0.234	0.407	0.651	0.03
90	0.039	0.703	0.593	0.46	0.724	0.434
90	0.045	0.659	0.624	0.68	0.592	0.122
90	0.029	0.309	0.498	0.269	0.567	0.042
90	0.05	0.038	0.144	0.064	0.16	0.101
100	0.033	0.206	0.114	0.032	0.371	0.062
100	0.082	0.306	0.263	0.44	0.705	0.029
100	0.04	0.776	0.767	0.542	0.854	0.488
100	0.047	0.758	0.736	0.794	0.732	0.12
100	0.029	0.307	0.515	0.263	0.642	0.056
100	0.056	0.035	0.158	0.074	0.176	0.106

Table 41. 0013-2-2a Line Detection t_{total}, Grid = 8 x 8

P	t_{total}							
10	0.027	0.068	0.024	0.057	0.033	0.074	0.102	0.132
10	0.044	0.073	0.074	0.078	0.071	0.077	0.085	0.058
10	0.031	0.069	0.071	0.075	0.07	0.073	0.069	0.157
10	0.054	0.072	0.072	0.068	0.071	0.069	0.069	0.071
10	0.032	0.07	0.074	0.066	0.068	0.07	0.071	0.097
10	0.027	0.069	0.069	0.075	0.07	0.074	0.077	0.111
10	0.028	0.069	0.071	0.071	0.071	0.101	0.071	0.07
10	0.043	0.03	0.03	0.066	0.038	0.075	0.08	0.107
20	0.028	0.078	0.022	0.054	0.035	0.07	0.104	0.129
20	0.047	0.124	0.123	0.124	0.12	0.119	0.122	0.058
20	0.032	0.09	0.124	0.119	0.125	0.164	0.12	0.161
20	0.053	0.12	0.123	0.118	0.12	0.121	0.12	0.086
20	0.032	0.123	0.122	0.121	0.122	0.121	0.121	0.147
20	0.027	0.114	0.121	0.123	0.163	0.12	0.121	0.104
20	0.027	0.122	0.12	0.123	0.127	0.166	0.122	0.129
20	0.044	0.03	0.028	0.063	0.041	0.064	0.086	0.096
30	0.027	0.078	0.024	0.057	0.033	0.07	0.104	0.131
30	0.044	0.174	0.173	0.18	0.175	0.185	0.193	0.06
30	0.034	0.098	0.192	0.194	0.198	0.24	0.206	0.167
30	0.054	0.207	0.179	0.178	0.174	0.176	0.181	0.097
30	0.038	0.137	0.197	0.198	0.235	0.236	0.18	0.188
30	0.026	0.117	0.177	0.179	0.222	0.178	0.177	0.111
30	0.028	0.149	0.164	0.224	0.179	0.221	0.18	0.154
30	0.045	0.026	0.03	0.068	0.038	0.067	0.091	0.097
40	0.031	0.09	0.028	0.059	0.035	0.077	0.112	0.137
40	0.066	0.221	0.251	0.246	0.195	0.192	0.275	0.064
40	0.033	0.101	0.242	0.258	0.273	0.305	0.335	0.194
40	0.054	0.354	0.309	0.245	0.244	0.246	0.271	0.108
40	0.043	0.151	0.245	0.242	0.301	0.256	0.263	0.189
40	0.028	0.129	0.259	0.264	0.291	0.268	0.248	0.111
40	0.028	0.157	0.185	0.317	0.318	0.354	0.284	0.196
40	0.047	0.033	0.031	0.074	0.044	0.071	0.093	0.108
50	0.03	0.092	0.031	0.062	0.049	0.077	0.118	0.148
50	0.049	0.201	0.267	0.291	0.241	0.195	0.299	0.062
50	0.035	0.094	0.306	0.333	0.315	0.364	0.34	0.179
50	0.056	0.37	0.391	0.402	0.317	0.332	0.331	0.102
50	0.039	0.147	0.316	0.327	0.374	0.275	0.342	0.202
50	0.03	0.133	0.304	0.304	0.368	0.334	0.312	0.119
50	0.032	0.159	0.181	0.405	0.348	0.366	0.336	0.177
50	0.051	0.031	0.033	0.078	0.051	0.083	0.099	0.111
60	0.03	0.088	0.027	0.056	0.036	0.073	0.114	0.145
60	0.046	0.184	0.27	0.264	0.194	0.184	0.35	0.065
60	0.036	0.102	0.391	0.233	0.292	0.399	0.38	0.168

Table 42. 0013-2-2a Line Detection t_{total}, Grid = 10 x 10

P	t_{total}									
10	0.032	0.026	0.077	0.070	0.077	0.033	0.083	0.062	0.091	0.050
10	0.025	0.056	0.058	0.040	0.116	0.054	0.049	0.072	0.058	0.032
10	0.025	0.059	0.058	0.058	0.057	0.060	0.061	0.068	0.059	0.020
10	0.025	0.055	0.057	0.061	0.087	0.059	0.057	0.056	0.058	0.051
10	0.030	0.059	0.061	0.059	0.058	0.057	0.056	0.059	0.056	0.060
10	0.018	0.041	0.062	0.061	0.059	0.061	0.059	0.075	0.058	0.057
10	0.057	0.054	0.060	0.056	0.056	0.058	0.055	0.057	0.057	0.058
10	0.018	0.055	0.059	0.086	0.054	0.058	0.059	0.055	0.058	0.037
10	0.019	0.058	0.058	0.070	0.056	0.057	0.056	0.059	0.090	0.070
10	0.039	0.042	0.025	0.032	0.057	0.056	0.035	0.059	0.086	0.031
20	0.022	0.021	0.101	0.102	0.102	0.032	0.101	0.102	0.131	0.045
20	0.026	0.103	0.071	0.047	0.170	0.103	0.052	0.129	0.103	0.034
20	0.029	0.060	0.106	0.105	0.100	0.080	0.102	0.101	0.103	0.018
20	0.021	0.101	0.099	0.135	0.177	0.114	0.122	0.105	0.101	0.054
20	0.030	0.101	0.101	0.114	0.097	0.105	0.131	0.104	0.106	0.086
20	0.020	0.040	0.103	0.104	0.104	0.110	0.101	0.132	0.162	0.105
20	0.056	0.117	0.119	0.102	0.099	0.105	0.099	0.100	0.127	0.106
20	0.019	0.102	0.076	0.132	0.106	0.132	0.078	0.133	0.106	0.038
20	0.019	0.105	0.128	0.145	0.108	0.135	0.114	0.102	0.137	0.079
20	0.041	0.039	0.034	0.036	0.073	0.077	0.044	0.113	0.134	0.034
30	0.022	0.023	0.150	0.113	0.088	0.030	0.164	0.175	0.161	0.048
30	0.027	0.159	0.084	0.056	0.244	0.145	0.083	0.178	0.148	0.033
30	0.029	0.068	0.148	0.147	0.147	0.076	0.128	0.145	0.143	0.020
30	0.023	0.148	0.100	0.179	0.179	0.145	0.146	0.147	0.177	0.050
30	0.029	0.151	0.149	0.147	0.162	0.144	0.153	0.147	0.149	0.087
30	0.017	0.041	0.147	0.151	0.151	0.146	0.143	0.177	0.209	0.108
30	0.058	0.091	0.154	0.144	0.140	0.144	0.159	0.188	0.144	0.167
30	0.019	0.165	0.089	0.153	0.146	0.178	0.079	0.177	0.145	0.037
30	0.023	0.147	0.170	0.216	0.156	0.208	0.193	0.148	0.244	0.106
30	0.048	0.057	0.035	0.049	0.080	0.078	0.052	0.153	0.172	0.043
40	0.028	0.024	0.207	0.145	0.087	0.043	0.176	0.232	0.170	0.047
40	0.030	0.152	0.086	0.047	0.289	0.222	0.074	0.246	0.265	0.051
40	0.031	0.065	0.210	0.168	0.209	0.083	0.142	0.209	0.227	0.030
40	0.029	0.232	0.139	0.294	0.255	0.184	0.182	0.264	0.224	0.051
40	0.031	0.201	0.209	0.208	0.240	0.222	0.156	0.197	0.193	0.089
40	0.018	0.040	0.200	0.195	0.193	0.190	0.184	0.227	0.250	0.106
40	0.060	0.094	0.202	0.188	0.194	0.197	0.201	0.235	0.188	0.140
40	0.025	0.189	0.077	0.137	0.192	0.312	0.080	0.224	0.188	0.040
40	0.019	0.192	0.163	0.209	0.197	0.220	0.219	0.108	0.262	0.080
40	0.045	0.043	0.022	0.034	0.064	0.072	0.037	0.168	0.173	0.032
50	0.026	0.025	0.222	0.134	0.082	0.033	0.173	0.226	0.189	0.050
50	0.030	0.150	0.079	0.057	0.340	0.267	0.054	0.287	0.343	0.043
50	0.038	0.067	0.240	0.189	0.300	0.083	0.157	0.277	0.271	0.031
50	0.026	0.284	0.116	0.248	0.304	0.208	0.254	0.261	0.279	0.055
50	0.032	0.268	0.259	0.256	0.296	0.273	0.165	0.257	0.265	0.094

Table 42 (Continued). 0013-2-2a Line Detection t_{total}, Grid = 10 x 10

P	t_{total}									
50	0.018	0.045	0.269	0.263	0.257	0.262	0.215	0.322	0.331	0.114
50	0.066	0.095	0.209	0.252	0.251	0.254	0.265	0.309	0.203	0.142
50	0.022	0.256	0.089	0.151	0.256	0.382	0.085	0.286	0.230	0.038
50	0.022	0.240	0.179	0.224	0.249	0.281	0.285	0.114	0.349	0.082
50	0.041	0.049	0.024	0.043	0.078	0.071	0.042	0.185	0.179	0.036
60	0.026	0.020	0.214	0.121	0.083	0.029	0.180	0.232	0.173	0.052
60	0.026	0.140	0.084	0.048	0.366	0.317	0.052	0.330	0.288	0.034
60	0.029	0.060	0.235	0.157	0.290	0.080	0.140	0.300	0.254	0.022
60	0.024	0.296	0.108	0.247	0.331	0.193	0.251	0.275	0.327	0.057
60	0.033	0.343	0.302	0.247	0.602	0.299	0.166	0.250	0.297	0.098
60	0.018	0.037	0.337	0.289	0.279	0.296	0.198	0.365	0.307	0.112
60	0.061	0.091	0.195	0.252	0.282	0.244	0.296	0.328	0.200	0.139
60	0.021	0.308	0.084	0.135	0.243	0.401	0.072	0.312	0.211	0.043
60	0.020	0.280	0.166	0.221	0.257	0.291	0.309	0.109	0.335	0.078
60	0.040	0.040	0.025	0.032	0.059	0.073	0.043	0.169	0.169	0.032
70	0.024	0.027	0.224	0.126	0.085	0.033	0.179	0.231	0.188	0.053
70	0.031	0.152	0.096	0.056	0.410	0.390	0.054	0.412	0.371	0.039
70	0.029	0.070	0.217	0.169	0.368	0.088	0.146	0.374	0.273	0.023
70	0.031	0.369	0.116	0.247	0.407	0.236	0.277	0.359	0.282	0.062
70	0.037	0.385	0.364	0.269	0.415	0.313	0.180	0.278	0.381	0.095
70	0.026	0.045	0.389	0.364	0.303	0.373	0.215	0.459	0.340	0.120
70	0.063	0.100	0.224	0.262	0.364	0.281	0.371	0.389	0.216	0.152
70	0.030	0.323	0.088	0.156	0.270	0.491	0.085	0.356	0.243	0.036
70	0.022	0.357	0.180	0.235	0.284	0.318	0.385	0.120	0.399	0.084
70	0.052	0.048	0.026	0.038	0.075	0.083	0.052	0.189	0.183	0.038
80	0.028	0.020	0.198	0.113	0.077	0.026	0.172	0.224	0.179	0.051
80	0.034	0.147	0.078	0.043	0.393	0.385	0.048	0.390	0.375	0.040
80	0.029	0.063	0.210	0.163	0.403	0.091	0.146	0.436	0.279	0.019
80	0.031	0.390	0.119	0.223	0.393	0.192	0.244	0.412	0.255	0.053
80	0.032	0.349	0.374	0.256	0.439	0.295	0.177	0.278	0.401	0.102
80	0.022	0.049	0.384	0.390	0.270	0.388	0.190	0.453	0.314	0.111
80	0.059	0.091	0.188	0.251	0.339	0.253	0.389	0.363	0.198	0.141
80	0.018	0.284	0.079	0.138	0.245	0.508	0.078	0.336	0.220	0.042
80	0.019	0.340	0.170	0.224	0.277	0.298	0.362	0.115	0.352	0.083
80	0.039	0.045	0.030	0.044	0.068	0.072	0.042	0.168	0.172	0.037
90	0.024	0.024	0.209	0.114	0.088	0.029	0.162	0.215	0.160	0.047
90	0.029	0.138	0.085	0.045	0.363	0.426	0.050	0.385	0.335	0.035
90	0.029	0.062	0.206	0.148	0.395	0.086	0.135	0.428	0.245	0.023
90	0.024	0.424	0.107	0.233	0.407	0.195	0.250	0.375	0.265	0.054
90	0.031	0.360	0.387	0.244	0.464	0.284	0.156	0.262	0.341	0.096
90	0.021	0.042	0.365	0.386	0.265	0.440	0.194	0.497	0.321	0.110
90	0.058	0.092	0.192	0.250	0.348	0.251	0.399	0.362	0.207	0.135
90	0.019	0.289	0.077	0.132	0.247	0.535	0.083	0.321	0.214	0.046
90	0.023	0.319	0.166	0.214	0.263	0.287	0.345	0.105	0.339	0.092
90	0.040	0.043	0.024	0.035	0.067	0.081	0.036	0.171	0.177	0.064
100	0.027	0.026	0.224	0.123	0.084	0.036	0.163	0.225	0.176	0.050
100	0.027	0.145	0.078	0.050	0.380	0.449	0.053	0.396	0.354	0.037
100	0.028	0.067	0.209	0.159	0.447	0.082	0.144	0.444	0.257	0.025

Table 42 (Continued). 0013-2-2a Line Detection t_{total}, Grid = 10 x 10

P	t_{total}									
100	0.024	0.437	0.113	0.240	0.420	0.203	0.259	0.387	0.267	0.062
100	0.030	0.361	0.405	0.255	0.545	0.306	0.154	0.241	0.384	0.090
100	0.029	0.054	0.369	0.389	0.276	0.519	0.210	0.586	0.318	0.121
100	0.059	0.094	0.201	0.270	0.368	0.261	0.413	0.374	0.199	0.130
100	0.019	0.286	0.087	0.153	0.239	0.579	0.075	0.310	0.209	0.037
100	0.031	0.366	0.170	0.221	0.261	0.284	0.338	0.104	0.328	0.079
100	0.040	0.042	0.027	0.032	0.073	0.069	0.039	0.165	0.181	0.037

Appendix B: Analysis of Image fiber02a

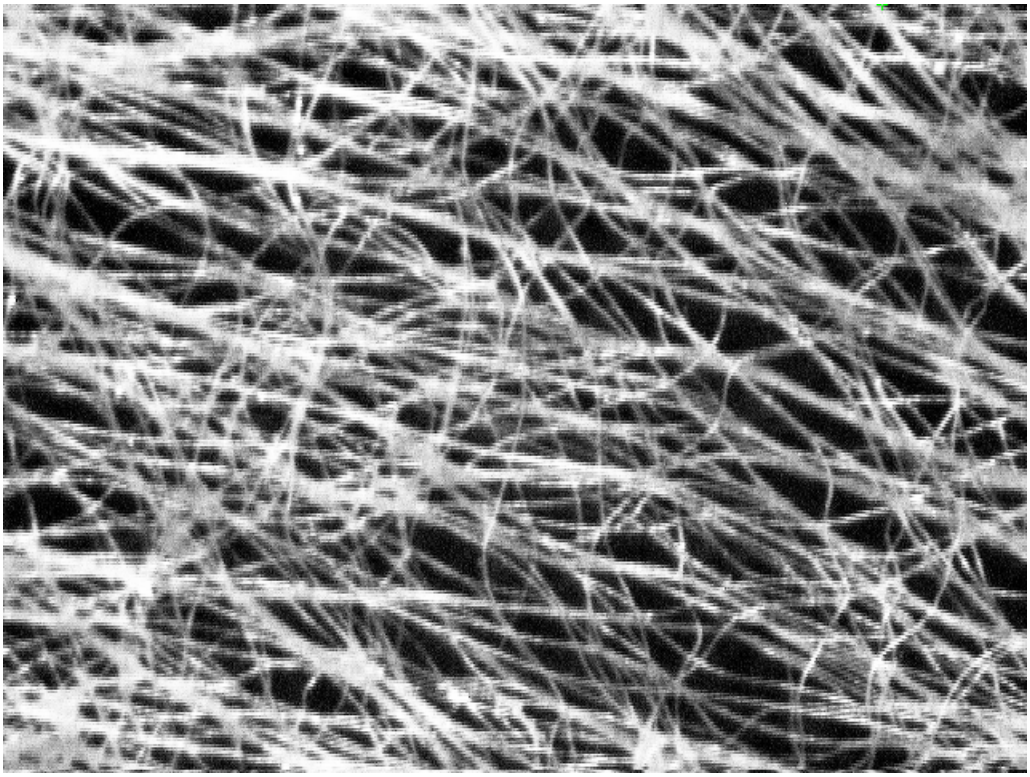


Figure 120. fiber02a

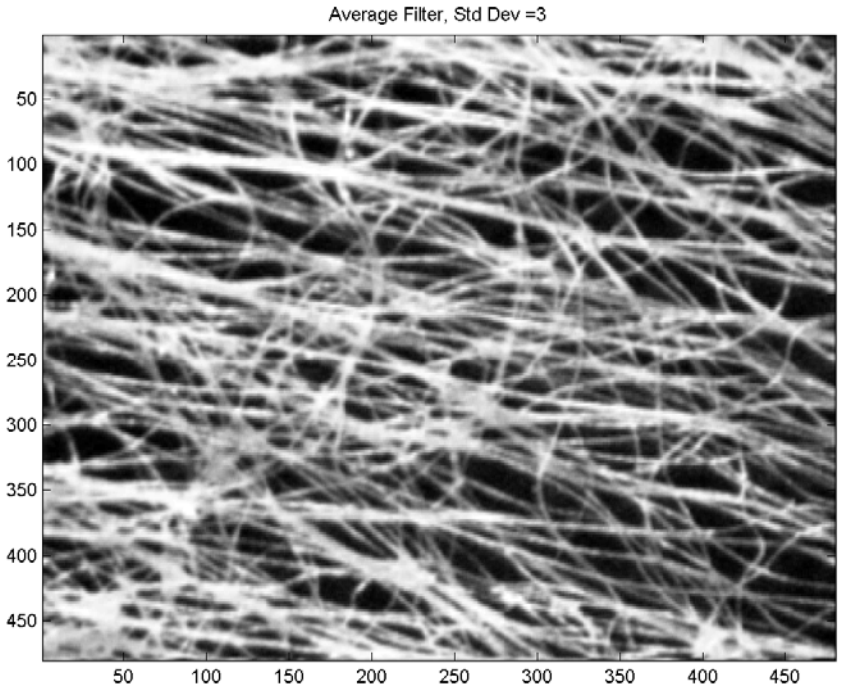


Figure 121. fiber02a Averaging Smoothing, 3 x 3 kernel

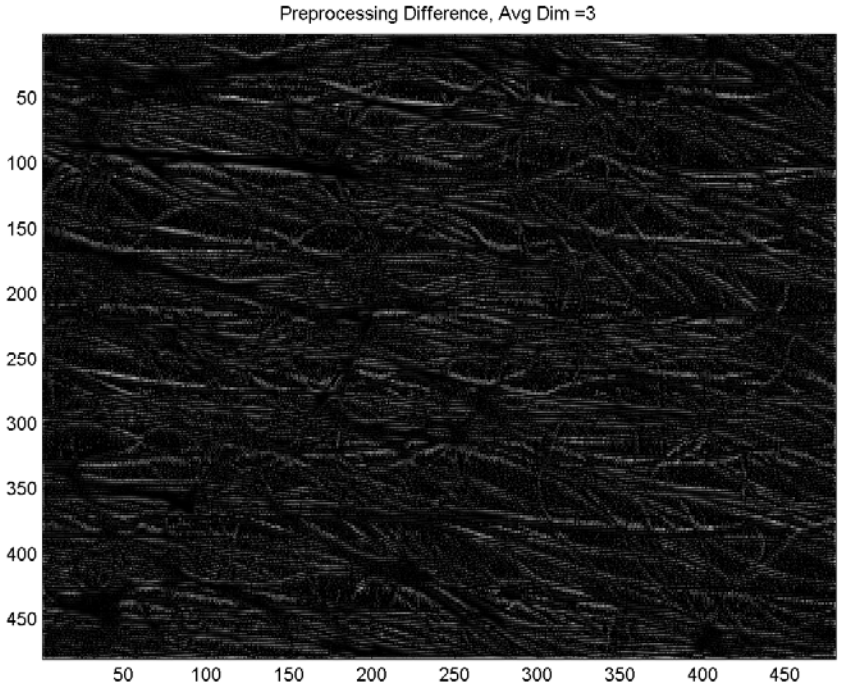


Figure 122. fiber02a Averaging Smoothing Noise, 3 x 3 kernel

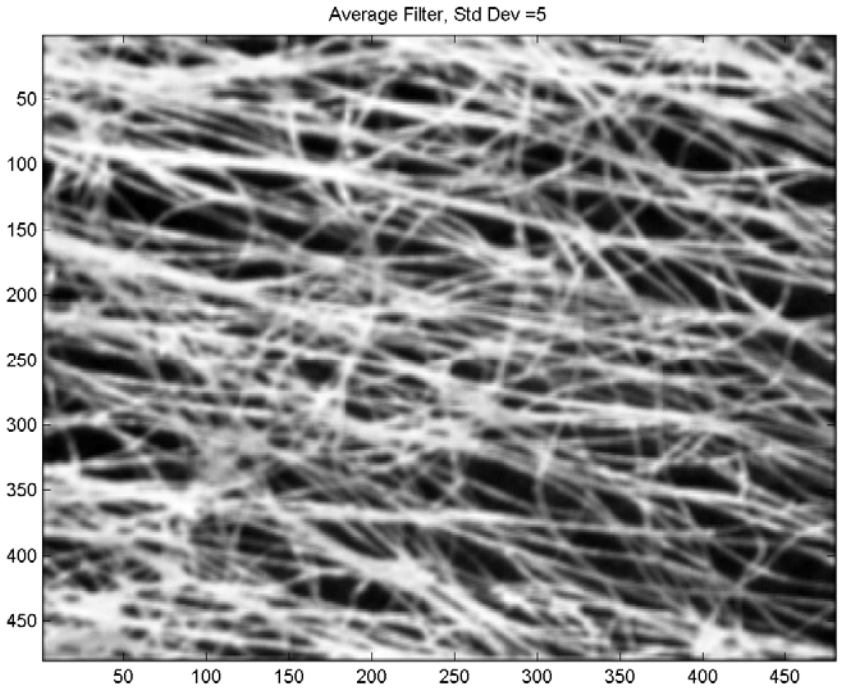


Figure 123. fiber02a Averaging Smoothing, 5 x 5 kernel

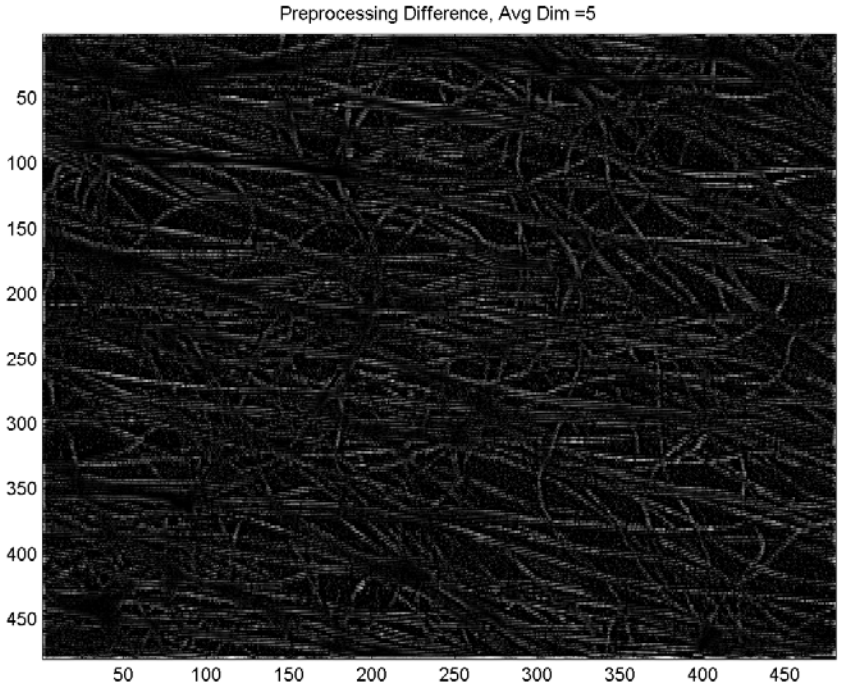


Figure 124. fiber02a Averaging Smoothing Noise, 5 x 5 kernel

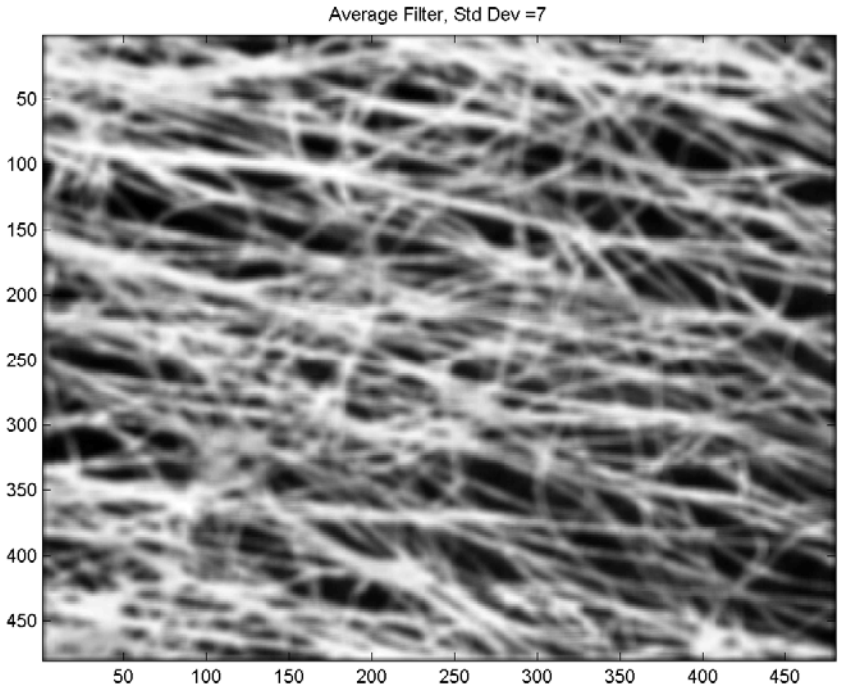


Figure 125. fiber02a Averaging Smoothing, 7 x 7 kernel

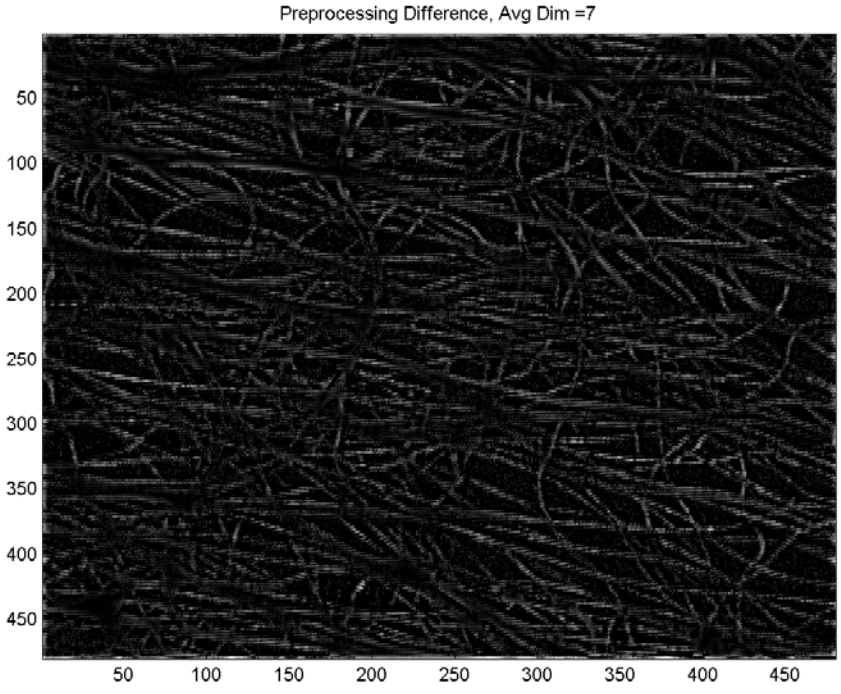


Figure 126. fiber02a Averaging Smoothing Noise, 7 x 7 kernel

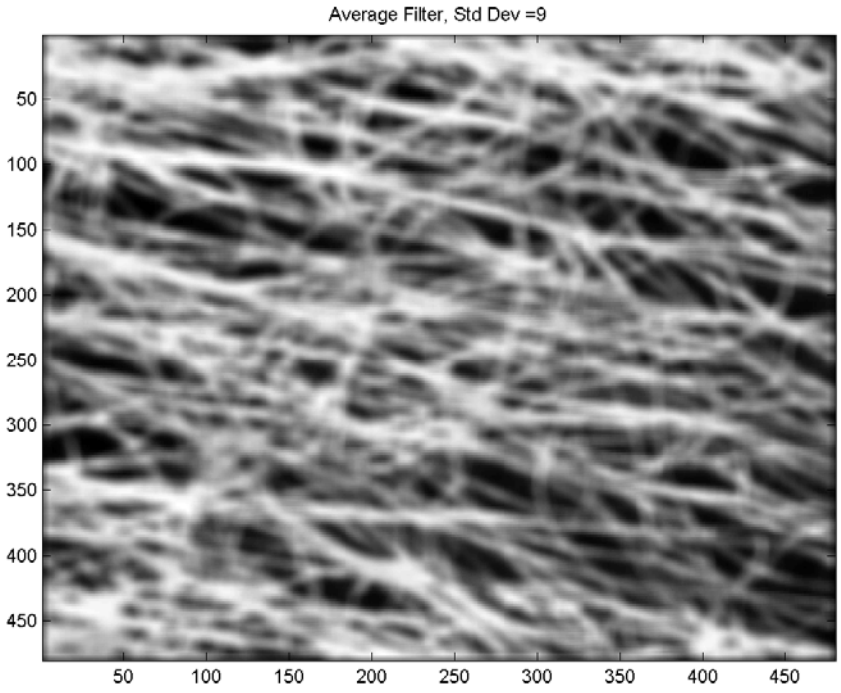


Figure 127. fiber02a Averaging Smoothing, 9 x 9 kernel

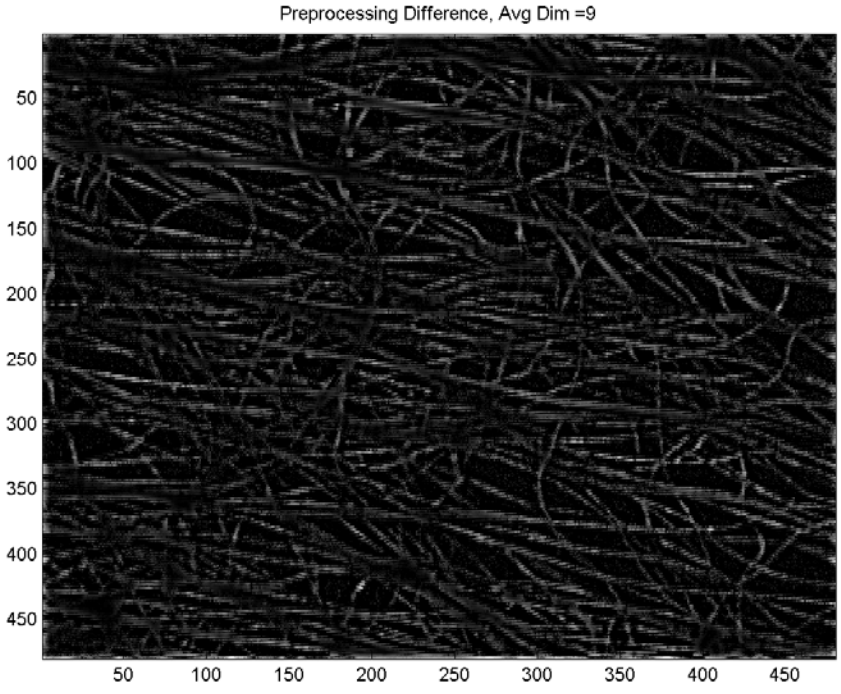


Figure 128. fiber02a Averaging Smoothing Noise, 9 x 9 kernel

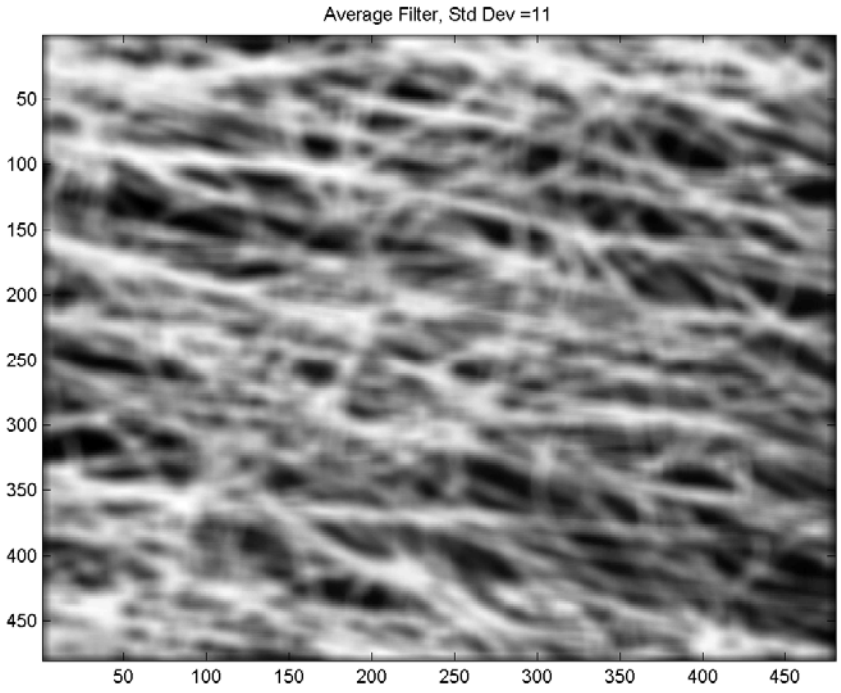


Figure 129. fiber02a Averaging Smoothing, 11 x 11 kernel

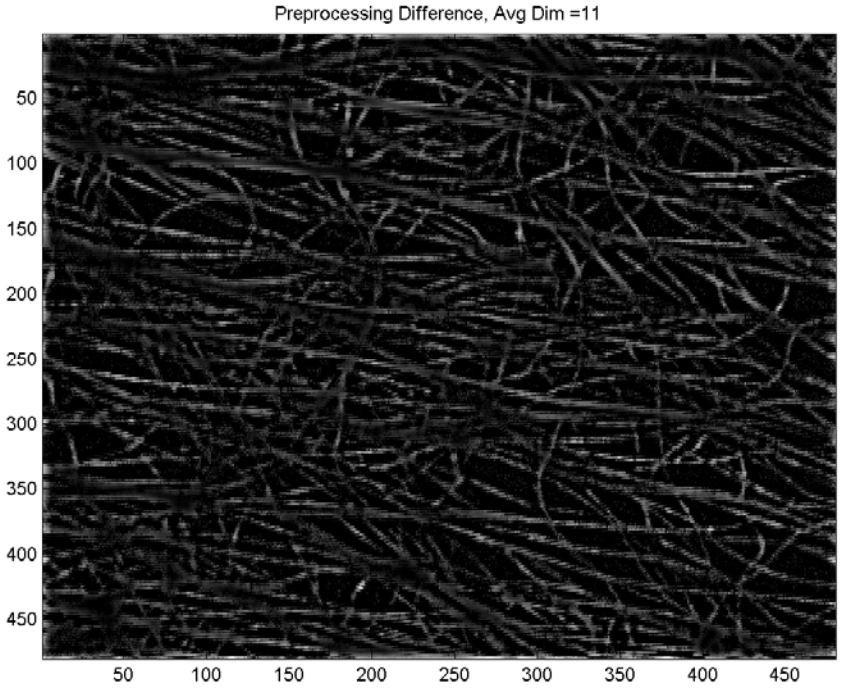


Figure 130. fiber02a Averaging Smoothing Noise, 11 x 11 kernel

Table 43. fiber02a Averaging Smoothing Histogram Data

Grayscale	1	2	3	4	5
0	114515	112981	112564	112364	111975
1	4009	3686	2848	2259	1952
2	4009	3841	2908	2318	1917
3	3801	3702	2885	2282	1914
4	3720	3798	2917	2294	1936
5	3691	3769	2956	2286	1935
6	3406	3677	3093	2507	1986
7	3464	3567	3043	2341	2041
8	3241	3568	2931	2299	1957
9	3134	3381	2905	2392	2038
10	3084	3287	2880	2389	2072
11	3092	3262	2789	2372	1987
12	2964	3108	2769	2258	2037
13	2837	3036	2707	2333	2024
14	2761	2937	2716	2393	2075
15	2645	2823	2589	2309	2075
16	2650	2758	2568	2274	2106
17	2546	2677	2473	2300	2074
18	2516	2667	2493	2198	1969
19	2391	2479	2393	2200	2029
20	2273	2366	2362	2170	2008
21	2264	2329	2258	2169	1971
22	2216	2327	2257	2159	1930
23	2100	2102	2089	2089	1918
24	2049	2061	2173	2005	1984
25	2033	1974	2009	1919	1915
26	1912	1978	1966	1997	1867
27	1780	1825	1954	1837	1879
28	1764	1792	1861	1853	1797
29	1669	1696	1806	1884	1802
30	1715	1682	1765	1813	1781
31	1602	1586	1705	1743	1770
32	1586	1572	1699	1718	1728
33	1467	1479	1574	1665	1833
34	1456	1396	1579	1590	1639
35	1370	1308	1571	1626	1569
36	1317	1363	1476	1601	1677
37	1285	1282	1417	1514	1561
38	1220	1145	1349	1524	1585
39	1187	1154	1405	1461	1556
40	1208	1066	1330	1458	1519
41	1082	1063	1252	1403	1392
42	1048	1042	1255	1370	1395
43	1012	991	1145	1298	1388

Table 43 (Continued). fiber02a Averaging Smoothing Histogram Data

Grayscale	1	2	3	4	5
44	932	890	1093	1206	1393
45	943	862	1065	1213	1317
46	852	852	1075	1158	1275
47	812	794	1009	1112	1288
48	809	795	961	1084	1274
49	723	705	977	1051	1174
50	779	676	860	1040	1114
51	707	661	880	1037	1193
52	671	606	788	972	1087
53	618	639	761	1020	1035
54	603	583	757	889	1042
55	521	536	716	863	1035
56	534	501	674	862	997
57	523	471	673	829	919
58	478	452	640	767	864
59	458	425	595	796	889
60	455	401	535	744	796
61	417	375	562	696	815
62	394	381	497	696	786
63	339	306	455	661	782
64	393	345	453	675	783
65	315	329	457	603	706
66	318	256	438	583	730
67	273	243	395	588	669
68	249	240	390	576	629
69	241	228	342	493	608
70	223	216	334	521	628
71	207	198	339	504	611
72	169	176	305	437	616
73	161	168	290	439	597
74	187	161	272	416	522
75	155	146	256	371	493
76	153	145	235	392	501
77	140	132	219	393	474
78	121	111	226	353	476
79	104	118	225	318	414
80	145	94	171	322	379
81	104	82	166	321	405
82	99	83	178	274	346
83	102	80	161	263	384
84	88	71	141	206	351
85	94	74	122	243	344
86	83	69	133	237	301
87	80	64	99	229	307

Table 43 (Continued). fiber02a Averaging Smoothing Histogram Data

Grayscale	1	2	3	4	5
88	64	59	106	234	300
89	45	62	97	191	290
90	33	47	68	197	248
91	49	44	85	166	274
92	38	49	81	187	230
93	31	49	80	175	225
94	31	45	62	158	217
95	23	57	75	153	182
96	25	54	76	143	204
97	18	32	48	147	209
98	24	40	41	107	165
99	19	57	51	100	179
100	14	36	46	95	168
101	11	37	50	102	133
102	6	32	63	83	140
103	10	37	48	69	156
104	12	25	47	89	106
105	14	35	45	94	122
106	6	23	40	65	128
107	5	23	30	65	128
108	9	23	38	72	105
109	4	19	30	73	83
110	5	19	30	51	95
111	3	17	42	55	90
112	4	10	30	44	72
113	6	14	30	50	82
114	6	7	23	42	67
115	2	6	30	53	61
116	3	13	17	45	68
117	1	3	16	41	59
118	3	7	20	37	53
119	1	8	22	21	62
120	2	5	13	39	49
121	1	5	19	27	41
122	2	4	7	26	36
123	1	8	20	25	50
124	0	4	5	15	27
125	2	7	5	22	33
126	3	7	14	18	34
127	0	3	17	24	26
128	0	5	8	22	30
129	0	6	5	18	29
130	0	2	13	26	23
131	0	1	7	12	29

Table 43 (Continued). fiber02a Averaging Smoothing Histogram Data

Grayscale	1	2	3	4	5
132	0	3	5	21	25
133	0	5	2	9	20
134	0	3	2	12	24
135	0	2	5	17	18
136	0	1	8	12	15
137	0	0	2	13	19
138	0	4	8	10	14
139	0	0	4	7	16
140	0	1	3	11	7
141	0	1	2	8	18
142	0	1	8	12	16
143	0	4	4	4	20
144	0	3	1	4	4
145	0	0	7	6	2
146	0	0	2	3	12
147	0	2	4	5	9
148	1	1	1	4	12
149	0	0	3	2	7
150	0	0	1	10	7
151	0	0	3	4	10
152	0	0	0	6	7
153	0	0	3	6	2
154	0	0	2	5	7
155	0	0	2	5	4
156	0	0	3	0	5
157	0	0	1	4	6
158	0	0	1	6	7
159	0	0	1	2	10
160	0	0	0	1	7
161	0	0	2	1	5
162	0	0	0	3	8
163	0	0	0	5	6
164	0	0	0	0	0
165	0	0	0	1	3
166	0	0	0	1	2
167	0	0	1	3	2
168	0	0	1	1	1
169	0	0	0	2	3
170	0	0	1	1	2
171	0	0	1	1	1
172	0	0	0	0	3
173	0	0	2	1	1
174	0	0	0	2	2
175	0	0	0	2	0

Table 43 (Continued). fiber02a Averaging Smoothing Histogram Data

Grayscale	1	2	3	4	5
176	0	0	0	0	2
177	0	0	0	0	0
178	0	0	0	0	0
179	0	0	0	0	1
180	0	0	0	0	0
181	0	0	0	0	0
182	0	0	0	0	3
183	0	0	0	0	2
184	0	0	0	0	1
185	0	0	0	1	0
186	0	0	0	0	0
187	0	0	0	1	0
188	0	0	0	0	0
189	0	0	0	0	0
190	0	0	0	0	0
191	0	0	0	0	1
192	0	0	0	0	1
193	0	0	0	0	0
194	0	0	0	0	0
195	0	0	0	0	0
196	0	0	0	0	0
197	0	0	0	0	0
198	0	0	0	0	0
199	0	0	0	0	0
200	0	0	0	0	0
201	0	0	0	0	0
202	0	0	0	0	0
203	0	0	0	0	0
204	0	0	0	0	0
205	0	0	0	0	0
206	0	0	0	0	0
207	0	0	0	0	0
208	0	0	0	0	0
209	0	0	0	0	0
210	0	0	0	0	0
211	0	0	0	0	0
212	0	0	0	0	0
213	0	0	0	0	0
214	0	0	0	0	0
215	0	0	0	0	0
216	0	0	0	0	0
217	0	0	0	0	0
218	0	0	0	0	0
219	0	0	0	0	0

Table 43 (Continued). fiber02a Averaging Smoothing Histogram Data

Grayscale	1	2	3	4	5
220	0	0	0	0	0
221	0	0	0	0	0
222	0	0	0	0	0
223	0	0	0	0	0
224	0	0	0	0	0
225	0	0	0	0	0
226	0	0	0	0	0
227	0	0	0	0	0
228	0	0	0	0	0
229	0	0	0	0	0
230	0	0	0	0	0
231	0	0	0	0	0
232	0	0	0	0	0
233	0	0	0	0	0
234	0	0	0	0	0
235	0	0	0	0	0
236	0	0	0	0	0
237	0	0	0	0	0
238	0	0	0	0	0
239	0	0	0	0	0
240	0	0	0	0	0
241	0	0	0	0	0
242	0	0	0	0	0
243	0	0	0	0	0
244	0	0	0	0	0
245	0	0	0	0	0
246	0	0	0	0	0
247	0	0	0	0	0
248	0	0	0	0	0
249	0	0	0	0	0
250	0	0	0	0	0
251	0	0	0	0	0
252	0	0	0	0	0
253	0	0	0	0	0
254	0	0	0	0	0
255	0	0	0	0	0
Min:	0	0	0	0	0
μ:	900	900	900	900	900
Max:	114515	112981	112564	112364	111975
Median:	0	4	8	21	29
σ:	7188.1491	7095.5302	7057.1614	7034.3391	7004.3923
% Black:	49.70%	49.04%	48.86%	48.77%	48.60%
% Gray:	50.30%	50.96%	51.14%	51.23%	51.40%

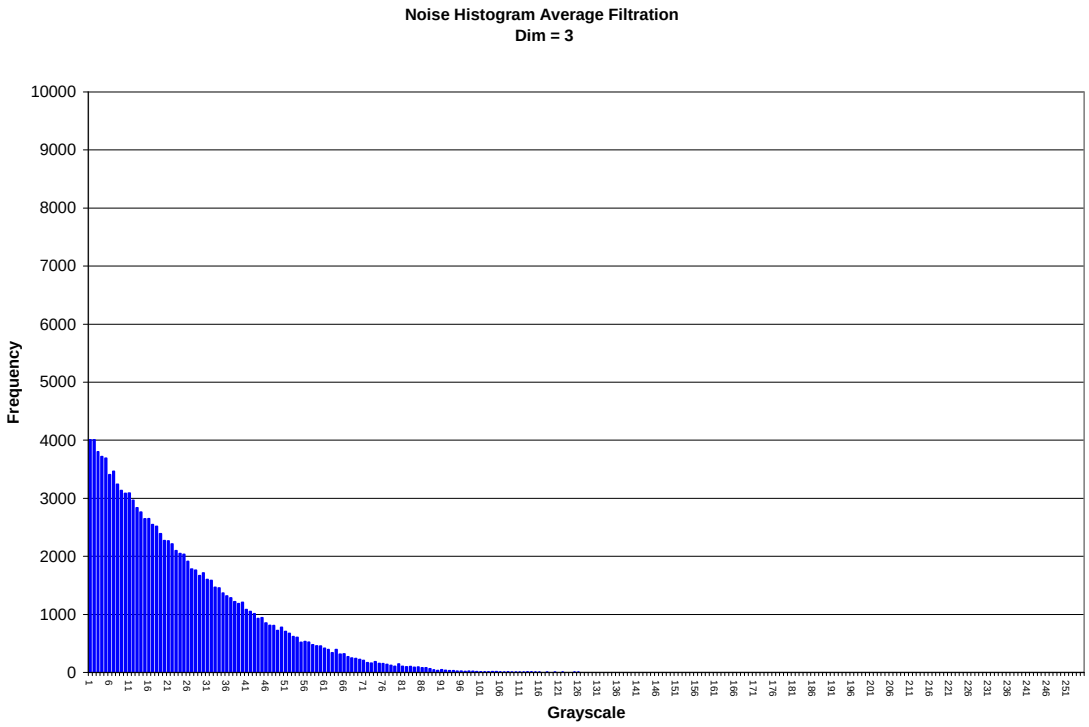


Figure 131. fiber02a Averaging Smoothing Noise Histogram, 3 x 3 kernel

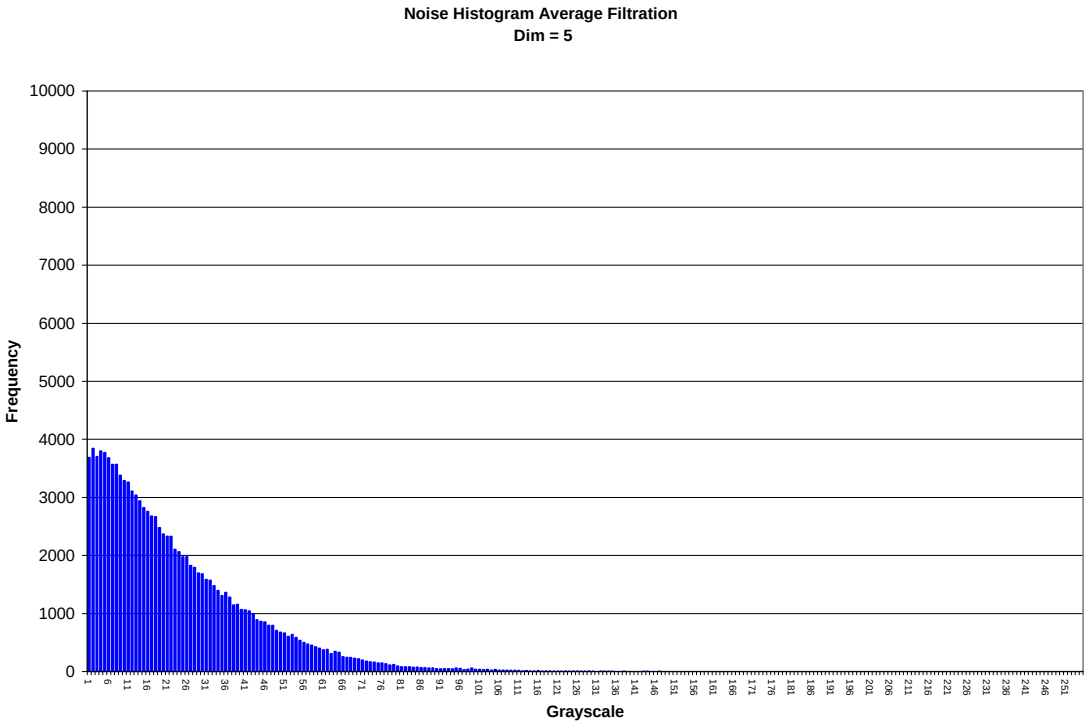


Figure 132. fiber02a Averaging Smoothing Noise Histogram, 5 x 5 kernel

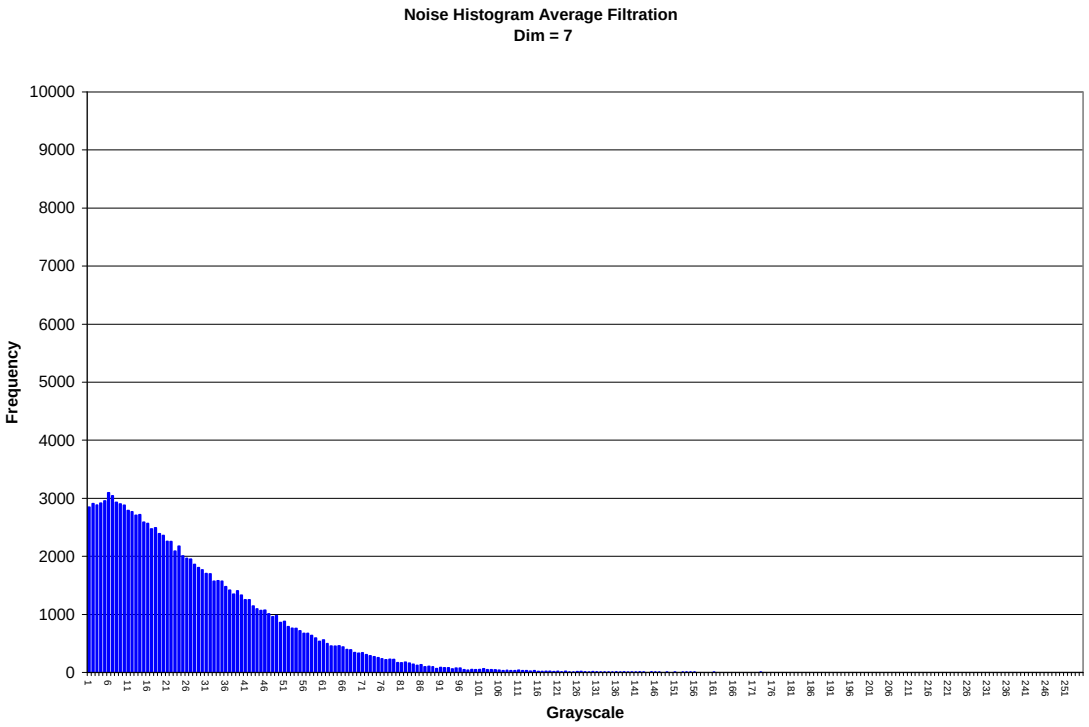


Figure 133. fiber02a Averaging Smoothing Noise Histogram, 7 x 7 kernel

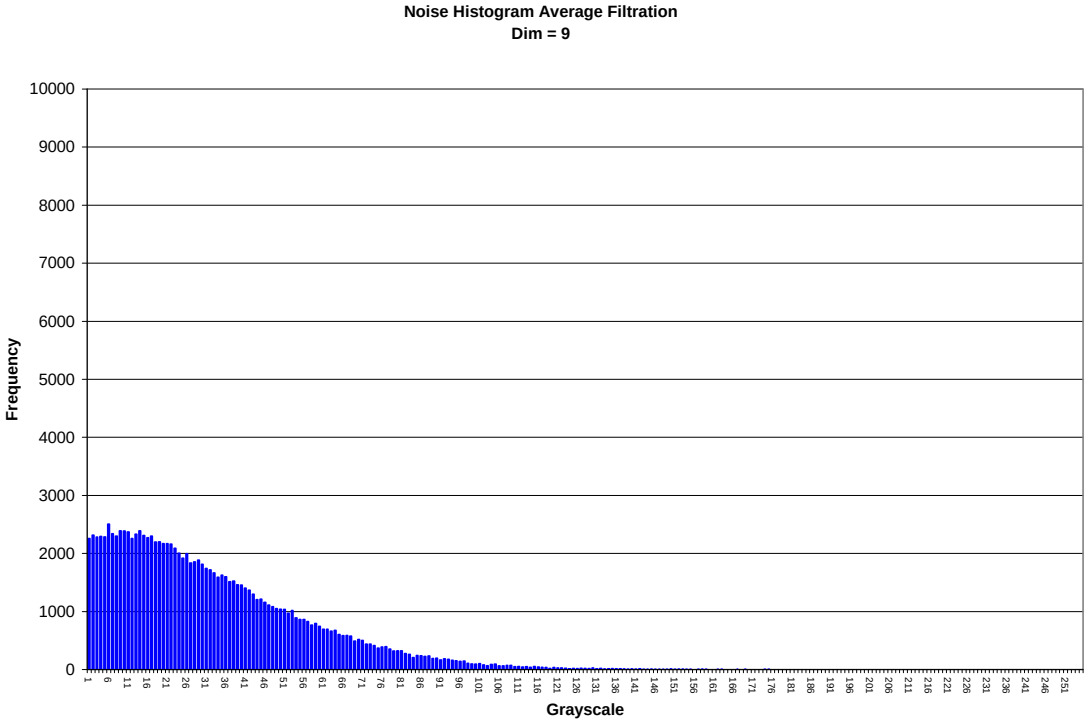


Figure 134. fiber02a Averaging Smoothing Noise Histogram, 9 x 9 kernel

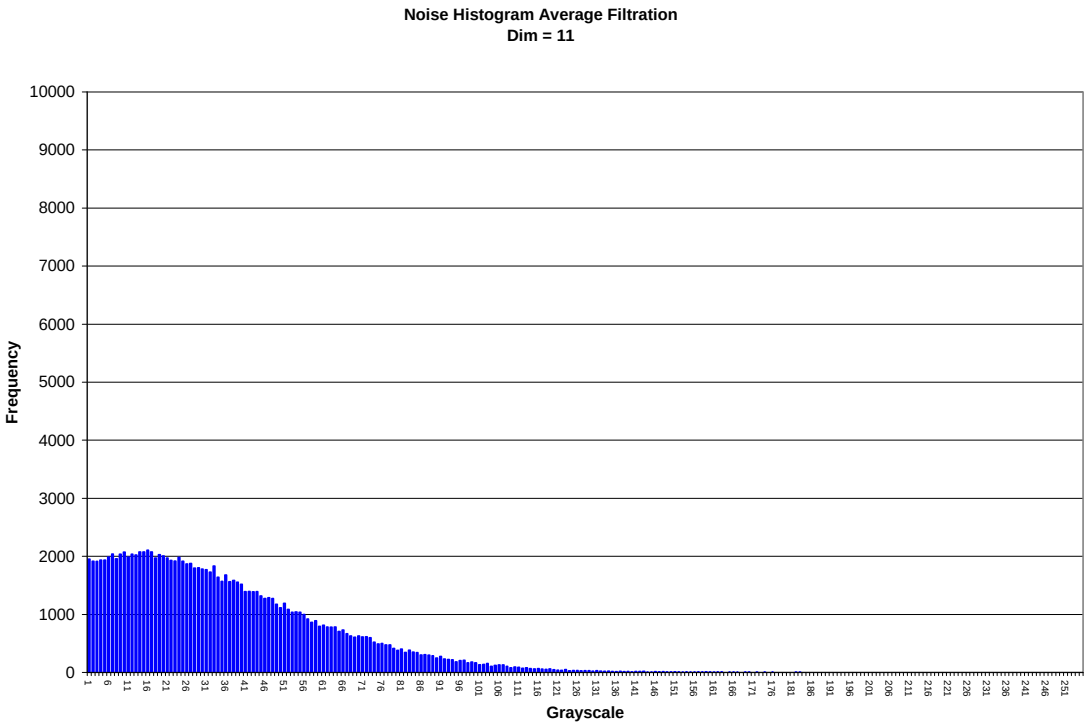


Figure 135. fiber02a Averaging Smoothing Noise Histogram, 11 x 11 kernel

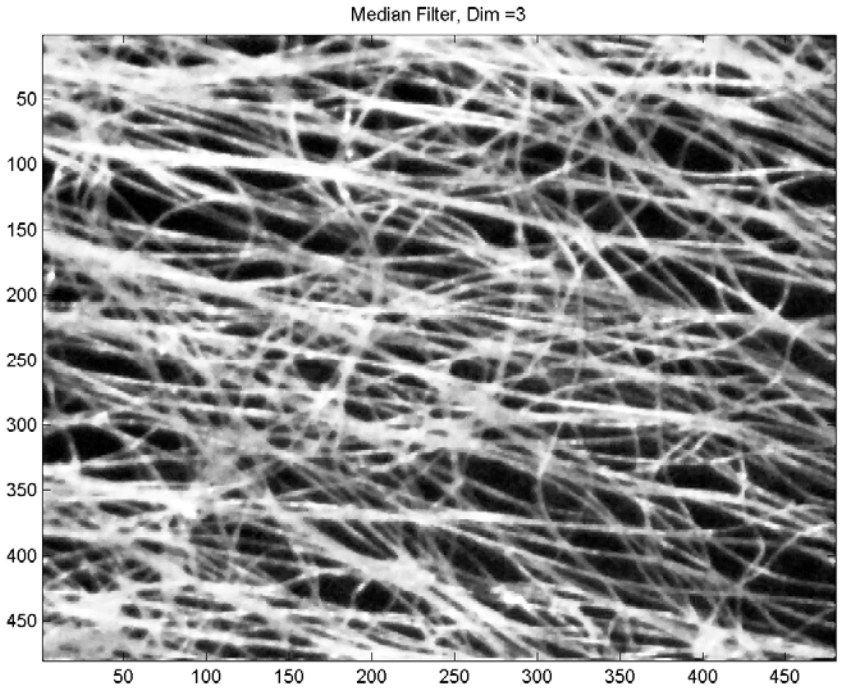


Figure 136. fiber02a Median Smoothing, 3 x 3 kernel

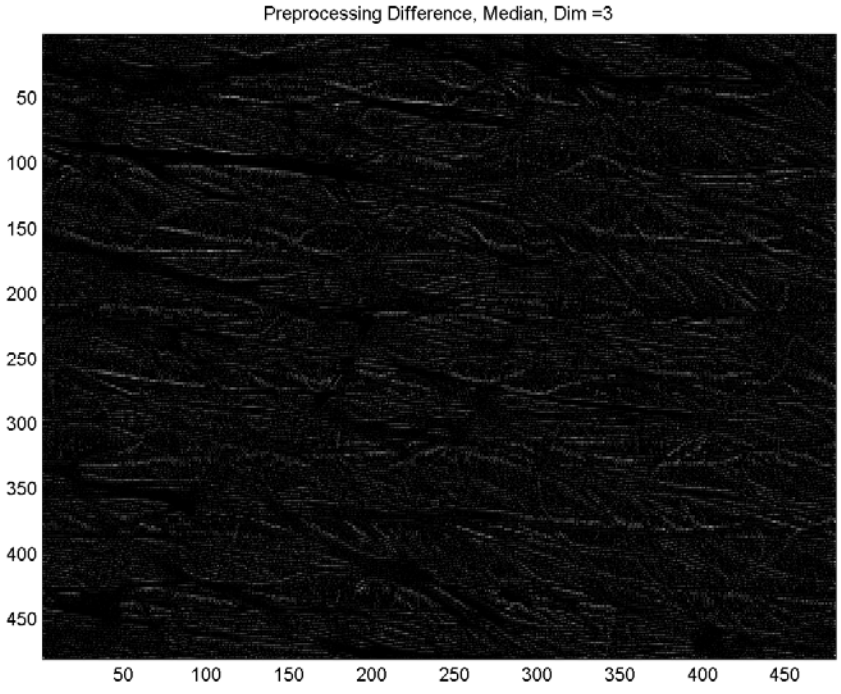


Figure 137. fiber02a Median Smoothing Noise, 3 x 3 kernel

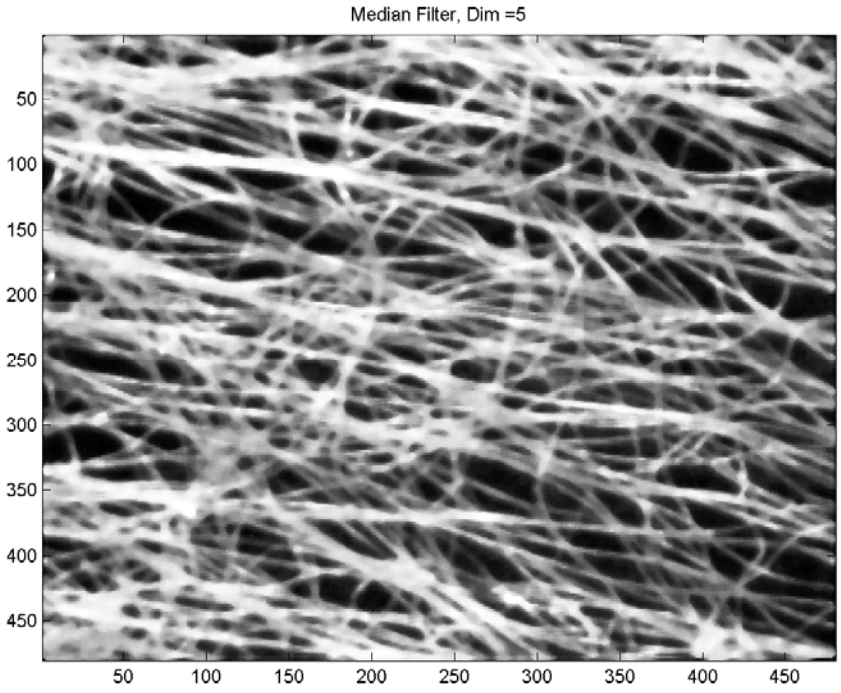


Figure 138. fiber02a Median Smoothing, 5 x 5 kernel

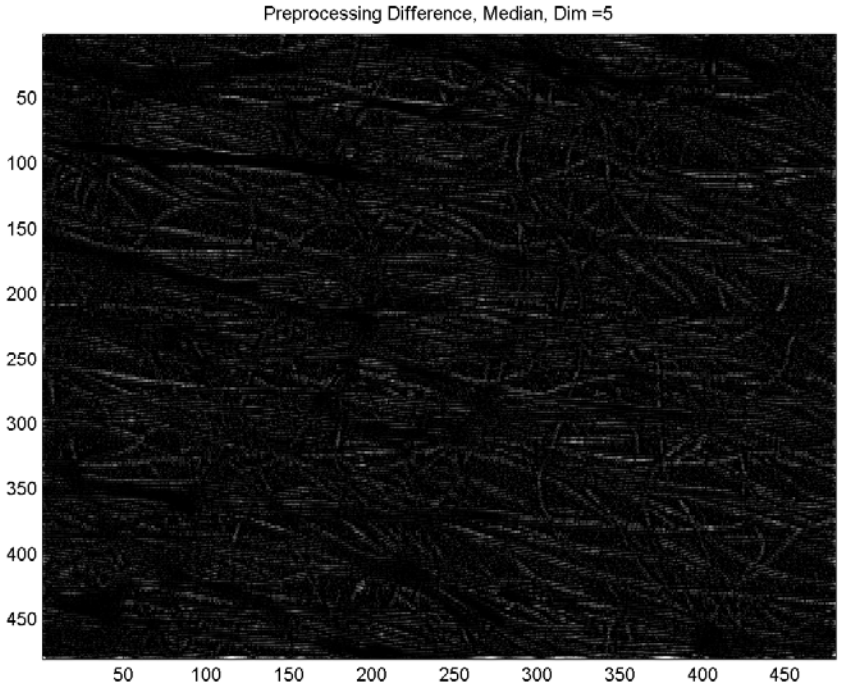


Figure 139. fiber02a Median Smoothing Noise, 5 x 5 kernel

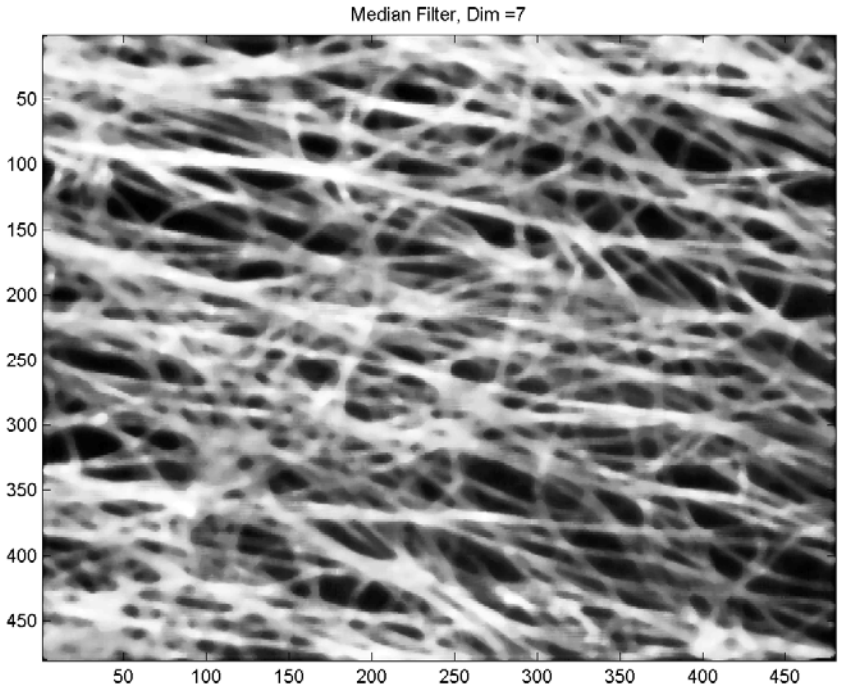


Figure 140. fiber02a Median Smoothing, 7 x 7 kernel

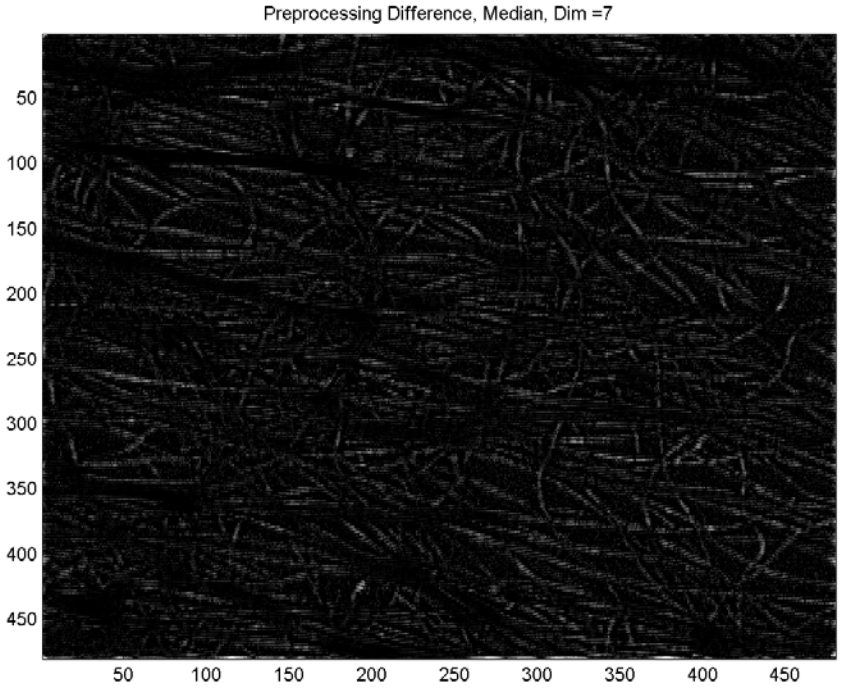


Figure 141. fiber02a Median Smoothing Noise, 7 x 7 kernel

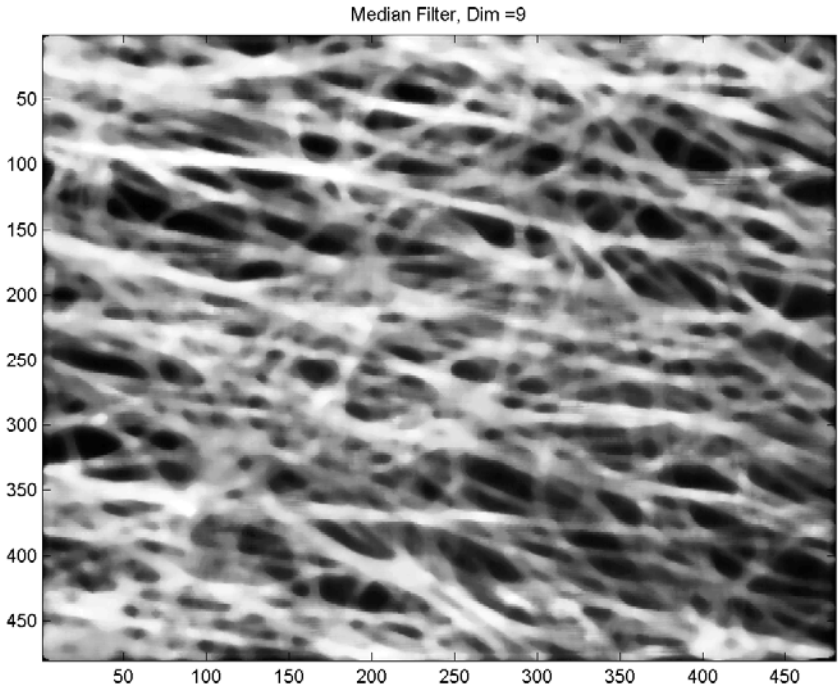


Figure 142. fiber02a Median Smoothing, 9 x 9 kernel

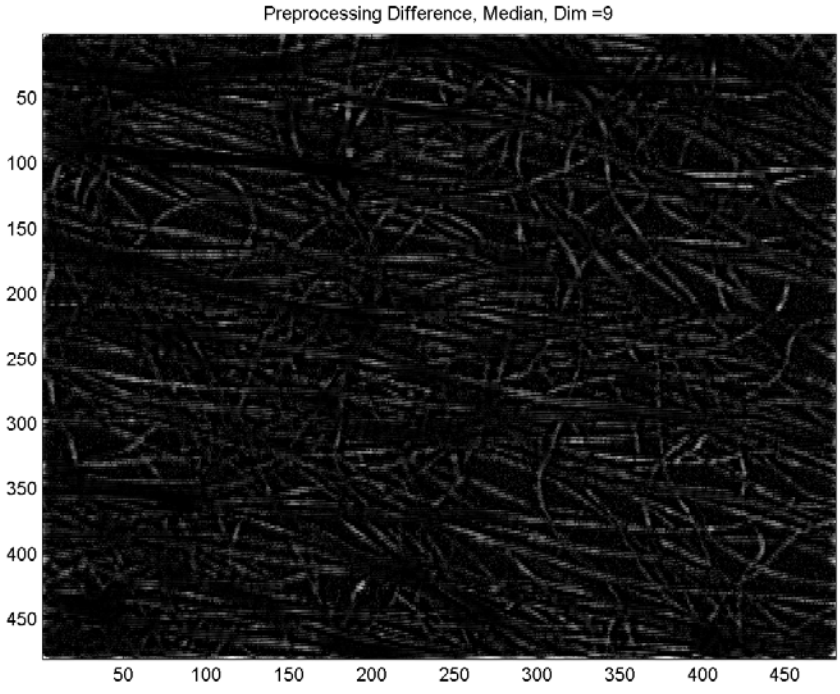


Figure 143. fiber02a Median Smoothing Noise, 9 x 9 kernel

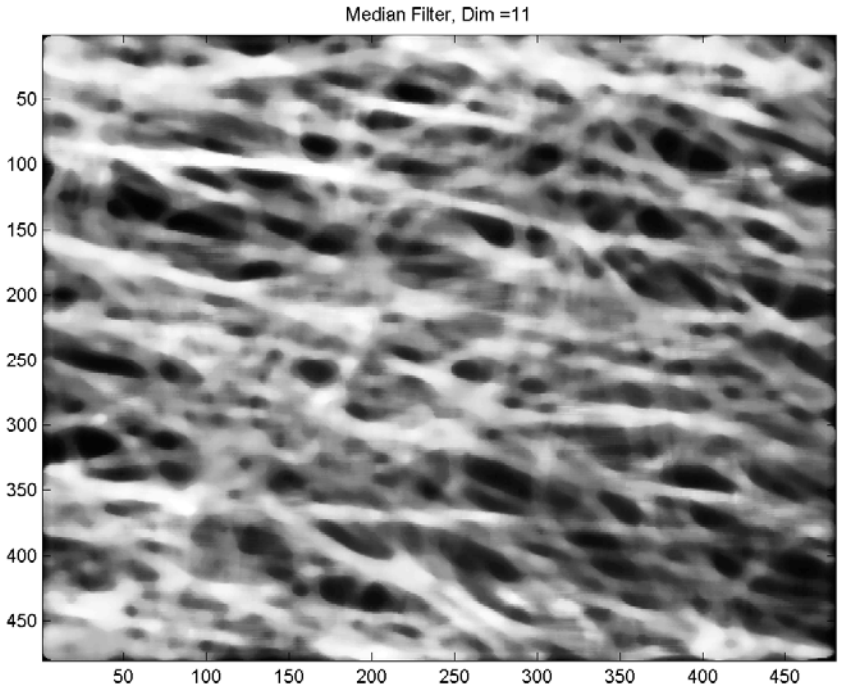


Figure 144. fiber02a Median Smoothing, 11 x 11 kernel

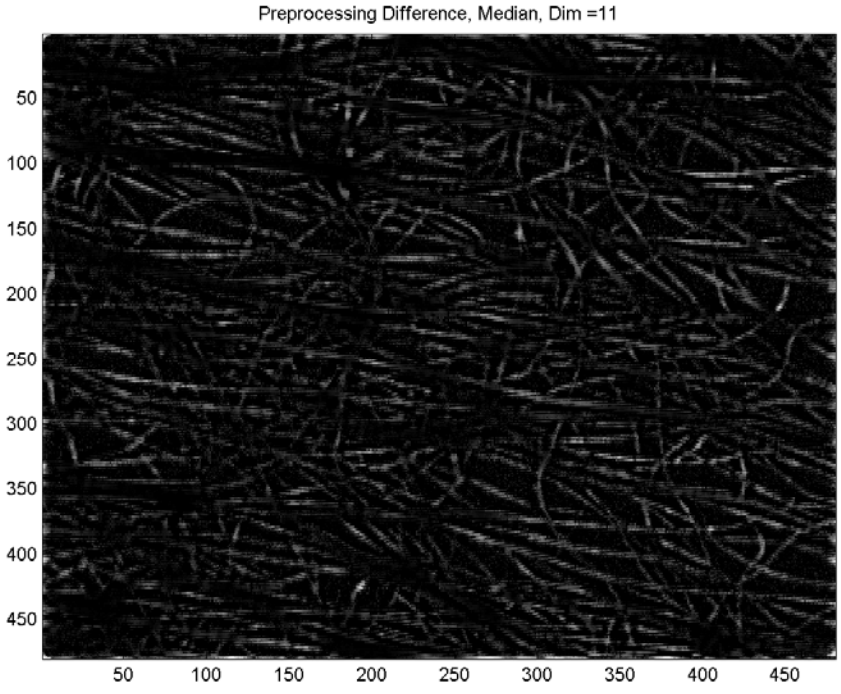


Figure 145. fiber02a Median Smoothing Noise, 11 x 11 kernel

Table 44. fiber02a Median Smoothing Histogram Data

Grayscale	1.00	2.00	3.00	4.00	5.00
0	131018	123966	121223	119007	118034
1	2908	2556	2371	1892	1596
2	3737	3606	3366	2690	2395
3	3540	3463	3243	2762	2371
4	3603	3820	3658	3246	2978
5	3824	4021	3871	3354	3089
6	3557	3659	3684	3226	2869
7	2899	3209	3133	2767	2588
8	3069	3203	3192	2961	2632
9	3054	3229	3266	2952	2817
10	2844	2984	2987	2651	2607
11	3017	3348	3370	2979	2848
12	2482	2566	2571	2336	2198
13	2638	2800	2782	2629	2388
14	2340	2572	2607	2397	2337
15	2760	2844	2971	2741	2703
16	2447	2694	2690	2435	2290
17	2306	2408	2464	2363	2282
18	1864	1936	1911	1861	1736
19	2339	2409	2423	2393	2282
20	1776	1867	1812	1792	1743
21	2286	2379	2560	2473	2415
22	1623	1661	1688	1625	1667
23	2125	2335	2338	2295	2194
24	1672	1653	1698	1681	1584
25	1809	1942	1984	1947	1943
26	1393	1564	1633	1570	1574
27	1911	1996	2029	2034	2007
28	1299	1356	1457	1411	1436
29	1676	1824	1752	1732	1775
30	1153	1253	1289	1305	1250
31	1367	1553	1649	1661	1679
32	1224	1257	1355	1399	1407
33	1221	1324	1439	1505	1533
34	1232	1263	1372	1413	1443
35	1010	1128	1135	1232	1312
36	1060	1093	1110	1178	1208
37	1185	1297	1406	1420	1459
38	985	1087	1191	1223	1301
39	698	772	723	893	905
40	905	1001	1043	1175	1194
41	711	824	910	1041	1025
42	1021	1182	1298	1404	1513
43	542	551	604	669	686

Table 44 (Continued). fiber02a Median Smoothing Histogram Data

Grayscale	1.00	2.00	3.00	4.00	5.00
44	837	937	1029	1160	1195
45	543	569	610	751	778
46	723	809	873	1085	1148
47	600	674	716	855	848
48	703	829	873	983	1121
49	467	567	590	730	823
50	585	616	662	767	856
51	427	534	563	661	731
52	430	501	549	672	773
53	500	560	615	795	773
54	336	391	398	533	568
55	304	399	418	563	629
56	557	646	679	865	905
57	342	445	467	610	646
58	385	413	470	627	717
59	257	292	316	435	505
60	215	255	305	410	427
61	353	469	524	682	772
62	212	254	350	419	487
63	279	337	429	570	601
64	179	204	270	369	429
65	224	293	320	502	572
66	162	231	252	359	453
67	198	258	266	384	448
68	128	199	218	330	389
69	189	245	274	414	458
70	169	194	255	395	509
71	162	185	229	352	434
72	150	178	207	343	374
73	103	162	183	303	362
74	102	129	178	264	326
75	163	185	227	376	484
76	48	61	100	156	180
77	96	137	160	285	344
78	97	137	177	314	389
79	68	82	112	220	281
80	75	104	137	263	351
81	65	80	126	203	296
82	73	98	124	213	312
83	53	70	100	196	233
84	67	95	114	198	306
85	43	66	90	182	244
86	57	73	93	202	316
87	33	43	65	163	187

Table 44 (Continued). fiber02a Median Smoothing Histogram Data

Grayscale	1.00	2.00	3.00	4.00	5.00
88	41	48	63	147	205
89	37	66	87	160	221
90	28	57	86	159	194
91	27	36	67	158	191
92	31	52	60	139	155
93	41	48	57	155	213
94	33	39	50	120	187
95	24	44	62	125	189
96	19	22	19	106	156
97	19	29	43	114	157
98	9	23	51	135	168
99	14	24	40	82	124
100	15	29	41	124	147
101	2	10	25	78	106
102	19	33	41	97	143
103	11	12	33	75	118
104	16	25	30	76	138
105	8	14	25	68	121
106	7	16	22	88	127
107	5	13	27	50	84
108	7	16	20	47	73
109	14	21	28	64	95
110	6	14	24	53	99
111	5	10	11	47	76
112	5	8	9	40	73
113	4	15	23	56	56
114	7	11	18	49	60
115	6	8	16	39	58
116	3	6	19	34	67
117	3	8	25	48	71
118	7	13	10	48	57
119	2	6	10	36	67
120	3	7	13	31	48
121	1	13	6	27	42
122	2	7	17	28	56
123	0	6	8	24	50
124	2	5	9	21	29
125	2	8	11	23	31
126	2	0	12	21	26
127	0	3	5	28	46
128	0	4	5	27	34
129	1	5	7	8	25
130	0	3	8	20	28
131	0	1	10	16	27

Table 44 (Continued). fiber02a Median Smoothing Histogram Data

Grayscale	1.00	2.00	3.00	4.00	5.00
132	1	1	6	10	35
133	2	4	7	18	38
134	0	2	3	20	26
135	0	2	3	10	20
136	0	4	4	10	20
137	1	2	2	15	26
138	3	7	6	21	28
139	2	2	6	12	18
140	0	1	5	24	21
141	2	3	6	11	19
142	0	0	3	5	12
143	2	4	6	11	19
144	0	1	1	12	21
145	0	3	4	5	9
146	0	3	5	8	17
147	0	0	5	6	12
148	1	2	5	13	13
149	1	1	3	18	8
150	0	1	4	7	13
151	0	1	4	12	12
152	0	2	1	4	10
153	0	1	3	6	9
154	4	4	3	9	13
155	0	2	1	5	9
156	0	1	2	9	12
157	0	1	3	3	5
158	1	1	1	3	6
159	0	2	5	14	12
160	0	0	2	4	11
161	0	1	1	2	8
162	0	1	2	5	9
163	0	3	1	3	10
164	0	1	2	4	6
165	0	1	1	7	10
166	0	1	0	4	4
167	1	2	3	4	7
168	0	0	1	4	11
169	0	0	0	2	4
170	0	0	3	4	4
171	0	0	2	0	5
172	0	1	2	2	5
173	0	1	1	4	3
174	0	0	1	5	5
175	0	0	0	2	5

Table 44 (Continued). fiber02a Median Smoothing Histogram Data

Grayscale	1.00	2.00	3.00	4.00	5.00
176	0	0	2	3	5
177	0	2	3	2	3
178	0	1	1	2	6
179	0	1	0	3	1
180	0	3	1	2	3
181	0	0	0	2	5
182	0	2	4	2	3
183	0	1	1	0	5
184	0	2	2	0	5
185	0	0	1	1	3
186	0	1	1	1	1
187	0	1	0	3	4
188	0	0	2	5	2
189	0	0	3	4	6
190	0	3	0	0	3
191	0	0	0	2	0
192	0	0	1	0	2
193	0	0	0	1	2
194	0	2	2	6	4
195	0	0	1	1	2
196	0	2	4	2	1
197	0	0	0	2	3
198	0	1	0	0	0
199	0	0	0	0	1
200	0	1	2	5	8
201	0	0	0	2	3
202	0	0	2	2	4
203	0	1	3	1	1
204	0	0	0	0	1
205	0	0	1	0	3
206	0	0	0	0	0
207	0	0	0	1	2
208	0	0	0	0	1
209	0	0	0	1	1
210	0	2	0	0	0
211	1	2	3	4	5
212	0	0	0	0	1
213	0	0	1	2	1
214	0	0	1	1	1
215	0	0	0	0	0
216	1	3	3	4	5
217	0	0	0	0	1
218	0	0	0	1	1
219	0	0	0	0	2

Table 44 (Continued). fiber02a Median Smoothing Histogram Data

Grayscale	1.00	2.00	3.00	4.00	5.00
220	0	0	0	0	1
221	0	0	1	0	1
222	0	0	0	1	1
223	0	0	1	1	1
224	0	0	0	0	0
225	0	0	0	0	1
226	0	0	0	1	1
227	0	0	0	2	1
228	0	0	0	0	0
229	0	0	0	0	1
230	0	0	0	0	0
231	0	0	0	0	0
232	0	0	0	0	0
233	0	0	0	0	0
234	0	0	0	0	0
235	0	0	0	0	0
236	0	0	0	0	0
237	0	0	0	0	0
238	0	0	0	0	0
239	0	0	0	0	0
240	0	0	0	0	0
241	0	0	0	0	0
242	0	0	0	0	0
243	0	0	0	0	0
244	0	0	0	0	0
245	0	0	0	0	0
246	0	0	0	0	0
247	0	0	0	0	0
248	0	0	0	0	0
249	0	0	0	0	0
250	0	0	0	0	0
251	0	0	0	0	0
252	0	0	0	0	0
253	0	0	0	0	0
254	0	0	0	0	0
255	0	0	0	0	0
Min:	0	0	0	0	0
μ:	900	900	900	900	900
Max:	131018	123966	121223	119007	118034
Median:	2	4.5	7.5	22	32.5
σ:	8207.244	7771.048	7599.415	7453.108	7387.992
% Black:	56.87%	53.80%	52.61%	51.65%	51.23%
% Gray:	43.13%	46.20%	47.39%	48.35%	48.77%

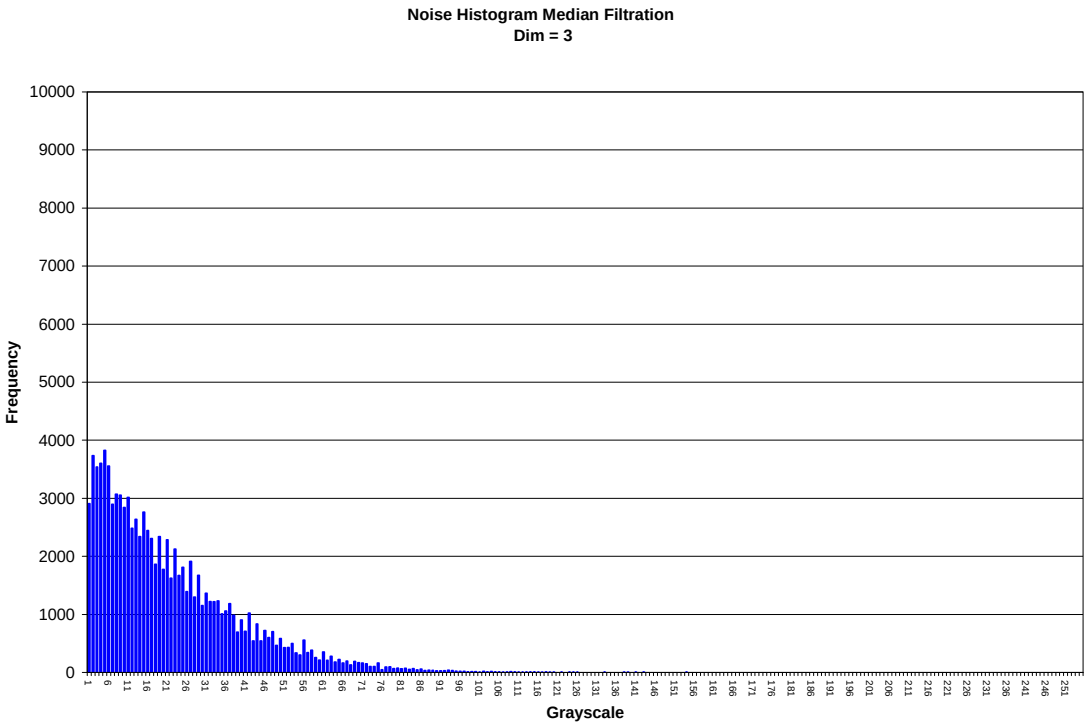


Figure 146. fiber02a Median Smoothing Noise Histogram, 3 x 3 kernel

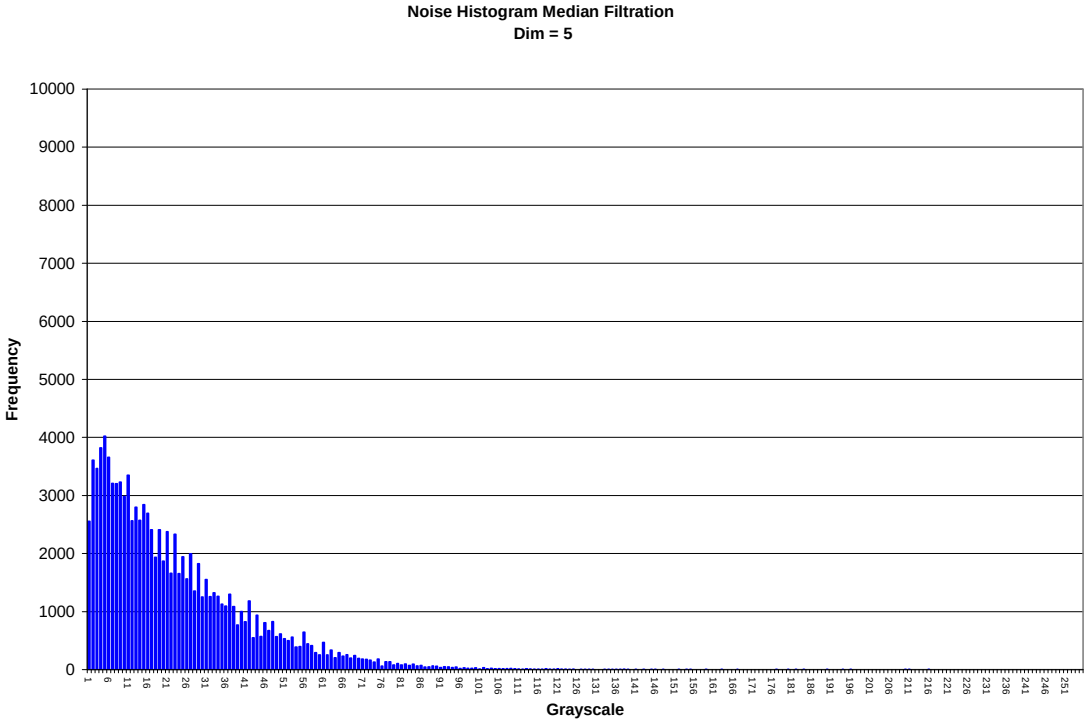


Figure 147. fiber02a Median Smoothing Noise Histogram, 5 x 5 kernel

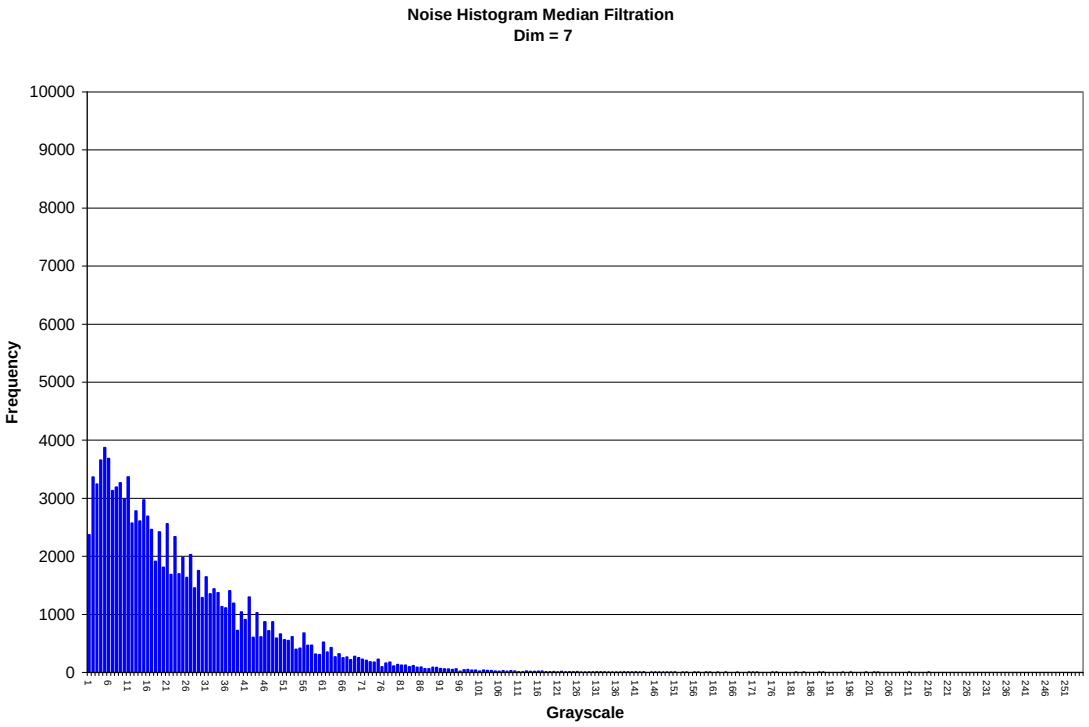


Figure 148. fiber02a Median Smoothing Noise Histogram, 7 x 7 kernel

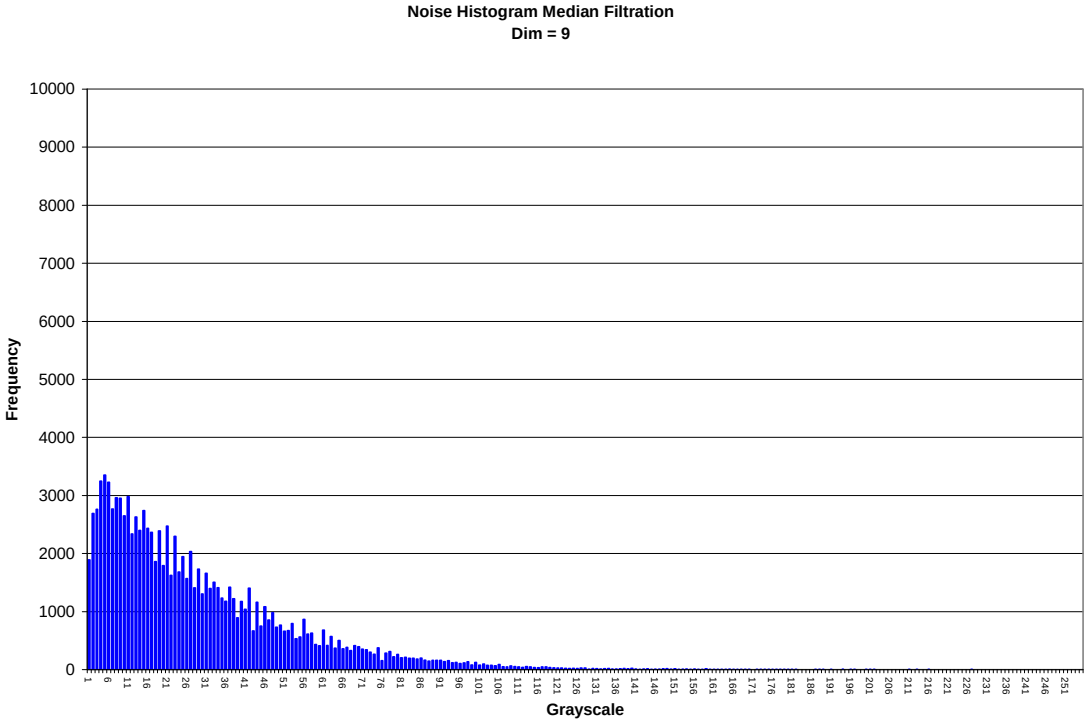


Figure 149. fiber02a Median Smoothing Noise Histogram, 9 x 9 kernel

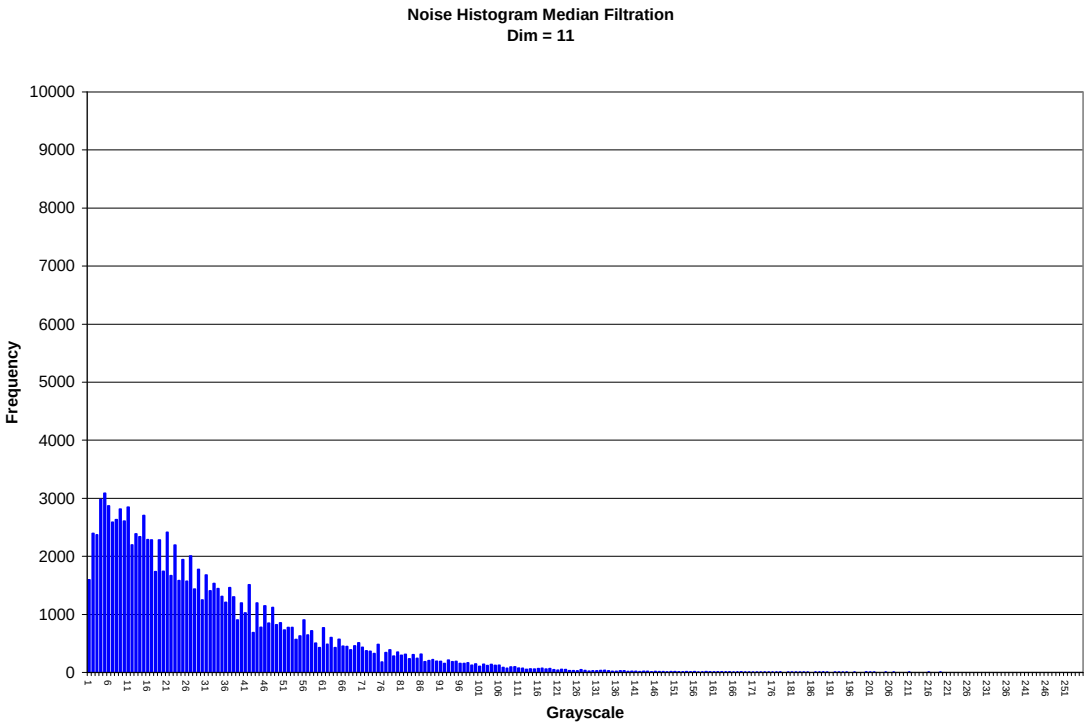


Figure 150. fiber02a Median Smoothing Noise Histogram, 11 x 11 kernel

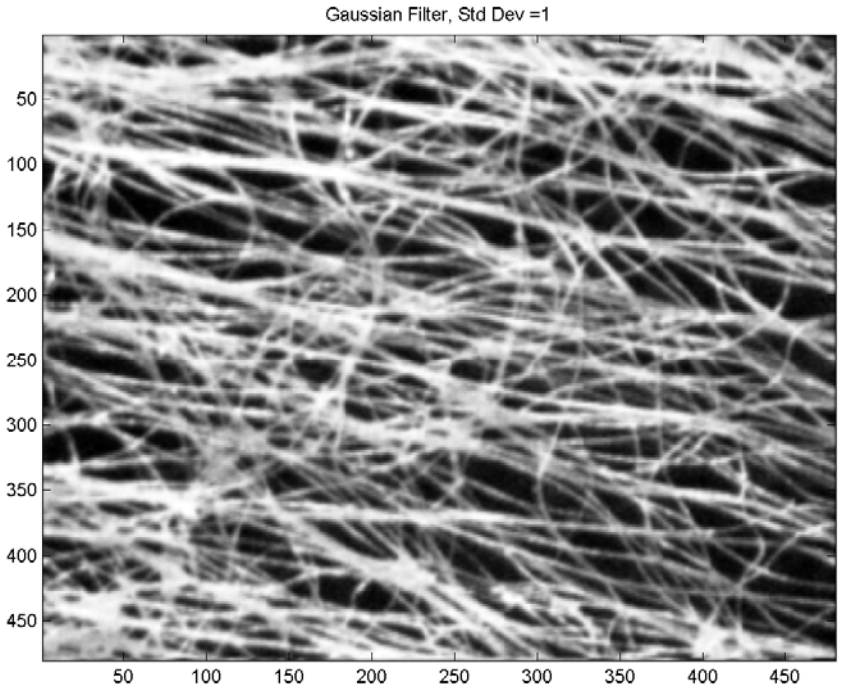


Figure 151. fiber02a Gaussian Smoothing, σ = 1.00 kernel

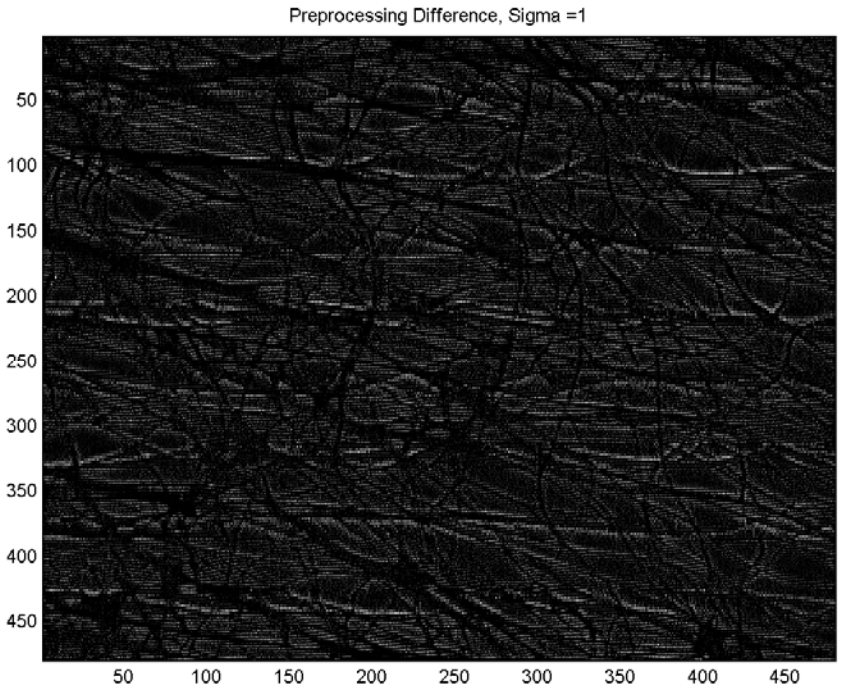


Figure 152. fiber02a Gaussian Smoothing Noise, σ = 1.00 kernel

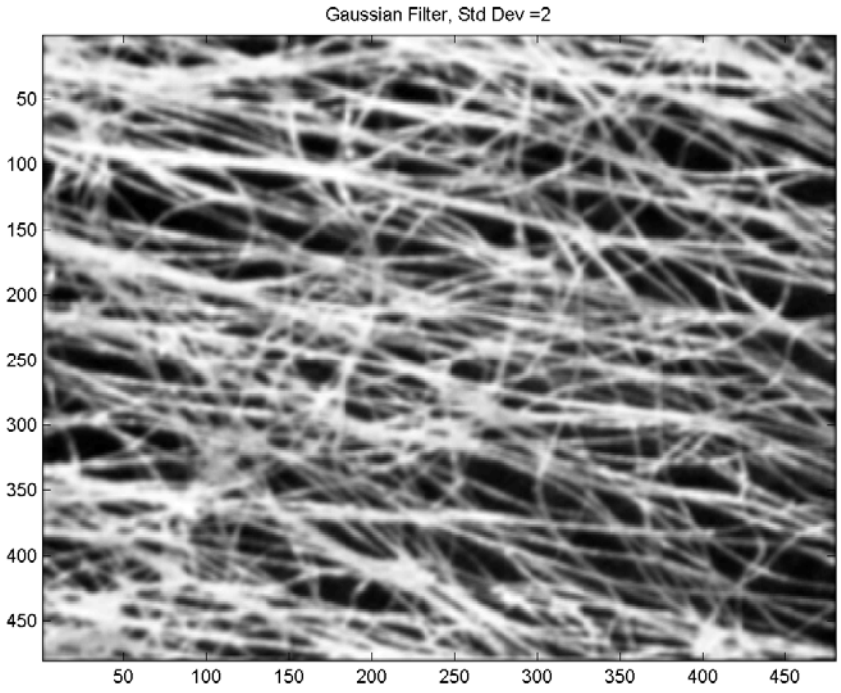


Figure 153. fiber02a Gaussian Smoothing, σ = 2.00 kernel

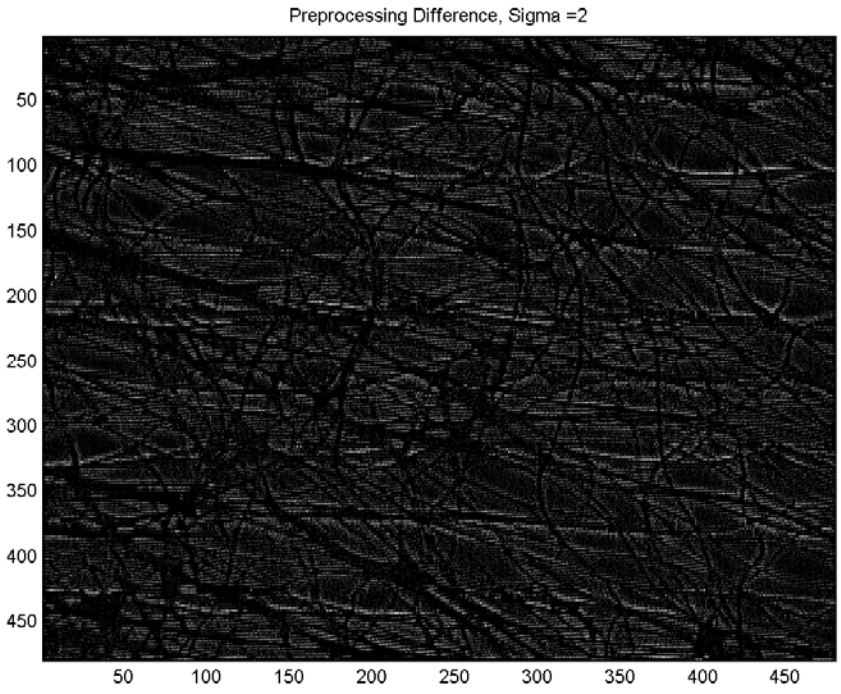


Figure 154. fiber02a Gaussian Smoothing Noise, σ = 2.00 kernel

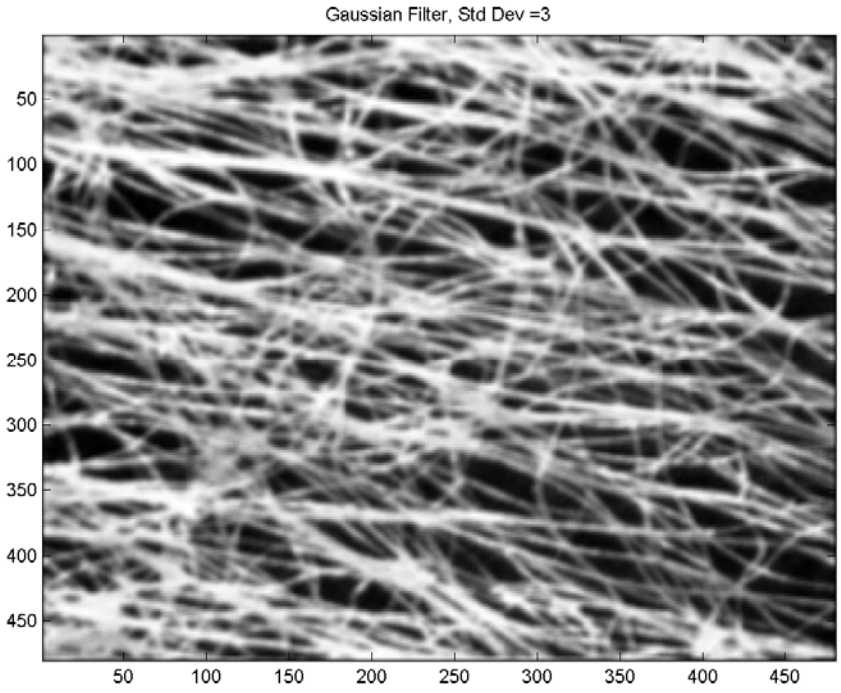


Figure 155. fiber02a Gaussian Smoothing, σ = 3.00 kernel

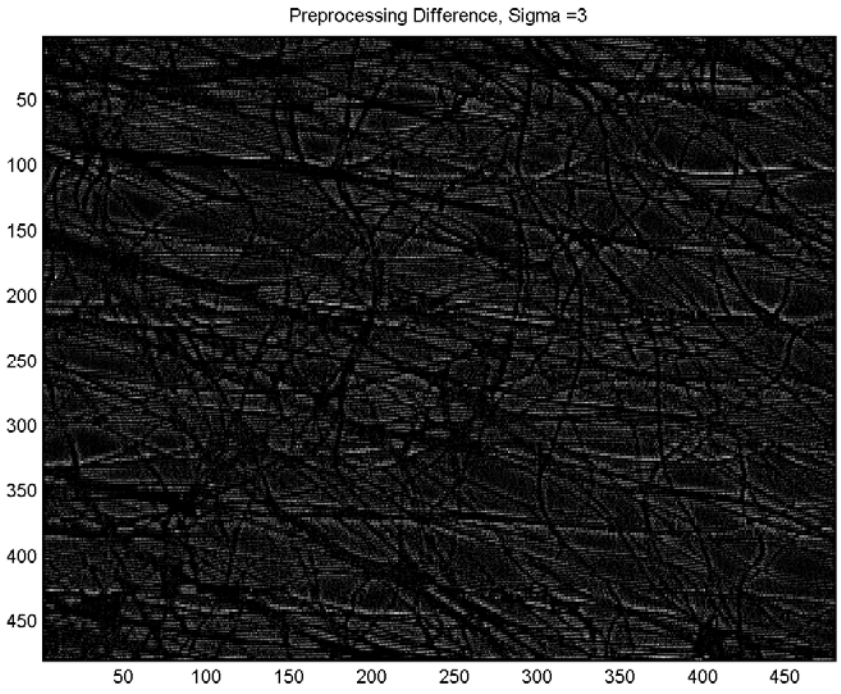


Figure 156. fiber02a Gaussian Smoothing Noise, σ = 3.00 kernel

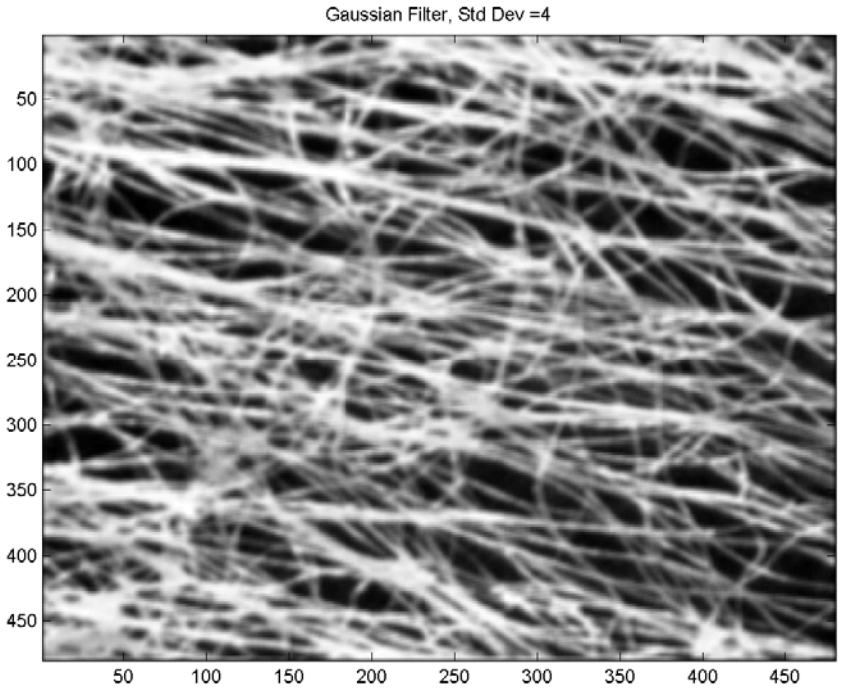


Figure 157. fiber02a Gaussian Smoothing, σ = 4.00 kernel

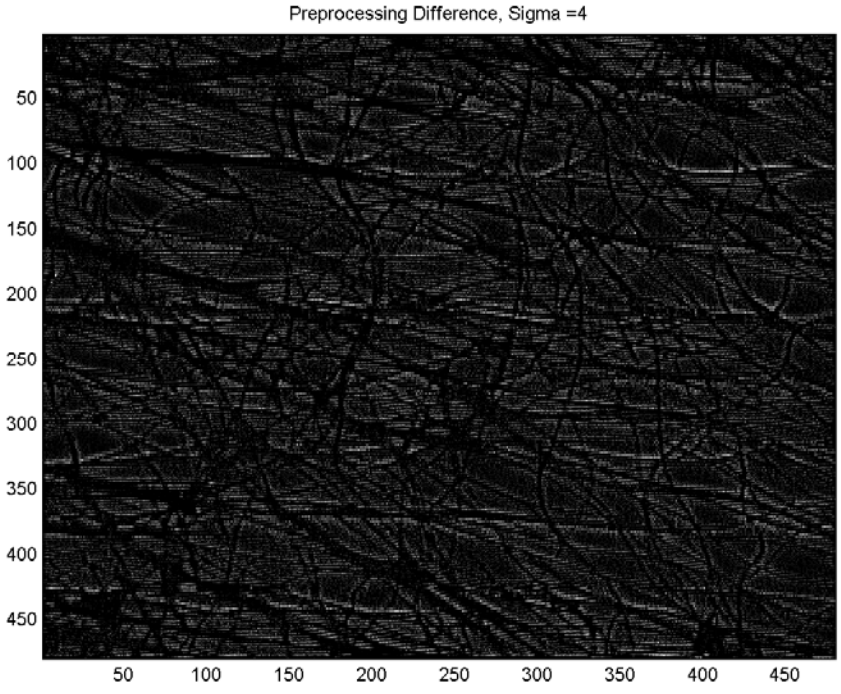


Figure 158. fiber02a Gaussian Smoothing Noise, σ = 4.00 kernel

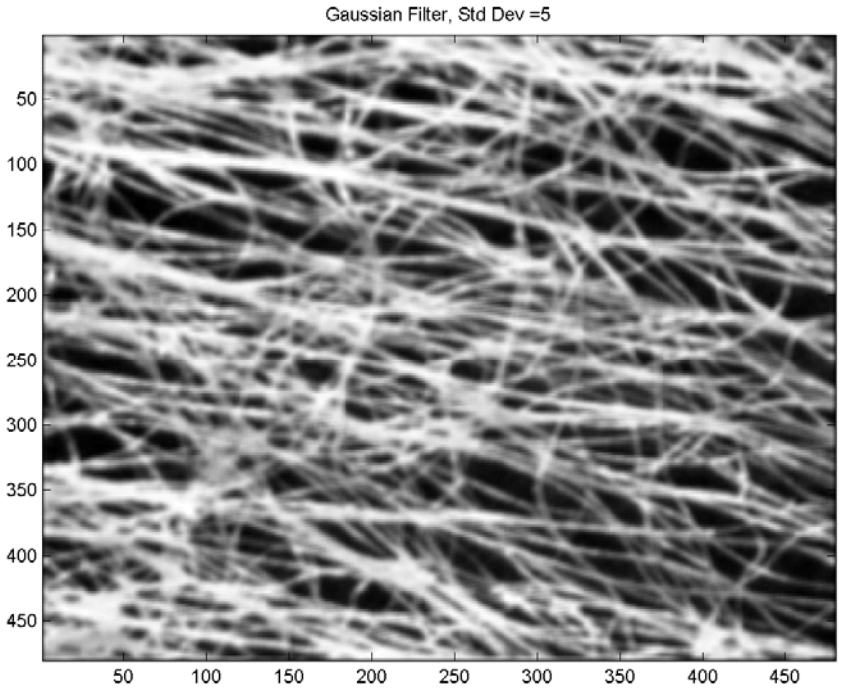


Figure 159. fiber02a Gaussian Smoothing, σ = 5.00 kernel

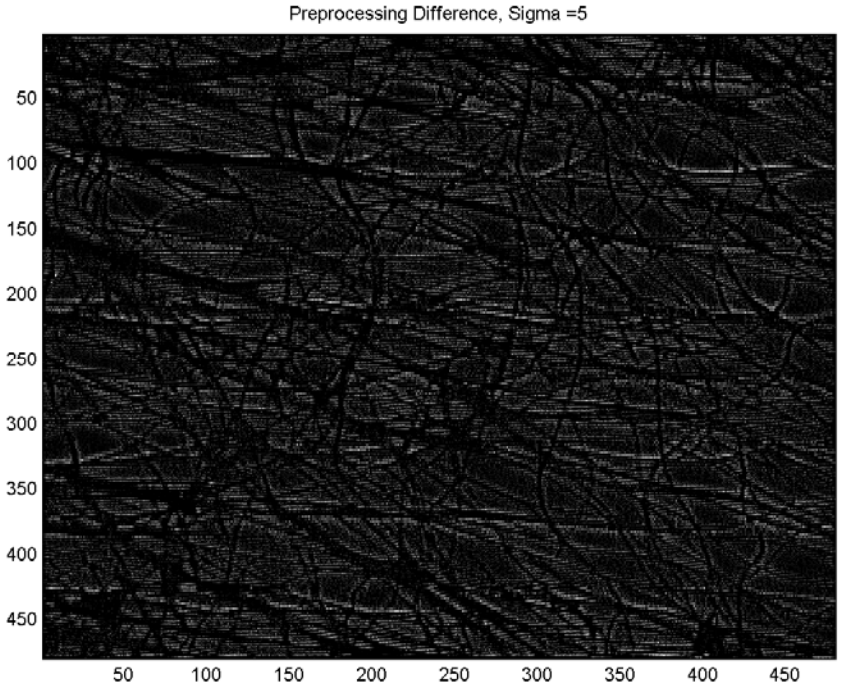


Figure 160. fiber02a Gaussian Smoothing Noise, σ = 5.00 kernel

Table 45. fiber02a Gaussian Smoothing Histogram Data

Grayscale	1.00	2.00	3.00	4.00	5.00
0	131018	123966	121223	119007	118034
1	2908	2556	2371	1892	1596
2	3737	3606	3366	2690	2395
3	3540	3463	3243	2762	2371
4	3603	3820	3658	3246	2978
5	3824	4021	3871	3354	3089
6	3557	3659	3684	3226	2869
7	2899	3209	3133	2767	2588
8	3069	3203	3192	2961	2632
9	3054	3229	3266	2952	2817
10	2844	2984	2987	2651	2607
11	3017	3348	3370	2979	2848
12	2482	2566	2571	2336	2198
13	2638	2800	2782	2629	2388
14	2340	2572	2607	2397	2337
15	2760	2844	2971	2741	2703
16	2447	2694	2690	2435	2290
17	2306	2408	2464	2363	2282
18	1864	1936	1911	1861	1736
19	2339	2409	2423	2393	2282
20	1776	1867	1812	1792	1743
21	2286	2379	2560	2473	2415
22	1623	1661	1688	1625	1667
23	2125	2335	2338	2295	2194
24	1672	1653	1698	1681	1584
25	1809	1942	1984	1947	1943
26	1393	1564	1633	1570	1574
27	1911	1996	2029	2034	2007
28	1299	1356	1457	1411	1436
29	1676	1824	1752	1732	1775
30	1153	1253	1289	1305	1250
31	1367	1553	1649	1661	1679
32	1224	1257	1355	1399	1407
33	1221	1324	1439	1505	1533
34	1232	1263	1372	1413	1443
35	1010	1128	1135	1232	1312
36	1060	1093	1110	1178	1208
37	1185	1297	1406	1420	1459
38	985	1087	1191	1223	1301
39	698	772	723	893	905
40	905	1001	1043	1175	1194
41	711	824	910	1041	1025
42	1021	1182	1298	1404	1513
43	542	551	604	669	686

Table 45 (Continued). fiber02a Gaussian Smoothing Histogram Data

Grayscale	1.00	2.00	3.00	4.00	5.00
44	837	937	1029	1160	1195
45	543	569	610	751	778
46	723	809	873	1085	1148
47	600	674	716	855	848
48	703	829	873	983	1121
49	467	567	590	730	823
50	585	616	662	767	856
51	427	534	563	661	731
52	430	501	549	672	773
53	500	560	615	795	773
54	336	391	398	533	568
55	304	399	418	563	629
56	557	646	679	865	905
57	342	445	467	610	646
58	385	413	470	627	717
59	257	292	316	435	505
60	215	255	305	410	427
61	353	469	524	682	772
62	212	254	350	419	487
63	279	337	429	570	601
64	179	204	270	369	429
65	224	293	320	502	572
66	162	231	252	359	453
67	198	258	266	384	448
68	128	199	218	330	389
69	189	245	274	414	458
70	169	194	255	395	509
71	162	185	229	352	434
72	150	178	207	343	374
73	103	162	183	303	362
74	102	129	178	264	326
75	163	185	227	376	484
76	48	61	100	156	180
77	96	137	160	285	344
78	97	137	177	314	389
79	68	82	112	220	281
80	75	104	137	263	351
81	65	80	126	203	296
82	73	98	124	213	312
83	53	70	100	196	233
84	67	95	114	198	306
85	43	66	90	182	244
86	57	73	93	202	316
87	33	43	65	163	187

Table 45 (Continued). fiber02a Gaussian Smoothing Histogram Data

Grayscale	1.00	2.00	3.00	4.00	5.00
88	41	48	63	147	205
89	37	66	87	160	221
90	28	57	86	159	194
91	27	36	67	158	191
92	31	52	60	139	155
93	41	48	57	155	213
94	33	39	50	120	187
95	24	44	62	125	189
96	19	22	19	106	156
97	19	29	43	114	157
98	9	23	51	135	168
99	14	24	40	82	124
100	15	29	41	124	147
101	2	10	25	78	106
102	19	33	41	97	143
103	11	12	33	75	118
104	16	25	30	76	138
105	8	14	25	68	121
106	7	16	22	88	127
107	5	13	27	50	84
108	7	16	20	47	73
109	14	21	28	64	95
110	6	14	24	53	99
111	5	10	11	47	76
112	5	8	9	40	73
113	4	15	23	56	56
114	7	11	18	49	60
115	6	8	16	39	58
116	3	6	19	34	67
117	3	8	25	48	71
118	7	13	10	48	57
119	2	6	10	36	67
120	3	7	13	31	48
121	1	13	6	27	42
122	2	7	17	28	56
123	0	6	8	24	50
124	2	5	9	21	29
125	2	8	11	23	31
126	2	0	12	21	26
127	0	3	5	28	46
128	0	4	5	27	34
129	1	5	7	8	25
130	0	3	8	20	28
131	0	1	10	16	27

Table 45 (Continued). fiber02a Gaussian Smoothing Histogram Data

Grayscale	1.00	2.00	3.00	4.00	5.00
132	1	1	6	10	35
133	2	4	7	18	38
134	0	2	3	20	26
135	0	2	3	10	20
136	0	4	4	10	20
137	1	2	2	15	26
138	3	7	6	21	28
139	2	2	6	12	18
140	0	1	5	24	21
141	2	3	6	11	19
142	0	0	3	5	12
143	2	4	6	11	19
144	0	1	1	12	21
145	0	3	4	5	9
146	0	3	5	8	17
147	0	0	5	6	12
148	1	2	5	13	13
149	1	1	3	18	8
150	0	1	4	7	13
151	0	1	4	12	12
152	0	2	1	4	10
153	0	1	3	6	9
154	4	4	3	9	13
155	0	2	1	5	9
156	0	1	2	9	12
157	0	1	3	3	5
158	1	1	1	3	6
159	0	2	5	14	12
160	0	0	2	4	11
161	0	1	1	2	8
162	0	1	2	5	9
163	0	3	1	3	10
164	0	1	2	4	6
165	0	1	1	7	10
166	0	1	0	4	4
167	1	2	3	4	7
168	0	0	1	4	11
169	0	0	0	2	4
170	0	0	3	4	4
171	0	0	2	0	5
172	0	1	2	2	5
173	0	1	1	4	3
174	0	0	1	5	5
175	0	0	0	2	5

Table 45 (Continued). fiber02a Gaussian Smoothing Histogram Data

Grayscale	1.00	2.00	3.00	4.00	5.00
176	0	0	2	3	5
177	0	2	3	2	3
178	0	1	1	2	6
179	0	1	0	3	1
180	0	3	1	2	3
181	0	0	0	2	5
182	0	2	4	2	3
183	0	1	1	0	5
184	0	2	2	0	5
185	0	0	1	1	3
186	0	1	1	1	1
187	0	1	0	3	4
188	0	0	2	5	2
189	0	0	3	4	6
190	0	3	0	0	3
191	0	0	0	2	0
192	0	0	1	0	2
193	0	0	0	1	2
194	0	2	2	6	4
195	0	0	1	1	2
196	0	2	4	2	1
197	0	0	0	2	3
198	0	1	0	0	0
199	0	0	0	0	1
200	0	1	2	5	8
201	0	0	0	2	3
202	0	0	2	2	4
203	0	1	3	1	1
204	0	0	0	0	1
205	0	0	1	0	3
206	0	0	0	0	0
207	0	0	0	1	2
208	0	0	0	0	1
209	0	0	0	1	1
210	0	2	0	0	0
211	1	2	3	4	5
212	0	0	0	0	1
213	0	0	1	2	1
214	0	0	1	1	1
215	0	0	0	0	0
216	1	3	3	4	5
217	0	0	0	0	1
218	0	0	0	1	1
219	0	0	0	0	2

Table 45 (Continued). fiber02a Gaussian Smoothing Histogram Data

Grayscale	1.00	2.00	3.00	4.00	5.00
220	0	0	0	0	1
221	0	0	1	0	1
222	0	0	0	1	1
223	0	0	1	1	1
224	0	0	0	0	0
225	0	0	0	0	1
226	0	0	0	1	1
227	0	0	0	2	1
228	0	0	0	0	0
229	0	0	0	0	1
230	0	0	0	0	0
231	0	0	0	0	0
232	0	0	0	0	0
233	0	0	0	0	0
234	0	0	0	0	0
235	0	0	0	0	0
236	0	0	0	0	0
237	0	0	0	0	0
238	0	0	0	0	0
239	0	0	0	0	0
240	0	0	0	0	0
241	0	0	0	0	0
242	0	0	0	0	0
243	0	0	0	0	0
244	0	0	0	0	0
245	0	0	0	0	0
246	0	0	0	0	0
247	0	0	0	0	0
248	0	0	0	0	0
249	0	0	0	0	0
250	0	0	0	0	0
251	0	0	0	0	0
252	0	0	0	0	0
253	0	0	0	0	0
254	0	0	0	0	0
255	0	0	0	0	0
Min:	0	0	0	0	0
μ:	900	900	900	900	900
Max:	131018	123966	121223	119007	118034
Median:	2	4.5	7.5	22	32.5
σ:	8207.244	7771.048	7599.415	7453.108	7387.992
% Black:	56.87%	53.80%	52.61%	51.65%	51.23%
% Gray:	43.13%	46.20%	47.39%	48.35%	48.77%

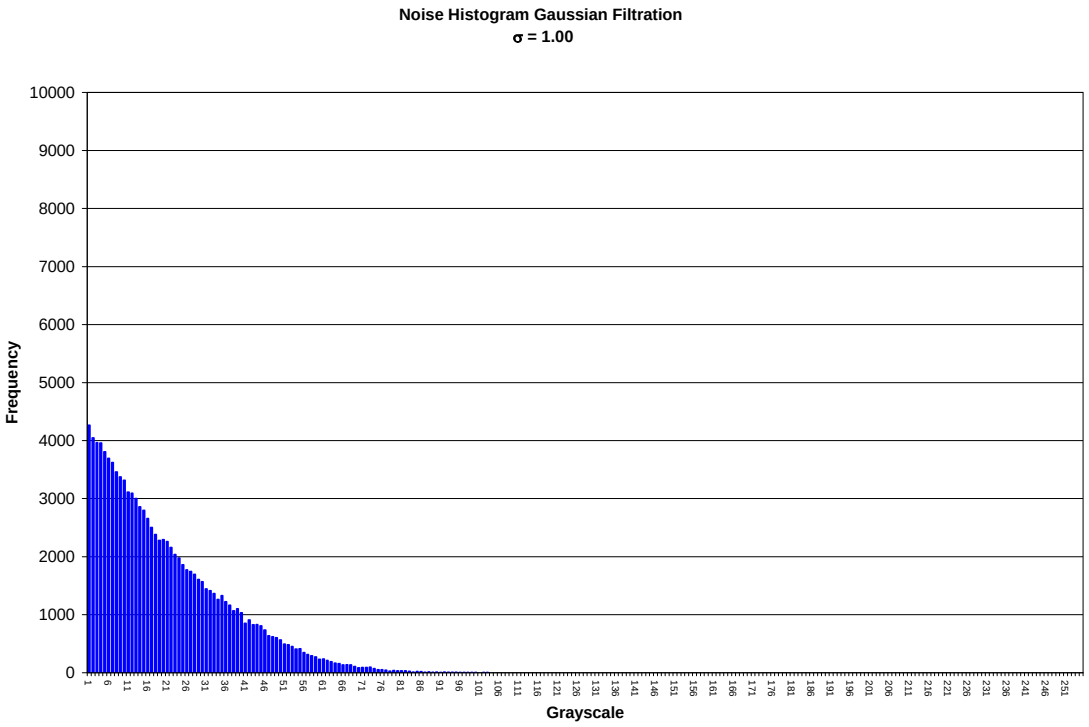


Figure 161. fiber02a Gaussian Smoothing Histogram, σ = 1.00 kernel

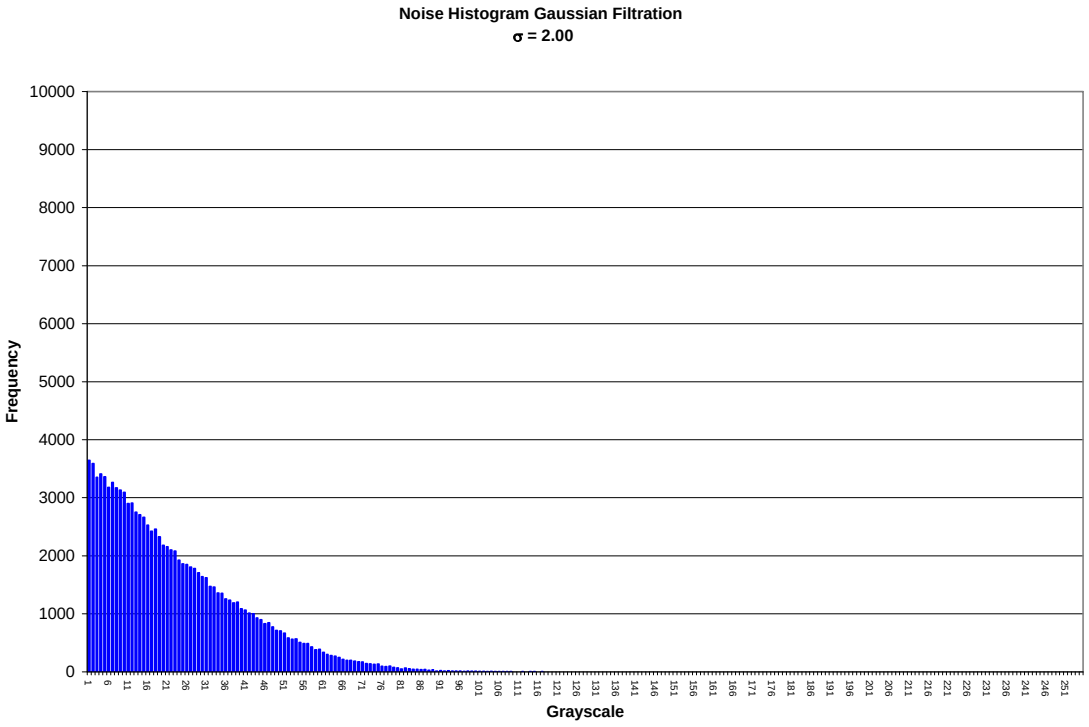


Figure 162. fiber02a Gaussian Smoothing Histogram, σ = 2.00 kernel

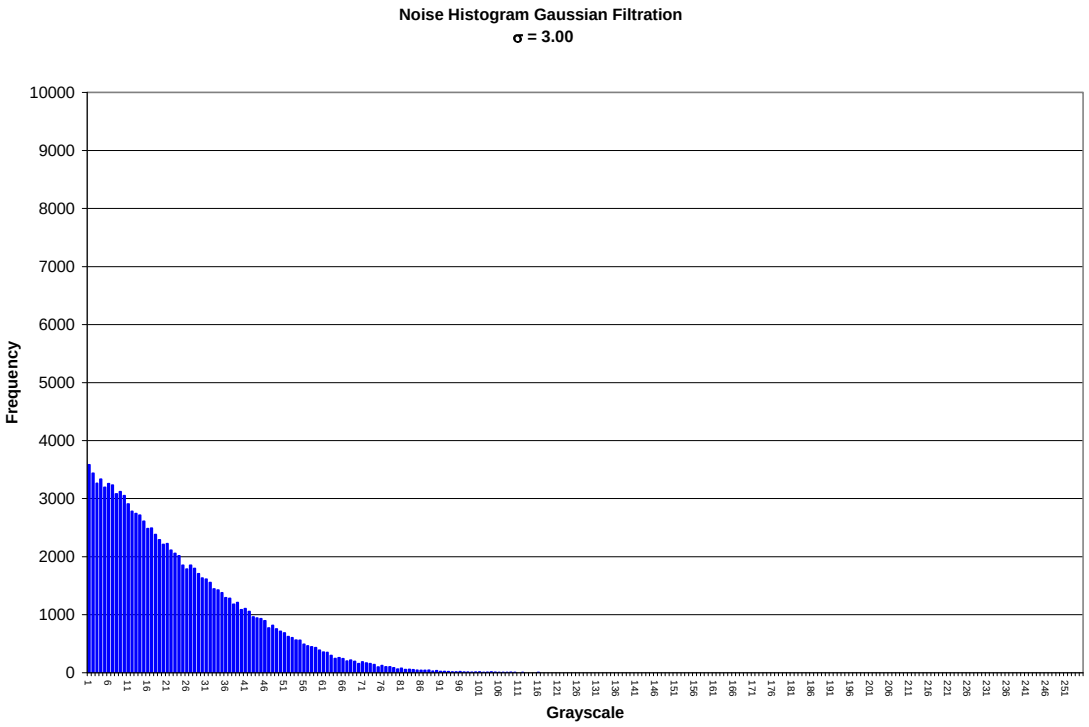


Figure 163. fiber02a Gaussian Smoothing Histogram, σ = 3.00 kernel

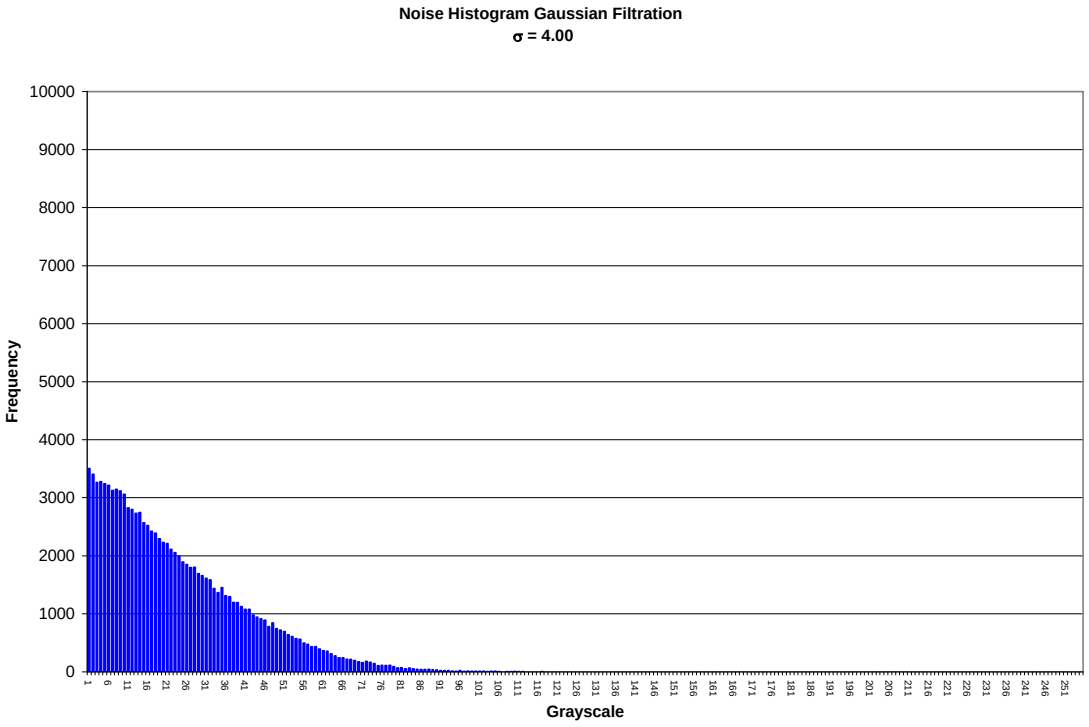


Figure 164. fiber02a Gaussian Smoothing Histogram, σ = 4.00 kernel

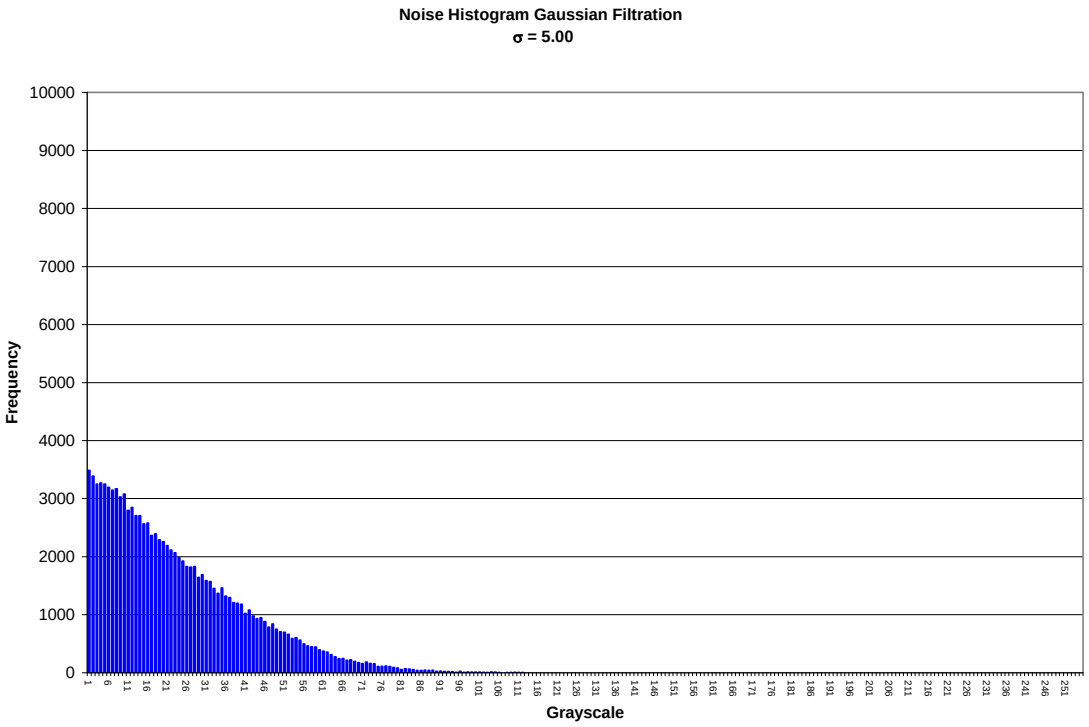


Figure 165. fiber02a Gaussian Smoothing Histogram, σ = 5.00 kernel

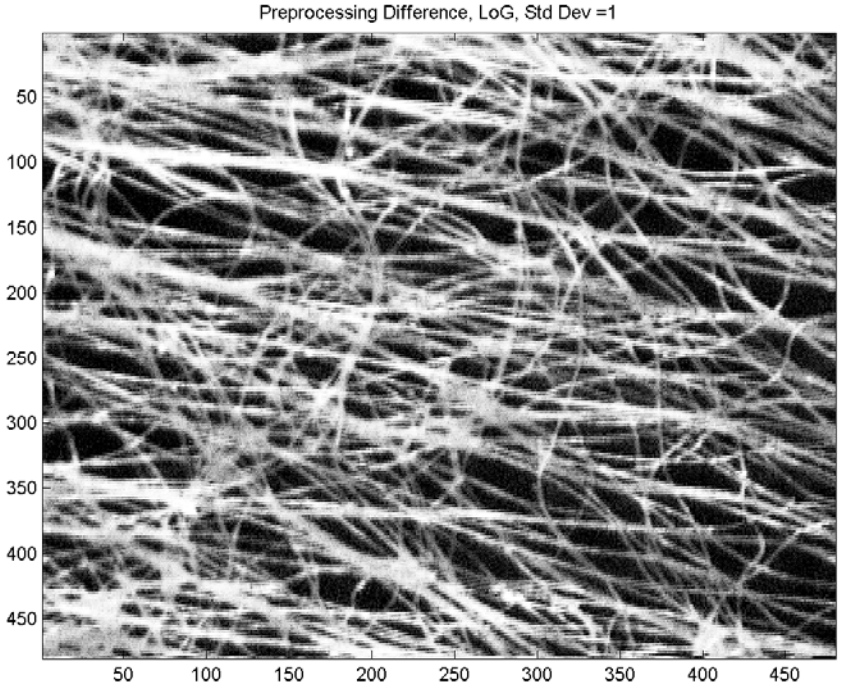


Figure 166. fiber02a LoG Smoothing, σ = 1.00 kernel

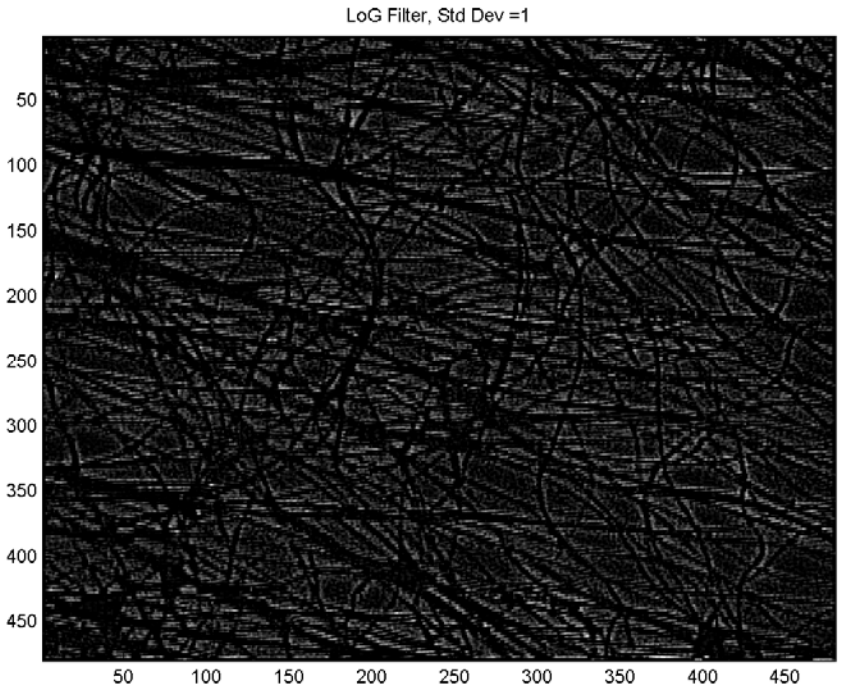


Figure 167. fiber02a LoG Smoothing Noise, σ = 1.00 kernel

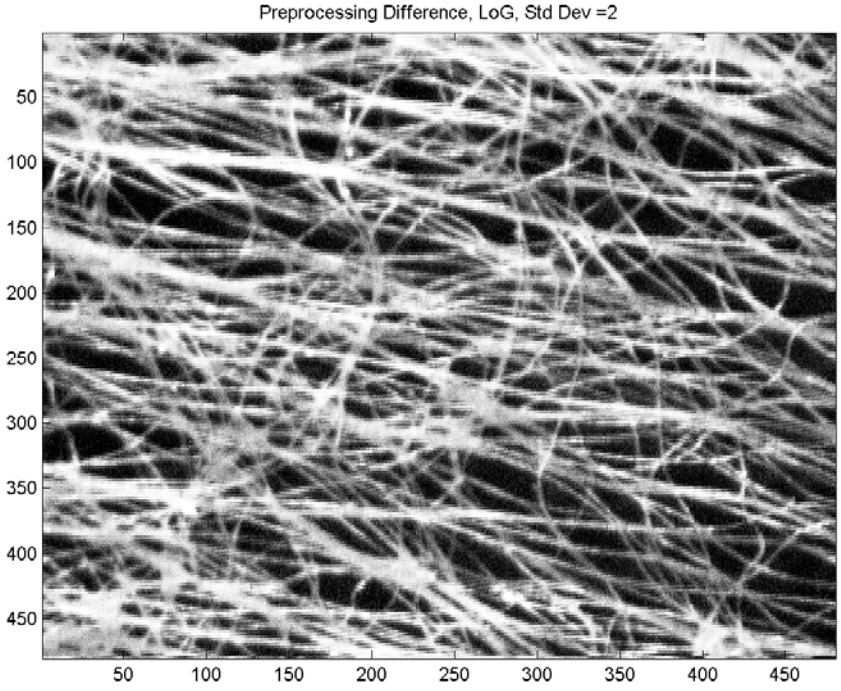


Figure 168. fiber02a LoG Smoothing, σ = 2.00 kernel

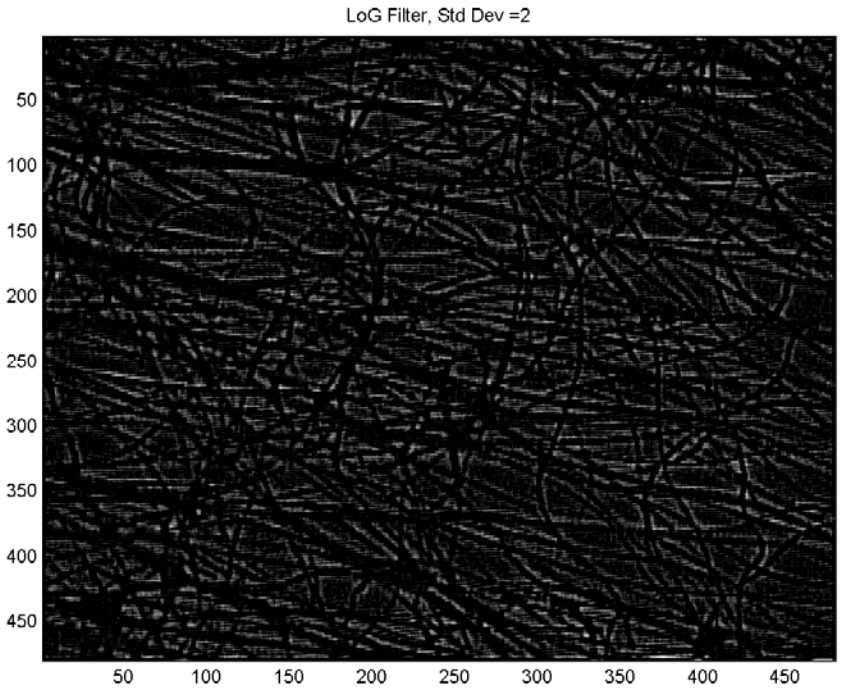


Figure 169. fiber02a LoG Smoothing Noise, σ = 2.00 kernel

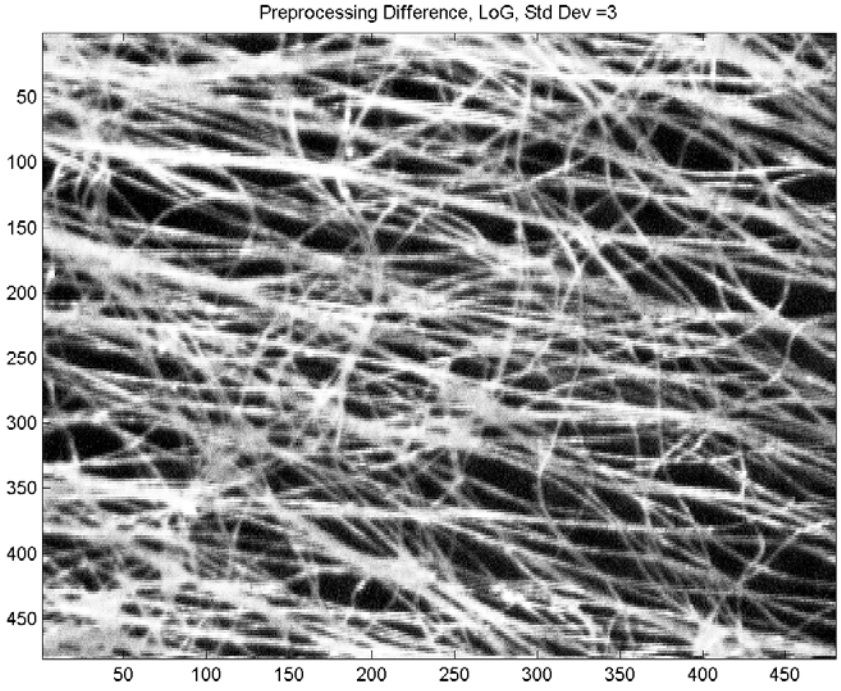


Figure 170. fiber02a LoG Smoothing, σ = 3.00 kernel

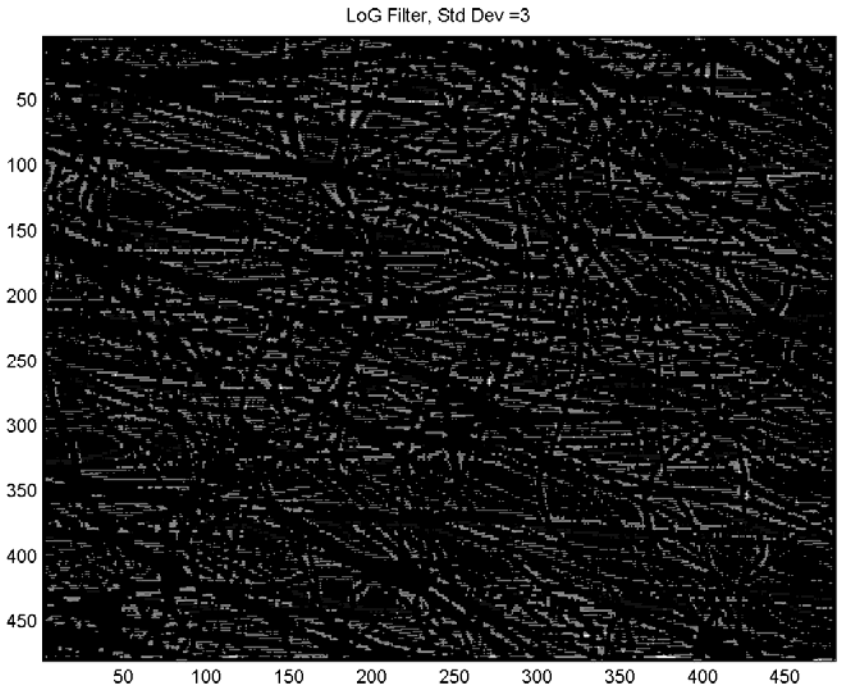


Figure 171. fiber02a LoG Smoothing Noise, σ = 3.00 kernel

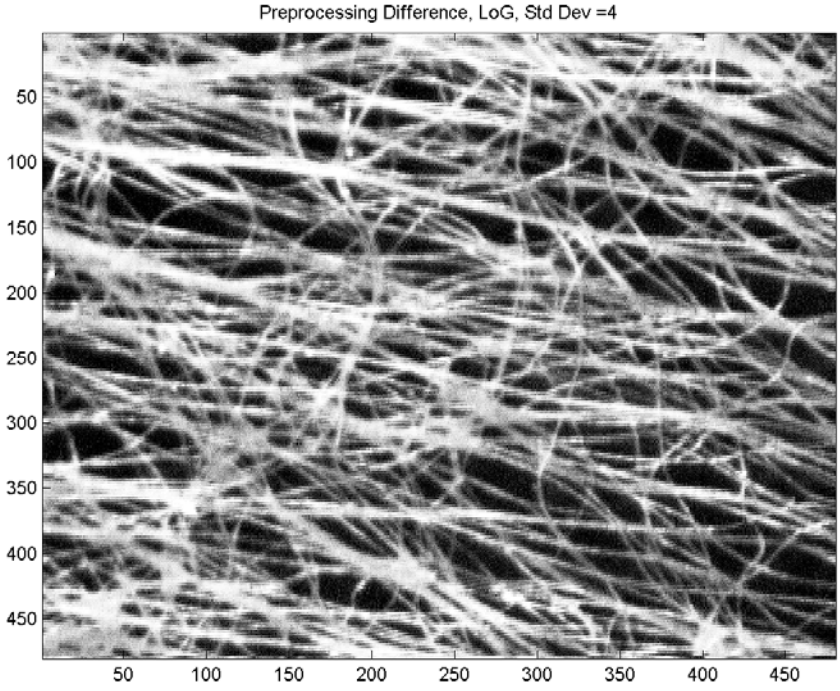


Figure 172. fiber02a LoG Smoothing, σ = 4.00 kernel

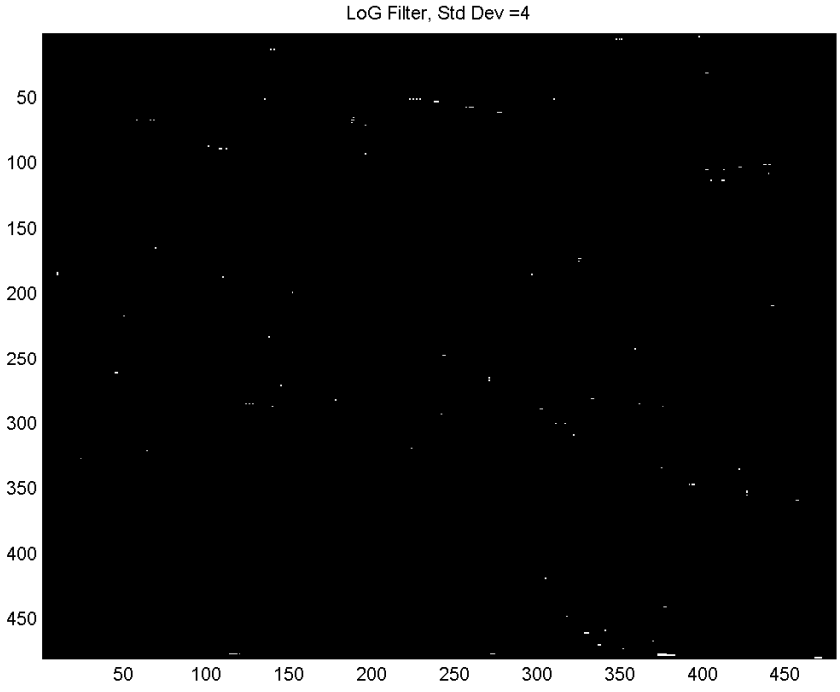


Figure 173. fiber02a LoG Smoothing Noise, σ = 4.00 kernel

Table 46. fiber02a LoG Smoothing Histogram Data

Grayscale	1.00	2.00	3.00	4.00	5.00
0	7691	1263	810	778	778
1	824	735	795	802	802
2	787	695	526	480	480
3	832	849	994	1027	1026
4	797	735	535	488	489
5	857	802	1122	1179	1179
6	772	562	292	267	267
7	839	785	790	813	813
8	763	883	445	295	293
9	908	1118	1678	1826	1828
10	785	614	486	394	392
11	812	655	974	1098	1100
12	778	473	65	0	0
13	818	897	661	625	624
14	931	1141	1204	1142	1142
15	881	1000	1301	1369	1369
16	850	677	754	848	849
17	758	649	167	1	0
18	924	1029	1307	1355	1355
19	857	824	881	903	903
20	813	706	624	718	719
21	780	792	347	3	0
22	1052	1168	2020	2367	2370
23	682	323	126	0	0
24	884	528	677	802	802
25	829	450	159	1	0
26	954	731	946	1105	1106
27	779	574	4	0	0
28	827	1092	471	4	0
29	1387	1670	2578	2910	2913
30	894	892	738	875	876
31	789	888	313	2	0
32	1102	1285	1906	1895	1896
33	1109	850	1441	1765	1766
34	756	302	1	0	0
35	810	529	221	1	0
36	1008	936	946	1165	1166
37	842	759	391	2	0
38	1137	1236	1676	1908	1908
39	905	873	673	830	832
40	788	919	382	3	0
41	1092	1337	1873	1903	1903
42	986	857	1303	1653	1656
43	760	489	213	2	0

Table 46 (Continued). fiber02a LoG Smoothing Histogram Data

Grayscale	1.00	2.00	3.00	4.00	5.00
44	927	935	763	973	975
45	794	770	406	2	0
46	985	1226	1738	1929	1931
47	888	835	688	902	902
48	793	735	471	1	0
49	1081	1136	1513	1975	1976
50	763	656	469	10	0
51	1018	1082	1417	1881	1891
52	699	583	261	3	0
53	920	997	1008	1007	1005
54	878	1054	860	1118	1123
55	783	884	499	6	0
56	999	1295	1940	1957	1959
57	957	906	1333	1812	1816
58	712	363	276	3	0
59	800	664	678	953	956
60	670	599	8	0	0
61	745	896	578	10	0
62	1064	1426	1912	2192	2201
63	829	999	812	1104	1105
64	649	805	656	5	0
65	1067	1269	1632	2281	2286
66	659	588	611	8	0
67	1023	1017	1485	2094	2102
68	692	355	252	0	0
69	846	741	694	946	946
70	706	673	4	0	0
71	705	805	712	4	0
72	1125	1442	1964	2430	2431
73	847	872	687	931	934
74	688	695	641	2	0
75	1141	1426	1618	2259	2261
76	644	731	6	0	0
77	648	803	1132	7	0
78	1451	1778	2960	4091	4098
79	591	209	0	0	0
80	632	468	0	0	0
81	643	657	6	0	0
82	650	752	924	7	0
83	1360	1720	2500	3420	3427
84	606	452	254	4	0
85	811	964	764	1017	1021
86	609	738	2	0	0
87	617	857	1003	3	0

Table 46 (Continued). fiber02a LoG Smoothing Histogram Data

Grayscale	1.00	2.00	3.00	4.00	5.00
88	1525	1987	3111	3879	3881
89	797	649	698	932	933
90	524	377	5	0	0
91	550	609	297	5	0
92	959	1182	1052	1345	1350
93	569	729	652	4	0
94	1356	1661	2008	2659	2663
95	546	556	595	1	0
96	1196	1397	1685	2280	2281
97	492	580	0	0	0
98	545	711	388	0	0
99	1009	1364	1904	1588	1587
100	1403	1591	2265	2969	2970
101	465	171	0	0	0
102	489	275	260	0	0
103	900	798	956	1216	1216
104	478	447	0	0	0
105	528	720	2	0	0
106	505	944	657	2	0
107	1646	2172	3100	3157	3159
108	1448	1548	2198	2798	2798
109	431	231	0	0	0
110	427	442	0	0	0
111	463	593	268	0	0
112	1007	1224	1572	1311	1310
113	1581	1721	2369	2898	2899
114	363	178	0	0	0
115	426	250	0	0	0
116	478	353	372	0	0
117	1235	1198	1535	1907	1907
118	454	363	0	0	0
119	479	683	1	0	0
120	494	970	551	1	0
121	1887	2466	2947	3063	3064
122	1506	1777	2439	2515	2515
123	1266	1326	1729	2088	2088
124	333	208	0	0	0
125	352	342	0	0	0
126	355	464	434	0	0
127	1665	1770	2385	2819	2819
128	340	165	0	0	0
129	368	320	1	0	0
130	363	479	241	1	0
131	1236	1306	1623	1600	1601

Table 46 (Continued). fiber02a LoG Smoothing Histogram Data

Grayscale	1.00	2.00	3.00	4.00	5.00
132	1177	1172	1508	1772	1772
133	330	324	0	0	0
134	374	595	0	0	0
135	394	871	667	0	0
136	2770	3138	4064	4731	4731
137	263	283	222	0	0
138	1133	1023	1418	1640	1640
139	261	8	0	0	0
140	310	50	0	0	0
141	319	213	0	0	0
142	333	343	0	0	0
143	387	555	395	0	0
144	2285	2263	2969	3364	3364
145	295	204	0	0	0
146	329	406	0	0	0
147	365	614	414	0	0
148	2556	2622	3249	3663	3663
149	300	268	138	0	0
150	1249	1224	1424	1562	1562
151	293	308	1	0	0
152	284	650	277	1	0
153	2161	2310	2633	2910	2911
154	275	537	311	0	0
155	2431	2401	3144	3455	3455
156	190	80	0	0	0
157	254	216	0	0	0
158	254	289	187	0	0
159	1537	1412	1815	2002	2002
160	247	99	0	0	0
161	259	312	0	0	0
162	290	622	231	0	0
163	2519	2499	3018	3249	3249
164	257	326	159	0	0
165	1537	1410	1858	2017	2017
166	228	103	0	0	0
167	243	290	0	0	0
168	275	590	225	0	0
169	2616	2653	3098	3323	3323
170	239	420	183	0	0
171	2185	2139	2674	2857	2857
172	197	138	0	0	0
173	188	291	74	0	0
174	1446	1260	1637	1711	1711
175	202	55	0	0	0

Table 46 (Continued). fiber02a LoG Smoothing Histogram Data

Grayscale	1.00	2.00	3.00	4.00	5.00
176	240	238	0	0	0
177	246	568	145	0	0
178	2612	2522	3100	3245	3245
179	235	290	73	0	0
180	1527	1543	1697	1770	1770
181	223	353	91	0	0
182	1946	1879	2314	2405	2405
183	188	184	0	0	0
184	208	485	99	0	0
185	2677	2540	3127	3226	3226
186	169	92	0	0	0
187	177	309	49	0	0
188	1238	1253	1332	1337	1337
189	1282	1143	1419	1463	1463
190	180	158	0	0	0
191	203	426	69	0	0
192	2372	2381	2768	2837	2837
193	179	416	49	0	0
194	2313	2219	2729	2778	2778
195	140	56	0	0	0
196	163	197	19	0	0
197	1268	1130	1354	1373	1373
198	160	97	0	0	0
199	187	438	35	0	0
200	2379	2441	2717	2729	2729
201	1237	1145	1384	1407	1407
202	127	13	0	0	0
203	150	87	0	0	0
204	180	413	34	0	0
205	2493	2653	2775	2792	2792
206	1908	1836	2190	2207	2207
207	130	34	0	0	0
208	154	200	13	0	0
209	1445	1367	1528	1541	1541
210	165	339	18	0	0
211	2302	2289	2655	2673	2673
212	122	125	6	0	0
213	1022	918	1051	1057	1057
214	184	62	0	0	0
215	186	441	15	0	0
216	3216	3153	3614	3629	3629
217	148	251	7	0	0
218	2029	2104	2269	2275	2275
219	816	784	893	894	894

Table 46 (Continued). fiber02a LoG Smoothing Histogram Data

Grayscale	1.00	2.00	3.00	4.00	5.00
220	109	26	0	0	0
221	135	266	8	0	0
222	2250	2263	2456	2463	2463
223	827	737	817	818	818
224	131	138	3	0	0
225	1155	1291	1185	1183	1183
226	2528	2578	2791	2795	2795
227	660	625	662	663	663
228	93	69	2	0	0
229	875	812	876	878	878
230	125	189	3	0	0
231	2523	2508	2697	2700	2700
232	109	119	1	0	0
233	1636	1712	1709	1707	1707
234	1657	1648	1771	1774	1774
235	60	35	0	0	0
236	612	616	567	565	565
237	1622	1662	1713	1715	1715
238	750	726	707	705	705
239	1128	1166	1154	1156	1156
240	1381	1381	1423	1423	1423
241	751	756	724	724	724
242	1125	1124	1127	1127	1127
243	1687	1717	1741	1741	1741
244	906	894	901	901	901
245	505	522	482	482	482
246	2387	2404	2457	2457	2457
247	274	276	259	259	259
248	986	979	986	986	986
249	1102	1115	1110	1110	1110
250	772	783	774	774	774
251	1571	1558	1577	1577	1577
252	981	1004	986	986	986
253	1154	1140	1156	1156	1156
254	816	813	818	818	818
255	871	863	873	873	873
Min:	60	8	0	0	0
μ:	900	900	900	900	900
Max:	7691	3153	4064	4731	4731
Median:	788.5	754	659	437	436
σ:	763.508	666.081	942.693	1102.044	1102.894
% Black:	3.34%	0.55%	0.35%	0.34%	0.34%
% Gray:	96.66%	99.45%	99.65%	99.66%	99.66%

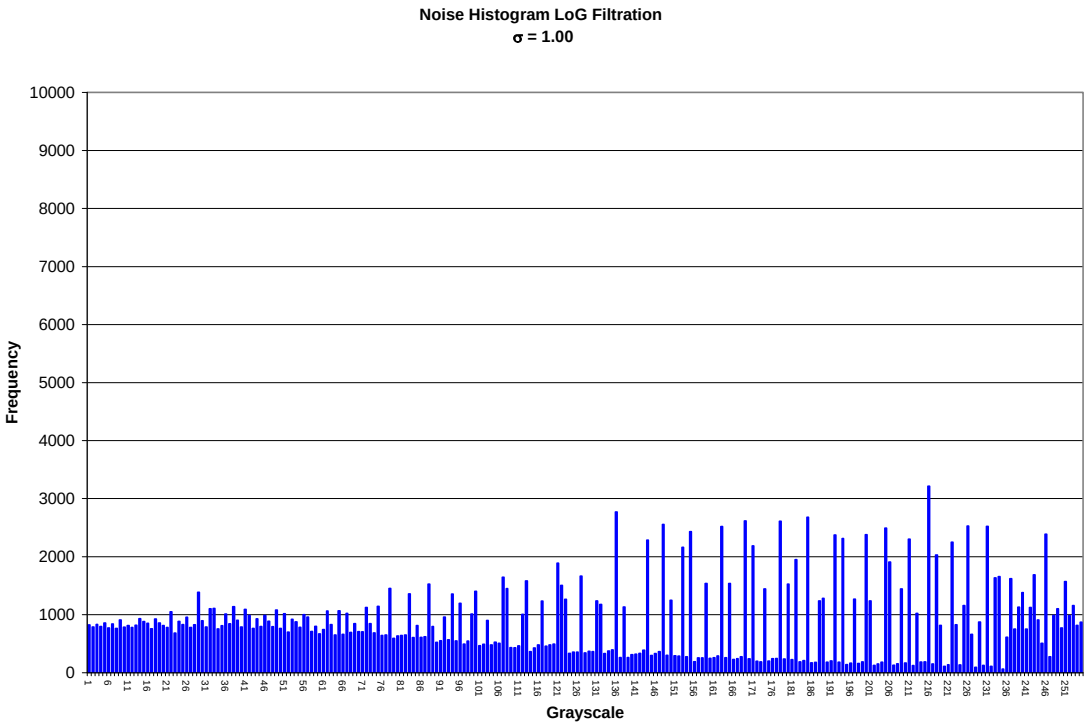


Figure 174. fiber02a LoG Smoothing Histogram, σ = 1.00 kernel

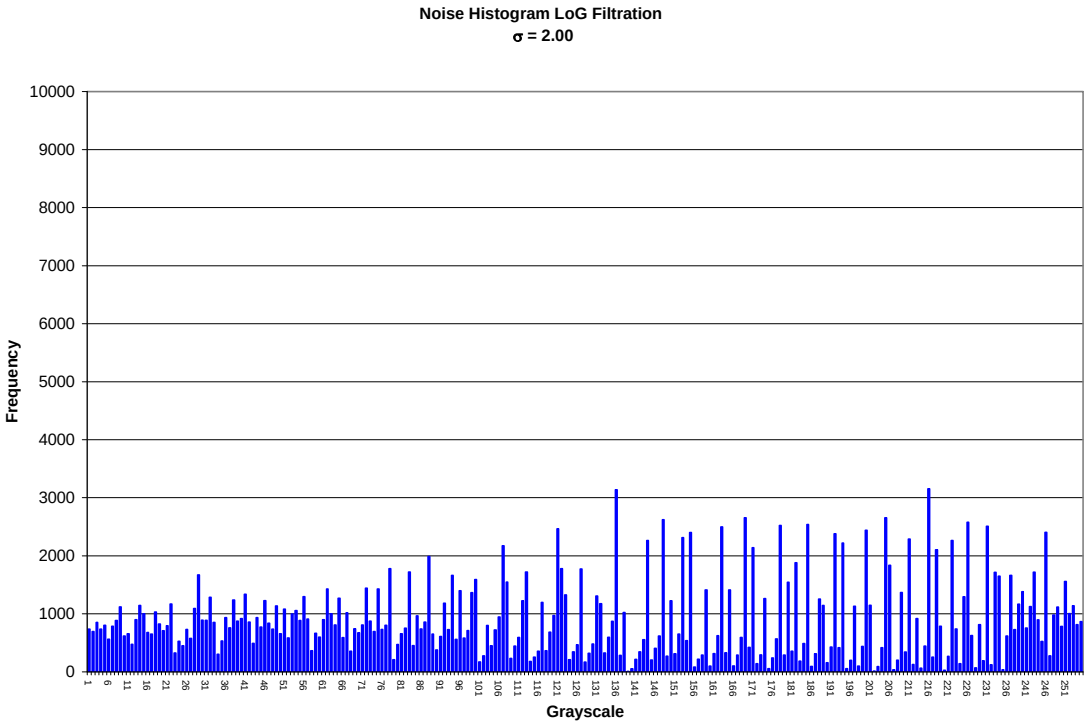


Figure 175. fiber02a LoG Smoothing Histogram, σ = 2.00 kernel

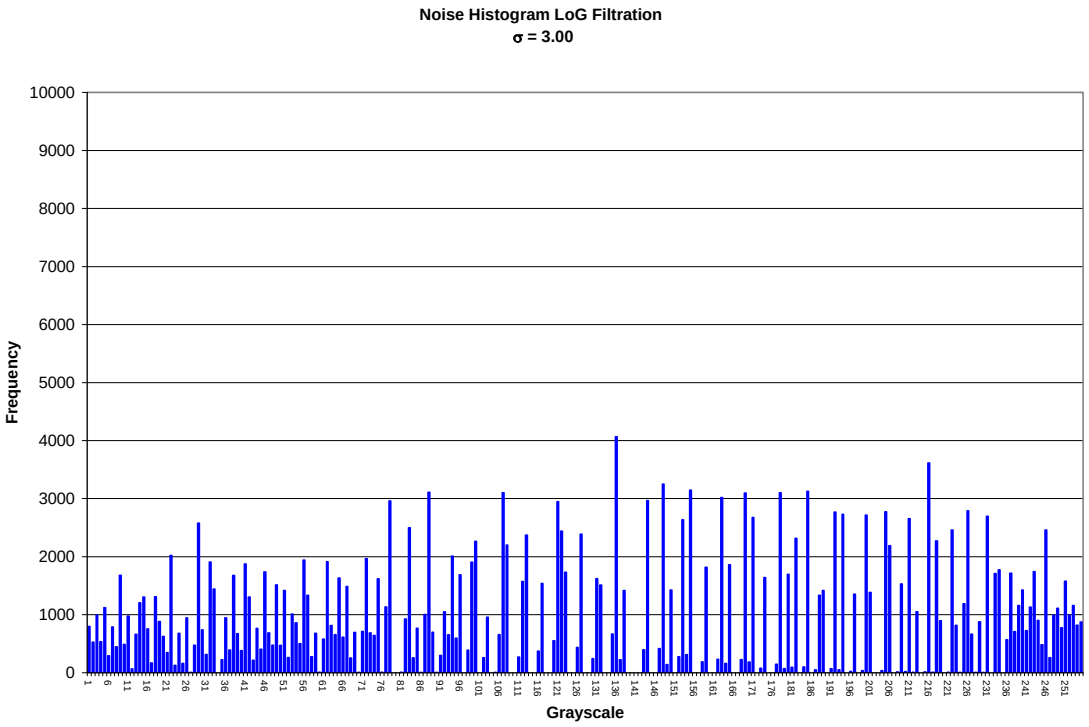


Figure 176. fiber02a LoG Smoothing Histogram, σ = 3.00 kernel

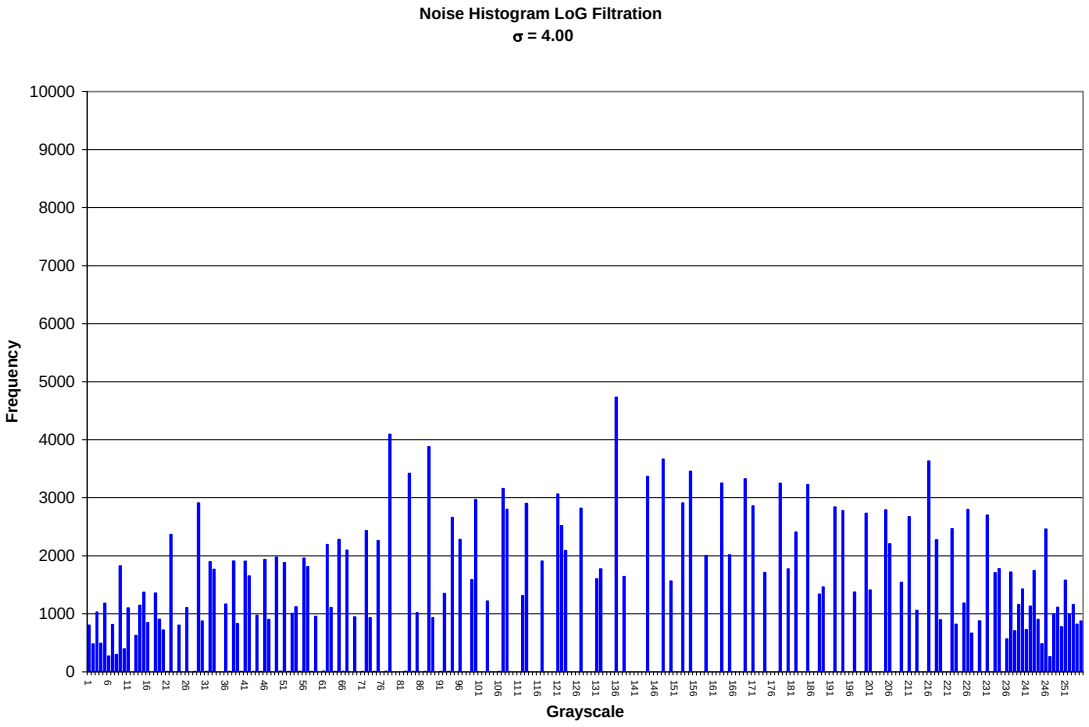


Figure 177. fiber02a LoG Smoothing Histogram, σ = 4.00 kernel

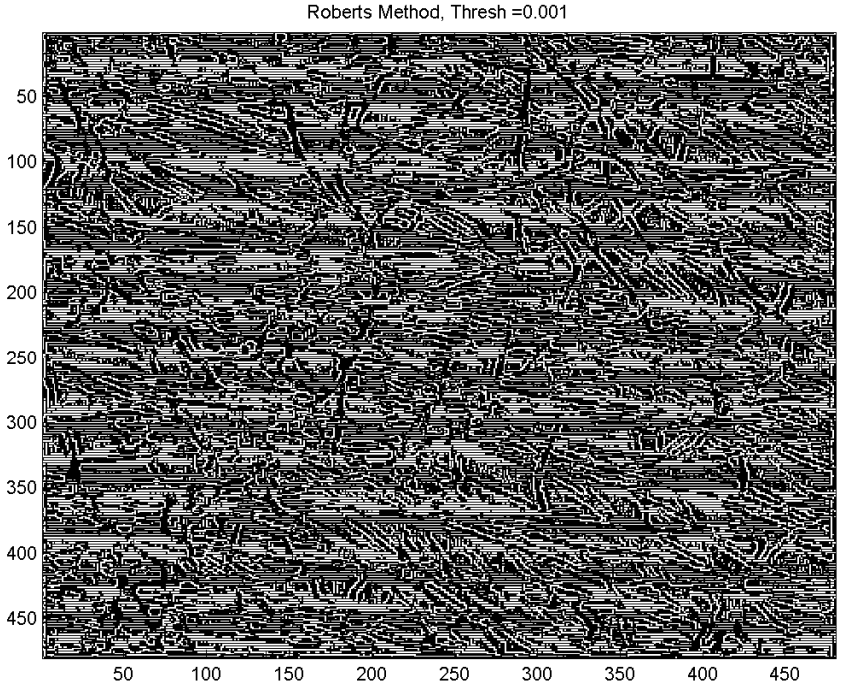


Figure 178. fiber2a Roberts Edge Detection, Threshold = 0.001

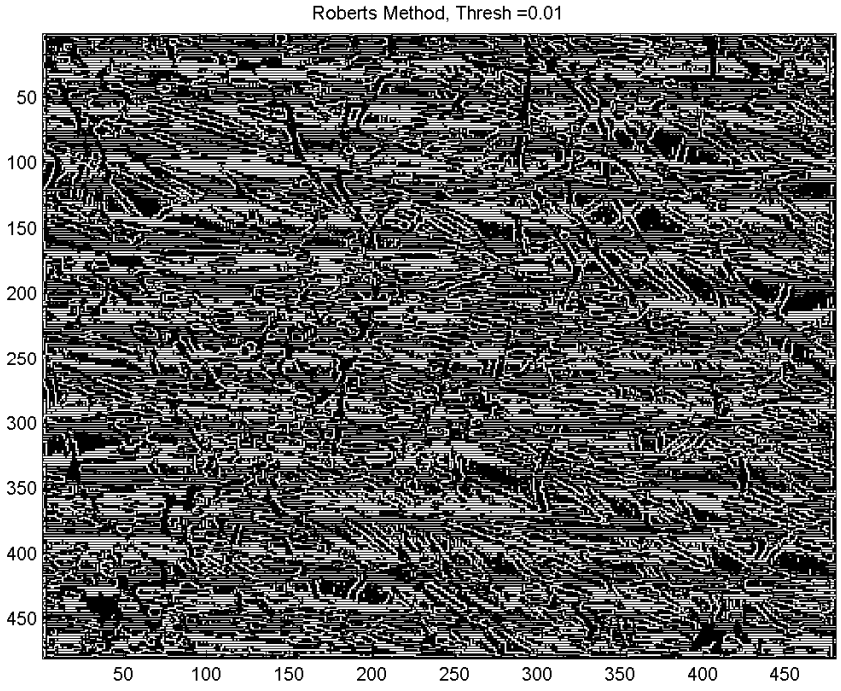


Figure 179. fiber2a Roberts Edge Detection, Threshold = 0.010

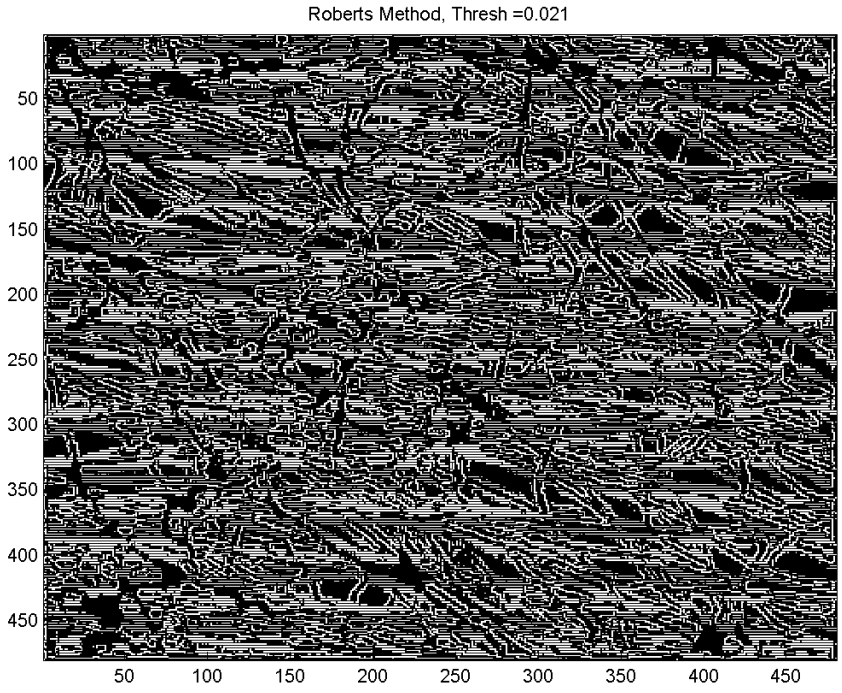


Figure 180. fiber2a Roberts Edge Detection, Threshold = 0.021

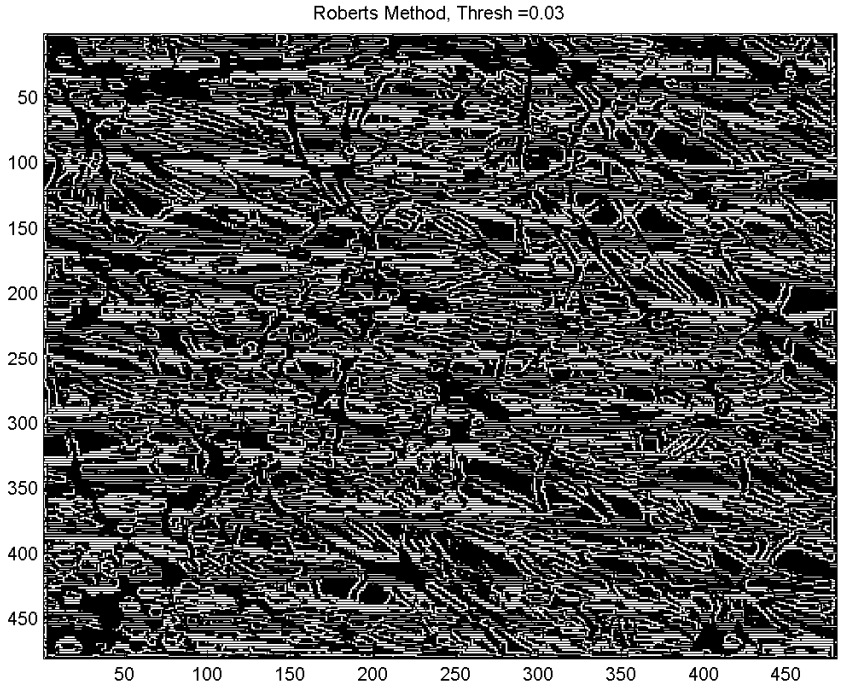


Figure 181. fiber02a Roberts Edge Detection, Threshold = 0.030

Table 47. fiber02a Roberts Edge Detection Histogram Data

	Edge Hist		90 Rotation		Difference		
Thresh	**0**	**1**	**0**	**1**	**0**	**1**	**Percent**
0.001	0.001	154461	75939	154495	75905	34	0.01476%
0.002	0.002	154470	75930	154509	75891	39	0.01693%
0.003	0.003	154573	75827	154608	75792	35	0.01519%
0.004	0.004	154653	75747	154686	75714	33	0.01432%
0.005	0.005	154864	75536	154891	75509	27	0.01172%
0.006	0.006	155146	75254	155172	75228	26	0.01128%
0.007	0.007	155379	75021	155404	74996	25	0.01085%
0.008	0.008	155768	74632	155801	74599	33	0.01432%
0.009	0.009	156296	74104	156330	74070	34	0.01476%
0.010	0.010	156746	73654	156777	73623	31	0.01345%
0.011	0.011	156924	73476	156956	73444	32	0.01389%
0.012	0.012	157495	72905	157531	72869	36	0.01563%
0.013	0.013	157833	72567	157867	72533	34	0.01476%
0.014	0.014	158304	72096	158332	72068	28	0.01215%
0.015	0.015	158723	71677	158753	71647	30	0.01302%
0.016	0.016	159205	71195	159233	71167	28	0.01215%
0.017	0.017	159718	70682	159746	70654	28	0.01215%
0.018	0.018	159969	70431	159997	70403	28	0.01215%
0.019	0.019	160524	69876	160552	69848	28	0.01215%
0.020	0.020	161191	69209	161213	69187	22	0.00955%
0.021	0.021	161636	68764	161657	68743	21	0.00911%
0.022	0.022	162290	68110	162314	68086	24	0.01042%
0.023	0.023	162929	67471	162959	67441	30	0.01302%
0.024	0.024	163671	66729	163698	66702	27	0.01172%
0.025	0.025	164135	66265	164159	66241	24	0.01042%
0.026	0.026	164802	65598	164822	65578	20	0.00868%
0.027	0.027	165530	64870	165551	64849	21	0.00911%
0.028	0.028	166293	64107	166310	64090	17	0.00738%
0.029	0.029	166937	63463	166956	63444	19	0.00825%
0.030	0.030	168035	62365	168054	62346	19	0.00825%

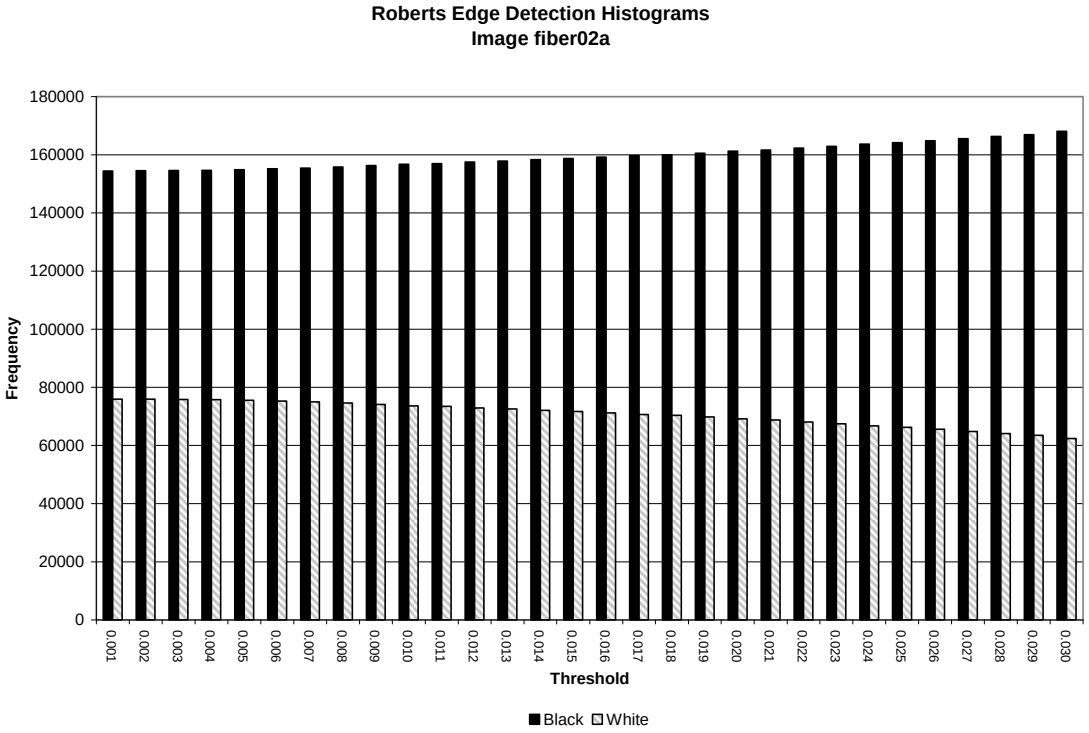


Figure 182. fiber02a Roberts Edge Detection Histograms

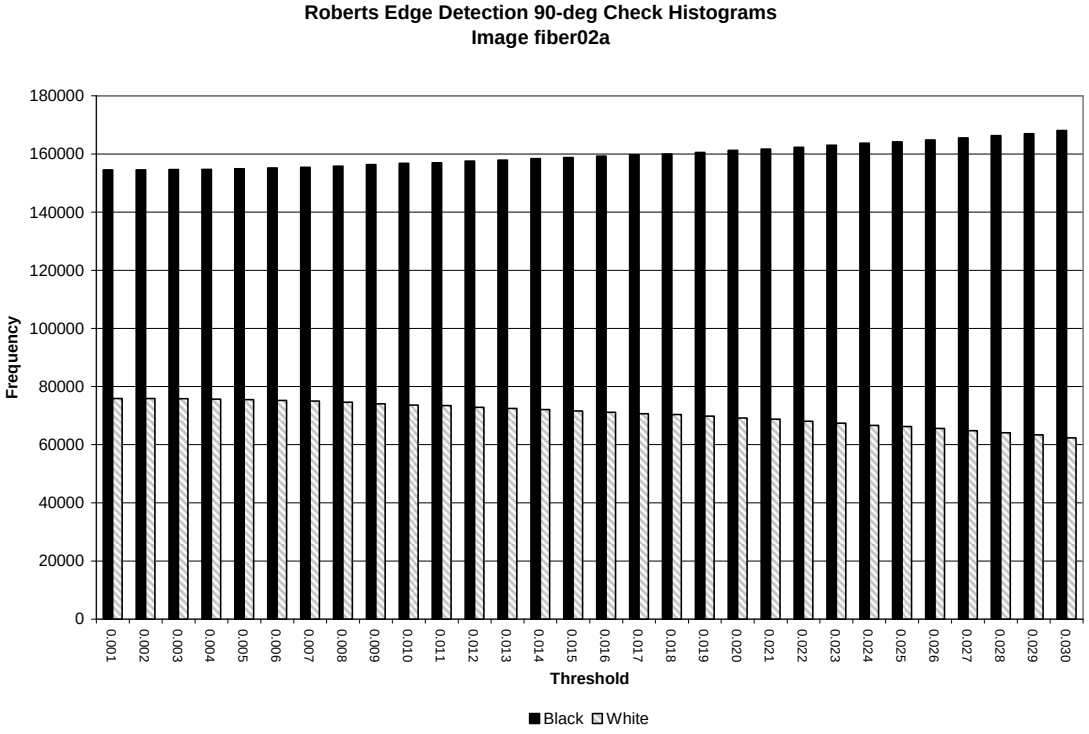


Figure 183. fiber02a Roberts Edge Detection 90° Rotation Histograms

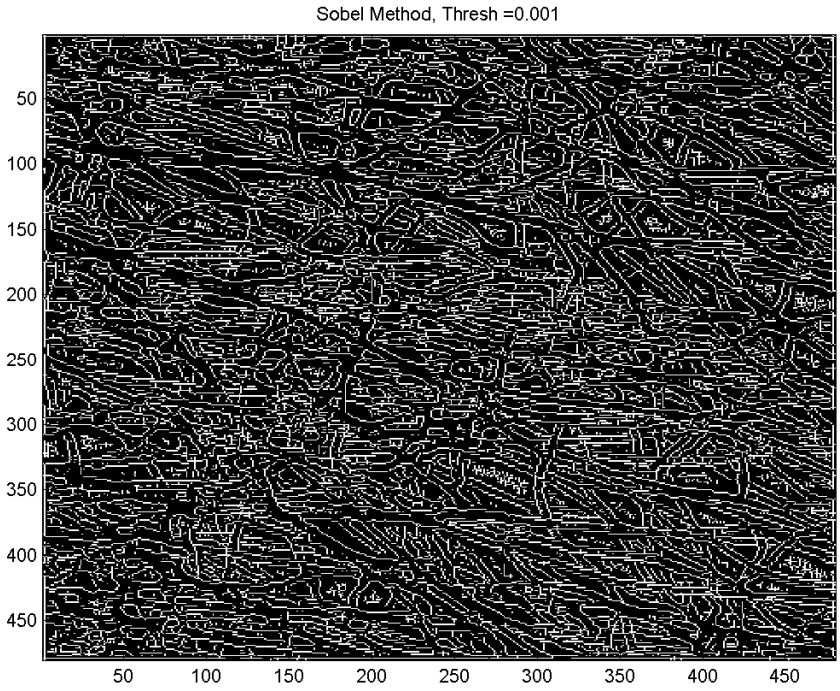


Figure 184. fiber2a Sobel Edge Detection, Threshold = 0.001

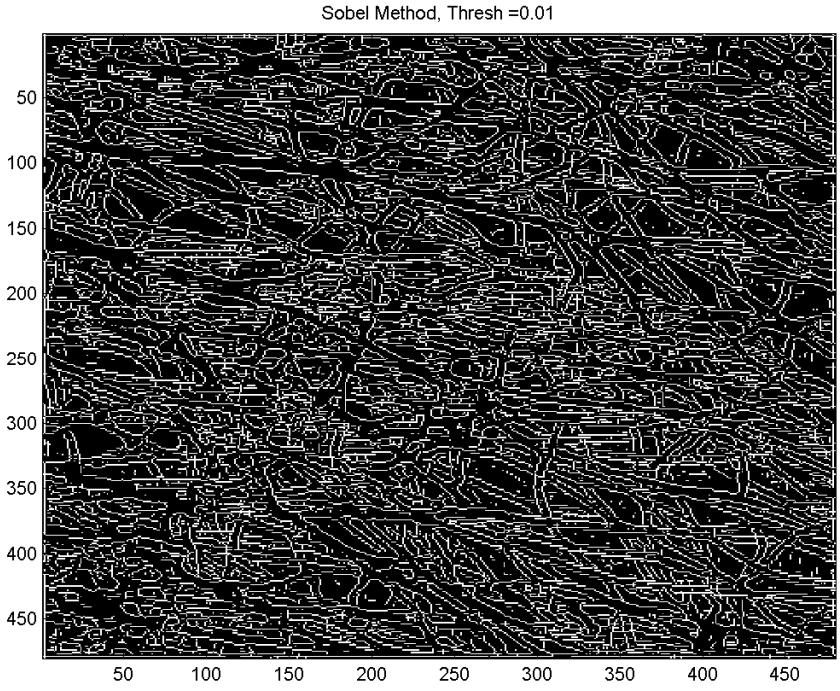


Figure 185. fiber2a Sobel Edge Detection, Threshold = 0.010

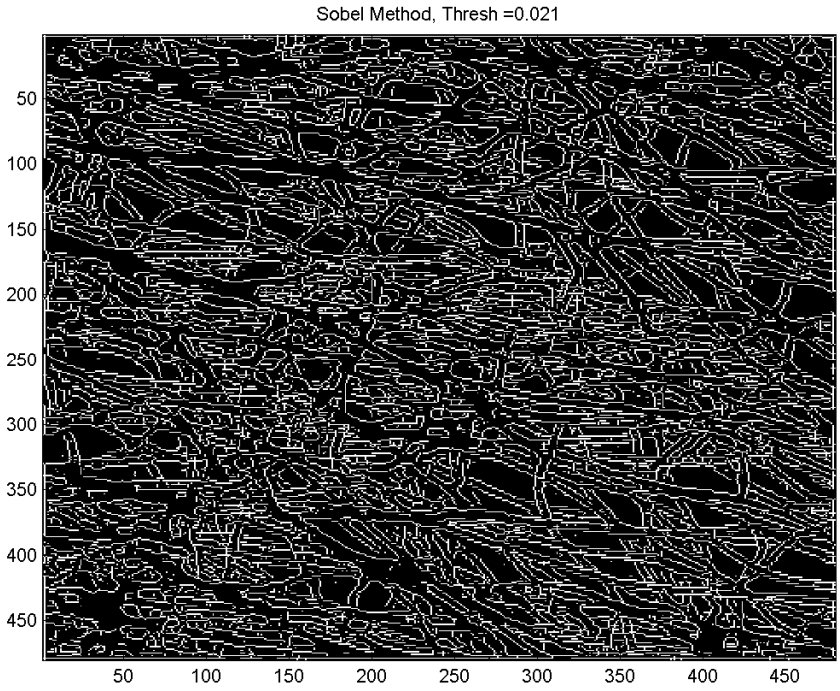


Figure 186. fiber2a Sobel Edge Detection, Threshold = 0.021

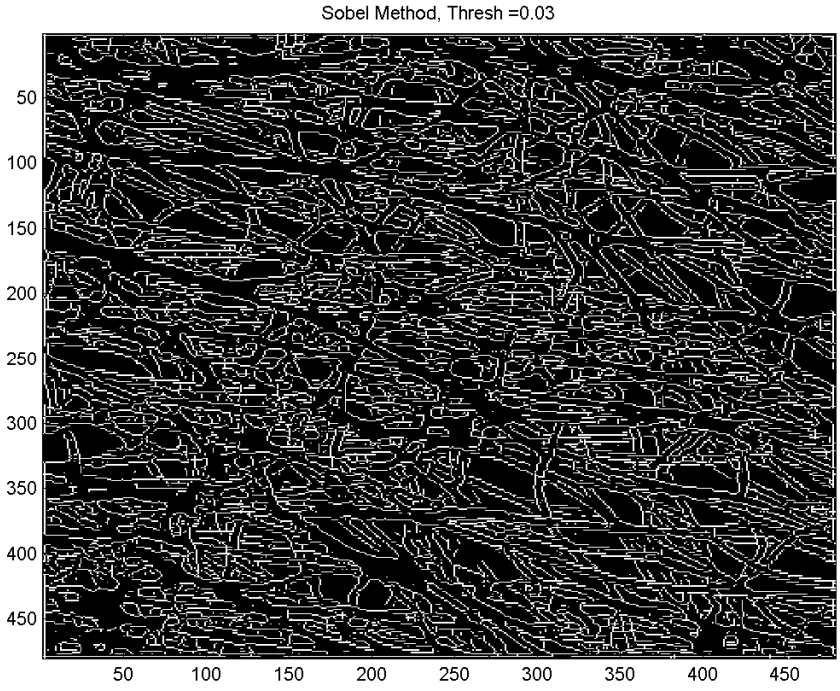


Figure 187. fiber2a Sobel Edge Detection, Threshold = 0.030

Table 48. fiber02a Sobel Edge Detection Histogram Data

	Edge Hist		90 Rotation		Difference		
Thresh	**0**	**1**	**0**	**1**	**0**	**1**	**Percent**
0.001	185873	44527	185853	44547	-20	20	0.00868%
0.002	185897	44503	185875	44525	-22	22	0.00955%
0.003	185989	44411	185970	44430	-19	19	0.00825%
0.004	186104	44296	186081	44319	-23	23	0.00998%
0.005	186363	44037	186343	44057	-20	20	0.00868%
0.006	186611	43789	186589	43811	-22	22	0.00955%
0.007	186852	43548	186834	43566	-18	18	0.00781%
0.008	187089	43311	187075	43325	-14	14	0.00608%
0.009	187260	43140	187244	43156	-16	16	0.00694%
0.010	187513	42887	187495	42905	-18	18	0.00781%
0.011	187706	42694	187690	42710	-16	16	0.00694%
0.012	187920	42480	187907	42493	-13	13	0.00564%
0.013	188086	42314	188074	42326	-12	12	0.00521%
0.014	188291	42109	188276	42124	-15	15	0.00651%
0.015	188519	41881	188506	41894	-13	13	0.00564%
0.016	188686	41714	188676	41724	-10	10	0.00434%
0.017	188879	41521	188871	41529	-8	8	0.00347%
0.018	189089	41311	189083	41317	-6	6	0.00260%
0.019	189299	41101	189288	41112	-11	11	0.00477%
0.020	189525	40875	189514	40886	-11	11	0.00477%
0.021	189760	40640	189747	40653	-13	13	0.00564%
0.022	189981	40419	189969	40431	-12	12	0.00521%
0.023	190226	40174	190211	40189	-15	15	0.00651%
0.024	190490	39910	190473	39927	-17	17	0.00738%
0.025	190782	39618	190765	39635	-17	17	0.00738%
0.026	191058	39342	191040	39360	-18	18	0.00781%
0.027	191327	39073	191312	39088	-15	15	0.00651%
0.028	191632	38768	191619	38781	-13	13	0.00564%
0.029	191916	38484	191902	38498	-14	14	0.00608%
0.030	192259	38141	192244	38156	-15	15	0.00651%

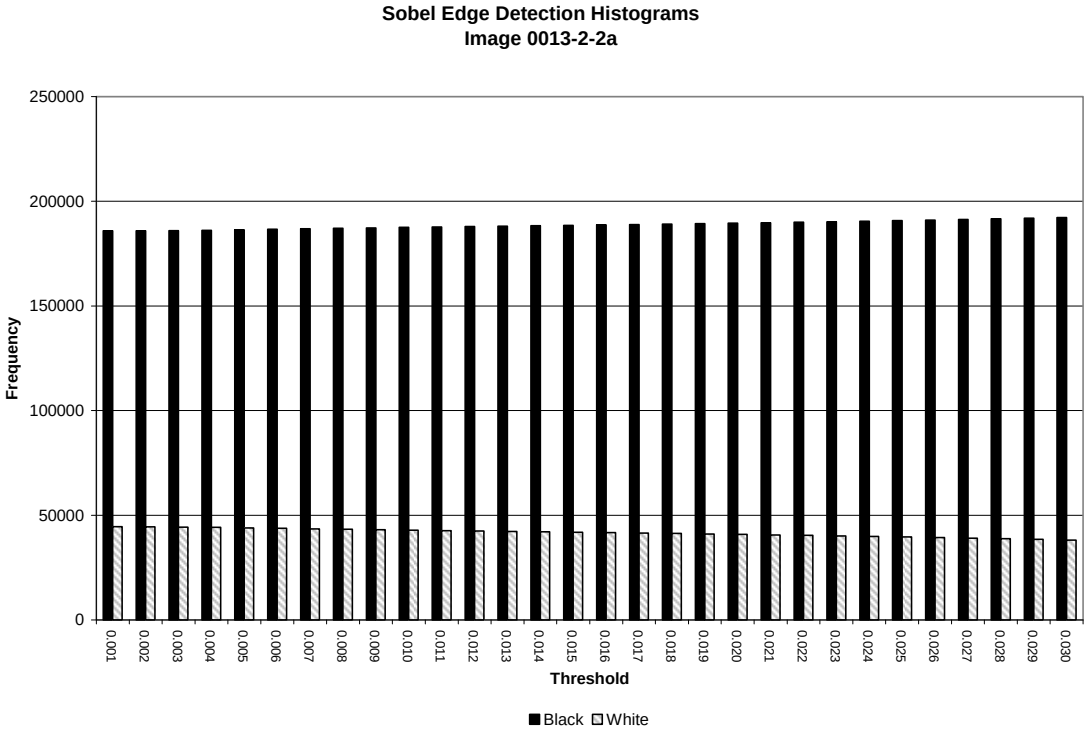


Figure 188. fiber02a Sobel Edge Detection Histograms

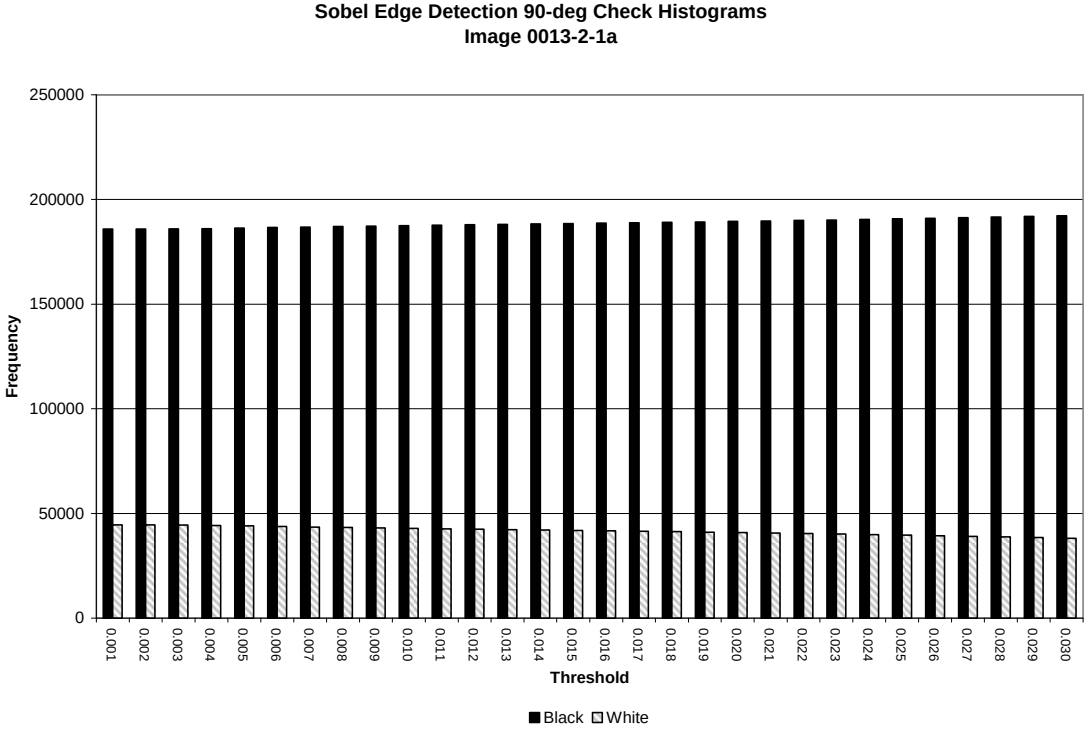


Figure 189. fiber02a Sobel Edge Detection 90° Rotation Histograms

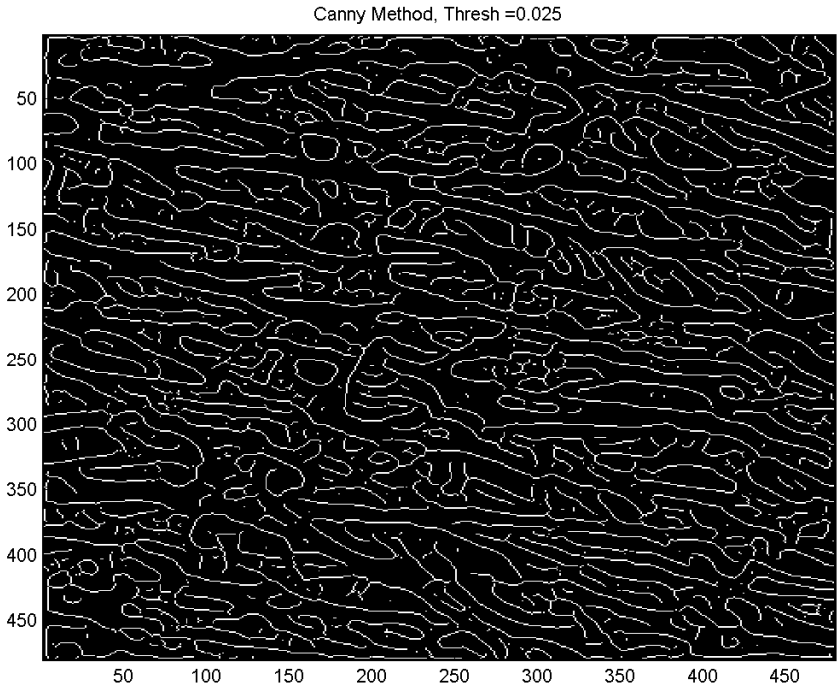


Figure 190. fiber02a Canny Edge Detection, Threshold = [0.010 0.025]

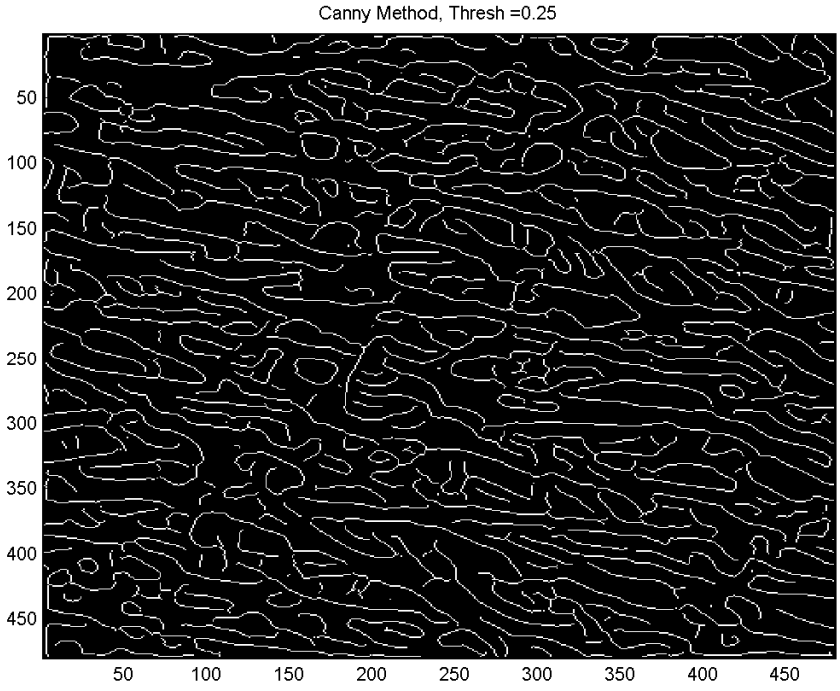


Figure 191. fiber02a Canny Edge Detection, Threshold = [0.100 0.250]

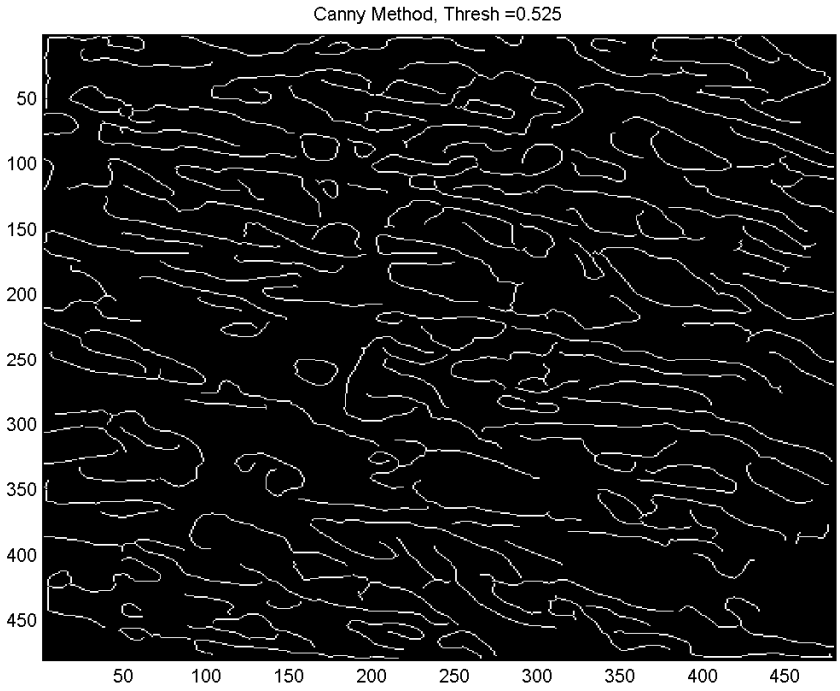


Figure 192. fiber02a Canny Edge Detection, Threshold = [0.210 0.525]

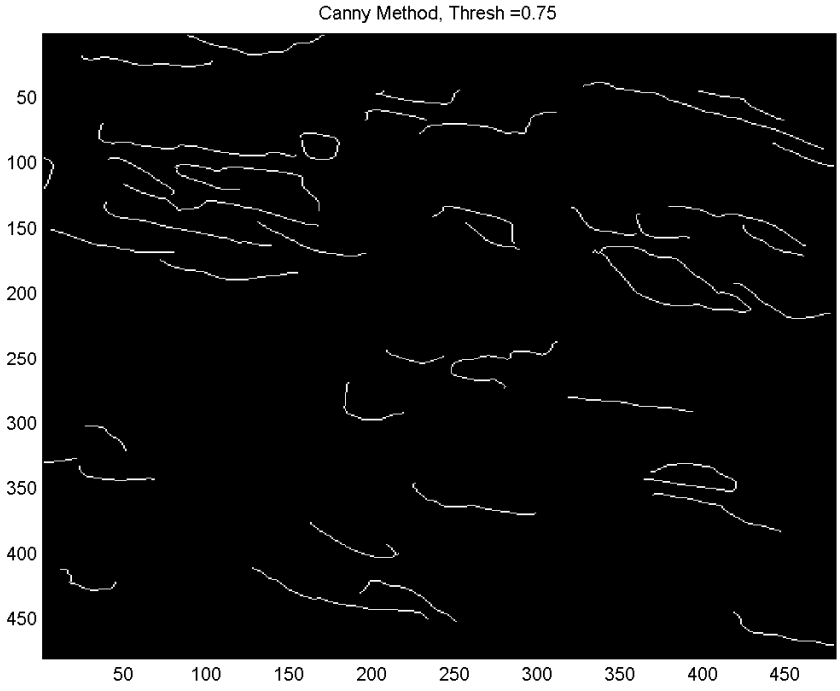


Figure 193. fiber02a Canny Edge Detection, Threshold = [0.300 0.750]

Table 49. fiber02a Canny Edge Detection Histogram Data

		Edge Hist		90 Rotation		Difference		
$Thresh_L$	**$Thresh_H$**	**0**	**1**	**0**	**1**	**0**	**1**	**Percent**
0.025	0.010	210627	19773	210617	19783	-10	10	0.00434%
0.050	0.020	210655	19745	210645	19755	-10	10	0.00434%
0.075	0.030	210719	19681	210710	19690	-9	9	0.00391%
0.100	0.040	210815	19585	210805	19595	-10	10	0.00434%
0.125	0.050	210961	19439	210951	19449	-10	10	0.00434%
0.150	0.060	211184	19216	211175	19225	-9	9	0.00391%
0.175	0.070	211441	18959	211432	18968	-9	9	0.00391%
0.200	0.080	211843	18557	211829	18571	-14	14	0.00608%
0.225	0.090	212201	18199	212182	18218	-19	19	0.00825%
0.250	0.100	212552	17848	212537	17863	-15	15	0.00651%
0.275	0.110	212872	17528	212856	17544	-16	16	0.00694%
0.300	0.120	213372	17028	213360	17040	-12	12	0.00521%
0.325	0.130	213833	16567	213818	16582	-15	15	0.00651%
0.350	0.140	214462	15938	214450	15950	-12	12	0.00521%
0.375	0.150	215048	15352	215038	15362	-10	10	0.00434%
0.400	0.160	215438	14962	215425	14975	-13	13	0.00564%
0.425	0.170	215929	14471	215918	14482	-11	11	0.00477%
0.450	0.180	216372	14028	216369	14031	-3	3	0.00130%
0.475	0.190	216855	13545	216848	13552	-7	7	0.00304%
0.500	0.200	217380	13020	217376	13024	-4	4	0.00174%
0.525	0.210	218266	12134	218260	12140	-6	6	0.00260%
0.550	0.220	219360	11040	219353	11047	-7	7	0.00304%
0.575	0.230	220028	10372	220025	10375	-3	3	0.00130%
0.600	0.240	221206	9194	221197	9203	-9	9	0.00391%
0.625	0.250	222143	8257	222136	8264	-7	7	0.00304%
0.650	0.260	222724	7676	222718	7682	-6	6	0.00260%
0.675	0.270	224143	6257	224146	6254	3	-3	0.00130%
0.700	0.280	225234	5166	225237	5163	3	-3	0.00130%
0.725	0.290	226220	4180	226223	4177	3	-3	0.00130%
0.750	0.300	227389	3011	227391	3009	2	-2	0.00087%

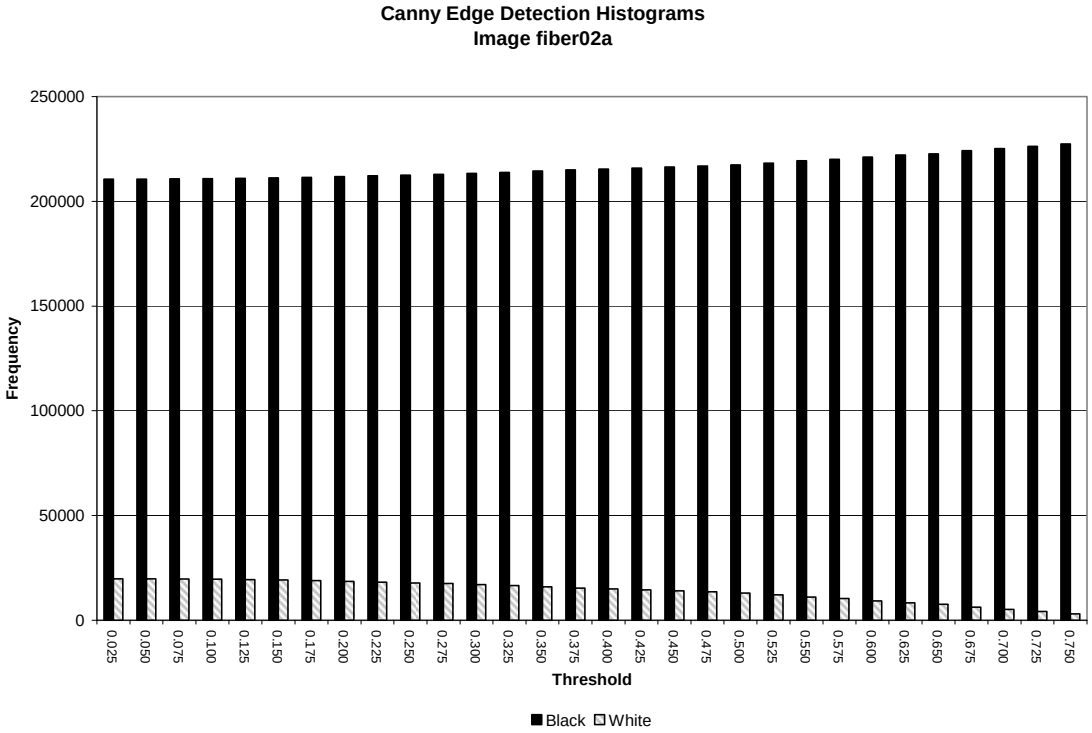


Figure 194. fiber02a Canny Edge Detection Histograms

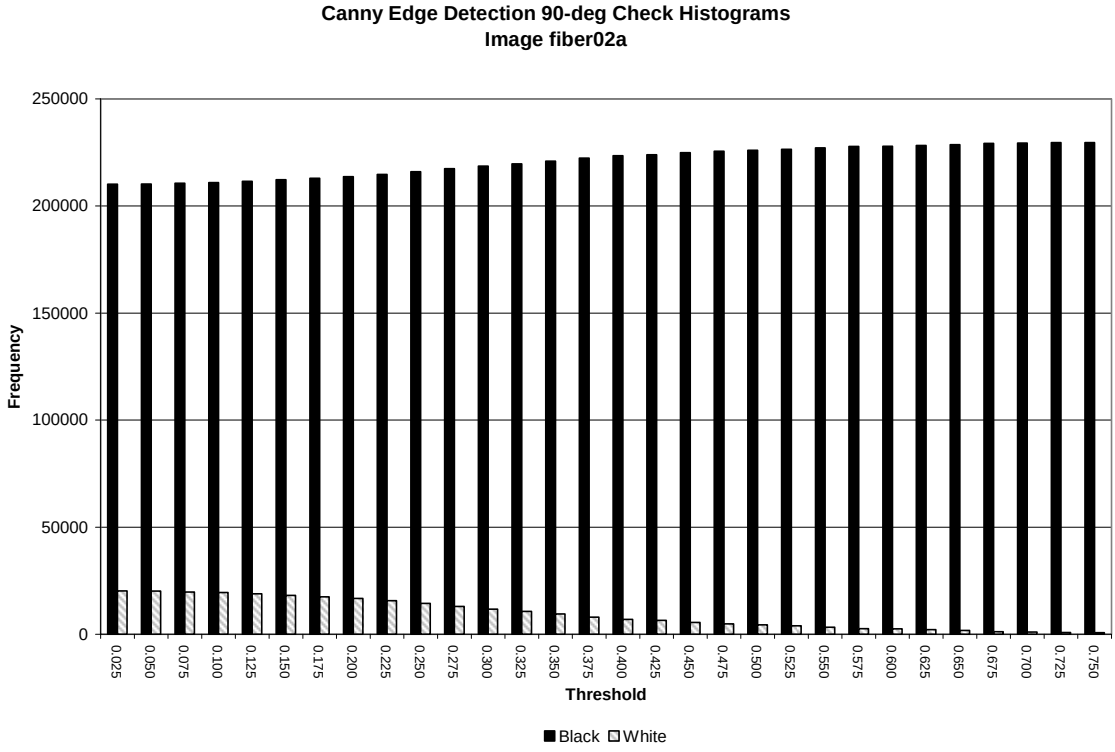


Figure 195. fiber02a Canny Edge Detection 90° Rotation Histograms

Table 50. fiber02a Line Detection θ_{mean}, Grid = 1 x 1

P	θ_{mean}
10	32.471
20	21.118
30	41.544
40	42.038
50	45.295
60	50.133
70	55.654
80	59.565
90	61.343
100	62.170

Table 51. fiber02a Line Detection θ_{mean}, Grid = 2 x 2

P	θ_{mean}	
10	34.008	30.949
10	49.069	26.543
20	35.031	35.955
20	46.600	29.780
30	43.279	44.468
30	52.022	31.820
40	38.374	38.289
40	45.422	30.748
50	44.168	45.380
50	50.651	38.816
60	45.612	50.494
60	54.482	45.709
70	50.350	52.125
70	57.242	48.699
80	59.537	64.483
80	71.102	62.435
90	59.108	65.438
90	72.619	66.417
100	56.623	62.697
100	66.363	59.176

Table 52. fiber02a Line Detection θ_{mean}, Grid = 4 x 4

P	θ_{mean}			
10	31.725	10.492	21.434	25.025
10	32.410	42.546	14.317	14.495
10	33.374	31.024	29.662	28.491
10	28.954	13.022	17.343	23.158
20	37.380	25.339	36.253	36.596
20	39.413	49.350	40.767	42.205
20	51.929	49.822	49.672	46.487
20	54.587	47.733	48.361	48.082
30	38.111	31.169	47.819	32.718
30	33.606	49.263	49.076	40.031
30	47.463	56.601	55.249	53.392
30	48.156	43.931	44.341	48.159
40	34.384	31.408	47.090	35.598
40	37.843	48.834	42.002	37.031
40	42.194	49.281	51.659	50.368
40	36.325	39.755	40.039	39.164
50	47.530	48.956	62.302	53.127
50	54.920	61.431	56.195	45.798
50	49.919	60.321	62.219	61.189
50	46.972	47.404	47.631	48.000
60	50.291	52.816	61.021	53.491
60	54.962	61.295	56.998	47.720
60	51.103	62.476	64.035	63.189
60	49.925	51.118	51.304	51.607
70	52.584	54.726	63.689	57.304
70	58.551	64.271	60.628	50.098
70	52.967	63.580	64.901	64.184
70	53.459	54.775	54.932	55.190
80	65.859	67.747	76.413	70.786
80	71.885	76.854	73.643	65.251
80	67.780	78.152	79.317	78.685
80	69.232	70.391	70.530	70.757
90	69.423	71.080	79.700	74.760
90	75.725	81.075	78.256	70.889
90	73.109	80.112	81.134	80.579
90	72.281	73.299	73.421	73.620
100	61.933	63.452	67.885	63.355
100	64.240	69.146	66.560	59.805
100	61.841	73.413	74.350	73.841
100	66.232	67.165	67.277	67.460

Table 53. fiber02a Line Detection θ_{mean}, Grid = 5 x 5

P	θ_{mean}				
10	50.054	25.220	22.840	25.945	26.313
10	24.591	24.407	32.827	25.710	29.350
10	25.293	29.848	31.944	21.276	22.643
10	43.661	38.968	33.475	33.863	27.829
10	30.728	27.527	30.062	29.386	35.809
20	40.214	31.281	32.148	39.295	32.155
20	31.919	38.505	39.490	37.456	34.656
20	32.297	35.002	42.900	44.272	31.555
20	56.715	49.843	37.349	37.575	38.620
20	37.042	38.660	31.599	33.879	35.012
30	45.604	46.689	47.254	46.005	37.210
30	39.725	43.637	42.414	46.474	45.027
30	43.490	46.438	52.446	49.354	47.234
30	63.626	57.211	46.630	46.777	47.539
30	61.273	63.833	57.727	49.078	51.187
40	38.716	42.453	42.846	45.748	39.637
40	41.385	44.977	46.393	39.972	37.859
40	36.791	36.460	49.862	48.113	40.350
40	51.738	46.139	43.197	43.299	44.456
40	52.890	54.668	50.426	44.820	48.866
50	47.643	51.858	52.172	55.941	51.063
50	52.458	55.325	56.456	43.191	41.503
50	40.651	40.386	51.758	50.362	42.700
50	51.792	55.579	49.729	49.811	49.576
50	55.061	56.481	53.095	46.300	49.530
60	51.314	55.852	56.109	56.886	52.883
60	54.027	56.381	57.309	49.010	47.626
60	46.926	46.709	58.730	57.584	51.193
60	58.655	61.763	54.907	54.974	57.113
60	61.614	62.780	60.000	53.147	55.798
70	54.941	58.789	59.007	63.983	60.588
70	61.559	63.554	64.341	54.469	53.295
70	52.701	52.517	65.953	64.982	57.017
70	63.344	65.979	63.650	63.707	63.124
70	66.941	67.930	65.573	59.778	62.026
80	70.537	73.930	74.122	70.966	67.974
80	68.829	70.588	71.282	66.075	65.040
80	64.517	64.355	77.265	76.409	69.389
80	74.966	77.289	75.806	75.856	74.296
80	77.661	78.532	76.455	70.589	72.570
90	73.428	76.405	76.574	70.825	68.199
90	68.950	70.494	71.103	66.759	65.851
90	65.392	65.249	76.582	75.831	69.668

Table 53 (Continued). fiber02a Line Detection θ_{mean}, Grid = 5 x 5

P	θ_{mean}				
90	74.564	76.603	72.715	72.759	71.390
90	74.344	75.108	73.285	68.135	69.875
100	67.283	70.014	70.169	65.619	63.210
100	63.899	65.314	65.873	61.890	61.057
100	60.636	60.505	70.898	70.209	64.557
100	69.047	70.916	65.494	65.535	64.279
100	66.987	67.689	66.016	61.294	62.889

Table 54. fiber02a Line Detection θ_{mean}, Grid = 6 x 6

P	θ_{mean}					
10	59.261	50.612	46.085	47.229	41.590	30.499
10	29.989	30.655	34.977	47.159	25.225	35.345
10	57.718	37.499	45.167	32.693	36.628	42.663
10	26.139	26.498	28.755	31.639	24.924	40.104
10	33.919	31.227	29.043	40.774	31.726	47.224
10	30.271	49.883	44.328	37.593	36.686	37.935
20	47.916	28.713	42.708	37.699	38.799	37.748
20	34.768	31.830	46.306	53.614	40.094	45.978
20	45.128	29.224	51.264	37.314	52.346	43.508
20	37.950	36.114	40.251	45.962	42.058	47.285
20	49.901	41.843	41.656	48.263	46.872	55.515
20	48.997	52.303	49.073	44.010	48.768	45.425
30	59.671	48.424	57.880	53.558	60.502	47.632
30	45.269	42.906	49.579	54.341	42.900	46.733
30	46.006	36.497	50.003	49.122	56.829	49.106
30	50.174	43.904	48.111	60.184	57.640	51.105
30	52.598	50.554	48.548	52.565	52.771	52.765
30	48.519	55.316	53.212	44.793	44.114	41.936
40	54.899	48.477	55.046	51.197	51.178	43.843
40	42.761	41.119	47.118	50.426	41.094	43.757
40	44.506	39.570	48.954	47.480	50.622	46.539
40	47.281	42.925	41.736	55.678	53.911	46.393
40	47.430	53.295	51.901	49.452	48.905	46.008
40	43.058	47.780	46.318	46.114	51.493	49.980
50	54.346	49.219	54.464	51.456	54.205	48.350
50	50.446	49.135	46.635	49.276	46.487	48.613
50	49.211	45.385	52.876	48.508	54.404	51.144
50	51.736	48.259	54.087	65.218	63.807	50.762
50	51.590	58.936	57.823	53.477	53.040	50.745
50	48.390	52.160	50.993	54.860	55.109	53.901
60	59.750	55.543	59.847	57.378	60.034	55.229
60	56.949	55.874	56.883	59.050	51.716	53.460
60	53.951	52.481	58.629	56.242	55.767	53.091
60	53.578	50.724	54.512	63.647	62.489	53.654
60	54.333	61.675	60.762	57.195	56.837	59.005
60	57.072	60.166	59.208	61.249	63.151	62.159
70	65.378	61.810	65.459	63.366	66.941	62.866
70	64.324	63.412	64.741	66.579	58.112	59.592
70	60.008	58.761	63.974	60.036	58.762	56.494
70	56.906	54.486	60.433	68.179	67.197	58.897
70	59.473	65.981	65.206	62.182	61.878	64.865
70	63.226	65.850	65.038	69.461	71.074	70.233
80	75.525	72.380	75.596	73.751	76.902	73.311

Table 54 (Continued). fiber02a Line Detection θ_{mean}, Grid = 6 x 6

P	θ_{mean}					
10	59.261	50.612	46.085	47.229	41.590	30.499
10	29.989	30.655	34.977	47.159	25.225	35.345
10	57.718	37.499	45.167	32.693	36.628	42.663
10	26.139	26.498	28.755	31.639	24.924	40.104
10	33.919	31.227	29.043	40.774	31.726	47.224
10	30.271	49.883	44.328	37.593	36.686	37.935
20	47.916	28.713	42.708	37.699	38.799	37.748
20	34.768	31.830	46.306	53.614	40.094	45.978
20	45.128	29.224	51.264	37.314	52.346	43.508
20	37.950	36.114	40.251	45.962	42.058	47.285
20	49.901	41.843	41.656	48.263	46.872	55.515
20	48.997	52.303	49.073	44.010	48.768	45.425
30	59.671	48.424	57.880	53.558	60.502	47.632
30	45.269	42.906	49.579	54.341	42.900	46.733
30	46.006	36.497	50.003	49.122	56.829	49.106
30	50.174	43.904	48.111	60.184	57.640	51.105
30	52.598	50.554	48.548	52.565	52.771	52.765
30	48.519	55.316	53.212	44.793	44.114	41.936
40	54.899	48.477	55.046	51.197	51.178	43.843
40	42.761	41.119	47.118	50.426	41.094	43.757
40	44.506	39.570	48.954	47.480	50.622	46.539
40	47.281	42.925	41.736	55.678	53.911	46.393
40	47.430	53.295	51.901	49.452	48.905	46.008
40	43.058	47.780	46.318	46.114	51.493	49.980
50	54.346	49.219	54.464	51.456	54.205	48.350
50	50.446	49.135	46.635	49.276	46.487	48.613
50	49.211	45.385	52.876	48.508	54.404	51.144
50	51.736	48.259	54.087	65.218	63.807	50.762
50	51.590	58.936	57.823	53.477	53.040	50.745
50	48.390	52.160	50.993	54.860	55.109	53.901
60	59.750	55.543	59.847	57.378	60.034	55.229
60	56.949	55.874	56.883	59.050	51.716	53.460
60	53.951	52.481	58.629	56.242	55.767	53.091
60	53.578	50.724	54.512	63.647	62.489	53.654
60	54.333	61.675	60.762	57.195	56.837	59.005
60	57.072	60.166	59.208	61.249	63.151	62.159
70	65.378	61.810	65.459	63.366	66.941	62.866
70	64.324	63.412	64.741	66.579	58.112	59.592
70	60.008	58.761	63.974	60.036	58.762	56.494
70	56.906	54.486	60.433	68.179	67.197	58.897
70	59.473	65.981	65.206	62.182	61.878	64.865
70	63.226	65.850	65.038	69.461	71.074	70.233
80	75.525	72.380	75.596	73.751	76.902	73.311

Table 55. fiber02a Line Detection θ_{mean}, Grid = 8 x 8

P	θ_{mean}							
10	45.61	38.13	56.71	17.91	25.26	20.04	23.84	44.78
10	33.38	27.21	46.69	28.23	39.93	40.27	43.33	35.16
10	36.71	36.74	34.21	40.64	37.69	33.51	27.55	34.57
10	27.05	31.00	31.22	27.05	35.88	40.22	29.97	38.54
10	29.58	28.50	31.88	40.31	28.43	28.62	23.21	31.22
10	41.78	26.32	39.33	34.09	34.50	38.28	38.28	29.71
10	26.75	30.94	53.41	27.53	28.46	21.79	40.53	41.30
10	42.98	40.11	32.66	34.78	31.52	42.36	35.79	44.60
20	60.80	56.64	71.31	48.25	48.97	32.49	37.39	50.29
20	50.07	42.47	53.79	34.85	45.18	40.46	42.24	38.13
20	43.67	43.69	42.21	45.95	44.24	43.21	34.17	33.48
20	36.35	37.90	45.06	41.68	44.47	47.86	41.90	46.88
20	37.87	32.75	40.42	51.33	44.97	44.21	42.98	40.41
20	46.55	38.78	46.36	42.61	42.85	37.80	37.80	36.48
20	43.82	36.53	46.54	41.27	41.67	29.73	46.59	43.70
20	44.67	40.11	35.78	37.51	41.72	50.15	39.18	49.84
30	51.96	47.16	56.71	41.69	47.08	40.70	43.90	52.30
30	54.26	42.63	50.01	44.55	51.24	50.61	51.77	47.38
30	50.99	51.00	50.04	52.48	51.36	45.31	39.42	37.64
30	44.63	45.64	50.31	48.11	49.90	51.68	47.80	51.05
30	43.87	42.62	48.72	51.44	44.66	44.16	43.37	45.07
30	49.07	44.94	50.27	49.82	49.97	48.89	48.89	44.43
30	52.91	47.14	53.66	50.27	50.54	42.32	43.72	42.54
30	43.17	37.07	34.25	35.38	44.08	46.18	42.69	49.40
40	56.94	52.90	59.54	49.10	46.60	36.88	39.10	44.93
40	46.30	38.22	43.34	38.05	45.40	43.74	44.55	41.49
40	44.00	44.01	43.34	45.03	44.26	41.00	36.91	35.68
40	44.24	44.94	48.18	50.27	46.74	49.39	46.69	48.95
40	44.23	44.48	48.23	49.78	45.07	44.73	44.17	44.96
40	47.73	43.20	51.83	50.86	50.97	50.93	50.93	47.83
40	52.26	46.60	51.13	48.78	48.96	43.62	47.24	47.25
40	47.69	45.78	43.82	44.60	47.49	48.68	46.26	50.92
50	59.46	60.14	65.44	57.11	47.37	49.49	51.26	55.92
50	57.01	50.56	54.65	52.44	58.30	56.98	57.62	55.19
50	57.19	57.20	56.66	58.01	57.39	54.80	51.53	50.55
50	53.49	54.05	56.63	57.01	57.80	59.91	57.75	59.56
50	55.79	55.99	58.46	59.77	56.01	55.74	55.30	53.60
50	55.82	54.22	61.10	59.83	59.92	62.30	62.30	59.82
50	63.35	58.84	62.46	60.58	60.73	56.46	55.36	59.15
50	59.51	56.25	54.68	55.30	57.61	58.56	56.63	60.34
60	66.72	67.28	71.63	64.79	54.78	53.36	54.81	58.64
60	59.53	54.23	57.59	56.05	60.87	59.78	60.31	58.31
60	59.95	59.96	59.52	60.63	60.12	57.99	55.31	54.50

Table 55 (Continued). fiber02a Line Detection θ_{mean}, Grid = 8 x 8

P								
60	54.04	54.50	56.63	58.76	60.37	62.10	60.33	61.81
60	58.72	58.89	55.85	57.64	54.55	54.33	53.96	54.61
60	56.43	52.58	57.92	57.17	57.24	59.20	59.20	57.17
60	60.06	56.36	59.33	57.78	57.91	54.40	52.21	55.70
60	55.99	53.31	52.03	52.54	54.43	55.21	53.62	56.67
70	74.10	74.57	78.26	72.46	63.61	62.24	63.47	66.71
70	67.47	62.98	65.83	62.23	66.31	65.39	65.84	64.14
70	65.53	65.54	65.17	66.11	65.68	63.87	61.60	60.91
70	63.54	63.94	65.74	67.54	67.76	69.23	67.73	68.99
70	66.37	66.51	66.74	65.72	63.10	62.91	62.60	63.14
70	64.69	65.15	70.08	67.37	67.43	69.09	69.09	67.37
70	69.83	66.68	69.20	67.90	68.00	65.03	63.99	68.09
70	68.34	66.07	64.98	65.41	67.02	67.68	66.34	68.92
80	81.52	81.93	85.19	80.07	72.27	70.91	72.00	74.86
80	75.53	71.57	74.08	72.80	76.40	75.59	75.98	74.49
80	75.71	75.72	75.39	76.22	75.84	74.25	72.24	71.64
80	72.58	72.92	74.51	76.10	76.58	77.87	76.55	77.66
80	75.35	75.47	75.68	74.62	72.32	72.15	71.87	72.35
80	73.71	75.33	80.57	77.98	78.03	79.49	79.49	77.97
80	80.14	77.37	79.59	78.44	78.53	75.91	70.04	75.50
80	75.71	73.71	72.75	73.13	74.55	75.13	73.95	76.23
90	79.19	79.56	82.41	77.92	71.07	69.88	70.83	73.34
90	73.93	70.46	72.66	71.54	74.70	73.98	74.33	73.02
90	74.10	74.10	73.81	74.54	74.21	72.81	71.05	70.52
90	71.34	71.64	73.04	74.43	74.85	75.99	74.83	75.80
90	73.77	73.88	74.06	73.14	71.11	70.96	70.73	71.15
90	72.34	73.76	78.36	76.08	76.13	77.41	77.41	76.08
90	77.98	75.55	77.50	76.49	76.56	74.27	69.12	75.39
90	75.58	73.82	72.98	73.32	74.56	75.07	74.03	76.03
100	70.84	71.18	73.80	69.68	63.40	62.31	63.18	65.48
100	66.02	62.83	64.85	63.83	66.72	66.07	66.39	65.18
100	66.17	66.18	65.91	66.58	66.27	64.99	63.38	62.89
100	63.65	63.92	65.20	66.48	66.87	67.91	66.85	67.74
100	65.88	65.98	66.14	65.29	63.44	63.30	63.08	63.47
100	64.56	65.86	70.08	67.99	68.04	69.21	69.21	67.99
100	69.73	67.51	69.29	68.36	68.44	66.33	61.60	68.45
100	68.63	67.02	66.24	66.55	67.69	68.16	67.20	69.04

Table 56. fiber02a Line Detection θ_{mean}, Grid = 10 x 10

P	θ_{mean}									
10	57.58	67.65	56.94	56.92	48.83	62.40	43.52	67.58	52.80	46.03
10	59.12	58.29	30.80	51.92	48.06	27.59	51.96	57.89	48.55	44.60
10	52.42	47.07	32.24	49.64	48.73	37.03	38.94	43.74	39.94	45.34
10	36.07	33.12	34.88	48.74	48.62	53.87	60.38	47.59	45.69	45.10
10	39.06	50.39	40.81	34.21	48.02	42.62	35.96	57.51	40.44	40.38
10	43.25	41.70	44.57	44.62	51.99	44.19	54.51	36.04	37.17	41.58
10	51.09	52.16	41.67	49.98	60.97	39.97	38.41	38.24	34.73	39.10
10	39.10	33.65	39.13	37.32	35.71	42.29	37.96	43.21	47.13	49.95
10	54.18	35.49	46.43	51.16	45.17	39.38	43.36	35.68	46.14	44.24
10	50.02	48.82	42.29	36.25	62.95	47.28	36.43	36.10	47.30	39.28
20	57.38	63.24	57.01	61.28	57.65	54.45	49.61	62.73	54.13	55.54
20	62.10	54.03	38.84	57.26	52.64	44.54	55.31	59.86	54.46	52.18
20	65.05	50.10	47.64	57.60	53.28	46.52	48.75	45.11	43.91	49.77
20	45.28	43.57	45.19	46.05	45.97	49.31	51.83	44.47	44.19	43.93
20	47.51	52.04	40.61	36.68	47.69	50.17	42.01	46.73	36.86	36.79
20	38.54	37.64	39.16	44.02	49.78	38.48	54.72	37.77	37.24	43.80
20	49.29	45.39	44.83	52.53	55.77	41.96	41.06	47.28	38.25	40.78
20	40.78	45.73	43.55	46.83	49.62	45.04	47.11	48.99	51.25	47.37
20	49.70	42.17	45.85	53.00	39.86	52.30	55.24	39.11	43.60	43.12
20	46.45	47.55	47.61	42.81	58.24	57.03	40.66	43.00	47.37	41.96
30	54.31	58.12	54.07	52.30	49.94	49.29	45.87	53.11	47.51	49.37
30	53.65	55.19	36.91	58.20	55.19	49.91	62.46	58.38	54.70	53.14
30	65.73	56.07	54.55	62.46	56.11	51.50	55.07	51.39	50.56	60.68
30	57.62	56.46	57.56	56.13	56.08	59.53	60.89	55.75	57.92	57.73
30	61.49	64.60	54.48	51.80	61.45	60.98	55.41	59.42	52.70	54.25
30	55.44	54.83	55.87	59.18	61.53	56.05	66.11	55.03	55.27	59.26
30	63.01	55.72	55.33	61.23	63.36	58.78	58.16	62.40	56.24	57.97
30	57.97	54.88	54.95	57.19	59.09	55.96	57.56	55.33	56.87	56.77
30	58.36	54.26	56.76	61.64	53.07	61.56	63.56	51.32	58.09	58.24
30	60.52	56.96	57.00	53.73	64.25	66.50	49.44	48.02	54.01	50.32
40	54.33	56.98	54.16	52.93	51.29	52.70	50.32	55.35	51.46	52.75
40	55.73	58.19	45.49	52.19	50.10	46.43	54.68	52.74	50.19	49.11
40	53.23	46.52	45.46	53.32	48.91	45.70	49.25	44.07	43.49	50.87
40	48.74	47.93	48.70	47.70	47.67	50.07	51.64	48.07	49.58	49.45
40	46.40	48.56	41.76	39.90	50.93	51.71	47.85	49.82	45.15	46.23
40	47.06	46.63	47.35	49.65	51.21	46.28	53.27	45.57	45.74	45.47
40	48.07	43.01	42.74	48.81	49.94	46.76	46.33	49.28	45.00	46.20
40	46.20	49.53	49.58	51.14	52.46	50.29	51.40	50.18	51.25	51.18
40	52.28	46.36	48.10	51.49	45.53	51.43	52.82	44.32	50.63	50.74
40	52.32	45.14	45.17	42.89	50.20	51.77	43.55	42.57	46.73	44.17
50	63.07	65.19	62.94	61.95	60.65	59.23	57.33	61.34	58.24	59.27
50	61.64	63.61	53.47	60.28	58.61	55.69	63.04	60.72	58.68	57.82
50	61.83	56.47	55.63	62.17	58.65	56.09	58.92	54.79	54.33	60.22
50	58.52	57.87	58.48	57.69	57.66	59.58	60.38	57.53	58.73	58.63
50	54.46	56.18	53.52	52.03	58.26	58.89	55.80	57.63	53.90	54.77

Table 56 (Continued). fiber02a Line Detection θ_{mean}, Grid = 10 x 10

P	θ_{mean}									
50	55.43	55.09	55.66	57.50	57.53	54.77	60.35	54.21	54.34	54.13
50	56.21	52.16	51.95	56.04	59.00	56.46	56.12	58.47	55.06	56.01
50	56.01	58.12	58.15	59.40	60.45	58.72	59.60	58.63	59.48	59.43
50	60.31	55.61	57.00	59.70	54.95	59.66	60.77	53.98	59.08	59.16
50	60.42	54.69	54.71	52.90	58.73	59.98	52.93	52.14	55.46	53.42
60	58.91	60.65	58.80	58.00	56.92	52.39	50.83	54.13	51.58	52.42
60	54.37	55.99	47.66	55.18	53.81	51.41	56.62	55.56	53.88	53.17
60	56.46	52.07	51.37	57.73	54.84	52.74	55.06	51.67	51.29	56.12
60	54.73	54.20	54.70	54.05	54.03	55.60	56.49	54.15	55.14	55.05
60	53.91	55.32	53.14	51.92	57.03	57.54	55.01	56.51	53.45	54.16
60	54.70	54.42	54.90	56.40	60.33	58.88	63.46	58.42	58.53	58.35
60	60.06	56.74	56.56	59.43	59.41	57.33	57.05	58.98	56.17	56.96
60	56.96	59.42	59.45	60.47	61.34	59.91	60.64	59.84	60.54	60.50
60	61.22	57.36	58.50	60.72	56.82	60.68	61.59	56.02	60.92	60.99
60	62.03	57.32	57.34	55.85	60.64	61.67	56.05	55.40	58.13	56.45
70	70.82	72.29	70.73	70.04	69.13	64.73	63.41	66.20	64.04	64.76
70	66.41	67.78	60.73	67.10	65.94	63.90	70.74	69.84	68.42	67.82
70	70.61	66.88	66.29	69.98	67.53	65.75	67.72	64.84	64.53	68.62
70	67.44	66.99	67.42	66.86	66.84	68.18	68.21	66.22	67.06	66.99
70	65.43	66.63	64.78	63.75	68.08	68.52	66.37	67.64	65.05	65.65
70	66.11	65.87	66.27	67.55	71.80	70.57	74.45	70.17	70.27	70.12
70	71.57	68.75	68.60	71.03	71.16	69.39	69.15	70.79	68.41	69.08
70	69.08	71.16	71.19	72.06	72.79	71.58	72.20	71.52	72.12	72.08
70	72.69	69.42	70.39	72.27	68.96	72.24	73.01	68.28	72.44	72.50
70	73.37	69.39	69.40	68.14	72.20	73.07	68.17	67.62	69.93	68.51
80	77.90	79.20	77.82	77.21	76.41	73.11	71.94	74.41	72.50	73.14
80	74.59	75.80	69.58	75.20	74.17	72.38	78.40	77.61	76.36	75.83
80	78.29	75.00	74.49	77.74	75.58	74.01	75.75	73.21	72.93	76.54
80	75.50	75.10	75.48	74.99	74.97	76.15	76.17	74.43	75.16	75.10
80	72.29	73.35	71.71	70.80	74.62	75.01	73.11	74.24	71.95	72.48
80	72.89	72.68	73.03	74.16	77.90	76.82	80.24	76.47	76.55	76.42
80	77.70	75.22	75.08	77.23	77.58	76.02	75.81	77.26	75.16	75.75
80	75.75	77.59	77.61	78.37	79.02	77.96	78.50	77.90	78.43	78.39
80	78.93	76.05	76.90	78.56	75.64	78.53	79.21	75.05	78.71	78.76
80	79.53	76.02	76.03	74.92	78.50	79.27	74.70	74.22	76.26	75.00
90	77.50	78.64	77.43	76.90	76.19	73.29	72.27	74.43	72.76	73.32
90	74.59	75.66	70.19	75.13	74.23	72.65	77.94	77.24	76.15	75.68
90	77.84	74.95	74.50	77.36	75.46	74.08	75.61	73.38	73.13	76.30
90	75.39	75.04	75.37	74.94	74.93	75.96	75.98	74.45	75.10	75.04
90	72.57	73.50	72.07	71.27	74.62	74.96	73.30	74.29	72.28	72.74
90	73.10	72.91	73.22	74.21	77.50	76.55	79.55	76.24	76.32	76.20
90	77.32	75.14	75.03	76.91	77.22	75.85	75.67	76.93	75.10	75.61
90	75.61	77.22	77.24	77.91	78.48	77.55	78.03	77.50	77.96	77.93
90	78.40	75.87	76.62	78.08	75.52	78.05	78.65	75.00	78.21	78.25
90	78.93	75.85	75.86	74.88	78.02	78.70	74.69	74.27	76.06	74.95
100	70.39	71.43	70.32	69.83	69.19	66.53	65.59	67.58	66.04	66.55
100	67.72	68.70	63.69	68.21	67.39	65.94	70.79	70.15	69.15	68.72
100	70.70	68.05	67.64	70.26	68.52	67.26	68.65	66.61	66.38	69.29

Table 56 (Continued). fiber02a Line Detection θ_{mean}, Grid = 10 x 10

P	θ_{mean}									
100	68.45	68.13	68.44	68.04	68.03	68.98	69.00	67.59	68.18	68.13
100	65.87	66.72	65.41	64.67	67.75	68.06	66.53	67.44	65.60	66.02
100	66.35	66.18	66.47	67.37	70.39	69.51	72.27	69.23	69.30	69.20
100	70.22	68.23	68.12	69.85	70.13	68.88	68.71	69.87	68.18	68.66
100	68.66	70.13	70.15	70.77	71.29	70.43	70.87	70.39	70.81	70.78
100	71.22	68.90	69.58	70.92	68.57	70.90	71.44	68.09	71.04	71.08
100	71.70	68.87	68.88	67.99	70.87	71.49	67.81	67.42	69.06	68.05

Table 57. fiber02a Line Detection L_{total}, Grid = 1 x 1

P	L_{total}
10	82.565
20	50.695
30	48.836
40	71.309
50	82.201
60	52.811
70	66.408
80	54.571
90	63.032
100	46.098

Table 58. fiber02a Line Detection L_{total}, Grid = 2 x 2

P	L_{total}	
10	49.477	57.280
10	40.000	52.393
20	53.141	96.000
20	66.910	72.180
30	56.143	41.049
30	126.830	59.228
40	70.612	50.220
40	63.781	178.930
50	121.020	49.980
50	55.731	52.479
60	52.240	41.000
60	41.146	128.690
70	129.400	105.800
70	66.851	60.166
80	64.008	47.802
80	45.044	76.688
90	71.694	120.920
90	42.059	65.856
100	43.324	75.664
100	130.510	57.009

Table 59. fiber02a Line Detection L_{total}, Grid = 4 x 4

P	L_{total}			
10	88.459	115.000	53.852	55.946
10	52.154	50.636	63.032	60.208
10	45.011	119.820	52.479	106.080
10	53.367	62.008	49.396	51.108
20	46.098	46.872	47.434	50.090
20	97.268	50.596	158.030	49.396
20	48.083	86.816	56.294	53.038
20	76.007	49.041	89.269	62.201
30	62.801	46.487	85.563	48.083
30	64.000	40.311	73.539	54.452
30	58.600	41.976	41.195	47.885
30	162.370	82.024	89.269	121.120
40	95.415	42.720	42.485	48.083
40	112.020	108.580	73.539	42.012
40	58.600	97.417	70.349	47.885
40	57.280	46.000	89.269	99.825
50	100.660	50.220	84.380	48.083
50	112.020	285.250	73.539	108.850
50	58.600	66.370	70.349	47.885
50	41.773	90.443	89.269	55.154
60	40.311	52.154	90.697	48.083
60	112.020	122.800	73.539	99.705
60	58.600	56.921	70.349	47.885
60	42.059	86.023	89.269	55.154
70	40.311	52.154	40.311	48.083
70	112.020	64.140	73.539	99.705
70	58.600	57.871	70.349	47.885
70	42.059	86.023	89.269	55.154
80	40.311	52.154	126.290	48.083
80	112.020	101.600	73.539	99.705
80	58.600	66.648	70.349	47.885
80	42.059	86.023	89.269	55.154
90	40.311	52.154	56.719	48.083
90	112.020	101.140	73.539	99.705
90	58.600	136.500	70.349	47.885
90	42.059	86.023	89.269	55.154
100	40.311	52.154	184.050	48.083
100	112.020	101.140	73.539	99.705
100	58.600	63.071	70.349	47.885
100	42.059	86.023	89.269	55.154

Table 60. fiber02a Line Detection L_{total}, Grid = 5 x 5

P	L_{total}				
10	114.790	42.450	41.485	57.271	56.569
10	54.120	48.260	41.437	206.240	41.437
10	46.141	42.000	51.624	46.690	97.949
10	55.317	48.374	46.400	49.366	43.738
10	42.107	65.788	137.570	49.396	95.713
20	42.202	82.298	60.166	48.104	56.400
20	44.407	41.146	87.092	50.596	60.440
20	46.141	52.010	221.000	45.100	43.105
20	68.411	242.330	69.296	49.366	45.000
20	58.898	48.765	74.726	46.098	61.522
30	121.020	61.074	60.166	41.869	49.477
30	40.311	45.891	63.032	40.249	56.321
30	46.141	60.539	55.317	118.830	65.008
30	68.411	41.785	43.658	49.366	79.158
30	40.050	45.044	74.726	83.006	41.773
40	78.772	44.283	60.166	57.035	49.477
40	40.311	42.048	69.354	47.760	120.920
40	46.141	64.413	54.918	101.140	194.180
40	68.411	41.725	70.007	49.366	74.726
40	68.118	45.044	74.726	50.695	62.514
50	78.772	57.280	60.166	79.404	49.477
50	40.311	42.048	69.354	255.620	120.920
50	46.141	64.413	213.530	101.140	84.149
50	68.411	43.012	85.006	49.366	48.166
50	68.118	45.044	74.726	45.651	62.514
60	78.772	118.000	60.166	194.440	49.477
60	40.311	42.048	69.354	43.932	120.920
60	46.141	64.413	85.563	101.140	94.847
60	68.411	43.012	40.497	49.366	94.048
60	68.118	45.044	74.726	74.733	62.514
70	78.772	118.000	60.166	40.224	49.477
70	40.311	42.048	69.354	50.804	120.920
70	46.141	64.413	68.118	101.140	75.664
70	68.411	43.012	50.040	49.366	74.545
70	68.118	45.044	74.726	69.642	62.514
80	78.772	118.000	60.166	56.886	49.477
80	40.311	42.048	69.354	42.297	120.920
80	46.141	64.413	40.012	101.140	75.664
80	68.411	43.012	72.471	49.366	74.545
80	68.118	45.044	74.726	47.518	62.514
90	78.772	118.000	60.166	55.036	49.477
90	40.311	42.048	69.354	42.297	120.920
90	46.141	64.413	40.012	101.140	75.664

Table 60 (Continued). fiber02a Line Detection L_{total}, Grid = 5 x 5

P	L_{total}				
90	68.411	43.012	49.041	49.366	74.545
90	68.118	45.044	74.726	47.518	62.514
100	78.772	118.000	60.166	42.297	49.477
100	40.311	42.048	69.354	42.297	120.920
100	46.141	64.413	40.012	101.140	75.664
100	68.411	43.012	85.563	49.366	74.545
100	68.118	45.044	74.726	47.518	62.514

Table 61. fiber02a Line Detection L_{total}, Grid = 6 x 6

P	L_{total}					
10	100.720	108.160	64.195	98.433	73.824	72.173
10	57.871	50.220	45.607	59.304	137.180	93.606
10	46.400	51.245	45.541	42.426	57.280	102.240
10	49.820	41.183	79.712	64.351	91.241	44.553
10	43.186	64.351	64.351	44.385	64.195	60.531
10	57.079	74.108	40.804	96.021	115.320	65.924
20	121.020	74.953	47.096	67.417	41.593	49.254
20	57.315	75.180	43.012	59.304	84.172	93.606
20	60.415	104.550	40.025	43.290	46.840	101.240
20	58.600	46.043	48.166	45.651	91.241	47.634
20	84.528	68.264	40.460	46.271	75.000	41.617
20	77.078	68.877	40.804	57.079	45.453	42.012
30	59.540	141.480	47.096	53.141	79.712	47.802
30	60.638	71.169	41.195	59.304	70.831	93.606
30	42.048	57.271	40.025	146.820	65.620	71.694
30	50.249	120.000	67.119	51.420	91.241	95.635
30	51.894	49.041	54.129	93.434	50.249	58.138
30	77.078	51.624	40.804	142.860	57.871	42.012
40	59.540	47.707	47.096	193.020	52.887	47.802
40	262.940	71.169	48.000	59.304	40.460	93.606
40	83.259	79.196	40.025	120.000	40.162	40.162
40	50.249	120.000	84.528	62.225	91.241	65.490
40	51.894	50.249	54.129	108.560	81.320	40.311
40	77.078	51.624	40.804	46.840	77.078	42.012
50	59.540	47.707	47.096	46.065	45.706	47.802
50	129.190	71.169	290.120	59.304	51.264	93.606
50	83.259	84.149	40.025	51.624	77.279	40.162
50	50.249	120.000	100.000	62.225	91.241	117.000
50	51.894	100.210	54.129	108.560	81.320	43.417
50	77.078	51.624	40.804	41.049	49.477	42.012
60	59.540	47.707	47.096	46.065	85.843	47.802
60	129.190	71.169	60.108	59.304	51.264	93.606
60	83.259	79.555	40.025	68.007	132.910	40.162
60	50.249	120.000	46.228	62.225	91.241	86.539
60	51.894	51.624	54.129	108.560	81.320	45.222
60	77.078	51.624	40.804	120.000	60.133	42.012
70	59.540	47.707	47.096	46.065	49.649	47.802
70	129.190	71.169	47.011	59.304	51.264	93.606
70	83.259	79.555	40.025	44.102	41.617	40.162
70	50.249	120.000	45.100	62.225	91.241	158.400
70	51.894	51.624	54.129	108.560	81.320	51.923
70	77.078	51.624	40.804	70.520	60.133	42.012
80	59.540	47.707	47.096	46.065	49.649	47.802

Table 61 (Continued). fiber02a Line Detection L_{total}, Grid = 6 x 6

P	L_{total}					
80	129.19	71.169	101.64	59.304	51.264	93.606
80	83.259	79.555	40.025	88.459	44.922	40.162
80	50.249	120	183.07	62.225	91.241	42.485
80	51.894	51.624	54.129	108.56	81.32	44.204
80	77.078	51.624	40.804	50.329	60.133	42.012
90	59.54	47.707	47.096	46.065	49.649	47.802
90	129.19	71.169	105.12	59.304	51.264	93.606
90	83.259	79.555	40.025	53.413	43.566	40.162
90	50.249	120	42.297	62.225	91.241	120
90	51.894	51.624	54.129	108.56	81.32	44.204
90	77.078	51.624	40.804	57.28	60.133	42.012
100	59.54	47.707	47.096	46.065	49.649	47.802
100	129.19	71.169	76.158	59.304	51.264	93.606
100	83.259	79.555	40.025	53.413	43.566	40.162
100	50.249	120	42.297	62.225	91.241	57.079
100	51.894	51.624	54.129	108.56	81.32	44.204
100	77.078	51.624	40.804	99.247	60.133	42.012

Table 62. fiber02a Line Detection L_{total}, Grid = 8 x 8

P	L_{total}							
10	57.28	60.02	56.29	47.00	95.26	78.26	46.17	48.10
10	97.49	52.24	110.86	86.00	48.37	63.64	94.05	48.37
10	57.28	50.09	72.84	112.27	50.93	137.18	64.35	153.53
10	65.15	85.29	80.01	88.81	57.49	44.10	60.41	121.02
10	41.62	48.00	49.20	49.98	63.00	44.00	100.12	52.70
10	103.12	86.31	51.62	76.56	92.20	44.10	44.10	57.28
10	63.60	64.51	45.00	80.01	93.56	120.70	80.60	50.92
10	40.71	85.00	41.05	98.47	101.14	60.08	81.25	73.17
20	59.14	184.00	64.08	56.04	52.00	43.68	65.80	61.98
20	44.27	86.02	110.86	50.00	53.34	49.50	94.05	62.13
20	60.08	50.09	72.84	112.27	50.93	46.39	111.25	91.00
20	54.12	79.61	51.11	48.70	125.30	42.38	60.41	121.02
20	41.73	46.49	69.12	104.12	45.54	42.01	44.94	60.14
20	103.12	68.01	43.19	56.75	92.20	64.35	64.35	51.00
20	56.14	69.86	69.30	62.64	43.42	61.13	61.21	43.19
20	40.71	45.49	41.05	47.43	40.31	57.28	54.63	44.10
30	59.14	259.98	64.08	56.04	184.00	42.15	65.80	61.98
30	70.26	58.31	110.86	222.17	61.10	45.28	94.05	62.13
30	60.08	50.09	72.84	112.27	50.93	42.01	111.25	74.20
30	96.68	79.61	51.11	160.64	53.71	43.93	60.41	121.02
30	44.82	43.27	80.81	48.09	93.86	42.01	44.94	79.31
30	103.12	46.01	87.30	64.35	92.20	49.58	49.58	51.00
30	111.80	84.85	69.30	62.64	43.42	63.57	51.74	42.43
30	40.71	121.76	41.05	47.43	47.01	63.60	85.70	44.10
40	59.14	64.85	64.08	56.04	221.00	59.06	65.80	61.98
40	70.26	58.31	110.86	98.01	54.56	110.37	94.05	62.13
40	60.08	50.09	72.84	112.27	50.93	42.01	111.25	74.20
40	73.03	79.61	51.11	44.92	131.88	43.93	60.41	121.02
40	44.82	84.17	46.04	68.03	93.86	42.01	44.94	100.90
40	103.12	53.23	42.54	55.61	92.20	48.04	48.04	51.00
40	111.80	100.40	69.30	62.64	43.42	63.57	54.23	60.83
40	40.71	43.32	41.05	47.43	47.01	47.20	85.70	44.10
50	59.14	45.04	64.08	56.04	47.52	68.25	65.80	61.98
50	70.26	58.31	110.86	65.07	54.56	110.37	94.05	62.13
50	60.08	50.09	72.84	112.27	50.93	42.01	111.25	74.20
50	86.00	79.61	51.11	98.88	67.19	43.93	60.41	121.02
50	44.82	84.17	75.43	44.10	93.86	42.01	44.94	43.42
50	103.12	43.17	81.15	52.47	92.20	48.04	48.04	51.00
50	111.80	100.40	69.30	62.64	43.42	63.57	41.05	103.02
50	40.71	43.32	41.05	47.43	47.01	47.20	85.70	44.10
60	59.14	45.04	64.08	56.04	43.42	178.06	65.80	61.98
60	70.26	58.31	110.86	59.01	54.56	110.37	94.05	62.13
60	60.08	50.09	72.84	112.27	50.93	42.01	111.25	74.20

Table 62 (Continued). fiber02a Line Detection L_{total}, Grid = 8 x 8

P	L_{total}							
60	62.10	79.61	51.11	52.20	52.17	43.93	60.41	121.02
60	44.82	84.17	184.00	63.16	93.86	42.01	44.94	43.42
60	103.12	40.61	62.80	100.12	92.20	48.04	48.04	51.00
60	111.80	100.40	69.30	62.64	43.42	63.57	107.04	61.52
60	40.71	43.32	41.05	47.43	47.01	47.20	85.70	44.10
70	59.14	45.04	64.08	56.04	176.71	46.53	65.80	61.98
70	70.26	58.31	110.86	74.11	54.56	110.37	94.05	62.13
70	60.08	50.09	72.84	112.27	50.93	42.01	111.25	74.20
70	76.42	79.61	51.11	52.20	60.17	43.93	60.41	121.02
70	44.82	84.17	45.22	40.11	93.86	42.01	44.94	43.42
70	103.12	50.99	61.85	49.04	92.20	48.04	48.04	51.00
70	111.80	100.40	69.30	62.64	43.42	63.57	41.40	42.20
70	40.71	43.32	41.05	47.43	47.01	47.20	85.70	44.10
80	59.14	45.04	64.08	56.04	176.71	40.31	65.80	61.98
80	70.26	58.31	110.86	47.27	54.56	110.37	94.05	62.13
80	60.08	50.09	72.84	112.27	50.93	42.01	111.25	74.20
80	76.42	79.61	51.11	52.20	43.42	43.93	60.41	121.02
80	44.82	84.17	45.22	87.48	93.86	42.01	44.94	43.42
80	103.12	50.60	58.31	43.17	92.20	48.04	48.04	51.00
80	111.80	100.40	69.30	62.64	43.42	63.57	92.91	143.78
80	40.71	43.32	41.05	47.43	47.01	47.20	85.70	44.10
90	59.14	45.04	64.08	56.04	176.71	40.31	65.80	61.98
90	70.26	58.31	110.86	47.27	54.56	110.37	94.05	62.13
90	60.08	50.09	72.84	112.27	50.93	42.01	111.25	74.20
90	76.42	79.61	51.11	52.20	43.42	43.93	60.41	121.02
90	44.82	84.17	45.22	87.48	93.86	42.01	44.94	43.42
90	103.12	50.60	58.31	43.17	92.20	48.04	48.04	51.00
90	111.80	100.40	69.30	62.64	43.42	63.57	92.91	43.83
90	40.71	43.32	41.05	47.43	47.01	47.20	85.70	44.10
100	59.14	45.04	64.08	56.04	176.71	40.31	65.80	61.98
100	70.26	58.31	110.86	47.27	54.56	110.37	94.05	62.13
100	60.08	50.09	72.84	112.27	50.93	42.01	111.25	74.20
100	76.42	79.61	51.11	52.20	43.42	43.93	60.41	121.02
100	44.82	84.17	45.22	87.48	93.86	42.01	44.94	43.42
100	103.12	50.60	58.31	43.17	92.20	48.04	48.04	51.00
100	111.80	100.40	69.30	62.64	43.42	63.57	92.91	42.49
100	40.71	43.32	41.05	47.43	47.01	47.20	85.70	44.10

Table 63. fiber02a Line Detection L_{total}, Grid = 10 x 10

P	L_{total}									
10	40.03	42.76	58.31	54.82	54.45	55.90	83.55	149.00	116.73	346.55
10	51.25	43.01	48.09	81.30	72.92	42.38	40.01	77.62	45.45	78.03
10	101.97	72.84	59.41	167.59	43.11	50.49	133.70	61.39	46.84	100.90
10	61.56	47.07	69.64	44.05	253.00	47.42	52.15	64.29	139.30	61.52
10	73.06	41.59	45.71	64.50	45.10	41.05	59.03	124.20	120.37	44.94
10	46.82	50.49	42.20	41.77	45.54	47.42	71.45	40.71	98.08	57.28
10	44.01	88.62	91.98	93.81	79.23	65.07	44.05	45.88	42.01	78.23
10	78.23	40.61	40.46	43.68	47.20	50.25	81.58	50.93	110.45	94.13
10	71.18	46.17	129.55	77.16	44.05	86.37	50.70	94.64	60.41	139.09
10	91.14	45.04	42.01	74.69	40.20	68.41	41.01	46.87	56.57	54.59
20	40.03	42.76	58.31	49.20	54.33	67.96	58.52	46.10	116.73	71.70
20	61.52	72.01	46.53	68.26	57.28	42.38	161.07	47.17	45.45	78.03
20	41.20	205.76	57.49	43.42	59.30	50.49	84.87	50.36	42.43	91.66
20	142.64	47.07	80.13	53.85	253.00	73.11	76.16	76.32	59.91	99.25
20	81.32	50.61	41.30	64.50	70.46	221.00	68.82	57.28	120.37	66.53
20	44.05	50.49	54.57	80.81	43.57	40.00	44.28	79.65	57.01	115.00
20	44.01	68.01	47.51	65.77	43.05	121.02	44.05	40.03	59.48	124.20
20	124.20	52.47	106.23	97.64	87.73	49.74	99.02	61.52	110.45	64.35
20	71.18	66.53	129.55	81.49	111.66	222.64	76.32	44.15	71.42	54.01
20	91.14	82.49	42.49	54.45	40.20	56.22	67.90	49.48	67.90	78.77
30	40.03	42.76	58.31	58.55	54.33	99.36	62.48	82.66	116.73	71.70
30	61.52	60.11	46.53	129.34	57.28	42.38	71.45	60.75	45.45	78.03
30	147.80	205.76	57.49	64.50	82.10	50.49	106.38	61.40	42.43	51.42
30	142.64	47.07	80.13	179.51	253.00	73.11	55.58	58.24	51.55	74.69
30	64.29	50.61	79.61	64.50	55.66	149.00	68.82	46.01	120.37	67.27
30	44.05	50.49	54.57	80.81	63.33	149.00	77.82	79.65	57.01	117.80
30	44.01	40.80	47.51	80.06	121.07	45.10	44.05	40.03	59.48	124.20
30	124.20	174.61	166.43	97.64	87.73	49.74	219.23	90.21	110.45	59.91
30	71.18	76.84	129.55	81.49	111.66	222.64	76.32	68.01	40.72	41.44
30	91.14	140.01	42.49	54.45	40.20	56.22	47.00	137.18	67.90	78.77
40	40.03	42.76	58.31	58.55	54.33	55.08	62.48	82.66	116.73	71.70
40	61.52	43.83	46.53	159.77	57.28	42.38	59.94	60.41	45.45	78.03
40	114.13	205.76	57.49	74.22	82.10	50.49	149.00	103.04	42.43	65.97
40	142.64	47.07	80.13	179.51	253.00	73.11	163.37	58.24	51.55	74.69
40	48.08	50.61	150.66	64.50	60.42	149.00	68.82	43.01	120.37	67.27
40	44.05	50.49	54.57	80.81	66.04	148.95	77.82	79.65	57.01	104.71
40	44.01	40.80	47.51	115.52	46.76	45.10	44.05	40.03	59.48	124.20
40	124.20	41.11	166.43	97.64	87.73	49.74	219.23	59.30	110.45	59.91
40	71.18	41.40	129.55	81.49	111.66	222.64	76.32	68.01	144.03	41.44
40	91.14	61.72	42.49	54.45	40.20	56.22	40.46	137.18	67.90	78.77
50	40.03	42.76	58.31	58.55	54.33	90.38	62.48	82.66	116.73	71.70
50	61.52	43.83	46.53	159.77	57.28	42.38	211.12	60.41	45.45	78.03
50	127.28	205.76	57.49	74.67	82.10	50.49	149.00	103.04	42.43	65.97
50	142.64	47.07	80.13	179.51	253.00	73.11	46.67	58.24	51.55	74.69
50	148.17	50.61	40.03	64.50	60.21	149.00	68.82	80.62	120.37	67.27

Table 63 (Continued). fiber02a Line Detection L_{total}, Grid = 10 x 10

P	L_{total}									
50	44.05	50.49	54.57	80.81	76.84	43.83	77.82	79.65	57.01	104.71
50	44.01	40.80	47.51	115.52	66.48	45.10	44.05	40.03	59.48	124.20
50	124.20	51.89	166.43	97.64	87.73	49.74	219.23	59.30	110.45	59.91
50	71.18	42.52	129.55	81.49	111.66	222.64	76.32	68.01	59.30	41.44
50	91.14	61.72	42.49	54.45	40.20	56.22	57.14	137.18	67.90	78.77
60	40.03	42.76	58.31	58.55	54.33	145.58	62.48	82.66	116.73	71.70
60	61.52	43.83	46.53	159.77	57.28	42.38	93.81	60.41	45.45	78.03
60	127.28	205.76	57.49	74.67	82.10	50.49	149.00	103.04	42.43	65.97
60	142.64	47.07	80.13	179.51	253.00	73.11	46.67	58.24	51.55	74.69
60	101.12	50.61	40.03	64.50	60.21	149.00	68.82	80.62	120.37	67.27
60	44.05	50.49	54.57	80.81	68.00	43.83	77.82	79.65	57.01	104.71
60	44.01	40.80	47.51	115.52	134.83	45.10	44.05	40.03	59.48	124.20
60	124.20	51.89	166.43	97.64	87.73	49.74	219.23	59.30	110.45	59.91
60	71.18	42.52	129.55	81.49	111.66	222.64	76.32	68.01	59.30	41.44
60	91.14	61.72	42.49	54.45	40.20	56.22	57.14	137.18	67.90	78.77
70	40.03	42.76	58.31	58.55	54.33	77.67	62.48	82.66	116.73	71.70
70	61.52	43.83	46.53	159.77	57.28	42.38	43.11	60.41	45.45	78.03
70	127.28	205.76	57.49	74.67	82.10	50.49	149.00	103.04	42.43	65.97
70	142.64	47.07	80.13	179.51	253.00	73.11	46.67	58.24	51.55	74.69
70	101.12	50.61	40.03	64.50	60.21	149.00	68.82	80.62	120.37	67.27
70	44.05	50.49	54.57	80.81	41.77	43.83	77.82	79.65	57.01	104.71
70	44.01	40.80	47.51	115.52	49.41	45.10	44.05	40.03	59.48	124.20
70	124.20	51.89	166.43	97.64	87.73	49.74	219.23	59.30	110.45	59.91
70	71.18	42.52	129.55	81.49	111.66	222.64	76.32	68.01	59.30	41.44
70	91.14	61.72	42.49	54.45	40.20	56.22	57.14	137.18	67.90	78.77
80	40.03	42.76	58.31	58.55	54.33	77.67	62.48	82.66	116.73	71.70
80	61.52	43.83	46.53	159.77	57.28	42.38	43.11	60.41	45.45	78.03
80	127.28	205.76	57.49	74.67	82.10	50.49	149.00	103.04	42.43	65.97
80	142.64	47.07	80.13	179.51	253.00	73.11	46.67	58.24	51.55	74.69
80	101.12	50.61	40.03	64.50	60.21	149.00	68.82	80.62	120.37	67.27
80	44.05	50.49	54.57	80.81	41.77	43.83	77.82	79.65	57.01	104.71
80	44.01	40.80	47.51	115.52	44.05	45.10	44.05	40.03	59.48	124.20
80	124.20	51.89	166.43	97.64	87.73	49.74	219.23	59.30	110.45	59.91
80	71.18	42.52	129.55	81.49	111.66	222.64	76.32	68.01	59.30	41.44
80	91.14	61.72	42.49	54.45	40.20	56.22	57.14	137.18	67.90	78.77
90	40.03	42.76	58.31	58.55	54.33	77.67	62.48	82.66	116.73	71.70
90	61.52	43.83	46.53	159.77	57.28	42.38	43.11	60.41	45.45	78.03
90	127.28	205.76	57.49	74.67	82.10	50.49	149.00	103.04	42.43	65.97
90	142.64	47.07	80.13	179.51	253.00	73.11	46.67	58.24	51.55	74.69
90	101.12	50.61	40.03	64.50	60.21	149.00	68.82	80.62	120.37	67.27
90	44.05	50.49	54.57	80.81	41.77	43.83	77.82	79.65	57.01	104.71
90	44.01	40.80	47.51	115.52	44.05	45.10	44.05	40.03	59.48	124.20
90	124.20	51.89	166.43	97.64	87.73	49.74	219.23	59.30	110.45	59.91
90	71.18	42.52	129.55	81.49	111.66	222.64	76.32	68.01	59.30	41.44
90	91.14	61.72	42.49	54.45	40.20	56.22	57.14	137.18	67.90	78.77
100	40.03	42.76	58.31	58.55	54.33	77.67	62.48	82.66	116.73	71.70
100	61.52	43.83	46.53	159.77	57.28	42.38	43.11	60.41	45.45	78.03
100	127.28	205.76	57.49	74.67	82.10	50.49	149.00	103.04	42.43	65.97

Table 63 (Continued). fiber02a Line Detection L_{total}, Grid = 10 x 10

P	L_{total}									
100	142.64	47.07	80.13	179.51	253.00	73.11	46.67	58.24	51.55	74.69
100	101.12	50.61	40.03	64.50	60.21	149.00	68.82	80.62	120.37	67.27
100	44.05	50.49	54.57	80.81	41.77	43.83	77.82	79.65	57.01	104.71
100	44.01	40.80	47.51	115.52	44.05	45.10	44.05	40.03	59.48	124.20
100	124.20	51.89	166.43	97.64	87.73	49.74	219.23	59.30	110.45	59.91
100	71.18	42.52	129.55	81.49	111.66	222.64	76.32	68.01	59.30	41.44
100	91.14	61.72	42.49	54.45	40.20	56.22	57.14	137.18	67.90	78.77

Table 64. fiber02a Line Detection t_{total}, Grid = 1 x 1

P	t_{total}
10	0.421
20	0.560
30	0.710
40	0.856
50	1.218
60	1.165
70	1.295
80	1.438
90	1.576
100	1.727

Table 65. fiber02a Line Detection t_{total}, Grid = 2 x 2

P	t_{total}	
10	0.200	0.152
10	0.154	0.154
20	0.293	0.258
20	0.263	0.253
30	0.381	0.338
30	0.339	0.361
40	0.460	0.430
40	0.421	0.428
50	0.580	0.519
50	0.521	0.550
60	0.628	0.596
60	0.598	0.600
70	0.714	0.679
70	0.678	0.676
80	0.797	0.763
80	0.852	0.777
90	0.926	0.881
90	0.966	0.882
100	0.994	0.939
100	1.026	0.940

Table 66. fiber02a Line Detection t_{total}, Grid = 4 x 4

P	t_{total}			
10	0.130	0.082	0.082	0.087
10	0.086	0.084	0.090	0.087
10	0.083	0.086	0.083	0.084
10	0.082	0.081	0.088	0.082
20	0.199	0.167	0.160	0.157
20	0.146	0.151	0.164	0.164
20	0.189	0.165	0.179	0.165
20	0.168	0.161	0.146	0.197
30	0.246	0.200	0.212	0.203
30	0.213	0.206	0.205	0.203
30	0.244	0.226	0.228	0.183
30	0.210	0.220	0.125	0.209
40	0.306	0.254	0.286	0.187
40	0.237	0.252	0.219	0.253
40	0.217	0.254	0.227	0.175
40	0.265	0.261	0.121	0.263
50	0.375	0.323	0.372	0.220
50	0.418	0.400	0.232	0.334
50	0.235	0.336	0.257	0.196
50	0.359	0.322	0.129	0.287
60	0.362	0.323	0.372	0.192
60	0.231	0.369	0.198	0.366
60	0.202	0.369	0.227	0.170
60	0.350	0.361	0.118	0.274
70	0.352	0.322	0.423	0.187
70	0.235	0.415	0.199	0.359
70	0.203	0.420	0.221	0.170
70	0.338	0.358	0.118	0.272
80	0.359	0.332	0.485	0.193
80	0.235	0.479	0.203	0.361
80	0.207	0.546	0.234	0.173
80	0.347	0.359	0.115	0.275
90	0.366	0.331	0.558	0.198
90	0.246	0.559	0.218	0.362
90	0.212	0.613	0.223	0.184
90	0.352	0.393	0.123	0.280
100	0.380	0.320	0.598	0.192
100	0.229	0.537	0.200	0.372
100	0.211	0.711	0.234	0.169
100	0.353	0.347	0.116	0.273

Table 67. fiber02a Line Detection t_{total}, Grid = 5 x 5

P	t_{total}				
10	0.117	0.069	0.073	0.108	0.073
10	0.070	0.074	0.075	0.073	0.075
10	0.093	0.078	0.074	0.087	0.094
10	0.075	0.076	0.070	0.060	0.079
10	0.083	0.072	0.078	0.084	0.084
20	0.184	0.130	0.118	0.124	0.134
20	0.125	0.126	0.124	0.136	0.155
20	0.079	0.142	0.143	0.153	0.137
20	0.132	0.145	0.139	0.065	0.145
20	0.133	0.130	0.093	0.130	0.127
30	0.230	0.181	0.117	0.183	0.188
30	0.200	0.231	0.184	0.179	0.186
30	0.073	0.231	0.199	0.179	0.185
30	0.124	0.185	0.180	0.067	0.180
30	0.186	0.155	0.089	0.177	0.184
40	0.230	0.224	0.108	0.230	0.184
40	0.175	0.256	0.224	0.225	0.229
40	0.073	0.225	0.225	0.194	0.223
40	0.122	0.225	0.224	0.058	0.239
40	0.224	0.140	0.085	0.226	0.198
50	0.227	0.289	0.116	0.283	0.186
50	0.177	0.347	0.251	0.307	0.259
50	0.075	0.234	0.280	0.194	0.291
50	0.125	0.265	0.282	0.061	0.308
50	0.228	0.154	0.104	0.314	0.208
60	0.217	0.335	0.105	0.327	0.180
60	0.180	0.240	0.223	0.325	0.218
60	0.074	0.223	0.319	0.188	0.326
60	0.120	0.254	0.321	0.052	0.341
60	0.220	0.137	0.084	0.323	0.195
70	0.212	0.334	0.103	0.394	0.181
70	0.177	0.243	0.225	0.371	0.219
70	0.074	0.221	0.372	0.190	0.370
70	0.121	0.256	0.374	0.053	0.383
70	0.235	0.146	0.088	0.392	0.199
80	0.218	0.332	0.106	0.444	0.180
80	0.176	0.242	0.234	0.412	0.225
80	0.072	0.229	0.406	0.202	0.363
80	0.122	0.258	0.467	0.056	0.382
80	0.223	0.137	0.084	0.421	0.196
90	0.223	0.331	0.113	0.519	0.189
90	0.187	0.253	0.236	0.444	0.225
90	0.076	0.239	0.417	0.196	0.380

Table 67 (Continued). fiber02a Line Detection t_{total}, Grid = 5 x 5

P	t_{total}				
90	0.122	0.270	0.528	0.056	0.392
90	0.231	0.142	0.104	0.426	0.209
100	0.218	0.328	0.104	0.542	0.179
100	0.178	0.245	0.230	0.415	0.223
100	0.077	0.226	0.405	0.194	0.363
100	0.121	0.257	0.558	0.054	0.381
100	0.219	0.138	0.084	0.414	0.196

Table 68. fiber02a Line Detection t_{total}, Grid = 6 x 6

P	t_{total}					
10	0.124	0.071	0.072	0.067	0.072	0.072
10	0.072	0.065	0.075	0.051	0.068	0.069
10	0.066	0.068	0.067	0.066	0.081	0.067
10	0.064	0.077	0.067	0.074	0.053	0.076
10	0.065	0.071	0.066	0.153	0.072	0.081
10	0.066	0.070	0.064	0.069	0.067	0.066
20	0.156	0.118	0.121	0.116	0.126	0.113
20	0.121	0.120	0.125	0.051	0.118	0.068
20	0.129	0.140	0.125	0.127	0.133	0.132
20	0.142	0.123	0.132	0.121	0.063	0.127
20	0.138	0.144	0.114	0.201	0.119	0.114
20	0.110	0.113	0.066	0.117	0.118	0.106
30	0.236	0.168	0.132	0.181	0.184	0.176
30	0.185	0.132	0.203	0.056	0.189	0.076
30	0.181	0.190	0.124	0.171	0.197	0.185
30	0.128	0.218	0.199	0.191	0.073	0.170
30	0.120	0.156	0.162	0.269	0.185	0.167
30	0.113	0.179	0.073	0.205	0.182	0.101
40	0.193	0.196	0.112	0.206	0.280	0.152
40	0.203	0.132	0.231	0.067	0.235	0.074
40	0.202	0.212	0.132	0.274	0.223	0.181
40	0.125	0.224	0.213	0.202	0.055	0.213
40	0.121	0.205	0.148	0.263	0.173	0.206
40	0.113	0.155	0.067	0.206	0.213	0.102
50	0.208	0.213	0.110	0.234	0.330	0.167
50	0.306	0.127	0.319	0.049	0.246	0.073
50	0.205	0.276	0.124	0.345	0.270	0.196
50	0.166	0.268	0.288	0.208	0.082	0.297
50	0.127	0.265	0.151	0.278	0.180	0.335
50	0.114	0.157	0.070	0.272	0.288	0.121
60	0.183	0.194	0.106	0.227	0.353	0.152
60	0.285	0.129	0.342	0.048	0.233	0.066
60	0.199	0.287	0.115	0.352	0.323	0.266
60	0.142	0.205	0.318	0.204	0.053	0.297
60	0.126	0.309	0.147	0.242	0.171	0.400
60	0.112	0.157	0.231	0.338	0.261	0.097
70	0.180	0.206	0.123	0.235	0.364	0.151
70	0.278	0.127	0.396	0.049	0.230	0.068
70	0.196	0.267	0.119	0.399	0.361	0.171
70	0.123	0.214	0.353	0.203	0.059	0.346
70	0.122	0.298	0.147	0.241	0.169	0.453
70	0.113	0.150	0.063	0.394	0.268	0.101
80	0.187	0.195	0.111	0.231	0.394	0.150

Table 68 (Continued). fiber02a Line Detection t_{total}, Grid = 6 x 6

P	t_{total}					
80	0.286	0.126	0.435	0.048	0.239	0.066
80	0.199	0.272	0.118	0.467	0.411	0.170
80	0.125	0.208	0.402	0.201	0.053	0.389
80	0.120	0.295	0.147	0.248	0.172	0.560
80	0.111	0.151	0.063	0.445	0.274	0.100
90	0.182	0.212	0.111	0.236	0.374	0.152
90	0.295	0.139	0.490	0.050	0.249	0.068
90	0.204	0.279	0.118	0.491	0.424	0.171
90	0.128	0.210	0.518	0.205	0.055	0.492
90	0.124	0.300	0.147	0.246	0.175	0.492
90	0.118	0.160	0.066	0.512	0.276	0.102
100	0.182	0.192	0.107	0.228	0.379	0.177
100	0.303	0.130	0.528	0.050	0.24	0.069
100	0.205	0.282	0.119	0.494	0.424	0.175
100	0.129	0.216	0.537	0.206	0.053	0.565
100	0.127	0.306	0.153	0.257	0.175	0.490
100	0.119	0.157	0.063	0.565	0.287	0.102

Table 69. fiber02a Line Detection t_{total}, Grid = 8 x 8

P	t_{total}							
10	0.10	0.07	0.07	0.06	0.06	0.06	0.06	0.06
10	0.06	0.07	0.06	0.09	0.06	0.06	0.04	0.06
10	0.06	0.04	0.06	0.04	0.05	0.06	0.06	0.06
10	0.06	0.06	0.06	0.06	0.06	0.06	0.05	0.04
10	0.06	0.06	0.06	0.06	0.07	0.06	0.06	0.06
10	0.06	0.06	0.07	0.07	0.07	0.06	0.03	0.06
10	0.06	0.06	0.06	0.06	0.06	0.06	0.06	0.06
10	0.04	0.06	0.05	0.06	0.06	0.06	0.06	0.07
20	0.12	0.15	0.07	0.09	0.11	0.11	0.10	0.08
20	0.10	0.10	0.06	0.15	0.10	0.10	0.03	0.09
20	0.10	0.04	0.07	0.04	0.05	0.10	0.11	0.10
20	0.10	0.09	0.09	0.10	0.11	0.10	0.05	0.04
20	0.11	0.10	0.10	0.10	0.10	0.08	0.11	0.10
20	0.06	0.10	0.11	0.10	0.06	0.10	0.02	0.10
20	0.10	0.10	0.07	0.10	0.07	0.10	0.10	0.11
20	0.04	0.10	0.05	0.07	0.11	0.10	0.11	0.10
30	0.11	0.19	0.07	0.09	0.19	0.14	0.09	0.08
30	0.10	0.12	0.06	0.22	0.19	0.18	0.04	0.12
30	0.11	0.04	0.07	0.05	0.05	0.15	0.10	0.14
30	0.17	0.09	0.10	0.15	0.15	0.12	0.05	0.04
30	0.12	0.14	0.15	0.14	0.14	0.08	0.12	0.15
30	0.06	0.16	0.15	0.14	0.06	0.15	0.02	0.10
30	0.22	0.14	0.08	0.11	0.09	0.15	0.18	0.16
30	0.05	0.17	0.05	0.08	0.16	0.16	0.17	0.10
40	0.11	0.24	0.08	0.09	0.23	0.19	0.09	0.09
40	0.11	0.12	0.06	0.25	0.18	0.18	0.04	0.12
40	0.11	0.05	0.08	0.05	0.06	0.17	0.11	0.14
40	0.19	0.09	0.10	0.20	0.19	0.12	0.05	0.04
40	0.13	0.17	0.19	0.18	0.14	0.08	0.11	0.18
40	0.06	0.18	0.19	0.18	0.06	0.18	0.03	0.10
40	0.19	0.17	0.07	0.10	0.07	0.13	0.20	0.18
40	0.04	0.18	0.05	0.07	0.14	0.16	0.15	0.10
50	0.12	0.28	0.07	0.10	0.30	0.23	0.12	0.09
50	0.11	0.12	0.06	0.28	0.16	0.16	0.03	0.10
50	0.10	0.04	0.06	0.04	0.05	0.15	0.10	0.13
50	0.26	0.09	0.09	0.23	0.27	0.12	0.05	0.06
50	0.14	0.17	0.24	0.23	0.15	0.08	0.11	0.22
50	0.06	0.26	0.24	0.23	0.06	0.18	0.03	0.10
50	0.20	0.16	0.07	0.10	0.07	0.15	0.25	0.25
50	0.04	0.19	0.05	0.07	0.14	0.17	0.16	0.10
60	0.10	0.25	0.06	0.09	0.30	0.27	0.09	0.08
60	0.11	0.12	0.05	0.49	0.17	0.16	0.03	0.09
60	0.10	0.04	0.06	0.04	0.05	0.15	0.10	0.12

Table 69 (Continued). fiber02a Line Detection t_{total}, Grid = 8 x 8

P	t_{total}							
60	0.31	0.09	0.09	0.24	0.28	0.12	0.05	0.04
60	0.12	0.16	0.31	0.26	0.14	0.08	0.11	0.20
60	0.06	0.29	0.28	0.27	0.06	0.18	0.02	0.10
60	0.18	0.17	0.07	0.10	0.07	0.14	0.28	0.26
60	0.04	0.17	0.05	0.07	0.13	0.15	0.14	0.09
70	0.10	0.26	0.07	0.09	0.34	0.31	0.09	0.08
70	0.10	0.12	0.06	0.34	0.16	0.15	0.03	0.09
70	0.10	0.03	0.06	0.04	0.05	0.14	0.10	0.12
70	0.34	0.08	0.08	0.23	0.32	0.11	0.05	0.04
70	0.12	0.16	0.35	0.31	0.14	0.08	0.11	0.21
70	0.06	0.33	0.32	0.31	0.06	0.18	0.02	0.10
70	0.18	0.16	0.07	0.10	0.06	0.13	0.32	0.30
70	0.04	0.17	0.05	0.07	0.13	0.15	0.15	0.09
80	0.10	0.25	0.07	0.09	0.34	0.32	0.09	0.08
80	0.11	0.12	0.06	0.37	0.17	0.16	0.03	0.09
80	0.11	0.03	0.06	0.04	0.05	0.14	0.10	0.12
80	0.36	0.08	0.09	0.24	0.34	0.11	0.05	0.04
80	0.12	0.16	0.34	0.33	0.14	0.08	0.11	0.20
80	0.06	0.33	0.34	0.33	0.06	0.18	0.03	0.10
80	0.17	0.16	0.07	0.09	0.06	0.13	0.36	0.34
80	0.04	0.17	0.05	0.07	0.13	0.15	0.14	0.09
90	0.10	0.25	0.07	0.09	0.35	0.33	0.09	0.09
90	0.11	0.12	0.06	0.38	0.17	0.16	0.03	0.10
90	0.11	0.03	0.06	0.04	0.05	0.15	0.10	0.12
90	0.37	0.09	0.09	0.25	0.37	0.12	0.05	0.04
90	0.13	0.18	0.35	0.35	0.15	0.08	0.11	0.20
90	0.06	0.36	0.36	0.35	0.06	0.19	0.03	0.11
90	0.19	0.16	0.07	0.10	0.07	0.13	0.40	0.41
90	0.04	0.18	0.05	0.07	0.14	0.17	0.15	0.09
100	0.11	0.25	0.07	0.09	0.36	0.33	0.09	0.08
100	0.11	0.12	0.06	0.37	0.16	0.16	0.03	0.11
100	0.11	0.04	0.06	0.04	0.05	0.15	0.10	0.12
100	0.37	0.09	0.09	0.24	0.35	0.12	0.05	0.04
100	0.13	0.18	0.35	0.36	0.15	0.08	0.11	0.21
100	0.06	0.35	0.36	0.35	0.06	0.18	0.02	0.10
100	0.18	0.17	0.07	0.10	0.06	0.13	0.41	0.43
100	0.04	0.19	0.05	0.07	0.13	0.16	0.15	0.10

Table 70. fiber02a Line Detection t_{total}, Grid = 10 x 10

P	t_{total}									
10	0.05	0.06	0.06	0.06	0.06	0.06	0.06	0.10	0.05	0.06
10	0.10	0.05	0.06	0.12	0.06	0.06	0.05	0.06	0.04	0.06
10	0.05	0.05	0.06	0.06	0.06	0.05	0.06	0.06	0.05	0.06
10	0.06	0.03	0.05	0.06	0.05	0.06	0.05	0.06	0.07	0.09
10	0.05	0.06	0.06	0.05	0.05	0.06	0.06	0.06	0.06	0.05
10	0.05	0.04	0.06	0.07	0.05	0.07	0.05	0.06	0.06	0.06
10	0.05	0.05	0.06	0.06	0.06	0.05	0.05	0.05	0.08	0.08
10	0.03	0.06	0.06	0.06	0.06	0.05	0.06	0.06	0.06	0.06
10	0.05	0.06	0.06	0.06	0.06	0.06	0.06	0.06	0.05	0.07
10	0.05	0.07	0.06	0.07	0.05	0.06	0.06	0.06	0.06	0.06
20	0.05	0.06	0.06	0.10	0.09	0.10	0.10	0.16	0.06	0.08
20	0.13	0.10	0.09	0.18	0.10	0.06	0.10	0.16	0.04	0.06
20	0.10	0.07	0.08	0.17	0.10	0.05	0.11	0.10	0.08	0.10
20	0.07	0.03	0.07	0.10	0.05	0.08	0.10	0.11	0.10	0.13
20	0.10	0.10	0.10	0.06	0.10	0.10	0.11	0.10	0.06	0.10
20	0.09	0.05	0.07	0.10	0.11	0.10	0.11	0.08	0.09	0.11
20	0.05	0.10	0.09	0.10	0.11	0.10	0.03	0.08	0.09	0.08
20	0.04	0.10	0.10	0.09	0.07	0.10	0.10	0.16	0.06	0.10
20	0.05	0.11	0.06	0.08	0.09	0.22	0.06	0.10	0.10	0.10
20	0.04	0.18	0.07	0.07	0.05	0.10	0.10	0.10	0.09	0.07
30	0.06	0.06	0.06	0.14	0.08	0.14	0.11	0.20	0.07	0.08
30	0.14	0.16	0.09	0.19	0.12	0.06	0.14	0.20	0.04	0.06
30	0.13	0.07	0.08	0.20	0.14	0.05	0.14	0.14	0.08	0.14
30	0.06	0.03	0.08	0.13	0.04	0.08	0.14	0.14	0.13	0.16
30	0.14	0.12	0.14	0.05	0.13	0.19	0.11	0.14	0.06	0.12
30	0.08	0.04	0.06	0.10	0.14	0.18	0.11	0.06	0.09	0.14
30	0.05	0.13	0.09	0.13	0.14	0.10	0.03	0.08	0.09	0.08
30	0.04	0.14	0.11	0.10	0.07	0.09	0.10	0.19	0.06	0.11
30	0.05	0.14	0.06	0.08	0.09	0.15	0.06	0.11	0.14	0.11
30	0.03	0.20	0.09	0.06	0.05	0.10	0.15	0.12	0.08	0.07
40	0.05	0.06	0.06	0.13	0.09	0.17	0.10	0.20	0.06	0.08
40	0.13	0.16	0.11	0.26	0.11	0.07	0.21	0.24	0.04	0.06
40	0.18	0.08	0.08	0.25	0.15	0.05	0.25	0.21	0.09	0.20
40	0.08	0.03	0.09	0.17	0.06	0.09	0.20	0.15	0.14	0.18
40	0.20	0.12	0.21	0.05	0.21	0.25	0.12	0.19	0.07	0.13
40	0.10	0.05	0.07	0.11	0.20	0.25	0.13	0.07	0.10	0.17
40	0.06	0.15	0.10	0.19	0.19	0.11	0.04	0.08	0.10	0.10
40	0.04	0.21	0.11	0.09	0.07	0.11	0.11	0.25	0.06	0.12
40	0.05	0.22	0.08	0.09	0.09	0.16	0.08	0.15	0.18	0.13
40	0.04	0.31	0.07	0.07	0.05	0.11	0.36	0.14	0.12	0.09
50	0.05	0.06	0.06	0.13	0.08	0.22	0.11	0.23	0.06	0.08
50	0.11	0.16	0.09	0.20	0.10	0.06	0.21	0.19	0.04	0.05
50	0.20	0.07	0.07	0.25	0.14	0.05	0.19	0.18	0.08	0.15
50	0.06	0.03	0.06	0.14	0.04	0.08	0.21	0.13	0.12	0.15
50	0.21	0.12	0.20	0.07	0.20	0.20	0.11	0.20	0.06	0.12

Table 70 (Continued). fiber02a Line Detection t_{total}, Grid = 10 x 10

P	t_{total}									
50	0.10	0.04	0.06	0.10	0.21	0.24	0.10	0.06	0.09	0.23
50	0.06	0.13	0.08	0.18	0.21	0.10	0.03	0.08	0.08	0.08
50	0.03	0.20	0.10	0.08	0.06	0.09	0.11	0.22	0.05	0.11
50	0.05	0.18	0.05	0.07	0.09	0.13	0.06	0.11	0.18	0.10
50	0.03	0.21	0.07	0.06	0.04	0.10	0.26	0.10	0.08	0.06
60	0.05	0.05	0.05	0.13	0.08	0.25	0.10	0.17	0.05	0.07
60	0.11	0.16	0.09	0.21	0.10	0.06	0.25	0.19	0.04	0.05
60	0.19	0.07	0.07	0.25	0.14	0.05	0.18	0.18	0.08	0.15
60	0.06	0.03	0.07	0.14	0.04	0.07	0.20	0.13	0.12	0.15
60	0.26	0.11	0.19	0.05	0.19	0.20	0.11	0.19	0.06	0.12
60	0.08	0.04	0.07	0.10	0.31	0.24	0.11	0.06	0.08	0.16
60	0.05	0.13	0.09	0.17	0.26	0.10	0.03	0.08	0.08	0.08
60	0.03	0.20	0.10	0.09	0.06	0.09	0.10	0.21	0.05	0.11
60	0.05	0.18	0.06	0.08	0.09	0.13	0.06	0.10	0.19	0.11
60	0.04	0.21	0.07	0.06	0.04	0.09	0.25	0.11	0.08	0.07
70	0.05	0.05	0.05	0.13	0.08	0.28	0.10	0.19	0.05	0.07
70	0.11	0.16	0.09	0.21	0.10	0.06	0.29	0.19	0.04	0.05
70	0.20	0.07	0.08	0.26	0.14	0.05	0.19	0.18	0.09	0.18
70	0.07	0.03	0.07	0.15	0.04	0.07	0.21	0.13	0.12	0.15
70	0.27	0.11	0.19	0.05	0.19	0.20	0.11	0.20	0.05	0.11
70	0.08	0.04	0.06	0.10	0.30	0.25	0.10	0.06	0.08	0.16
70	0.05	0.13	0.08	0.17	0.29	0.10	0.03	0.08	0.08	0.08
70	0.04	0.20	0.10	0.08	0.06	0.10	0.10	0.22	0.05	0.11
70	0.05	0.18	0.06	0.08	0.10	0.13	0.06	0.11	0.18	0.10
70	0.03	0.21	0.06	0.06	0.04	0.10	0.26	0.11	0.08	0.06
80	0.05	0.05	0.05	0.12	0.08	0.27	0.10	0.17	0.05	0.07
80	0.11	0.16	0.09	0.21	0.10	0.06	0.29	0.18	0.03	0.05
80	0.19	0.07	0.07	0.25	0.14	0.05	0.18	0.18	0.08	0.15
80	0.06	0.03	0.07	0.14	0.04	0.08	0.20	0.13	0.12	0.15
80	0.27	0.11	0.19	0.05	0.19	0.20	0.11	0.19	0.06	0.12
80	0.08	0.04	0.06	0.10	0.31	0.24	0.10	0.06	0.08	0.16
80	0.05	0.13	0.08	0.17	0.31	0.10	0.03	0.08	0.09	0.08
80	0.03	0.19	0.10	0.08	0.06	0.09	0.10	0.22	0.06	0.11
80	0.05	0.18	0.05	0.08	0.09	0.13	0.06	0.11	0.18	0.10
80	0.03	0.20	0.07	0.06	0.04	0.10	0.26	0.11	0.08	0.06
90	0.05	0.05	0.05	0.13	0.08	0.27	0.10	0.17	0.05	0.07
90	0.11	0.16	0.09	0.21	0.10	0.06	0.29	0.19	0.03	0.05
90	0.20	0.07	0.08	0.25	0.14	0.05	0.19	0.18	0.08	0.15
90	0.06	0.03	0.07	0.14	0.04	0.07	0.21	0.13	0.12	0.15
90	0.28	0.11	0.19	0.05	0.19	0.20	0.10	0.19	0.05	0.11
90	0.08	0.04	0.06	0.10	0.31	0.24	0.10	0.06	0.08	0.16
90	0.05	0.13	0.08	0.17	0.31	0.10	0.03	0.08	0.08	0.08
90	0.03	0.20	0.10	0.08	0.06	0.09	0.10	0.21	0.06	0.11
90	0.05	0.18	0.05	0.08	0.09	0.13	0.06	0.11	0.18	0.10
90	0.03	0.21	0.07	0.06	0.04	0.10	0.27	0.11	0.08	0.06
100	0.05	0.06	0.05	0.13	0.08	0.27	0.11	0.17	0.05	0.07
100	0.12	0.16	0.09	0.21	0.10	0.06	0.30	0.19	0.04	0.05
100	0.19	0.07	0.08	0.26	0.14	0.05	0.19	0.18	0.08	0.16

Table 70 (Continued). fiber02a Line Detection t_{total}, Grid = 10 x 10

P	t_{total}									
100	0.06	0.03	0.07	0.14	0.04	0.08	0.22	0.14	0.12	0.15
100	0.27	0.11	0.20	0.05	0.19	0.20	0.11	0.19	0.06	0.11
100	0.08	0.04	0.06	0.10	0.31	0.24	0.10	0.06	0.09	0.16
100	0.05	0.13	0.08	0.18	0.31	0.10	0.03	0.08	0.08	0.08
100	0.03	0.20	0.10	0.08	0.06	0.09	0.10	0.22	0.05	0.11
100	0.05	0.18	0.05	0.08	0.09	0.13	0.06	0.11	0.18	0.11
100	0.03	0.21	0.07	0.06	0.04	0.10	0.26	0.11	0.08	0.06

Appendix C: Matlab™ Codes

```
function preprocess_avg

%Get Image
RGB = imread('0013-2-10a.bmp');

I  = rgb2gray(RGB);

n = 256;

for i = 3:2:11

    tic

    dim = i;

    H = fspecial('average',dim);

    B = imfilter(I,H,'same','conv');

    D = I - B;

    toc

    t = toc;

    [count, x] = imhist(D,n);
    hist_data = [x, count];
    hist_data = hist_data';

    run_number = i;

    run_string = num2str( run_number );
    dim_string = num2str( dim );



        figure(1); colormap(gray);
        imagesc(B);
        title(strcat('Average Filter, Std Dev = ',dim_string));

%            picname1 = strcat( 'data/Preprocessing/Average/0013-2-
9a/filter_run_', run_string);
%            saveas(gcf, picname1, 'fig' );
%            saveas(gcf, picname1, 'png');


        figure(2); colormap(gray);
```

```
        imagesc(D);
        title(strcat('Preprocessing Difference, Avg Dim =
',dim_string));

%            picname2 = strcat( 'data/Preprocessing/Average/0013-2-
9a/diff_run_', run_string);
%            saveas(gcf, picname2, 'fig' );
%            saveas(gcf, picname2, 'png');

        figure(3);
        imhist(D,n);

       title(strcat('Noise Histogram, Average Dist = ',dim_string));

            picname3 = strcat( 'data/Preprocessing/Average/0013-2-
10a/diff_run_', run_string, '_hist');
            saveas(gcf, picname3, 'fig' );
            saveas(gcf, picname3, 'png');

            fid = fopen(strcat('data/Preprocessing/Average/0013-2-
10a/diff_run_', run_string, '_hist.txt'), 'wt');
            fprintf(fid, '%6d %12d\n', hist_data );
            fclose(fid)

            fid = fopen(strcat('data/Preprocessing/Average/0013-2-
10a/diff_run_', run_string, '_time.txt'), 'wt');
            fprintf(fid, '%6.9d ', t);
            fclose(fid)

end
```

```
function preprocess_median

%Get Image
RGB = imread('fiber10a.bmp');

I  = rgb2gray(RGB);

n = 256;

for i = 3:2:11

    tic

    dim = i;

    B = medfilt2(I,[dim dim]);

    D = I - B;



    toc

    t = toc;

    [count, x] = imhist(D,n);
    hist_data = [x, count];
    hist_data = hist_data';

    run_number = i;

    run_string = num2str( run_number );
    dim_string = num2str( dim );



        figure(1); colormap(gray);
        imagesc(B);
        title(strcat('Median Filter, Dim = ',dim_string));

%            picname1 = strcat( 'data/Preprocessing/Median/0013-2-
12a/filter_run_', run_string);
%            saveas(gcf, picname1, 'fig' );
%            saveas(gcf, picname1, 'png');


        figure(2); colormap(gray);
        imagesc(D);
        title(strcat('Preprocessing Difference, Median, Dim =
',dim_string));
```

```
%            picname2 = strcat( 'data/Preprocessing/Median/0013-2-
12a/diff_run_', run_string);
%            saveas(gcf, picname2, 'fig' );
%            saveas(gcf, picname2, 'png');

        figure(3);
        imhist(D,n);

       title(strcat('Noise Histogram, Median Dim = ',dim_string));

            picname3 = strcat(
'data/Preprocessing/Median/fiber10a/diff_run_', run_string, '_hist');
            saveas(gcf, picname3, 'fig' );
            saveas(gcf, picname3, 'png');

            fid =
fopen(strcat('data/Preprocessing/Median/fiber10a/diff_run_',
run_string, '_hist.txt'), 'wt');
            fprintf(fid, '%6d %12d\n', hist_data );
            fclose(fid)

            fid =
fopen(strcat('data/Preprocessing/Median/fiber10a/diff_run_',
run_string, '_time.txt'), 'wt');
            fprintf(fid, '%6.9d ', t);
            fclose(fid)

end
```

```
function preprocess_gauss

%Get Image
[RGB,map1] = imread('fiber10a.bmp');

I  = rgb2gray(RGB);

n = 256;

for i = 1:1:25

    tic

    sigma = 0.25*i;

    H = fspecial('gaussian',[5 5],sigma);

    B = imfilter(I,H,'same','conv');

    D = B - I;

    toc

    t = toc;

    [count, x] = imhist(D,n);
    hist_data = [x, count];
    hist_data = hist_data';

    run_number = i;

    run_string = num2str( run_number );
    sigma_string = num2str( sigma );



        figure(1); colormap(gray);
        imagesc(B);
%        title(strcat('Gaussian Filter, Sigma = ',sigma_string));

%            picname1 = strcat(
'data/Preprocessing/Gaussian/fiber02a/filter_run_', run_string);
%            saveas(gcf, picname1, 'fig' );
%            saveas(gcf, picname1, 'png');


        figure(2); colormap(gray);
        imagesc(D);
        title(strcat('Preprocessing Difference, Sigma =
',sigma_string));
```

```
            picname2 = strcat(
'data/Preprocessing/Gaussian/fiber10a/diff_run_', run_string);
            saveas(gcf, picname2, 'fig' );
            saveas(gcf, picname2, 'png');

        figure(3);
        imhist(D,n);

       title(strcat('Noise Histogram, Gaussian Sigma =
',sigma_string));

            picname3 = strcat(
'data/Preprocessing/Gaussian/fiber10a/diff_run_', run_string, '_hist');
            saveas(gcf, picname3, 'fig' );
            saveas(gcf, picname3, 'png');

            fid =
fopen(strcat('data/Preprocessing/Gaussian/fiber10a/diff_run_',
run_string, '_hist.txt'), 'wt');
            fprintf(fid, '%6d %12d\n', hist_data );
            fclose(fid)

            fid =
fopen(strcat('data/Preprocessing/Gaussian/fiber10a/diff_run_',
run_string, '_time.txt'), 'wt');
            fprintf(fid, '%6.9d ', t);
            fclose(fid)

end
```

```
function preprocess_LoG

%Get Image
RGB = imread('fiber10a.bmp');

I  = rgb2gray(RGB);

n = 256;

for i = 1:1:25

    tic

    sigma = 0.25*i;

    H = fspecial('log',[5 5],sigma);

    B = imfilter(I,H,'same','conv');

    D = I - B;

    toc

    t = toc;

    [count, x] = imhist(D,n);
    hist_data = [x, count];
    hist_data = hist_data';

    run_number = i;

    run_string = num2str( run_number );
    sigma_string = num2str( sigma );



        figure(1); colormap(gray);
        imagesc(B);
%        title(strcat('LoG Filter, Std Dev = ',sigma_string));

%            picname1 = strcat( 'data/Preprocessing/LoG/0013-2-
12a/filter_run_', run_string);
%            saveas(gcf, picname1, 'fig' );
%            saveas(gcf, picname1, 'png');


        figure(2); colormap(gray);
        imagesc(D);
        title(strcat('Preprocessing Difference, LoG, Std Dev =
',sigma_string));
```

```
            picname2 = strcat(
'data/Preprocessing/LoG/fiber10a/diff_run_', run_string);
            saveas(gcf, picname2, 'fig' );
            saveas(gcf, picname2, 'png');

         figure(3);
         imhist(D,n);

       title(strcat('Noise Histogram, LoG Sigma = ',sigma_string));

            picname3 = strcat(
'data/Preprocessing/LoG/fiber10a/diff_run_', run_string, '_hist');
            saveas(gcf, picname3, 'fig' );
            saveas(gcf, picname3, 'png');

            fid =
fopen(strcat('data/Preprocessing/LoG/fiber10a/diff_run_', run_string,
'_hist.txt'), 'wt');
            fprintf(fid, '%6d %12d\n', hist_data );
            fclose(fid)

            fid =
fopen(strcat('data/Preprocessing/LoG/fiber10a/diff_run_', run_string,
'_time.txt'), 'wt');
            fprintf(fid, '%6.9d ', t);
            fclose(fid)

end
```

```
function edge_roberts

%% Define Variables

for j = 1:1:12

pic_string = strcat('0013-2-', num2str(j), 'a');

dim = 5; %Defines size of n x n smoothing kernel

RGB = imread( strcat( pic_string,'.bmp') ); %Get image

scale = 0.001; %Edge detection threshhold scale

%% Noise Reduction via Averaging

I = rgb2gray(RGB); %Converts image to grayscale

H = fspecial('average',dim); %Generate kernel

B = imfilter(I,H,'same','conv'); %Filter Image

B_90 = imrotate(B, 90); %Rotate image 90 degrees counter-clockwise

    figure(1); colormap(gray);
    imagesc(B);
    title(strcat('Average Smoothing, ', num2str(dim), ' x ',
num2str(dim) ) );

Iavg = mean(mean(I))
Bavg = mean(mean(B))

%% Edge Detection: Roberts

for i = 1:1:30

    threshold = i * scale;

    tic;

    [BW, thresh] = edge(B,'roberts', threshold );

    toc;

    t(i) = toc

    [count, x] = imhist(BW);
    hist_data = [x, count];
    hist_data = hist_data';
```

```
    [BW_90, thresh ] = edge(B_90, 'roberts', threshold );

    BW_90check = imrotate( BW_90, -90);

    [count_90, x_90] = imhist(BW_90check);
    hist_data_90 = [x_90, count_90];
    hist_data_90 = hist_data_90';

    Check = BW - BW_90check;

    [count_check, x_check] = imhist(BW_90check);
    hist_data_check = [x_check, count_check];
    hist_data_check = hist_data_check';

    run_string = num2str(i);

        figure(2); colormap(gray);
        imagesc(BW);
        title( strcat('Roberts Method, Thresh = ', num2str(threshold) )
);

                    picname1 = strcat( 'data/Edge_Detection/Roberts/',
pic_string, '/edges_thresh_', run_string );
                    saveas(gcf, picname1, 'fig' );
                    saveas(gcf, picname1, 'png');

        figure(3); imhist(BW);
        title( strcat('Edge Histogram, Roberts Method, Thresh = ',
num2str(threshold) ) );

                    picname2 = strcat( 'data/Edge_Detection/Roberts/',
pic_string, '/edges_thresh_', run_string, '_hist');
                    saveas(gcf, picname2, 'fig' );
                    saveas(gcf, picname2, 'png');

        figure(4); colormap(gray);
        imagesc(Check);
        title( strcat('90 Degree Rotation Check, Roberts Method, Thresh
= ', num2str(threshold) ) );

                    picname3 = strcat( 'data/Edge_Detection/Roberts/',
pic_string, '/edges90_thresh_', run_string );
                    saveas(gcf, picname3, 'fig' );
                    saveas(gcf, picname3, 'png');

        figure(5); imhist(Check);
        title( strcat('Error Histogram, Roberts Method, Thresh = ',
num2str(threshold) ) );

                    picname4 = strcat( 'data/Edge_Detection/Roberts/',
pic_string, '/error_thresh_', run_string, '_hist');
                    saveas(gcf, picname4, 'fig' );
```

```
                saveas(gcf, picname4, 'png');


            fid = fopen(strcat('data/Edge_Detection/Roberts/',
pic_string, '/edges_thresh_', run_string, '_hist.txt'), 'wt');
            fprintf(fid, '%6d %12d\n', hist_data );
            fclose(fid)

            fid = fopen(strcat('data/Edge_Detection/Roberts/',
pic_string, '/edges90_thresh_', run_string, '_hist.txt'), 'wt');
            fprintf(fid, '%6d %12d\n', hist_data_90 );
            fclose(fid)

            fid = fopen(strcat('data/Edge_Detection/Roberts/',
pic_string, '/error_thresh_', run_string, '_hist.txt'), 'wt');
            fprintf(fid, '%6d %12d\n', hist_data_check );
            fclose(fid)

end

fid = fopen(strcat('data/Edge_Detection/Roberts/0013-2-1a/time.txt'),
'wt');
fprintf(fid, '%12d %12d\n', t );
fclose(fid)

end
```

```
function edge_sobel

%% Define Variables

for j = 1:1:12

pic_string = strcat('0013-2-', num2str(j), 'a');

dim = 5; %Defines size of n x n smoothing kernel

RGB = imread( strcat( pic_string,'.bmp') ); %Get image

scale = 0.001; %Edge detection threshhold scale

%% Noise Reduction via Averaging

I = rgb2gray(RGB); %Converts image to grayscale

H = fspecial('average',dim); %Generate kernel

B = imfilter(I,H,'same','conv'); %Filter Image

B_90 = imrotate(B, 90); %Rotate image 90 degrees counter-clockwise

    figure(1); colormap(gray);
    imagesc(B);
    title(strcat('Average Smoothing, ', num2str(dim), ' x ',
num2str(dim) ) );

Iavg = mean(mean(I))
Bavg = mean(mean(B))

%% Edge Detection: Roberts

for i = 1:1:30

    threshold = i * scale;

    tic;

    [BW, thresh] = edge(B,'sobel', threshold );

    toc;

    t(i) = toc

    [count, x] = imhist(BW);
    hist_data = [x, count];
    hist_data = hist_data';
```

```
    [BW_90, thresh ] = edge(B_90, 'sobel', threshold );

    BW_90check = imrotate( BW_90, -90);

    [count_90, x_90] = imhist(BW_90check);
    hist_data_90 = [x_90, count_90];
    hist_data_90 = hist_data_90';

    Check = BW - BW_90check;

    [count_check, x_check] = imhist(BW_90check);
    hist_data_check = [x_check, count_check];
    hist_data_check = hist_data_check';

    run_string = num2str(i);

        figure(2); colormap(gray);
        imagesc(BW);
        title( strcat('Sobel Method, Thresh = ', num2str(threshold) )
);

                    picname1 = strcat( 'data/Edge_Detection/Sobel/',
pic_string, '/edges_thresh_', run_string );
                    saveas(gcf, picname1, 'fig' );
                    saveas(gcf, picname1, 'png');

        figure(3); imhist(BW);
        title( strcat('Edge Histogram, Sobel Method, Thresh = ',
num2str(threshold) ) );

                    picname2 = strcat( 'data/Edge_Detection/Sobel/',
pic_string, '/edges_thresh_', run_string, '_hist');
                    saveas(gcf, picname2, 'fig' );
                    saveas(gcf, picname2, 'png');

        figure(4); colormap(gray);
        imagesc(Check);
        title( strcat('90 Degree Rotation Check, Sobel Method, Thresh =
', num2str(threshold) ) );

                    picname3 = strcat( 'data/Edge_Detection/Sobel/',
pic_string, '/edges90_thresh_', run_string );
                    saveas(gcf, picname3, 'fig' );
                    saveas(gcf, picname3, 'png');

        figure(5); imhist(Check);
        title( strcat('Error Histogram, Sobel Method, Thresh = ',
num2str(threshold) ) );

                    picname4 = strcat( 'data/Edge_Detection/Sobel/',
pic_string, '/error_thresh_', run_string, '_hist');
                    saveas(gcf, picname4, 'fig' );
```

```
                saveas(gcf, picname4, 'png');


            fid = fopen(strcat('data/Edge_Detection/Sobel/',
pic_string, '/edges_thresh_', run_string, '_hist.txt'), 'wt');
            fprintf(fid, '%6d %12d\n', hist_data );
            fclose(fid)

            fid = fopen(strcat('data/Edge_Detection/Sobel/',
pic_string, '/edges90_thresh_', run_string, '_hist.txt'), 'wt');
            fprintf(fid, '%6d %12d\n', hist_data_90 );
            fclose(fid)

            fid = fopen(strcat('data/Edge_Detection/Sobel/',
pic_string, '/error_thresh_', run_string, '_hist.txt'), 'wt');
            fprintf(fid, '%6d %12d\n', hist_data_check );
            fclose(fid)

end

fid = fopen(strcat('data/Edge_Detection/Sobel/',
pic_string,'/time.txt'), 'wt');
fprintf(fid, '%18d\n', t );
fclose(fid)

end
```

```
function edge_canny

%% Define Variables

for j = 2:1:9

pic_string = strcat('fiber0', num2str(j), 'a');

dim = 5; %Defines size of n x n smoothing kernel

sigma = 2.75; %Defines standard deviation for Canny Method

RGB = imread( strcat( pic_string,'.bmp') ); %Get image

scale = 0.025; %Edge detection threshhold scale

%% Noise Reduction via Averaging

I = rgb2gray(RGB); %Converts image to grayscale

H = fspecial('average',dim); %Generate kernel

B = imfilter(I,H,'same','conv'); %Filter Image

B_90 = imrotate(B, 90); %Rotate image 90 degrees counter-clockwise

    figure(1); colormap(gray);
    imagesc(B);
    title(strcat('Average Smoothing, ', num2str(dim), ' x ',
num2str(dim) ) );

%% Edge Detection: Canny

for i = 1:1:30

    threshold = i * scale;

    tic;

    [BW, thresh] = edge(B,'canny', threshold, sigma );

    toc;

    t(i) = toc

    [count, x] = imhist(BW);
    hist_data = [x, count];
    hist_data = hist_data';

    [BW_90, thresh ] = edge(B_90, 'canny', threshold, sigma );
```

```
    BW_90check = imrotate( BW_90, -90);

    [count_90, x_90] = imhist(BW_90check);
    hist_data_90 = [x_90, count_90];
    hist_data_90 = hist_data_90';

    Check = BW - BW_90check;

    [count_check, x_check] = imhist(BW_90check);
    hist_data_check = [x_check, count_check];
    hist_data_check = hist_data_check';

    run_string = num2str(i);

        figure(2); colormap(gray);
        imagesc(BW);
        title( strcat('Canny Method, Thresh = ', num2str(threshold) )
);

                    picname1 = strcat( 'data/Edge_Detection/Canny/',
pic_string, '/edges_thresh_', run_string );
                    saveas(gcf, picname1, 'fig' );
                    saveas(gcf, picname1, 'png');

        figure(3); imhist(BW);
        title( strcat('Edge Histogram, Canny Method, Thresh = ',
num2str(threshold) ) );

                    picname2 = strcat( 'data/Edge_Detection/Canny/',
pic_string, '/edges_thresh_', run_string, '_hist');
                    saveas(gcf, picname2, 'fig' );
                    saveas(gcf, picname2, 'png');

        figure(4); colormap(gray);
        imagesc(Check);
        title( strcat('90 Degree Rotation Check, Canny Method, Thresh =
', num2str(threshold) ) );

                    picname3 = strcat( 'data/Edge_Detection/Canny/',
pic_string, '/edges90_thresh_', run_string );
                    saveas(gcf, picname3, 'fig' );
                    saveas(gcf, picname3, 'png');

        figure(5); imhist(Check);
        title( strcat('Error Histogram, Canny Method, Thresh = ',
num2str(threshold) ) );

                    picname4 = strcat( 'data/Edge_Detection/Canny/',
pic_string, '/error_thresh_', run_string, '_hist');
                    saveas(gcf, picname4, 'fig' );
                    saveas(gcf, picname4, 'png');
```

```
            fid = fopen(strcat('data/Edge_Detection/Canny/',
pic_string, '/edges_thresh_', run_string, '_hist.txt'), 'wt');
            fprintf(fid, '%6d %12d\n', hist_data );
            fclose(fid)

            fid = fopen(strcat('data/Edge_Detection/Canny/',
pic_string, '/edges90_thresh_', run_string, '_hist.txt'), 'wt');
            fprintf(fid, '%6d %12d\n', hist_data_90 );
            fclose(fid)

            fid = fopen(strcat('data/Edge_Detection/Canny/',
pic_string, '/error_thresh_', run_string, '_hist.txt'), 'wt');
            fprintf(fid, '%6d %12d\n', hist_data_check );
            fclose(fid)

end

fid = fopen(strcat('data/Edge_Detection/Canny/',
pic_string,'/time.txt'), 'wt');
fprintf(fid, '%18d\n', t );
fclose(fid)

end
```

```
function lines

%% Define Variables

for j = 2:1:2

pic_string = strcat('0013-2-', num2str(j), 'a');

dim = 5; %Defines size of n x n smoothing kernel

sigma = 2.75; %Defines standard deviation for Canny Method

RGB = imread( strcat( pic_string,'.bmp') ); %Get image

threshold = .005; %Edge detection threshhold

    % Line Detection Variables
    grids = 8; %Number of grids for line detection
    ThetaRes = 1; %Theta resolution for hough transform
    RhoRes = 1; %Rho resolution for hough transform
    nhoodsize = 9; %Supression area around hough peak
    fill_gap = 8; %Defines minimum gap distance for hough lines
    min_length = 24; %Minimum length of merged lines

%% Noise Reduction: Averaging

I = rgb2gray(RGB); %Converts image to grayscale
[ M, N ] = size(I); %Determines size of image

H = fspecial('average',dim); %Generate kernel

B = imfilter(I,H,'same','conv'); %Filter Image

    figure(1); colormap(gray);
    imagesc(B);
    title(strcat('Average Smoothing, ', num2str(dim), ' x ',
num2str(dim) ) );

%% Edge Detection: Canny

[BW, thresh] = edge(B,'canny', [threshold 2.5*threshold], sigma );

    figure(2); colormap(gray);
    imagesc(BW);
    title( strcat('Canny Method, Thresh = ', num2str(threshold) ) );

%% Line Extraction: Hough Transform
    for hough_peaks = 10:10:100

        hough_peaks_str = num2str(hough_peaks);
```

```
        for grid = [ 1 2 3 4 5 6 8 10 ]

            grid_str = num2str( grid );

            for m = 1 : 1 : grids

                for n = 1 : 1 : grids

                    tic

                    % Iteration scheme divides BW into grid
                    BWa = BW( ( M / grids ) * ( m - 1 ) + 1 : ( M /
grids ) * m , ( N / grids ) * ( n  - 1 ) + 1 : ( N / grids ) * n );

                    % Hough Transform
                    [H,T,R] =
hough(BWa,'RhoResolution',RhoRes,'ThetaResolution',ThetaRes);

                    hough_thresh_str = num2str(10*hough_thresh);

                    % Hough Peaks
                    peaks =
houghpeaks(H,hough_peaks,'NHoodsize',[nhoodsize nhoodsize]);

                    % Hough Lines
                    lines = houghlines(BW, T, R,
peaks,'FillGap',fill_gap,'MinLength',min_length);

                    for k = 1:length(lines)-1

                        xy = [lines(k).point1; lines(k).point2]

                        dx(k) = xy(2,1) - xy(1,1);
                        dy(k) = xy(2,2) - xy(1,2);
                        dtheta(k) = atan( dy(k) / dx(k) ) * 180 / pi;
                        len(k) = sqrt( dx(k) ^2 + d(y)^2 );


                        if dtheta(k) < 0

                            dtheta(k) = dtheta(k) + 180;

                        end

                    end

                    toc
                    t(m,n) = toc;

                    mean_theta(m,n) = mean( dtheta );
                    sum_len(m,n) = sum( len );
```

```
                end

                mean_theta;
                sum_len;
                t;

                file1 = strcat('data/Line_Detection/', pic_string,
'/grid_', grid_str,'_thresh_', hough_peaks_str,'_mean_theta.txt');
                dlmwrite(file1, mean_theta, '\t')

                file2 = strcat('data/Line_Detection/', pic_string,
'/grid_', grid_str,'_thresh_', hough_peaks_str,'_sum_len.txt');
                dlmwrite(file2, sum_len, '\t')

                file3 = strcat('data/Line_Detection/', pic_string,
'/grid_', grid_str,'_thresh_', hough_peaks_str,'_sum_len.txt');
                dlmwrite(file3, t, '\t')

            end

        end

    end

end
```

```
function alignment_analysis

%% Define Variables

pic_string = strcat('0013-2-1a');

dim = 5; %Defines size of n x n smoothing kernel

sigma = 2.75; %Defines standard deviation for Canny Method

RGB = imread( strcat( pic_string,'.bmp') ); %Get image

threshold = .005; %Edge detection threshhold

    % Line Detection Variables
    grids = 8; %Number of grids for line detection
    ThetaRes = 1; %Theta resolution for hough transform
    RhoRes = 1; %Rho resolution for hough transform
    hough_peaks = 50; %Defines threshold for hough lines
    nhoodsize = 9; %Supression area around hough peak
    fill_gap = 8; %Defines minimum gap distance for hough lines
    min_length = 24; %Minimum length of merged lines

    hough_peaks_str = num2str( hough_peaks ); %String formatting for
Hough Peaks
    grid_str = num2str( grids ); %String formatting for Grids

%% Noise Reduction: Averaging

I = rgb2gray(RGB); %Converts image to grayscale
[ M, N ] = size(I); %Determines size of image

H = fspecial('average',dim); %Generate kernel

B = imfilter(I,H,'same','conv'); %Filter Image

    figure(1); colormap(gray);
    imagesc(B);
    title(strcat('Average Smoothing, ', num2str(dim), ' x ',
num2str(dim) ) );

%% Edge Detection: Canny

[BW, thresh] = edge(B,'canny', [threshold 2.5*threshold], sigma );

    figure(2); colormap(gray);
    imagesc(BW);
    title( strcat('Canny Method, Thresh = ', num2str(threshold) ) );

%% Line Extraction: Hough Transform
```

```
    for m = 1 : 1 : grids

        for n = 1 : 1 : grids

            tic

            % Iteration scheme divides BW into grid
            BWa = BW( ( M / grids ) * ( m - 1 ) + 1 : ( M / grids ) * m
, ( N / grids ) * ( n  - 1 ) + 1 : ( N / grids ) * n );

            % Hough Transform
            [H,T,R] =
hough(BWa,'RhoResolution',RhoRes,'ThetaResolution',ThetaRes);

            % Hough Peaks
            peaks = houghpeaks(H,hough_peaks,'NHoodsize',[nhoodsize
nhoodsize]);

            % Hough Lines
            lines = houghlines(BW, T, R,
peaks,'FillGap',fill_gap,'MinLength',min_length);

            for k = 1:length(lines)-1

                xy = [lines(k).point1; lines(k).point2]

                dx(k) = xy(2,1) - xy(1,1);
                dy(k) = xy(2,2) - xy(1,2);
                dtheta(k) = atan( dy(k) / dx(k) ) * 180 / pi;
                len(k) = sqrt( dx(k) ^2 + dy(k)^2 );


                if dtheta(k) < 0

                    dtheta(k) = dtheta(k) + 180;

                end

            end

            toc
            t(m,n) = toc;

            mean_theta(m,n) = mean( dtheta );
            sum_len(m,n) = sum( len );

        end

        mean_theta
        sum_len
        t
```

```
        %file1 = strcat('data/Line_Detection/', pic_string, '/grid_',
grid_str,'_thresh_', hough_peaks_str,'_mean_theta.txt');
        %dlmwrite(file1, mean_theta, '\t')

        %file2 = strcat('data/Line_Detection/', pic_string, '/grid_',
grid_str,'_thresh_', hough_peaks_str,'_sum_len.txt');
        %dlmwrite(file2, sum_len, '\t')

        %file3 = strcat('data/Line_Detection/', pic_string, '/grid_',
grid_str,'_thresh_', hough_peaks_str,'_sum_len.txt');
        %dlmwrite(file3, t, '\t')

    end
```

VITA

Lee Allen was born and raised in Memphis, Tennessee. Upon graduating from Christian Brothers High School in 2001 he majored in mechanical engineering at Christian Brothers University. After graduating from CBU, he worked for a short time as at Smith & Nephew Orthopedics as an Associate Lean Engineer. Lee returned to graduate school in the fall of 2006 at the University of Tennessee Space Institute in Tullahoma, TN. While at UTSI, Lee worked under Dr. Ahmad Vakili as a GRA supporting low cost pitch-based carbon fiber manufacturing.

Lee plans to start work in mid-September 2008 for NASA as a ceramics engineer at Marshall Space Flight Center in Huntsville, AL.